

**Periodic bottlenecks in experimental antibiotic resistance
evolution of *Pseudomonas aeruginosa***

Dissertation

zur Erlangung des Doktorgrades (Dr. rer. nat.) der
Mathematisch-Naturwissenschaftlichen Fakultät der
Christian-Albrechts-Universität zu Kiel

Vorgelegt von

Niels Jonas Mahrt

aus Flensburg

Kiel, February 2020

Erstprüfer:

Prof. Dr. Hinrich Schulenburg

Evolutionary Ecology and Genetics, Christian-Albrechts-Universität zu Kiel

Zweitprüferin:

Prof. Dr. Eva Holtgrewe Stukenbrock

Environmental Genomics, Christian-Albrechts-Universität zu Kiel

Datum der mündlichen Prüfung: 24. April 2020

Summary

Over the past decades, the spread of antibiotic resistance among nosocomial bacterial pathogens has developed into a global problem. Population bottlenecks are an important factor for bacterial evolution. Their influence on antibiotic resistance evolution is however not yet fully understood. Bottlenecks are defined as a strong reduction of population size that can lower the population's genetic diversity drastically. Population bottlenecks frequently occur in nature and play a significant role in the evolutionary history of populations. Bacterial populations can evolve resistance by various adaptive paths. However, the serial bottlenecks experienced by bacteria both in nature and in experimental evolution influence the direction of adaptation. After surviving a narrow bottleneck, future adaptation is more likely influenced by selective sweeps and periodic selection, rendering the adaptive paths less predictable. In contrast, higher degrees of parallel evolution and clonal interference are expected in case of a wider bottleneck, as higher genetic diversity is likely maintained. In this thesis, I validated the influence of different bottleneck sizes at different levels of selectivity on the evolvability of resistance in populations of the pathogenic bacterium *Pseudomonas aeruginosa* (subclone PA14). Three different evolution experiments were performed to simulate single drug treatments with carbenicillin (beta-lactam), ciprofloxacin (quinolone) and gentamicin (aminoglycoside) against PA14, for approximately 100 generations. While high inhibitory concentrations selected for the highest resistance under large transfer sizes, the highest resistance in low inhibitory concentrations populations emerged when the transfer size was small. These different dynamics are reflected by mutational patterns in the evolving bacterial genomes. Even though the total number of mutations per population for each treatment depended on the treatment drug, the diversity of the most frequent mutations at the final growth season was higher for small transfer sizes than for large transfer sizes. Surprisingly, only few mutations have completely fixed by the final transfer. These results may indicate that clonal interference of *de novo* mutations occurs regularly at sub-inhibitory drug concentrations. Overall, my data suggests that bottlenecks, in combination with antibiotic-induced selective pressure, can be a key determinant of resistance evolution and can shape genetic diversity within and between populations.

Zusammenfassung

Im Laufe der letzten Jahrzehnte hat sich die Verbreitung von Antibiotikaresistenzen bei humanpathogenen Bakterien zu einem globalen Problem entwickelt. Genetische Flaschenhälse beschreiben eine starke Reduktion der Populationsgröße, welche die populationsgenetische Vielfalt drastisch vermindern kann. Flaschenhälse treten häufig in der Natur auf und spielen eine bedeutsame Rolle für die Evolution von Populationen. Ihr Einfluss auf die Evolution von Antibiotikaresistenz ist bislang jedoch noch nicht verstanden. Bakterienpopulationen können durch verschiedene adaptive Wege Resistenz entwickeln. Die genetischen Flaschenhälse, welche sie sowohl in der Natur als auch in der experimentellen Evolution erfahren, beeinflussen hingegen die Richtung der Anpassung. Nach dem Überleben eines engen genetischen Flaschenhalses wird die zukünftige Anpassung eher durch selektive Sweeps und periodische Selektion beeinflusst, was die adaptiven Pfade weniger vorhersehbar macht. Im Gegensatz dazu werden bei einem breiten genetischen Flaschenhals mehr parallele Evolution und klonale Interferenzen erwartet, da eine höhere genetische Vielfalt wahrscheinlich erhalten bleibt. In dieser Arbeit habe ich den Einfluss verschieden großer Flaschenhälse bei unterschiedlichem Selektionsdruck auf die Evolvierbarkeit von Resistenz in Populationen des humanpathogenen Bakteriums *Pseudomonas aeruginosa* (Subklon PA14) untersucht. Drei verschiedene Evolutionsexperimente wurden durchgeführt um eine medikamentöse Einzelbehandlung mit Carbenicillin (Beta-Lactam), Ciprofloxacin (Chinolon) und Gentamicin (Aminoglykosid) gegen PA14 über etwa 100 Generationen zu simulieren. Während sich bei hohen Hemmungskonzentrationen die höchste Resistenz unter großen Transfergrößen entwickelte, entstand die höchste Resistenz bei niedrigen Hemmungskonzentrationen, wenn die Transfergröße klein ist. Diese unterschiedlichen Dynamiken wurden durch entsprechende Mutationsmuster in den Genomen der evolvierenden Bakterien bestätigt. Auch wenn die Gesamtzahl an Mutationen pro Population für jede Behandlung vom Medikament abhing, war die Vielfalt der häufigsten Mutationen bei kleinen Transfergrößen höher als bei großen Transfergrößen. Überraschenderweise wurden beim letzten Transfer nur wenige Mutationen vollständig fixiert. Diese Ergebnisse kann darauf hindeuten, dass klonale Interferenz zwischen De-Novo-Mutationen bei subinhibitorischen Wirkstoffkonzentrationen regelmäßig auftritt. Insgesamt deuten meine Daten darauf hin, dass genetische Flaschenhälse in Kombination mit antibiotikabedingtem Selektionsdruck ein wichtiger Einflussfaktor für die Resistenzentwicklung sein können und die genetische Vielfalt sowohl innerhalb als auch zwischen Populationen prägen.

Contents

Summary.....	4
Zusammenfassung.....	5
List of figures.....	9
List of abbreviations	12
Introduction.....	13
Antibiotic resistance as a universal threat	13
What are antibiotics?	13
What are the consequences of high antibiotic usage?	14
How is antibiotic resistance conferred?	15
The threat of emerging multidrug resistance.....	17
Alternative strategies to combat infections while minimizing antibiotic resistance	18
Using experimental evolution to study the long-term effects of new treatment strategies.....	19
Neglected population properties	22
The effect of population size and epistasis on the adaptive path of bacterial populations	23
The influence of population bottlenecks on fixation probabilities of mutations	24
The influence of population bottlenecks on bacteria in natural populations.....	25
The potential influence of population bottlenecks on bacteria in evolution experiments	26
<i>Pseudomonas aeruginosa</i> & its role in cystic fibrosis	27
Objectives.....	29
Approach.....	31
Material and Methods	34
Material.....	34
Laboratory devices	34
Consumables	35
Media and buffers.....	35
Kits	36
Antibiotics.....	36
Bacterial strains	38
Software.....	39
Methods.....	40
Bacteria culturing	40

Flow cytometry	40
Dose-response curves and IC determinations	41
Growth curves and inferred fitness parameters	43
Design and general setup of evolution experiments	44
Resistance and fitness assays of evolved populations	47
DNA isolation	47
DNA sequencing and genomics	48
PCR for Sanger sequencing	49
Competition assays	50
Two-step PCR for amplicon sequencing	51
Analysis of amplicon sequencing	54
Statistics	54
Results	56
Evolutionary growth patterns	57
Large TS groups evolve higher yield in GEN evolution experiment	57
Yield improves faster under large TS in CIP evolution experiment	59
All treatment groups adapt gradually in CAR evolution experiment	61
Evolved resistance	63
IC20-k50 and IC80-M5 evolve the highest resistance in GEN evolution experiment	63
IC20-k50 and IC80-M5 evolve the highest resistance in CIP evolution experiment	67
IC80-treated groups evolve highest resistance in CAR evolution experiment	69
Evolutionary genomics	72
Mutations in two-component regulators and <i>ptsP</i> dominate populations of GEN evolution experiment	72
Mutations in multidrug efflux regulators dominate populations of CIP evolution experiment	76
Evolutionary allele dynamics	79
Populations adapt faster under large TS in GEN evolution experiment	79
Increased clonal competition during CIP evolution experiment	85
Fixation indices (FST)	88
Treatment groups show unique changes in diversity metrics during the GEN evolution experiment	88
Competition Assays	90
Growth advantage of <i>ptsP</i> over <i>pmrB</i> decreases under high IC	90
Growth characteristics under drug-free conditions	96

<i>ptsP</i> shows better growth than <i>pmrB</i> under drug-free conditions	96
Discussion.....	98
Synthesis of different evolution experiments	100
Bottleneck strength and selection strength cause contrasting yield dynamics	100
Combined effects of bottleneck and selective strength on resistance evolution.....	100
Different treatment groups show distinct genomic signatures.....	102
Allele dynamics are influenced by bottleneck strength.....	107
Clonal competition influenced by selective regimen	109
Distinct evolutionary dynamics for individual drugs.....	111
Revisiting the original hypotheses	114
Comparing this thesis to the state of the art	117
Colistin experiments.....	122
Outlook.....	123
References.....	125
Supplementary data	148
Acknowledgements.....	196
Curriculum vitae	198
Erklärung.....	201

List of figures

Figure 1: Antibiotic modes of action and common resistance mechanisms	16
Figure 2: Example of a dose-response curve (DRC).....	42
Figure 3: Example of a growth curve.....	44
Figure 4: Layout design of a 96-well plate for an evolution experiment	46
Figure 5: Design of the general experimental setup.	46
Figure 6: Systematic randomization of competition treatments on a 96-well plate.	51
Figure 7: Plate design of the second PCR-step with sequencing primers.....	53
Figure 8: Large TS groups evolve higher yield in GEN evolution experiment.....	58
Figure 9: Yield improves faster under large TS in CIP evolution experiment.	60
Figure 10: All treatment groups adapt slowly in CAR evolution experiment.	62
Figure 11: IC20-k50 and IC80-M5 evolve the highest resistance in GEN evolution experiment. A:	64
Figure 12: The most GEN-resistant group shows the lowest growth in drug-free medium.....	66
Figure 13: GEN resistance correlates negatively with maximum growth rate.....	66
Figure 14: IC20-k50 and IC80-M5 evolve the highest resistance in CIP evolution experiment. A:	67
Figure 15: Adaptation to CIP does not affect growth in drug-free medium for all treatment groups.....	69
Figure 16: IC80-treated groups evolved higher resistance than IC20-treated groups in CAR evolution experiment. A:.....	70
Figure 17: CAR-adapted lineages have slightly lower growth in drug-free medium.....	71
Figure 18: Most mutations in evolved populations of GEN evolution experiment found in two-component regulators and <i>ptsP</i>	73
Figure 19: Frequency of the most common mutation in a population decreases with the total number of mutations in GEN evolution experiment.....	74
Figure 20: Populations with the most frequent mutation in <i>ptsP</i> show lower resistance than populations with the most frequent mutation in <i>pmrB</i>	75
Figure 21: Most mutations in evolved populations of CIP evolution experiment found in multidrug efflux regulators. The.....	77
Figure 22: Frequency of the most common mutation in a population decreases with the total number of mutations in CIP evolution experiment.	78
Figure 23: Complex evolutionary allele dynamics between mutations in various genes found in IC20-k50 populations of GEN evolution experiment.	81

Figure 24: Mutations in <i>ptsP</i> dominate evolutionary allele dynamics in IC20-M5 populations of GEN evolution experiment.	82
Figure 25: Single mutations in different genes dominate evolutionary allele dynamics in IC80-k50 populations of GEN evolution experiment.	83
Figure 26: Mutations in <i>pmrB</i> dominate evolutionary allele dynamics in IC80-M5 populations of GEN evolution experiment.	84
Figure 27: Clonal interference between mutations in different genes shapes evolutionary allele dynamics in IC20-k50 populations of CIP evolution experiment.....	86
Figure 28: Mutations in <i>mexS</i> and <i>nfxB</i> dominate evolutionary allele dynamics in IC80-M5 populations of CIP evolution experiment.	87
Figure 29: Treatment groups show unique changes in diversity metrics during the GEN evolution experiment..	89
Figure 30: <i>ptsP</i> shows a growth advantage over <i>pmrB</i> in competitions under low IC. ...	92
Figure 31: Combined results of the three competition experiments.	94
Figure 32: Frequencies of <i>ptsP</i> mutants decrease when competing against <i>pmrB</i> mutants under high GEN concentrations.	95
Figure 33: AUC of single strain growth (k50).....	97
Figure 34: AUC of single strain growth (M5).....	97
Figure 35: Schematic interpretation of results.....	116

List of tables

Table 1: Examples of studies on antibiotic resistance that made use of experimental evolution.....	21
Table 2: Antibiotics used in this thesis.....	37
Table 3: Evolved clones used in competition experiments.	38
Table 4: Software used in this thesis.	39
Table 5: PCR mix for one reaction.....	49
Table 6: PCR protocol.	50
Table 7: Sequence-specific primers for amplicon sequencing.	52
Table 8: Sequencing primers for amplicon sequencing (second PCR step).	53
Table 9: Yield over time: Linear mixed model results for gentamicin.	58
Table 10: Yield over time: TukeyHSD results for gentamicin.	59
Table 11: Yield over time: Linear mixed model results for ciprofloxacin.....	60
Table 12: Yield over time: TukeyHSD results for ciprofloxacin.	61
Table 13: Yield over time: Linear mixed model results for carbenicillin.....	62
Table 14: Yield over time: TukeyHSD results for carbenicillin.	63
Table 15: Linear mixed effect model results for evolved gentamicin resistance.....	65
Table 16: TukeyHSD results for evolved gentamicin resistance.	65
Table 17: Linear model results for evolved ciprofloxacin resistance.....	68
Table 18: TukeyHSD results for evolved ciprofloxacin resistance.....	68
Table 19: Linear model results for evolved carbenicillin resistance.....	71
Table 20: TukeyHSD results for evolved carbenicillin resistance.....	71
Table 21: Gentamicin: Shannon’s diversity indices H and Hmax for each treatment group.	74
Table 22: Ciprofloxacin: Shannon’s diversity indices H and Hmax for each treatment group.	76
Table 23: Clones used in the three competition experiments.	91
Table 24: One-way ANOVA of frequency of <i>ptsP</i> mutants in competition against <i>pmrB</i> mutants based on treatment group.	94
Table 25: Tukey HSD for multiple pairwise-comparison of frequency of <i>ptsP</i> mutants in competition against <i>pmrB</i> mutants and treatment group.....	95
Table 26: Linear models to detect influence of single strain growth characteristics on the competition outcome.....	96
Table 27: Summary of results.....	99

List of abbreviations

CAR	carbenicillin
CF	cystic fibrosis
CIP	ciprofloxacin
COL	colistin
FST	Fixation index
GEN	gentamicin
HGT	horizontal gene transfer
HS	genetic diversity within populations
HT	genetic diversity between populations
IC	inhibitory concentration
INDEL	nucleotide insertion or deletion
LPS	lipopolysaccharides
MIC	minimum inhibitory concentration
NGS	next generation sequencing
OD	optical density
PA / PA14	<i>Pseudomonas aeruginosa</i> / sub strain 14
QS	quorum sensing
Ref.	reference code number
SNP	single nucleotide polymorphisms
TS	transfer size
WGS	whole genome sequencing
Wt	PA14 wild type

Introduction

Antibiotic resistance as a universal threat

What are antibiotics?

In 1906, the German chemist Alfred Bertheim started a test series with more than 600 synthesized organoarsenic compounds in the lab of Paul Ehrlich ¹. Three years later, Ehrlich and his colleague Sahachiro Hata identified compound #606 as an effective drug against syphilis. After one year of clinical tests, “Ehrlich-Hata 606“ was produced and distributed by Hoechst as a syphilis treatment drug under the name Salvarsan, making it the world’s first commercial antibiotic ²⁻⁴. Salvarsan remained the most prescribed drug until the 1940s, when it was replaced by penicillin as the standard drug for syphilis treatment ⁵. The large-scale production of penicillin and streptomycin as the main drugs against tuberculosis eventually started the golden era of antibiotics, which was characterized by the identification and production of several classes of treatment drugs against bacterial infections ⁶⁻⁸. Before the implementation of antibiotics for clinical therapy, bacterial infections were often fatal to those harboring the disease. The increased identification and mass production of antibiotics allowed physicians to treat otherwise fatal infections ⁹.

Antibiotics are competitive molecules that kill or inhibit the growth of bacteria and other microorganisms ¹⁰. Most antibiotics that are applied for clinical therapy of bacterial infections are derived from natural compounds that are produced by bacteria or fungi to inhibit the growth of other microbial species in the competition for resources ^{11,12}. Additional ecological functions of antibiotics include signaling, quorum sensing and virulence modulation ¹³⁻¹⁶. After the successful clinical application of the first antibiotics, dozens of antibiotics that target different molecular processes in bacteria have been developed and clinically applied in the last 60 years. The most common cellular processes targeted by antibiotics are cell wall synthesis (beta-lactam antibiotics), protein synthesis (aminoglycosides, macrolides, tetracyclins), DNA or RNA synthesis (quinolones, rifampin) and folate biosynthesis (sulfamethoxazole, trimethoprim) ¹⁷. In addition, some antibiotic classes, like antimicrobial peptides, have multiple target sites ¹⁸.

What are the consequences of high antibiotic usage?

Currently, the administration of antibiotics is common procedure not only to treat but also to prevent bacterial infections¹⁹. The success rate of common surgeries and organ transplantations can be greatly improved by the prophylactic use of antibiotics to prevent pathogenic infections^{20,21}. Antibiotics additionally allow for the successful treatment of cancer patients and other patients with suppressed immune systems^{20,21}. In addition to clinical application, the prophylactic use of antibiotics has also played a key role in the agricultural industry in the last couple of decades to improve the growth and overall yield of both farm animals and crops^{22,23}. It had been estimated in 2015 that ~80% of the annual antibiotic usage in the US is applied prophylactically to farm animals²⁴. In addition, antibiotics are distributed on crop fields when animal manure is used as a crop fertilizer. Animals previously treated with antibiotics excrete trace amounts of the drugs which are then redistributed to the soil when their manure is applied to crop fields²⁵.

Because of the great success of antibiotics for therapy, their usage has steadily increased over the past decades. However, this high usage has also resulted in increased contamination of natural environments with antibiotics via wastewater from all fields of antibiotic application^{26,27}. The contamination of natural environments selectively favors the spread of antibiotic resistance among bacteria. Even the low concentrations of antibiotics often found in wastewater can provoke the spread of strong resistance in bacteria and positively select for resistant variants^{28,29}. Over the last decade, scientists and government bodies alike have been warning the general public about the risk of entering a “post-antibiotic era”, in which the successful treatment of currently treatable infections will be no longer possible because of the high degree of antibiotic resistance^{19,30,31}. Antibiotic misuse by patients contrary to doctor’s recommendation, antibiotics being prescribed by doctors when not necessary and antibiotics release into the environment due to excessive use in agriculture and livestock have all certainly contributed to the increased spread of resistance^{6,9,19}. Ultimately, resistance is an evolutionary response: When bacteria are consistently challenged with antibiotics in their environment, the most resistant phenotypes will be positively selected over time. Antibiotic resistance was present long before the man-made discovery and application of antibiotics. For example, resistance genes have been found in 30,000-year-old permafrost soil samples³². This finding indicates that natural antibiotics have been a selective agent for microbial adaptation for a long time and may help us comprehend why antibiotic resistance can evolve so frequently and rapidly.

How is antibiotic resistance conferred?

Antibiotic resistance is generally conferred by mutations in genes that somehow influence the effect of the drug. According to evolutionary theory, randomly occurring mutations can increase their frequency in a population if they confer a growth advantage over the ancestral genotype³³. To fix in the population, the fitness advantage conferred by the mutation must also survive any population bottleneck, an event that results in a rapid decrease in size and genetic diversity of a population³³. The selection of resistance-conferring mutations is a textbook example of rapid evolutionary adaptation: Antibiotic treatment at dosages that are too low to effectively kill bacteria will eventually select for *de novo* mutations that improve the fitness of the pathogen under antibiotic therapy³⁴. Selection of mutants with increased resistance can subsequently enable the resistant variants to increase in frequency and to further spread to new environments. The mutation rates of bacteria are commonly about 10^{-10} to 10^{-9} mutations per site per generation³⁵. Antibiotics and other stressors can transiently increase the mutation rate of treated bacteria via activation of the SOS response, a global stress response cascade in bacteria that results in the arrest of the cell cycle and induction of mutagenesis³⁶. By increasing bacterial mutation rates, the risk of a resistance mutation to emerge in time is also increased. In addition, variants with elevated mutation rates (so-called hypermutators) are commonly present at low frequencies in bacterial populations³⁷.

Resistance due to *de novo* evolution is often conferred by single base pair mutations, either single nucleotide polymorphisms (SNPs) or single nucleotide insertions/deletions (Indels)³⁸⁻⁴⁰. Single base pair mutations can cause changes in the encoded protein sequence that is transcribed into mRNA, which ultimately results in an altered protein structure or premature stop of the translation. If structural alterations caused by the mutation change the binding site of the antibiotic, the drug will lose its efficacy. However, mutations can also result in a non-functioning regulatory gene, which will confer resistance^{41,42}. There are four general molecular mechanisms by which bacteria commonly resist antimicrobial agents: (1) restricted drug uptake, (2) increased drug efflux, (3) enzymatic drug inactivation and (4) alteration of the drug targets^{40,41,43}. In case of resistance by increased drug efflux, single point mutations commonly occur in negative regulators of multidrug efflux pumps that remove distinct substrates from the cytoplasm^{42,44}. An inactive regulator can also result in constitutively increased efflux pump activity that is causing resistance. Duplication of genes that are important for drug resistance will also confer increased resistance^{45,46}. A common result of

partial genomic duplications is heteroresistance, a mixed resistance profile of bacterial populations due to genetic heterogeneity. Heteroresistance is caused by genetically resistant variants within the population that occur at low frequencies and express higher resistance than the rest of the population ^{47,48}.

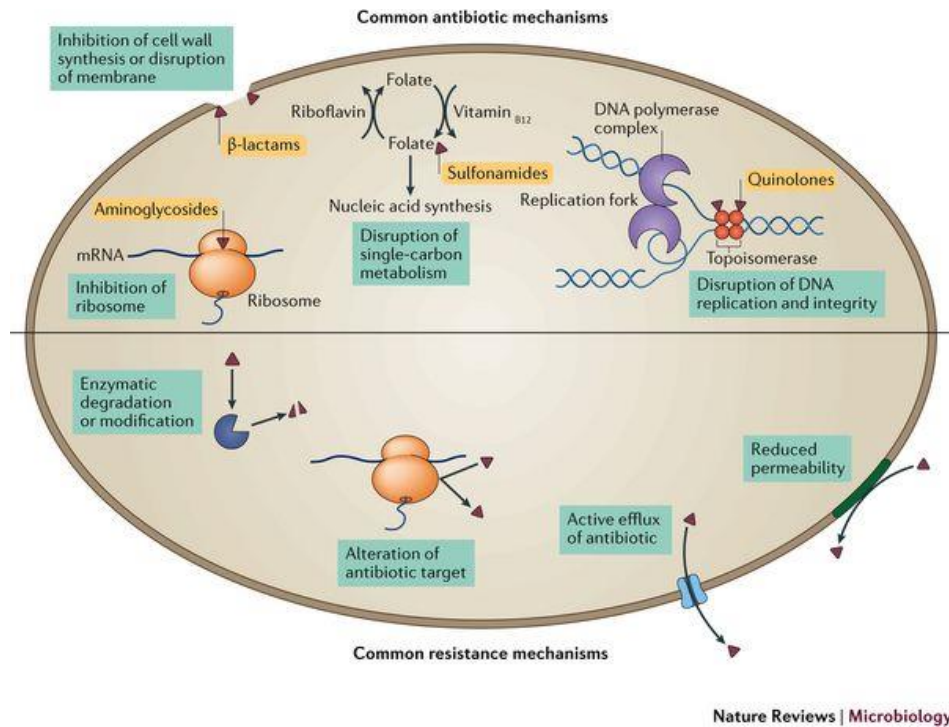


Figure 1: Antibiotic modes of action and common resistance mechanisms. The upper half of the schematic cell summarizes the target sites and the inhibitory effects of the most prevalent antibiotic classes (beta-lactam antibiotics, quinolones, sulfonamides and aminoglycosides). The lower half of the schematic cell summarizes the four most common adaptive changes in bacteria that ultimately cause antibiotic resistance. (Figure taken from Crofts *et al.* 2017 ⁴⁹.)

More than 20,000 different resistance genes with highly diverse functions have thus far been identified, demonstrating the substantial adaptive potential of bacteria to overcome antibiotic treatment from any class or function ⁶. To further complicate this matter, horizontal gene transfer (HGT) is an additional important route for bacteria to acquire resistance genes from extracellular sources ^{50,51}. Resistance can rapidly spread via conjugative plasmids that often carry multiple selective resistance-conferring genes ⁵². In addition, resistance genes can be inserted into the bacterial genome by bacteriophages via transduction ⁵³. Effective antibiotic therapy can reduce the size of the bacterial population to levels at which the mutation supply rate is too low to yield beneficial mutations in time for the population to survive the treatment ^{54,55}. However, bacteria can also express alternative phenotypic traits that enable them to survive the antibiotic treatment and may later contribute to resistance evolution. A common

phenomenon of phenotypic heterogeneity in bacterial populations is persistence. Persister cells are subpopulations of cells existing in a semi-dormant state with a drastically lower growth rate than genetically identical normal growing cells ^{57,58}. The reduced growth rate of persisters enables higher survival in stressful environments like high antibiotic concentrations. This is because cell division is necessary for many stressors, including antibiotics, to confer damage ^{56,57}. Non- or slow-growing cells can enable the survival of the population during transient stress exposure and may enable resistant mutants to emerge later ^{58,59}.

The threat of emerging multidrug resistance

After the 1970s, which marked the end of the golden era of antibiotics, the number of multidrug-resistant pathogenic bacterial strains has steadily increased ^{6,60,61}. These strains are resistant to the majority of clinically prescribed antibiotics, rendering successful treatment of these strains virtually impossible ⁶². In addition to the increased spread of multidrug-resistant pathogenic strains, the development of novel antibiotics for clinical application has simultaneously slowed down drastically over the past decades ⁶³. This is due to both challenges in the discovery of new antibiotic compounds and financial unattractiveness: The development of new drugs is very expensive and does not promise high profits, as new drugs would likely only be applied as a last resort effort to treat an infection ^{64,65}. Most European programs to promote new AB discovery and development are therefore funded by public sources and not by companies ⁶⁶.

Even though the call for new antibiotics has been continuously made public over the years, the development of alternative treatment strategies has only recently received more attention ⁶⁷. The ultimate reason for the delayed interest in new treatment strategies is increased desperation: With the increasing rate of resistance evolution trumping the limited treatment options, the threat of multidrug resistance has been increasing with each year ^{9,69}. However, experience has proven that bacteria always evolve ways to antagonize the effects of newly introduced treatment drugs within only a couple of years ^{6,68}. Therefore, it is crucial to study the evolutionary principles of antibiotic resistance to find new ways to effectively slow down resistance evolution with the help of both new and currently still effective drugs.

Alternative strategies to combat infections while minimizing antibiotic resistance

Alternative approaches to combat the evolution and spread of antibiotic-resistant bacteria include the application of bacteriophages and antimicrobial peptides as well as the development of novel vaccines^{70–74}. In addition, the rise of CRISPR/Cas-based technologies has inspired the development of “sequence-specific antimicrobials” that consist of phages or phagemids as delivery vectors for guide RNA that targets either essential or resistance / virulence genes of the bacterial genome⁷⁵.

Another promising alternative to conventional antibiotic therapy is using already established antibiotics more efficiently by considering research findings on evolutionary dynamics of resistance. Particular focus has been put on the application of treatments that make use of combined effects of two or more antibiotics to reduce resistance evolution⁷⁶. Bacteria that evolve resistance against single antibiotics also commonly become collaterally resistant against antibiotics of the same class, rendering them ineffective as additional treatment options^{77–80}. However, resistance against single antibiotics can also confer collateral sensitivity against antibiotics of different classes. In this case, evolving resistance against the main treatment drug would turn other drugs into viable treatment options. Thus, switching treatment to said drugs would dramatically increase the chance of treatment success^{77,81}. A common example of this pleiotropic effect is collateral sensitivity between aminoglycosides and beta-lactam antibiotics^{78,82,83}. Aminoglycoside resistance is commonly conferred by mutations that alter the structure of the outer membrane of bacteria^{84,85}. Aminoglycosides bind to the lipid A of the bacterial outer membrane for self-promoted uptake via diffusion^{86,87}. Mutations that cause lipid A modifications can disable aminoglycosides from entering the cells, thereby rendering the cells resistant^{86,87}. However, the structural changes in the outer membrane also confer a decreased membrane potential that is an important driver of multidrug efflux pumps⁸⁸. As a consequence, cells with an altered outer membrane have a reduced efflux rate and a higher susceptibility to beta-lactam antibiotics and other drugs for which resistance is mediated by efflux⁷⁸.

A different exploitable aspect of resistance evolution is the metabolic cost that typically accompanies resistance mutations⁸⁹. As mutations in resistance genes commonly affect key mechanisms of cellular metabolism, their alteration most likely results in decreased energy efficiency and therefore decreased ability to replicate^{38,90}. The metabolic fitness cost conferred by the mutation decreases the bacteria’s growth and its competitive ability when growing

together with its ancestor in a non-stressful environment ^{38,90}. Therefore, the severity of the fitness cost of a resistance mutation can have important consequences for its fixation and spread ³⁸. The lower fitness may cause the resistant variant to be outcompeted by less resistant types in nonselective environments and ultimately be lost from the population ^{90,91}. In addition to growth, decreased virulence and transmission rate can also occur as means of resistance-associated fitness cost ⁹²⁻⁹⁴. However, the degree to which fitness is compromised by resistance mutation varies and largely depends on selective strength, bacterial population size, generation time and the number of possible resistance mechanisms ^{95,96}. Compensatory mutations, which are secondary mutations that lower the fitness cost without affecting resistance, can occur and increase the fitness of the resistant variant ^{91,97}. However, the chance of fitness improvement by compensatory mutations greatly depends on the severity of the fitness cost ⁹⁸.

Using experimental evolution to study the long-term effects of new treatment strategies

To develop antibiotic treatment strategies that kill bacteria and at the same time reduce the chance of multidrug resistance evolution, it is necessary to understand the long-term effects of antibiotic treatments on bacteria. Since 24 February 1988, Richard Lenski of Michigan State University has been leading a long-term study of 12 initially identical populations of *Escherichia coli* bacteria that has led to key understandings about adaptive dynamics and evolution of key innovations ¹⁰⁰. The success of Lenski's long term evolution experiment proved that experimental evolution is a promising approach to investigate the long-term adaptation of bacterial populations over extended periods of time ¹⁰¹. The experimental evolution approach has since been applied to study a variety of scientific problems that involve the adaptive processes, including antibiotic resistance ¹⁰²⁻¹⁰⁴. In contrast to medical *in vivo* studies, *in vitro* evolution experiments offer long-term perspectives on the effects of treatment protocols. This way, experimental evolution can also add to the development of novel treatment strategies that might reduce the likelihood of resistance while still being able to minimize bacterial growth ⁸². A common experimental evolution protocol is based on serial transfers. It utilizes growth media with defined concentrations of antibiotics that are inoculated with bacteria, which are then allowed to grow under ideal conditions for a time period of 12-24 hours. After this growth period, a small sampling fraction of the culture is transferred to a

freshly prepared vessel containing the same medium. This process is continued until a desired number of generations has been achieved ^{83,101,104}.

By withdrawing other selective forces and confronting bacteria only with the antibiotic as the single environmental stressor, the adaptation of the bacteria to the antibiotic pressure can be studied in a very controlled and detailed manner ^{82,100,101}. With the help of modern molecular tools like next-generation sequencing (NGS), the underlying genetic mechanisms of resistance evolution can be identified and tracked down ^{104,105}. With NGS, the complete genomes of multiple strains from large numbers of evolved populations can be rapidly and economically sequenced ¹⁰⁶. Due to its high accuracy, NGS is also the most substantial method to detect mutations and, therefore, a vital tool to accompany modern-day experimental evolution ^{102,107}.

Over the last two decades, many studies used experimental evolution to simulate the effects that long-term multidrug treatments have on the resistance properties of bacteria. Several important observations have been made. In 2007, Perron *et al.* experimentally compared the effects of two antibiotics being applied either simultaneously or separately and are switched at every transfer. They identified that sequential treatment has the higher potential to slow down antibiotic resistance evolution, depending on the order the drugs are given in ¹⁰⁸. These findings were later confirmed by Kim *et al.* in 2014 ¹⁰⁹. In 2008, Hegreness *et al.* showed that adaptation rates are reduced by pairs of two drugs being less effective when applied together than alone (antagonism) compared to drug pairs that are more effective when applied together than alone (synergism) ¹¹⁰. Building on the findings of potentially slowing down resistance evolution with multidrug treatments, Imamovic & Sommer introduced the concept of collateral sensitivity cycling in 2013. In this treatment concept, two antibiotics with reciprocal collateral sensitivity are deployed cyclically to select against resistance to either drug ⁷⁷. In addition, Levin-Reisman *et al.* presented evidence that antibiotic tolerance can facilitate the evolution of resistance in 2017 ¹¹¹.

Table 1: Examples of studies on antibiotic resistance that made use of experimental evolution.

Studied factor	Main finding	Bacterium	Year	Reference
Antibiotic combinations	Alternating drugs slows the rate of resistance evolution compared with single-drug treatments	<i>Staphylococcus aureus</i>	2014	¹⁰⁹
Antibiotic combinations	Synergistic combinations select more strongly for resistance than single drugs or antagonistic combinations	<i>Escherichia coli</i>	2008	¹¹²
Antibiotic landscapes	Resistant mutants can be spatially and temporally outcompeted by more sensitive lineages	<i>Escherichia coli</i>	2015	¹⁰¹
Antibiotic tolerance	Tolerance facilitates the evolution of resistance	<i>Escherichia coli</i>	2017	¹¹¹
Collateral sensitivity	Aminoglycoside resistance through reduction in the proton-motive force diminish the activity of major efflux pumps, causing sensitivity	<i>Escherichia coli</i>	2013	⁷⁸
Collateral sensitivity	Two antibiotics can be deployed cyclically to select against resistance to either drug	<i>Escherichia coli</i>	2013	⁷⁷
Immigration under multidrug treatment	Migration into antibiotic environments increases the rate of resistance evolution and decreases the resistance costs, especially under cycling therapy	<i>Pseudomonas aeruginosa</i>	2007	¹¹³
Increasing antibiotic concentration	Ordered adaptive pathways lead to strong antibiotic resistance	<i>Escherichia coli</i>	2012	¹¹⁴
Low Antibiotic concentrations	Selection of resistant bacteria occurs at extremely low antibiotic concentrations	<i>Escherichia coli</i> <i>Salmonella enterica</i>	2011	²⁸
Resistance evolution in cystic fibrosis-like environment	Genes and genetic pathways are repeatedly involved in adaptation to antibiotics and cystic fibrosis-like conditions	<i>Pseudomonas aeruginosa</i>	2012	¹¹⁵

Research conducted in our own lab showed that the joint effect of two antibiotics that are applied simultaneously usually does not last long. Instead, bacteria regularly adapt quickly to the joint selective pressure. However, the evolvability of resistance in combination treatments depends on their respective long-term drug interaction properties. If two antibiotics maintain a synergistic effect over long time, resistance is less likely to evolve^{80,116}. In general, application of multiple drugs in a rapid cycling regimen shows a high inhibitory potential and a low likelihood of long-term adaptation¹¹⁷. One important reason for the high efficacy of switching the treatment drugs every 12 hours is cellular hysteresis. If one drug in the cycling regimen can induce change in the bacterial physiology that enhances susceptibility towards the following drug, resistance is less likely to evolve. A significant difference in adaptation rates was not observed when regular and random temporal drug cycling regimens were compared. In addition, cycling with two drugs and cycling with two two-drug combinations also did not yield a significant difference in resistance evolution¹¹⁷.

Overall, experimental evolution has shown to be a promising approach to test hypotheses about evolutionary concepts of multidrug treatment strategies. When applied effectively, combinations of antibiotics can slow down the *de novo* evolution of resistance. Experimental validation of promising concepts like collateral sensitivity cycling is essential to make the best use of all possible treatment options. As of now, the most precise testing of long-term effects of antibiotic therapy is achieved with evolution experiments.

Neglected population properties

The general interest in bacterial evolution has increased substantially over the last 20 years. At the same time, the experimental evaluation of long-term effects of antibiotic exposure has gained more attention. However, the influence of population biological principles on the evolution of antibiotic resistance has so far mainly been approached in a theoretical framework^{93,118–121}. Uncovering the population dynamics and their dependence on population biological factors remains a crucial challenge to address. This information might help us to make reliable predictions about antibiotic resistance evolution. It was demonstrated that bacterial population size can impact the outcome of drug cycling treatments because multidrug resistant mutants have a higher likelihood to appear in large populations¹²². This finding highlights that

translation of experimental findings for clinical application can be limited when the potential influence of population-related factors on treatment outcome is not sufficiently considered.

Studies, in which antibiotic resistance is investigated by experimental evolution, commonly focus on the characterization of single clonal lineages as study systems. In contrast, natural bacterial populations mostly show a high genetic diversity. Populations comprised of a single species can consist of several clonal lineages and differ in their genotypes because of previously acquired mutations^{123–127}. The genetic diversity of populations of both hosts and parasites plays a key role in determining the spread and evolution of infectious diseases. The genetic diversity of host populations can limit the spread of pathogens^{128,129}. On the other hand, the genetic diversity of the parasite increases its adaptability to local hosts¹³⁰. Clonal competitions commonly take place in genetically diverse bacterial populations. However, it has also been shown that lineages of multi-clonal populations can mutually coexist instead of competing against each other^{131–133}.

The effect of population size and epistasis on the adaptive path of bacterial populations

Beneficial mutations that increase the host fitness must not necessarily fix in the population. Apart from the fitness effect of the mutation itself, the likelihood of individual mutations to be fixed first is affected by the population size, the genetic diversity of the population and its mutation rate^{134,135}. All these factors can drastically change after a population bottleneck, an event that is characterized by the sudden, drastic reduction of population size¹³⁶. Population bottlenecks are common in host-pathogen interactions and can strongly reduce the genetic diversity of the antagonist^{137,138}. Apart from the normal infection cycle of a pathogen^{139–142}, the bottleneck strength can be further increased by clinical treatment, as in case of antibiotic therapy¹⁴³.

The adaptive path of a population describes the order by which selected beneficial mutations fix in the host's genome over time. Population size does not solely determine the likelihood of an organism to adapt to a stressful environment. However, it does influence the degrees of directions that the adaptive path can take because the likelihood of individual mutations to occur becomes higher with increasing population size^{144–147}. It is therefore critical not to ignore the influence that population size likely has on the dynamics of resistance evolution. Evolutionary theory predicts that the fate of alleles is subjected to genetic drift more strongly in small populations^{94,148}. Thus, small populations are commonly less genetically

diverse. Consequently, adaptation is more likely to be shaped by selective sweeps and periodic selection rather than by the simultaneous occurrence and establishment of several fit genetic variants in the population, also known as the Hill–Robertson effect or clonal interference^{33,92,99,149}. Instead, clonal interference is rather expected when the population size is large enough and the selective pressure low enough to allow for the simultaneous occurrence and selection of several independent beneficial mutations in the ancestral genetic background¹⁵⁰. Therefore, clonal interference is more likely to shape the path of adaptation for large populations^{92,151–153}. Clonal interference between different beneficial alleles and their respective frequencies also affects the dynamics of less beneficial mutations due to strong linkage disequilibrium^{154,155}. Large populations have a higher chance of fixing the mutation that confers the highest immediate fitness advantage early than small populations because of their higher mutational load¹⁴⁴. In comparison, one would expect a larger diversity in first-step mutations when the population size is small¹⁴⁴.

The effect of a mutation on its host's fitness can greatly depend on the host's genetic background. Epistatic interactions between individual mutations occur when their combined fitness effect is not additive, which can add to the complexity of multi-clonal populations^{156–158}. Mutations that are beneficial in one lineage can be deleterious for other lineages of the population^{159–161}. Therefore, the adaptive path of the population can be constrained by the epistatic interactions of the first selected mutations with any secondary mutation^{162–164}. As effective population size also influences the chance of epistatic mutations to arise, the adaptive path would then also be less predictable for populations of small size than it would be for large populations^{156,159,160,165}.

The influence of population bottlenecks on fixation probabilities of mutations

Population bottlenecks have a strong influence on the genetic diversity of bacterial populations and consequently on their genome evolution. When the population size is reduced, the chance of individual alleles to rapidly change in frequency due to genetic drift is drastically increased^{166,167}. In turn, drift will reduce the genetic diversity of the population because one genotype with an increased chance to fix will cause other, less fit variants to be lost from the population¹⁶⁸. However, drift effects must not necessarily be entirely random, as the chance of an individual to survive a bottleneck event strongly depends on the fitness of its genotype in the environment^{142,169}. Naturally fitter variants will sustain their competitive advantage if the

population bottleneck is not too severe to trump natural selection. Persisters, tolerant or resistant variants have an increased chance to be fixed under stressful, selective conditions due to both drift and natural selection ¹⁷⁰. If beneficial mutations occur at high frequencies during the bottleneck, they also have a higher likelihood of further increasing in frequency due to drift ¹⁷¹. In contrast, genetic drift causes low-frequency mutations of small effect to be stochastically lost from the population ¹⁷².

Beneficial mutations are more likely to survive in bottlenecked populations than in large populations of constant size because the benefits of population growth outweigh the impact of the bottleneck on survival ^{173,174}. The overall fixation rate may be increased in bottlenecked populations compared to populations of constant size because of sustained periods of exponential growth between bottlenecks ¹⁷⁵. Thus, strong bottlenecks are more likely to maintain mutations of small or even deleterious effect in the population ¹⁷⁶. In contrast, wide bottlenecks are expected to maintain a higher rate of adaptation. Under selective conditions, adaptation of bacterial populations under clonal interference is driven by highly beneficial mutations ^{133,153,177}. As the probability of these mutations to occur is high under wide bottlenecks, the adaptive process is thus characterized by a high probability of parallel evolution ^{92,144,147}. In contrast, adaptive dynamics by clonal interference are less likely to be maintained under strong selective bottlenecks, which decreases the chance of parallel evolution ^{175,178}. Thus, population bottlenecks can take great influence on adaptive allele dynamics and interfere with the selective processes. Both beneficial and deleterious alleles can either be maintained or excluded from the population, depending on both bottleneck size and selective strength.

The influence of population bottlenecks on bacteria in natural populations

Bottleneck events frequently occur in nature and play a critical role in the evolutionary history of bacterial populations. The impact of environmental factors on the size and genetic composition of bacterial populations can take place at regular (e.g. seasonal change) or irregular (e.g. stochastic perturbation) intervals and therefore take a great influence on the adaptive path of the population ^{92,147,151,152,179–181}. Whenever the transfer of a subpopulation from an environmental reservoir to a previously uninhabited environmental patch (being it a biotic or abiotic environment) takes place, only a fraction of the population will be part of the transfer, let alone survive it. This initial stage of new colonization by a small number of individuals is described as the founder effect: The genetic architecture of the founding

population will restrain the adaptive steps that the population can take via mutations to improve its fitness in the new environment ^{182,183}.

For pathogens, every infection cycle within a new host is accompanied by a strong reduction of effective population size, as host immune systems typically select for the survival of only few cells ^{142,169}. Once a resistant phenotype has been selected, it is unlikely that another variant with a very similar phenotype will be acquired, as the selective pressure of the antibiotic decreases in the presence of an already acquired resistance gene ¹⁸⁴. Pathogens are subjected to severe, successive bottlenecks by the transmission from host to host, but environmental factors such as seasonality, resource limitation and disease can impose bottlenecks on any natural population ^{148,164,175–179}. However, bottlenecks do not only influence the evolutionary path of pathogens. The life history of all of a host's microbiome is also shaped by population bottlenecks ^{190,191}. Symbiotic and commensal bacteria can be transmitted to new hosts either vertically (from the environment) or horizontally (passed on by ancestors). Both routes are examples of strong population bottlenecks, as only a small number of bacteria are transferred from a larger population to become the founding colonizers of the new host ^{190,192}. After the first bacteria colonize the host colonization as founders of the native microbiome, the chance of secondary colonizing bacteria to establish themselves as new microbiome members is restricted by the fitness and frequency of the first colonizers ^{193–195}. While the transmission of commensals is often aided by the host, pathogens are subjected to a strong selection pressure by the host's immune system ^{193–195}.

The potential influence of population bottlenecks on bacteria in evolution experiments

The impact of population bottlenecks on resistance evolution has thus far been greatly overlooked ^{151,196}. Population bottlenecks are an intrinsic feature of any experimental protocol that includes serial transfer of a small fraction of the evolving population to sustain microbial populations for hundreds or thousands of generations ^{100,189}. A common bias in most experimental protocols has been the relative bottleneck size that bacteria undergo when being transferred to new culture medium after each growth period. Populations that already carry a beneficial mutation will show higher yield at the end of a growth period than populations in which beneficial mutations have not yet been established ^{151,196,197}. In a common evolution experiment, the same percentage of each population is transferred to the next growth period at the end of every transfer cycle. This means that the number of cells that start the next growth

period will be higher for that population that already fixed the beneficial mutation than for the population that does not carry the mutation. This potentially provides the population with the beneficial mutation an increased chance to acquire additional beneficial mutations even sooner. In contrast, if a beneficial mutation has not occurred before the transfer, a small surviving population will likely require longer to acquire a beneficial mutation and is instead at higher risk of going extinct¹¹³. Even though the relative bottleneck size (percentage of bacteria that are transferred) remains the same over the course of the experiment, the absolute bottleneck size (number of bacteria that are transferred) is variable¹⁸⁹. Thus, a population bottleneck can be severe in either a relative sense, an absolute sense, or both¹⁹⁸. When the absolute bottleneck size is extremely small, adaptation is most likely limited if not impossible^{175,178,189}. In an evolution experiment, the population size is usually at its peak immediately before the transfer⁹⁷. Since more mutations occur when the population size is large, most beneficial mutations occur at late times during a growth period and therefore are unlikely to persist in the population after the bottleneck¹⁷⁸. An about fivefold population growth between bottlenecks is predicted to optimize the occurrence and survival of beneficial mutations in serial passage experiments¹⁷⁴. However, bottlenecks that are more severe than this optimal prediction substantially reduce the occurrence and survival of adaptive mutations¹⁷⁴.

***Pseudomonas aeruginosa* & its role in cystic fibrosis**

The model organism used for this study is the bacterium *Pseudomonas aeruginosa* (PA). It is a ubiquitous Gram-negative gamma-proteobacterium that can inhabit a great variety of environments such as plants, soil, freshwater, seawater, sewage and various surfaces^{123,199}. It is a non-fermenter that can utilize a wide range of carbon and energy sources and produce numerous competitive molecules such as antibiotics, siderophores including pyocyanin and pyoverdine that give the bacterium its characteristic green color, and other virulence factors^{200,201}. It has a small cell size (typically 1-3 μm in length), is a strict aerobe, highly motile and grows optimally at 37 °C^{123,200}. It also is an effective biofilm former²⁰². Its genome is one of the largest among bacteria (5.5- to 7.0 Mbp) and includes a high number of regulatory genes as well as metabolic features that enable the adaptation to various ecological niches^{123,202–204}. PA is an opportunistic pathogen of mammals, insects and plants^{205,206}.

In humans, PA can infect a multitude of different organs and tissues. Immuno-compromised patients are especially susceptible to PA infections, making it one of the most relevant causes of nosocomial infections. It is particularly notorious for wound and burn infections as well as infections after implantation of organs and prostheses but can also play a significant role in airway and urinary tract infections ^{207–209}. PA contains a large natural resistome to cope with the selective pressure of different antibiotics classes, which is limiting treatment options to manage PA infections successfully ^{202,210}. In addition, PA can readily evolve resistance by genetic adaptation ²¹¹. Its genome contains a broad set of genes that encode for various multidrug efflux pumps and deleterious mutations in regulatory genes like efflux repressors rapidly lead to multidrug resistance ^{212,213}. Both chromosomal mutations and genes acquired by HGT play a critical role in the evolution of antibiotic resistance in PA, to different degrees, depending on the clonal variant ^{96,211}. Only in 2017, the World Health Organization listed carbapenem-resistant PA in the highest priority class of critical pathogenic bacteria for which new antibiotic treatments are urgently needed ²⁰⁹.

Due to its ubiquitous lifestyle and high adaptability, PA can also colonize the human lung and cause pneumonia ^{214,215}. PA lung infections are a common problem for patients suffering from cystic fibrosis (CF) ^{216,217}. CF is a hereditary disease that affects the normal function of sodium chloride channels in human epithelia. The disease is caused by a loss-of-function mutation in the Cystic Fibrosis Transmembrane Conductance Regulator (CFTR) gene on chromosome 7 ^{218,219}. CFTR is a transmembrane channel that controls the movement of chloride and bicarbonate ions into and out of epithelial cells ^{220,221}. Defects in CFTR lead to significantly decreased chloride secretion, increased sodium absorption, excessive movement of water into the airway epithelial cells, dehydration of the periciliary matrix and the secretion of highly viscous mucus ^{221,222}. In the lung, those hypoxic plugs formed by heavy mucus are a suitable environment for the growth of foreign bacteria that can cause severe inflammation, which in turn leads to progressive deterioration in lung function ^{223,224}. Bacterial infections are the primary cause of death in CF patients. A wide range of microorganisms is associated with pulmonary infections in CF ^{225,226}. In addition, the composition of the lung's microbiome changes over the course of a patient's lifetime ^{226–228}. For most CF patients, PA eventually becomes the most abundant pathogen over the course of a patient's lifetime ^{226–228}.

PA colonizes about 80% of all CF patients and causes chronic lung infections that eventually cause respiratory failure in most cases ^{229–231}. Phenotypic indicators of chronic

infections by PA are decreased motility, virulence and quorum sensing, and increased auxotrophy, antibiotic resistance and mucoidy²³². Generally, drug-resistant phenotypes with an increased ability to form biofilms have the highest ability to colonize the CF airway²³³. In addition, a large fraction of PA found in CF lungs displays a mucoid phenotype due to increased secretion of the exopolysaccharide alginate²³². Because of the increased risk of CF patients to become chronically infected by foreign bacteria, CF therapy revolves heavily around controlling for pulmonary infections with antibiotic treatment^{216,234}. However, there is no consensus on the best combinations, dosages, or the length of treatment courses²³⁵. Commonly applied antibiotics are ciprofloxacin, ceftazidime, meropenem, tobramycin, colistin or aztreonam²³⁶. Antibiotic treatments are commonly done at home by inhalation of single drugs for 1-4 weeks, depending on the patient's wellbeing^{237,238}. In addition to antibiotic therapy at home, patients occasionally receive 2-week courses of rehabilitative therapy that often include additional treatment with combinations of two or even more antibiotics^{239,240}. However, constantly being exposed to the selective pressure of antibiotic therapy also drives the adaptation of PA clones to the CF lung environment^{241,242}.

Objectives

Over the past decades, antibiotic resistance among nosocomial pathogenic bacteria has turned into a global health crisis. In order to reduce the spread of multidrug-resistant bacteria, new treatment strategies that make effective use of current and future antibiotics need to be developed. To identify effective treatment strategies, the complex evolutionary mechanisms by which antibiotic resistance evolves in bacterial populations need to be studied in a comprehensive way. Experimental evolution is a powerful tool to study how bacteria adapt to their environments over extended periods of generations. In the context of antibiotic resistance, experimental evolution has served as an important control to verify theoretical concepts about bacterial resistance evolution. However, the likely contribution of population biological factors like population size and genetic composition to antibiotic resistance evolution has remained severely understudied. The influence of population size on the outcome of evolution experiments has likely been underestimated if not even completely ignored in the design and discussion of most experimental results. The combined effect of population bottlenecks and selective strength on allele frequency dynamics has so far not been quantified. This information

is especially important for our understanding of antibiotic resistance evolution, because bottlenecks are ubiquitous in natural bacterial populations and influence adaptation of human pathogens during infection and transmission processes. Therefore, it is necessary to systematically investigate the impact of different population biological factors on the evolution of bacteria. The influence of bottleneck size on bacterial adaptation to antibiotic selection has been greatly under-estimated for both natural and *in vitro* experimental populations. In my thesis, I thus want to specifically address the influence of bottleneck size on antibiotic resistance evolution.

The main objective of my thesis is to quantify the influence of bottleneck strength on the rate of adaptation to the selective pressure of antibiotics. To tackle this challenge, I performed evolution experiments for which I manipulated the transfer size of the evolving populations in the presence of stable antibiotic concentrations. Instead of relative sampling fractions, I always transferred a defined number of cells from the population between two growth periods. In addition to different bottleneck sizes, varying levels of selective pressure were applied to bacterial populations by exposing them to different antibiotic concentrations. This allowed me to quantify the impact of population size on the evolution of resistance. Bacterial populations were frozen at different transfers and their DNA was isolated for Whole Genome Sequencing. By identifying resistance mutations and the distribution of their respective frequencies over the course of the evolution experiment, their rate of adaptation can be determined on the genetic level. Theory predicts that the bottleneck strength affects the genetic diversity of the population depending on the environmental conditions. Thus, the adaptational process is expected to differ between the treatment regimens, with the treatment of the widest bottleneck and the highest inhibitory concentration expected to provoke the evolution of the highest resistance.

In addition, the experiments could help to investigate the impact of population composition and genetic diversity on resistance evolution, as population diversification will likely be influenced to different degrees in the individual treatment groups. Strong bottleneck treatments are expected to produce the highest diversity between different replicate populations and wide bottleneck treatments are expected to produce the highest diversity within different populations.

The following hypotheses are tested:

H_{1,1}: Wide rather than small bottleneck size reduces treatment efficacy in terms of strength and speed of resistance evolution.

H_{1,2}: High rather than low antibiotic selection strength reduces treatment efficacy in terms of strength and speed of resistance evolution.

H_{1,3}: Small rather than wide bottleneck size increases variation in accumulation of selectively favored mutations.

H_{1,4}: High rather than low antibiotic selection strength increases parallel evolution.

Approach

The model system for my experimental approach was the bacterium *Pseudomonas aeruginosa* subclone PA14 and a selection of antibiotics that specifically inhibit its growth by different mechanisms. PA is a facultative human pathogen with great intrinsic capacity to evolve resistance against any clinically relevant antibiotic. It has been established as a model organism for infection biology and its mechanisms of resistance evolution are well-studied. The antibiotics used in this thesis provide selective pressure with distinct modes of action. Carbenicillin is a penicillin targets the bacterial cell wall synthesis. Ciprofloxacin is a fluoroquinolone that inhibits the DNA gyrase. Gentamicin is an aminoglycoside that inhibits the 30S subunit of the bacterial ribosome. Colistin is a peptide that disrupts the bacterial outer membrane.

The general setup of the evolution experiments was based on previously published experimental studies from our lab^{80,83,117,243,244}. They were carried out in 96-well plates with a sample volume of 100 µl per culture. By reducing both the culture volume and the space to operate on, experiments could be performed in a semi-high-throughput manner. The experiments encompassed serial transfers of distinct cell numbers of bacterial populations after growth periods of > 9 hours. The bacteria were challenged against different concentrations of antibiotics to identify how populations adapt under different levels of selective strength. In addition, bacterial populations not challenged with antibiotics were run as controls for uninhibited growth and media adaptation under different bottleneck sizes. For each plate, six

wells were neither inoculated with bacteria nor with antibiotics to serve as controls for systematic contamination of the experimental setup. I propagated the evolving bacterial populations for a total of 15 growth periods, encompassing ~ 100 generations for the uninhibited control populations.

I introduced a new method to the experimental setup that ensured the maintenance of the same bottleneck size throughout the evolution experiment. In order to maintain a steady number of cells to be transferred between two growth periods, it was critical to quantify the actual cell concentration and subsequently calculate the transfer volume necessary to transfer the desired number of cells. I achieved this goal by counting the cells in subsamples of every replicate population with a flow cytometer before transferring the appropriate cell number to the next growth period. Cell counting of an entire 96-well plate was accomplished within < 2 hours and is much more precise than counting cells in a counting chamber. A small sample from each population was quantified in the flow cytometer from which the density of the main population was then extrapolated. Based on the approximated cell concentration, I could calculate the necessary resuspension volumes and applied them to the cultures to adjust the cell concentration before passaging to the next growth period.

In addition, it was crucial to avoid dilution effects when transferring different culture volumes from one experimental plate to the next. If different bacteria cultures grow at dissimilar rates, the transfer of the same volume will subsequently result in different nutrient availability for the next growth period. For example, in stationary phase, all nutrients in the medium have been consumed. In mid-exponential phase, only ~ 50% of the nutrients have been consumed. This potential “starvation effect” would develop into a systematic error over the course of the evolution experiment because the potential influence of different nutrient supply on the adaptive process will remain incomprehensible. Thus, it was essential to replace the old medium with fresh growth medium before performing the transfer. I solved this issue by separating the cells from the old medium after each growth period via centrifugation and subsequently resuspending the cell pellets in fresh medium before performing the transfer.

To approach the objectives, I ran different sets of evolution experiments. Three different bottleneck sizes of PA14 cultures (50,000; 500,000 and 5,000,000 cells) were challenged against four different inhibitory concentrations (IC0, IC20, IC50 and IC80) of four antibiotics (carbenicillin, ciprofloxacin, colistin and gentamicin) that inhibit yield of PA14 after 12 hours of growth by 0%, 20%, 50% or 80%. For each experiment, only a single antibiotic was used.

After the experiments, bacteria were frozen and later revived for phenotypic and genetic testing. The resistance of the evolved populations against the treatment drug was measured with standardized dose response curves. In addition, I obtained growth characteristics of the evolved populations in drug-free medium. I extracted DNA from the populations of the last growth period and WGS was performed to identify adaptive mutations. Subsequently, populations from intermediate time points of the experiments were also sequenced to uncover the presence, absence and proportion of beneficial mutations at the respective time points of the experiment and to identify additional beneficial alleles. This allowed me to trace the history of beneficial mutations within the populations over the course of the experiments and to evaluate the degree of parallel evolution among the replicate populations. Furthermore, I performed competition experiments with defined mutants from the experiment to validate the mutation's adaptive benefit under different bottleneck sizes and selective pressures. Thus, I could study the impact of serial bottlenecks on the rate of antibiotic resistance evolution in a detailed and comprehensive manner.

Material and Methods

Material

Laboratory devices

-20 °C freezer	AEV-TS; Thermo Fisher Scientific Inc., USA
-80 °C freezer	HFU 400TV; Thermo Fisher Scientific Inc., USA
Autoclave	Laboklav 135MSL-FA; SHP Steriltechnik AG, Germany
Centrifuge	Centrifuge 5810 R; Eppendorf AG, Germany
Clean bench	Biowizard Silver SL-200 Class II; Kojair Tech Oy, Finland
Flow cytometer	Guava EasyCyte HT Blue-Green; Merck KGaA, Germany
Fridge	AEV-TS; Thermo Fisher Scientific Inc., USA
Fume hood	Abzug NA 1500 EN; Lamed Vertriebs-GmbH, Germany
Gel photo documentation	ChemiDoc Touch; Bio-Rad Laboratories Inc., USA
Microplate shakers	Titramax 100, 1mm orbital; Heidolph Instruments, Germany
Multi-channel pipettes	Xplorer Plus; Eppendorf AG, Germany
PCR cycler	Labcycler; SensoQuest GmbH, Germany
pH meter	HI 221; Hanna Instruments Deutschland GmbH, Germany
Plate readers	Infinite M200Pro Nanoquant; Tecan Group, Switzerland
Serological pipette	Easypet 3; Eppendorf AG, Germany
Shaking incubators	Thermomixer Comfort; Eppendorf AG, Germany Titramax 1000; Heidolph Instruments GmbH & Co. KG
Single-channel pipettes	US-Patent No. 5,531,131; Eppendorf AG, Germany

Spectrophotometer	Jenway 6300 ViS; Cole-Parmer Instrument Company LLC, USA
Standing incubator	Heraeus B12; Thermo Fisher Scientific Inc., USA
Vortexer	Lab dancer; IKA-Werke GmbH & CO. KG, Germany

Consumables

96-well plates	Greiner Bio-One, Germany; Ref. 655161
Buffer Chemicals	Carl Roth GmbH; Germany
Centrifugal filters	Merck Millipore, USA; Ref. UFC505096
Culture vessels	Sarstedt, Germany; Ref. 62.547.004
Membrane filter	Sarstedt, Germany; Ref. 83.1826.001
Microtubes	Eppendorf AG, Germany; Ref. 0030120094
PCR plates	Sarstedt, Germany; Ref. 72.1978.202
Petri dish	Sarstedt, Germany; Ref. 82.1473.001
Pipette tips	Sarstedt, Germany; Ref. 70.765.100
Plate sealing foil	Sarstedt, Germany; Ref. 95.1994
Sealing film	Parafilm M (PM-996); Bemis Company Inc., USA
Serological pipettes	Sarstedt, Germany; Ref. 86.1254.001/ 86.1256.001/ 86.1685.001

Media and buffers

Bacteria were grown in sterile M9 minimal medium, consisting of 7 g/l K₂HPO₄, 2 g/l KH₂PO₄, 0.588 g/l trisodium citrate, 1 g/l (NH₄)₂SO₄, 0.1 g/l MgSO₄ and supplemented with 0.2% glucose and casamino acids.

For long-time storage, bacterial cultures were supplemented with 30% glycerol before freezing at -80 °C.

For cultivation of bacteria on solid surfaces, M9 medium was supplemented with 15 g/l of agar-agar before autoclaving to generate M9 agar.

Phosphate-buffered saline (PBS) - consisting of 0.2 g/l KCl, 8 g/l NaCl, 1.42 g/l Na₂HPO₄ and 0.24 g/l KH₂PO₄ - was used as a dilution buffer for the cell counting in the flow cytometer to prevent both cell growth and cell lysis during the measurements in the flow cytometer. 1.9 mM propidium iodide in water was used as a staining solution to identify dead cells during flow cytometry.

CTAB buffer was used for the extraction of DNA from the evolved and ancestral PA14 strains. The buffer consists of 2% CTAB (cetyl-trimethyl-ammonium-bromide), 0.1 M Tris-HCL, 0.02 M EDTA, 1.4 M NaCl. After autoclaving, 0.2% β-mercaptoethanol is added to the solution.

Kits

The GeneJET Gel Extraction Kit (Ref. K0691) by Thermo Fisher Scientific Inc., USA was used to purify DNA solutions from agarose gel extracts.

Antibiotics

The antibiotics used for this thesis are bactericidal antibiotics that are specifically used for the treatment of infections caused by *Pseudomonas aeruginosa* and other Gram-negative bacteria. They represent four of the major classes of bactericidal antibiotics (β-lactam antibiotics, fluoroquinolones, polypeptides and aminoglycosides).

Carbenicillin (CAR) is a member of the carboxypenicillin subgroup of the penicillins (beta-lactam ABs). It targets the bacterial cell wall synthesis by inhibiting DD-transpeptidase. It has been discontinued for clinical application in favor of ticarcillin²⁴⁵. It had previously been applied for the intravenous treatment of urinary tract infections because of its broad spectrum

against Gram-negative pathogens ²⁴⁵. However, it is inactive against Gram-positive bacteria and susceptible to degradation by beta-lactamases.

Ciprofloxacin (CIP) is a fluoroquinolone that inhibits the ligase activity of the type II topoisomerases, gyrase and topoisomerase IV which causes DNA with single and double-strand breaks that ultimately leads to cell death ²⁴⁶. Because of its broad-spectrum activity against both Gram-positive and –negative species and its various possible routes of administration (oral, topical, intravenous), it is one of the most widely used antibiotics in clinics worldwide ²⁴⁶. Side effects include tendinitis, nervous system defects & diarrhea.

Gentamicin (GEN) is an aminoglycoside that inhibits protein synthesis by binding to the 30S subunit of the bacterial ribosome. It is used for the treatment of respiratory tract infections, urinary tract infections, blood, bone and soft tissue infections ²⁴⁷. GEN treatments can cause neuropathy, kidney damage as well as inner ear problems ²⁴⁸. Nowadays, it is mostly used as a last-resort antibiotic for the treatment of resistant Gram-negative pathogens because of its severe side effects.

Colistin (COL), aka polymyxin E, is a polycationic peptide that disrupts the bacterial outer membrane by displacing magnesium and calcium ions in the lipopolysaccharide ²⁴⁹. Despite the recent spread of plasmid-borne mcr-1-conferred resistance, clinical resistance against colistin is still rarely observed ²⁵⁰. It is thus considered one of the most valuable last-resort antibiotics against multidrug resistant *Pseudomonas aeruginosa*, *Klebsiella pneumoniae*, and *Acinetobacter baumannii* ²⁴⁹. Common side effects include both nephro- and neuro-toxicity.

Table 2: Antibiotics used in this thesis.

Name	Abbr.	Antibiotic class	Distributor	MIC	IC80	IC20
Carbenicillin disodium salt	CAR	β -lactam antibiotic (Penicillins)	Roth Ref. 6344.2	35 μ g/ml	40 μ g/ml	18 μ g/ml
Ciprofloxacin	CIP	Fluoroquinolone	Sigma-Aldrich Ref. 17850-5G-F	60 ng/ml	40 ng/ml	15 ng/ml
Colistin sulfate salt	COL	Polypeptide	Sigma-Aldrich Ref. C4461-100MG	10 μ g/ml	6.5 μ g/ml	2.5 μ g/ml
Gentamicin	GEN	Aminoglycoside	Roth; Ref. HN09.1	600 ng/ml	510 ng/ml	380 ng/ml

Bacterial strains

The *Pseudomonas aeruginosa* strain UCBPP-PA14 (from here on referred to as either ‘PA14’ or as ‘Wt’ to distinguish it from experimentally evolved clones) has been chosen as the ancestral strain for my evolution experiments. PA14 is a clinically isolated strain of *Pseudomonas aeruginosa* that shows a particularly high virulence towards animal hosts in comparison to the common PA reference strain PAO1²⁵¹. Its genome has been fully sequenced and annotated²⁵². PA14 is the most common clonal group of *Pseudomonas aeruginosa* worldwide²⁵³. In the last couple of years, it has been established as a model organism for a broad set of experimental evolution studies^{254–257}. Pipelines for comparative genomics had previously been developed for the computer cluster of the lab and well-studied data of the model system has been published by other lab members over the last decade^{80,83,117,243,244}.

Additional evolved clones were selected for comparative experiments after the evolution experiments were run and identification of mutations by population genomic analyses was completed. The clones carry single point mutations (either a single nucleotide polymorphism (SNP) or a 1-base pair deletion) in either the gene *pmrB* or *ptsP*.

Table 3: Evolved clones used in competition experiments.

Mutated gene	Population	Clonality	Position of SNV in gene	Position in genome
<i>pmrB</i>	D12	mono	G239A	5636922
	A5	bi	G239A	5636922
	A6	bi	T521A	5637204
<i>ptsP</i>	A12	mono	Δ274	393042
	B11	mono	C1955T	394724
	E7	bi	C1480T	394249

Software

Table 4: Software used in this thesis.

Program	Developers / Main authors
Burrows-Wheeler Aligner ²⁵⁸	Sanger Institute
FastQC ²⁵⁹	Babraham Institute
FreeBayes ²⁶⁰	Erik Garrison
GIMP 2	The GIMP Development Team
guavaSoft	Merck-Millipore
GrowthRates ²⁶¹	Barry G Hall
i-control	Tecan
Inkscape	Inkscape Community
Integrative Genomics Viewer ²⁶²	Broad Institute
Mendeley	Mendeley Ltd.
Microsoft Office	Microsoft Corporation
PinDel ²⁶³	Kai Ye
PuTTY	Simon Tatham
R, RStudio and R packages ^{264,265}	R Core Team
SAMtools ²⁶⁶	Sanger Institute
Trimmomatic 0.39 ²⁶⁷	Bjoern Usadel
UGENE ²⁶⁸	Unipro
VarScan ²⁶⁹	Dan Koboldt
WinSCP	Martin Příkryl

Methods

Bacteria culturing

Frozen stocks of bacteria cultures were maintained at -80 °C. For experimental work, bacteria were reactivated by isolating clones from frozen cultures on M9 agar plates. The bacteria were streaked out and incubated at 37 °C for 12-16 hours. Single colonies were freshly picked with a sterile loop as inoculums to start liquid cultures of any given population. After inoculation of 5 ml M9 liquid medium, the culture vessels were incubated at 37 °C for approximately 6 hours at constant shaking (150 rpm) to achieve mid-exponential growth phase. The OD of the culture was measured in a spectrophotometer at 600 nm wavelength. A final OD of 0.1 was set to ensure an initial population size of 10^4 - 10^5 CFU/ml. If necessary, the OD was adjusted by adding sterile M9 medium. The adjusted cultures were subsequently used as inoculums for experimental work.

To prepare new stocks of PA14 or any other bacteria, single colonies were transferred to 5 ml M9 liquid medium and incubated for 16-24 hours at 37 °C and constant shaking to achieve exponential phase cultures. 1 ml of culture was then mixed with 600 µl 80 % glycerol in a cryogenic tube and subsequently stored at -80 °C for extended periods of time.

Flow cytometry

A Guava easyCyte flow cytometer was used to assess cell counts of bacterial cultures. In a flow cytometer, a sample consisting of a cell suspension is carried by sheath fluid into a flow cell where the cells are aligned single file. The cells then pass a laser light source at a given flow rate. The light deflection caused by the cells is detected by an analogue-to-digital conversion system. The detectors measure both forward scattered light (FSC) as a measure of cell size and side scattered light (SSC) as a measure of the cell granularity. Additional detectors measure fluorescence emitted by the cells that are passing the laser beam. By setting size thresholds for the individual detections, cells can be distinguished from particle noise. For flow cytometry of *Pseudomonas aeruginosa* cultures, cells were suspended at an appropriate concentration (< 2000 cells/µl) in PBS and injected into the flow cytometer instrument. This ensures that one cell at a time passes the laser light source. First, 4 µl of each culture were diluted in PBS at a ratio of 1:25, supplemented with 50 µl of propidium iodide to stain dead cells. After a second dilution step in PBS for a final dilution of $1:10^3$, the plate was read in the

flow cytometer. The machine parameters were set to measure the diluted culture at a flow rate of 0.236 $\mu\text{l/s}$ for either 30 seconds or until a total cell count of 5000 cells per sample was reached. The total number of cells in the population was calculated for each culture by correcting the cell concentration for the number of dead cells, sampling volume and dilution factor.

Dose-response curves and IC determinations

Dose-response Curves (DRCs) describe the effect that differing concentrations of a substance have on a set viability parameter of an organism after a certain time of exposure. Obtaining DRCs is a common procedure to determine the inhibitory effect that an antibiotic has on bacteria. Inhibitory concentrations (ICs) are named depending on the degree of inhibition that the respective drug concentration has on the growth of a bacterium in comparison to its uninhibited growth. For example, the IC₅₀ is the drug concentration for which the growth of the bacterium is inhibited by 50% in comparison to the growth in complete absence of the antibiotic. The minimal inhibitory concentration (MIC) is the lowest concentration for which the growth is inhibited by 100% or, put differently, the lowest IC₁₀₀. In order to obtain a DRC, broth microdilution tests were performed.

Ten different concentrations of the antibiotic in question were prepared as 10X stock solutions in M9 medium and added in 1:10 ratios onto a 96-well plate in a fully randomized design. For each plate, 8 wells were run as technical replicates for the same concentration, along with 8 wells for a no-drug control and 8 wells for which neither the drug nor the bacteria are added (from here on referred to as empty wells or 'E'). The latter wells served as a control for systematic contamination of the setup. The no-drug control wells served as a reference for the uninhibited growth. Single colonies of bacteria were transferred from an overnight agar culture to 6 ml M9 medium in a 50 ml falcon tube and grown for ~ 6 hours (h) at 37 °C and constant shaking (orbital, 150 rpm). The bacteria were then diluted to reach an OD of about 0.1 at 600 nm to ensure an initial population size of approximately 10^4 - 10^5 CFU/ml. The diluted culture was then transferred onto the freshly prepared 96-well plate by adding an appropriate volume of the culture to each well (except for the 'E' control wells), adding up to a total volume of 100 μl for every well. Inoculum volumes differed for the desired inoculum sizes of 50 000 (k50), 500 000 (k500) and 5 000 000 (M5) cells. M9-medium, antibiotic and bacteria culture were added in the following manner:

1. M9: 100 μ l to 'E' wells, 89.5 μ l to k50 wells, 85 μ l for k500 wells, 40 μ l to M5 wells and additional 10 μ l M9 to every IC0 well
2. Antibiotic: 10 μ l of each antibiotic concentration (10x stocks)
3. Bacteria culture ($OD \approx 0.1$): 50 μ l for M5, 5 μ l for k500, 0.5 μ l for k50

The plates were then sealed with sterile adhesive foil and incubated for 12 hours at 37 °C under constant shaking (double-orbital, 900 rpm) in the Tecan plate readers. Kinetic OD reads were performed at 600 nm of the entire 96-well plate at 15-minute intervals. The relative inhibition of growth after 12 hours of incubation can be determined for each drug by comparing the optical density (OD) of all replicates of the last OD read against that of the no-drug control wells.

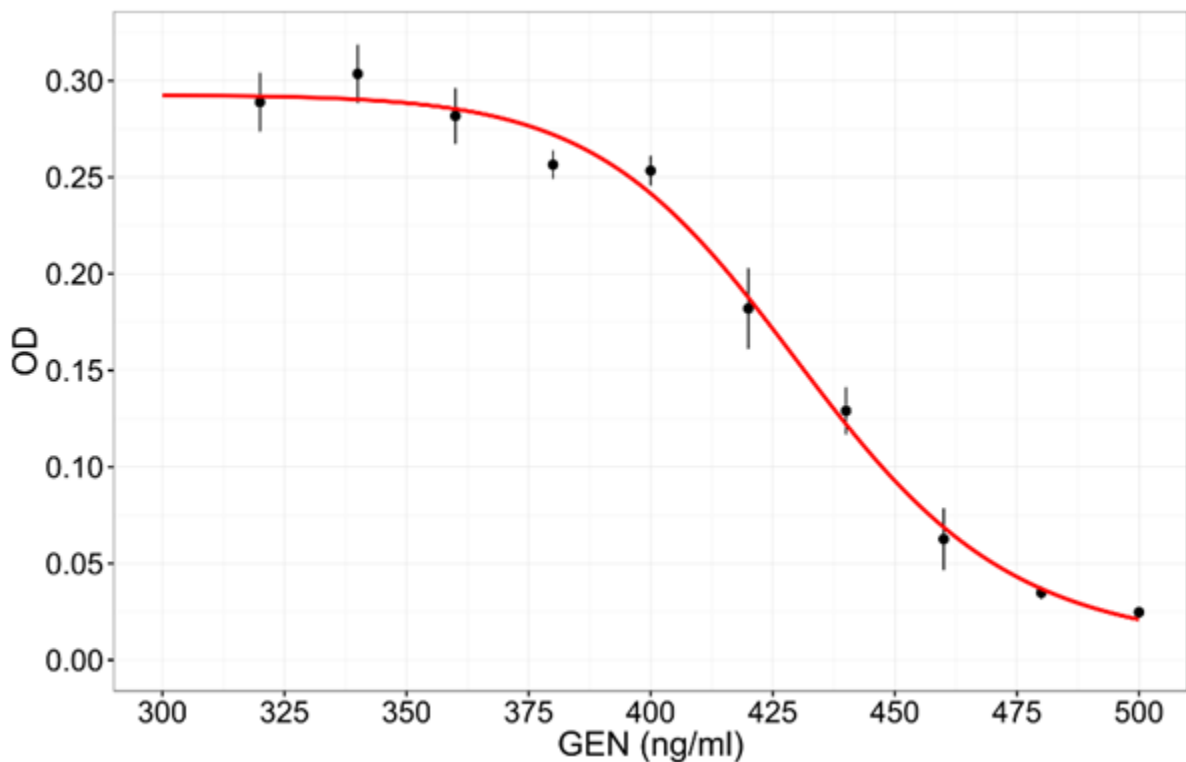


Figure 2: Example of a dose-response curve (DRC). The concentration of the antibiotic (in this case GEN) is given on the X-axis. The optical density (OD) after 12 hours of incubation is given on the Y-axis. Black dots represent the means of the obtained OD measurements at the respective concentrations. Error bars represent the standard error of the mean (8 replicates). The red line represents the model curve calculated in accordance with the obtained measurement results.

The lowest antibiotic concentration for which no visible growth was optically measurable was accepted as the drug's MIC. Experiments were performed until the below-MIC concentration range was uncovered and the desired ICs for the evolution experiments could be reliably identified. The 'drc' package for R was used to calculate a model curve of the dose-response effect based on the real obtained measurements.

Growth curves and inferred fitness parameters

The continuous OD measurements of cultures grown in the plate readers were used to construct growth curves and to infer fitness parameters. The obtained parameters can be used to evaluate fitness consequences of acquired mutations. For each individual replicate population, the change of the parameters can be monitored in relation to the fitness of the ancestral PA14 under the respective treatment conditions. The following fitness parameters were drawn from the growth kinetics of the populations:

- o Total yield: The total number of cells in the population by the end of the growth phase. It relates to the amount of replication events that have occurred during the period.
- o Maximum growth rate: The largest increase in OD over a few successive time points during exponential growth phase. It describes how quickly bacteria reach their optimal yield under the respective environmental conditions and, therefore, is a good measure of how well the bacteria are adapted to their specific environment.
- o Length of lag phase: The amount of time that surpasses until the bacteria enter their exponential growth phase. It describes how well bacteria can utilize the given nutrients and, therefore, is another indicator of how well they are adapted to their respective environment.
- o Area under the curve (AUC): This measure of average response during the growth period multiplied by the length of the growth period can be viewed as a summary of the cumulative response of the bacteria to the drug treatment over the observed time and is an often used factor to describe drug efficacy.

Maximum growth rate and length of lag phase were calculated with the software GrowthRates v2.1. The AUC was calculated with the cAUC function of the R package 'growthcurver'.

Instead of final OD as a prior for total yield, the flow cytometry results were used to infer change in population size.

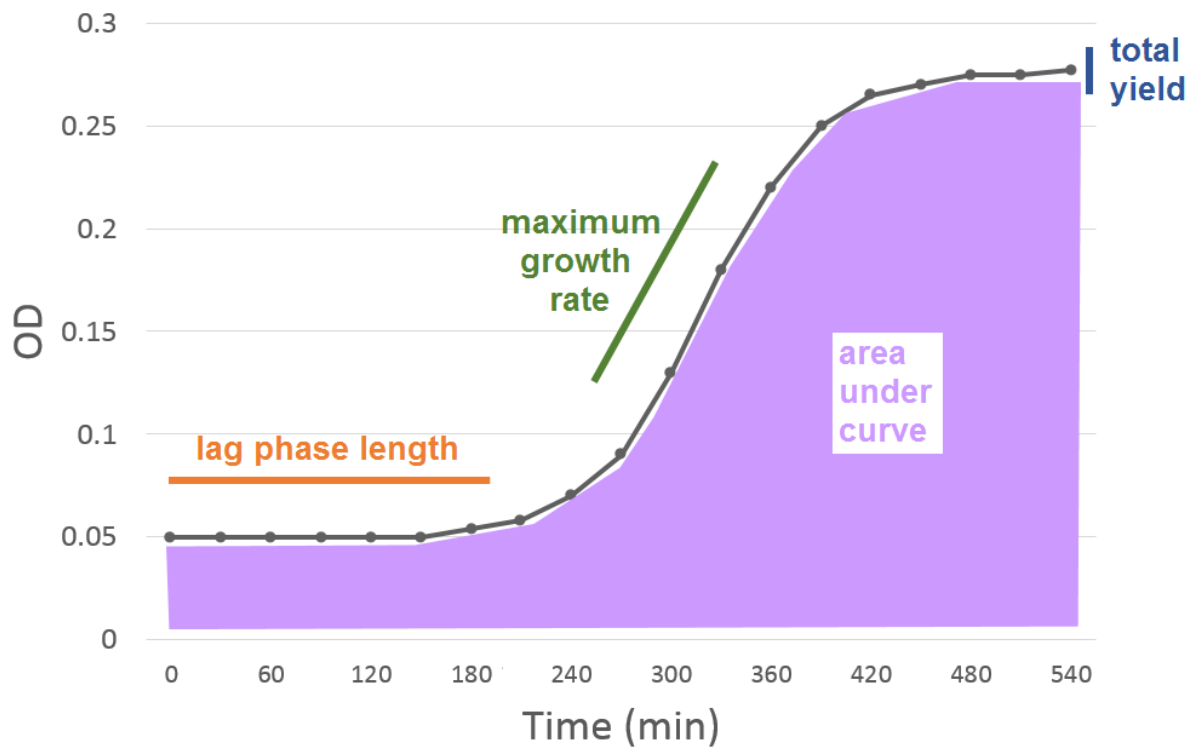


Figure 3: Example of a growth curve. The X-axis represents time in minutes. The Y-axis represents optical density. Black dots represent OD measurements at the respective time points and the black line represents the change in OD between two time points. Growth parameters are annotated in different colors.

Design and general setup of evolution experiments

The setup of the evolution experiment is summarized in Figure 5. The general prerequisites for the experiments were the transfer of a distinct number of cells from one growth period to the next and the removal of old growth medium and replacement with fresh growth medium before the transfer. The cultures were centrifuged after every growth period to discard the old medium with minimal loss of cells. The cell pellets were then resuspended in fresh medium. The cell concentration of each well was quantified by measuring the cell number in subsamples of the cultures in a flow cytometer and the volume that was needed to be transferred from the old plate to the new was extrapolated to achieve the distinct cell number for the next growth period.

Liquid cultures of PA14 were prepared as described before to obtain a culture with an OD_{600} of 0.1 and a concentration of $\sim 10^5$ to 10^6 cells/ μl . 4 μl of the culture were then diluted at a ratio of 1:1000 in PBS. Cells were counted in a Guava easyCyte flow cytometer and volumes were calculated that are needed to achieve a total of 50 000, 500 000, 5 000 000 cells, respectively. A 96-well flat bottom plate was prepared, using a systematic randomization of treatments as shown in Figure 4. Three different antibiotic concentrations (IC20, IC50 and IC80) were applied to every starting population size and seven replicates were run per treatment group. The calculated volumes of the PA14 culture were then transferred to the respective wells on the plate, with a total volume of 100 μl for each well. The plate was sealed with transparent foil and incubated in a plate reader at 37 °C under constant shaking (double-orbital, 900 rpm). OD measurements of each culture were taken at 600 nm wavelength every 15 minutes.

After 9.5 hours of incubation, the 96-well plate was taken out of the plate reader. 4 μl were removed from each culture and diluted 1:1000 in PBS in two dilution steps on separate 96-well plates. The dilutes were subsequently counted in a flow cytometer as previously described. Meanwhile, the 96-well plate with the original cultures was centrifuged at 5000 rpm for 90 minutes. The supernatant was discarded and replaced with fresh M9 medium. The resuspension volumes of fresh M9 were calculated individually based on the flow cytometry results. Resuspension volumes were set to achieve a concentration of 5×10^5 cells/ μl per culture. The plate for the next growth period was prepared accordingly (100 μl per well minus the calculated transfer volume) and the respective volumes were then transferred to the new plate: 0.1 μl for 50 000 cells, 1 μl for 500 000 cells and 10 μl for 5 000 000 cells. The freshly inoculated plate was then sealed and again incubated in the plate reader for 9.5 hours at 37 °C with continuous shaking and regular plate reading as described above. This protocol was continued for a total of 15 transfers. Bacteria from the evolution experiments were frozen at every second transfer by adding 30% glycerol to the culture wells after transfers to the next growth period had been performed. The plates were then frozen at -80 °C.

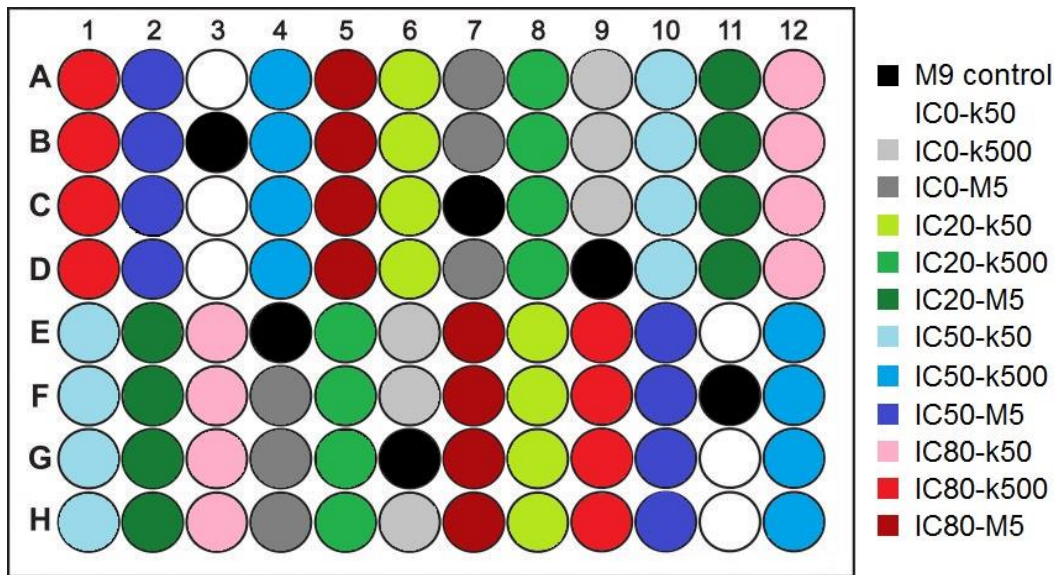


Figure 4: Layout design of a 96-well plate for an evolution experiment. Colored wells refer to the annotated treatment groups. White and grey wells refer to cultures in antibiotic-free medium (controls for uninhibited growth). Black wells refer to wells with only growth medium and neither bacteria nor antibiotics present (controls for contamination of the setup). Treatments were systematically randomized across the plate. Replicates of the same group are distributed in groups of three or four across the plate, thereby reducing the likelihood of pipetting mistakes.

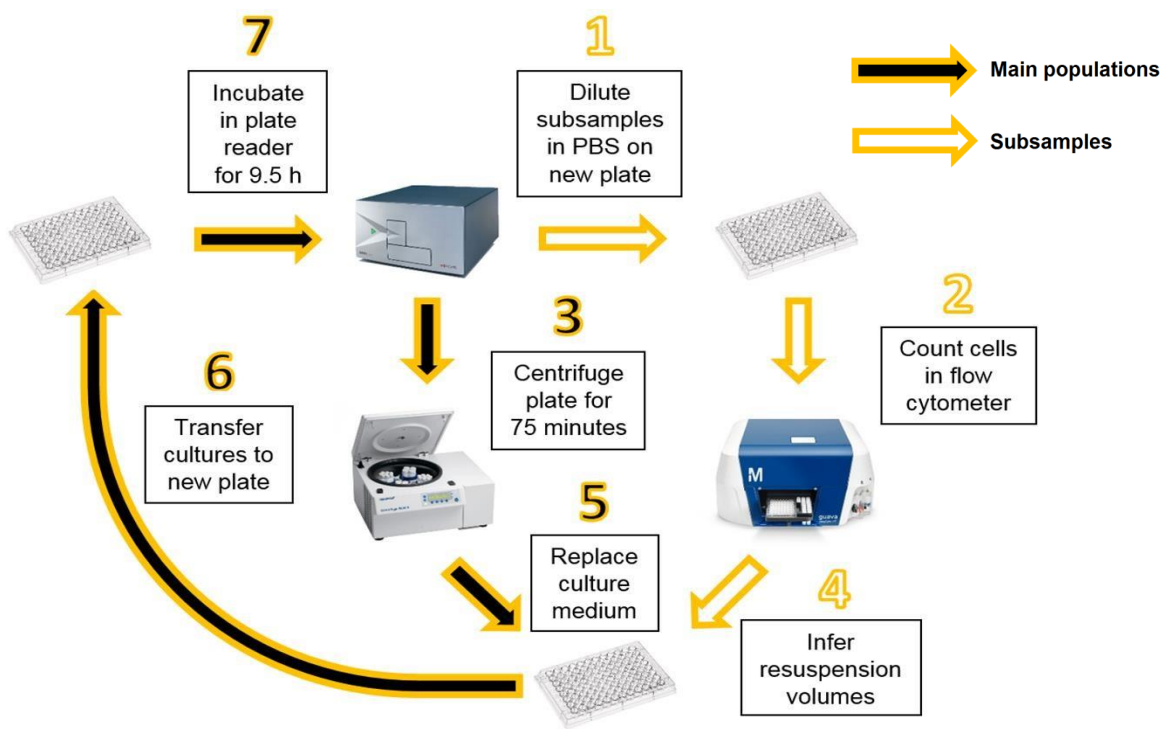


Figure 5: Design of the general experimental setup. Numbers mark the succession of steps taken in the protocol. Text in the boxes next to the numbers describe the experimental step. Arrows with black fill describe steps that are taken for the original experimental cultures. Arrows with white fill describe steps that are taken for subsamples of the experimental cultures. The annotated steps are repeated for a total of 15 growth periods.

Resistance and fitness assays of evolved populations

To investigate the resistance that evolved over the course of the evolution experiment as well as the change in fitness properties, populations of the last transfer period were challenged against different levels of antibiotic concentrations of the treatment drug. By exposing the evolved populations to a set of antibiotic concentrations after evolution has taken place, the change in relative resistance can be obtained and the effect of the population size on evolvability to different levels of resistance could be evaluated. The resistance tests were carried out as described for the dose-response curves. However, all cultures were standardized to the same population size of 500 000 cells (5 μ l inoculum). The antibiotic concentrations used for the test are distinct inhibitory concentrations below (IC₅₀, IC₈₀) and above the MIC (2xMIC, 4xMIC, 8xMIC and 16xMIC) of the ancestral population. In addition, the endpoint populations were also grown in drug-free M9 medium after the experiment. The cost of resistance can be reliably determined by comparing the previously described fitness parameters of the endpoint populations of each drug treatment to those of the uninhibited controls.

DNA isolation

DNA was isolated from populations of the experimentally evolved lineages from selected transfers as well as the original starting culture that was used as the starting inoculum of the experiment. The DNA was used for whole genome sequencing (WGS) to identify mutations that are under positive selection and likely drive the adaptation to the selective environment. 50 to 100 μ l of frozen cultures were transferred to 2 ml M9 medium and grown overnight at 37 °C and constant shaking. The CTAB buffer was used for DNA extraction. 2 ml of the overnight culture was transferred to a 2 ml Eppendorf tube. The tubes were centrifuged for 5 minutes at 13,000 rpm and the supernatant was subsequently discarded. 400 μ l CTAB buffer and 2 μ l proteinase K (20 mg/ml) were added to the bacteria pellet. The suspension was homogenized by mild vortexing and incubated overnight at 50 °C and 850 rpm. The next morning, 20 μ l RNase A (20 mg/ml) were added to the suspension, which was then vortexed and incubated for 30 minutes at room temperature. 800 μ l of a chloroform:isoamylalcohol (24:1) mix were added and the suspension was vortexed until the liquid was homogenous. After centrifugation for 5 minutes at 13,000 rpm, 300 μ l of the top phase was transferred into a new 1.5 ml Eppendorf tube and 200 μ l of ice-cold 100 % isopropanol was added. The suspension

was mixed by inverting and incubated at 4 °C for at least 60 minutes to precipitate the DNA. Samples were centrifuged for 30 minutes at 13.000 rpm. The supernatant was subsequently discarded, and the DNA pellet was washed in 1 ml 70 % ethanol and afterwards centrifuged for 1 minute at 13.000 rpm. After discarding the supernatant, the DNA pellet was airdried at 50 °C for 10 minutes and subsequently resuspended in 100 µl TE buffer. In some instances, the isolated DNA was concentrated further with the help of Amicon Ultra centrifugal filters.

DNA sequencing and genomics

Initially, DNA was only extracted from transfers 3 and 15. The DNA samples were stored at -20 °C and later sent to the sequencing facility at the Institute of Clinical Molecular Biology at the Kiel University Hospital for WGS. 25 µl with a DNA concentration of 20 µg/µl were submitted for library preparation. Sequencing libraries were built with the Nextera DNA Flex library preparation kit and sequencing was performed on the Illumina HiSeq 4000 platform using the Illumina paired-end technology with insert sizes of 150 bp and an average base coverage of >100²⁷⁰. In addition, DNA was also extracted from transfers 5, 7, 9, 11 and 13. Libraries were constructed with Nextera DNA library kit and sequenced on the Illumina NextSeq platform at the MPI for Evolutionary Biology in Plön/Germany with insert sizes of 150 bp and an average base coverage of >40.

Sequence reads of the WGS project were provided in the fastq format²⁷¹. Quality and quantity of reads were checked with FastQC²⁵⁹. The software trimmomatic was used to remove sequencing adapters from the Nextera library and to filter out low quality reads²⁶⁷. High quality reads were mapped to the UCBPP_PA14 reference genome with the software bwa^{252,258}. The generated .bam files were scanned for SNPs, insertions and deletions by using the variant calling programs FreeBayes, PinDel and VarScan^{263,269,272}. The resulting output files were filtered for duplicates, ancestral variants, and variants found in the evolved controls in R and subsequently double-checked by visually inspecting the called genome position provided by the .bam file in the IGV genome browser²⁶². Annotation of the detected alleles was done with the help of SnpEff²⁷³ as well as the *Pseudomonas* database (available at <http://pseudomonas.com>).

PCR for Sanger sequencing

To identify individual clones within multiclonal populations, it is necessary to identify the specific SNPs of the selected clones. Therefore, the regions of interest were amplified by PCR and sequenced by Sanger sequencing for a set of clones. Sanger sequencing is based on the selective incorporation of chain-terminating dideoxynucleotides by DNA polymerase during *in vitro* DNA replication^{274,275}.

DNA was extracted by boiling two to three colonies of individual clones in 20 μ l nuclease-free water for 15 minutes. 1 μ l of the supernatant was added to the PCR mix (Table 5). The PCR was performed for 30 cycles (Table 6), with hybridization at 60 °C and an elongation time according to the length of the amplified region. A gel electrophoresis was performed to verify correct amplification. Amplified DNA was sent to the IKMB molecular lab for Sanger sequencing. The received reads from the Sanger sequencing platform were aligned to the PA14 reference genes to identify SNPs²⁵².

Table 5: PCR mix for one reaction. 1 μ l of the lysed colony is added to 19 μ l of PCR Mix.

Volume (μ l)	Ingredient
12.3	dH ₂ O
2	10x DreamTaq Buffer
2.5	2 mM dNTPs
1	25 mM forward primer
1	25 mM reverse primer
0.2	DreamTaq Polymerase

Table 6: PCR protocol.

Step	Temperature	Duration	Cycles
Initial denaturation	95 °C	3 minutes	1
Denaturation	95 °C	30 seconds	30
Hybridization	Melting temperature	30 seconds	30
Elongation	72 °C	1 minutes/kb	30
Elongation	72 °C	10 minutes	1
Storage	4 °C	∞	

Competition assays

In each experiment of the competition assay, pairs of two strains were competed against one another. For this experiment, two resistant strains and PA14 were considered. Each assay was performed in a 96-well plate. As a control, each single strain was incubated in individual wells under the same conditions on a separate 96-well plate. Firstly, frozen clonal cultures were streaked out on M9-agar and incubated at 37 °C for about 20 hours. Liquid cultures were started by inoculating 5 ml M9-medium with a single colony of the respective clones. They were then incubated at 37 °C for six hours and set to an OD of 0.1. Cultures of competing strains were mixed at a 1:1 ratio before inoculation of the competition plate. Single strain cultures were used as controls. M9-medium, the antibiotic and the cultures were added following a semi-randomized plate design (Figure 6):

- M9: 100 μ l to blank wells (E), 89.5 μ l to k50 wells, 40 μ l to M5 wells and additional 10 μ l M9 to every IC0 well
- Antibiotic: 10 μ l of each concentration (10x stocks)
- Bacteria cultures (OD \approx 0.1): 50 μ l for M5, 0.5 μ l for k50

The plates were incubated in a plate reader for 12 hours at 37 °C under constant shaking. OD was measured every 15 minutes and results were used to analyze growth kinetics of the single strains on the control plate.

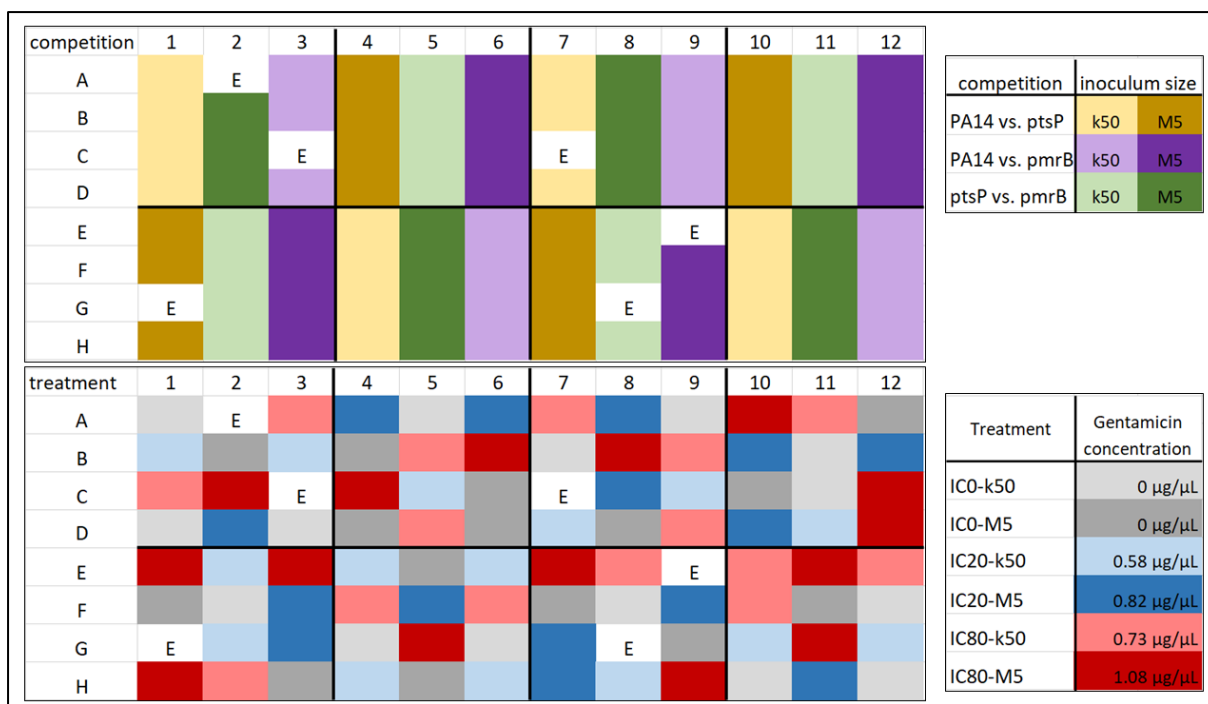


Figure 6: Systematic randomization of competition treatments on a 96-well plate. 5 replicates per treatment and a total of six blank wells (E).

Two-step PCR for amplicon sequencing

A two-step PCR was performed with the DNA obtained from cultures of the competition plates to amplify the region of interest and to ligate barcodes to the amplicons. The goal of the two-step PCR was to construct a library of DNA amplicons that contained all individual competitions. Within this library, every DNA fragment would be tagged with a combination of two barcode sequences that are individualized for every competition. By pooling all samples, the cost can be drastically reduced for determining clonal frequencies by DNA sequencing after competition.

As a first step, the 96-well competition plate was centrifuged, and the supernatant was subsequently discarded. The bacterial pellet was resuspended in 50 µl nuclease-free water, transferred onto a PCR plate and boiled for 15 minutes. 1 µl of each lysate was transferred to a new PCR plate containing the PCR mix (Table 5) with the sequence-specific overhang primers (Table 7). The first PCR was performed with 15 cycles and hybridization at 60 °C (Table 5). 1 µl of each PCR product was then used as a template for the second PCR plate containing the PCR mix (Table 5) with the sequencing primers (Table 8). Combining ten different barcodes

of the forward and reverse primers allows for up to 100 combinations to differentiate between the samples (Figure 7). The second PCR was performed with 15 cycles and hybridization at 47 °C (Table 6). A gel electrophoresis was performed to validate a successful PCR amplification.

After confirming the amplification, the DNA concentration of every sample was set to 100 ng/μl and 5 μl of every sample were pooled in a single Eppendorf tube for library generation. The library mix was then loaded on a 0.7% agarose gel and run for 1 hour at 120 mV. The desired fragments of appropriate size were then extracted from the gel by cutting them out, freezing them at -80 °C for 15 minutes in parafilm and squeezing out the DNA solution. The DNA solution was then purified with the GeneJET gel extraction kit (Thermo Fisher Scientific Inc.). Before Illumina sequencing, the DNA concentration was measured, and Sanger sequencing was performed to validate the successful amplification of the desired loci.

Table 7: Sequence-specific primers for amplicon sequencing. Names consist of the target gene, the position of the SNP in the genome and F or R for forward or reverse primer. The population(s) for which the primer amplifies the SNP region are listed. Overhangs of the primers are labelled in black. Sequence-specific parts of primers are in labelled in red.

1st PCR	Name	Population(s)	Sequence
forward	pmrB-5636922-F	A5, D12, A6	ACACTCTTCCCTACACGACGCTCTCCGATCTGACCTTGCCACCGAAGACC
	pmrB-5637204-F	A5, G8, A6	ACACTCTTCCCTACACGACGCTCTCCGATCTACCATGAACCTGCTGCTGTT
	ptsP-394249-F	E7	ACACTCTTCCCTACACGACGCTCTCCGATCTTCATGATCAACGACCGCTTC
	ptsP-393899-F	E7	ACACTCTTCCCTACACGACGCTCTCCGATCTCTCGGCTCGGGCAACTC
	ptsP-393042-F	A12	ACACTCTTCCCTACACGACGCTCTCCGATCTACAAGCGTTCATCGGCAA
	ptsP-394724-F	B11	ACACTCTTCCCTACACGACGCTCTCCGATCTAGGTCGACTTCCTTCGGTC
reverse	pmrB-5636922-R	A5, D12, A6	GTGACTGGAGTTCAGACGTGTGCTCTCCGATCTCACAGGGCGTAGCCGAG
	pmrB-5637204-R	A5, G8, A6	GTGACTGGAGTTCAGACGTGTGCTCTCCGATCTGACCTCGGCCTGCACTTC
	ptsP-394249-R	E7	GTGACTGGAGTTCAGACGTGTGCTCTCCGATCTCGGGTTGTCTTCCTTGATCGG
	ptsP-393899-R	E7	GTGACTGGAGTTCAGACGTGTGCTCTCCGATCTGGTAGCCATCGACGATCAGG
	ptsP-393042-R	A12	GTGACTGGAGTTCAGACGTGTGCTCTCCGATCTCCATCACCCGCCTATGGTG
	ptsP-394724-R	B11	GTGACTGGAGTTCAGACGTGTGCTCTCCGATCTCATCGTCGACCACCTTCTTCA

F-primers	1	2	3	4	5	6	7	8	9	10	11	12
A	F-1		F-3	F-4	F-5	F-6	F-7	F-8	F-9	F-10	F-1	F-1
B	F-1	F-2	F-3	F-4	F-5	F-6	F-7	F-8	F-9	F-10	F-2	F-2
C	F-1	F-2		F-4	F-5	F-6		F-8	F-9	F-10	F-3	F-3
D	F-1	F-2	F-3	F-4	F-5	F-6	F-7	F-8	F-9	F-10	F-4	F-4
E	F-1	F-2	F-3	F-4	F-5	F-6	F-7	F-8		F-10	F-5	F-5
F	F-1	F-2	F-3	F-4	F-5	F-6	F-7	F-8	F-9	F-10	F-6	F-6
G		F-2	F-3	F-4	F-5	F-6	F-7		F-9	F-10	F-7	F-7
H	F-1	F-2	F-3	F-4	F-5	F-6	F-7	F-8	F-9	F-10	F-8	F-8
R-primers	1	2	3	4	5	6	7	8	9	10	11	12
A	R-A		R-A	R-A	R-A	R-A	R-A	R-A	R-A	R-A	R-I	R-J
B	R-B	R-B	R-B	R-B	R-B	R-B	R-B	R-B	R-B	R-B	R-I	R-J
C	R-C	R-C		R-C	R-C	R-C		R-C	R-C	R-C	R-I	R-J
D	R-D	R-D	R-D	R-D	R-D	R-D	R-D	R-D	R-D	R-D	R-I	R-J
E	R-E	R-E	R-E	R-E	R-E	R-E	R-E	R-E		R-E	R-I	R-J
F	R-F	R-F	R-F	R-F	R-F	R-F	R-F	R-F	R-F	R-F	R-I	R-J
G		R-G	R-G	R-G	R-G	R-G	R-G		R-G	R-G	R-I	R-J
H	R-H	R-H	R-H	R-H	R-H	R-H	R-H	R-H	R-H	R-H	R-I	R-J

Figure 7: Plate design of the second PCR-step with sequencing primers. Combining ten different barcodes of the forward primers (F-primer) with ten different barcodes of the reverse primers (R-primer) allows to specifically tag up to 100 individual samples. For primer names see table 8.

Table 8: Sequencing primers for amplicon sequencing (second PCR step). Barcodes are labelled in blue. Illumina adapters are labelled in black.

2nd PCR	Name	Sequence
forward	F-1	AATGATACGGCGACCACCGAGATCTACACA AACCGCAT ACACTCTTCCCTACACG
	F-2	AATGATACGGCGACCACCGAGATCTACACA AAGGCCTT ACACTCTTCCCTACACG
	F-3	AATGATACGGCGACCACCGAGATCTACACA AGAGTGTG ACACTCTTCCCTACACG
	F-4	AATGATACGGCGACCACCGAGATCTACACA CACAAGTC ACACTCTTCCCTACACG
	F-5	AATGATACGGCGACCACCGAGATCTACACA CGTTCCTA ACACTCTTCCCTACACG
	F-6	AATGATACGGCGACCACCGAGATCTACACA CGTTGGAT ACACTCTTCCCTACACG
	F-7	AATGATACGGCGACCACCGAGATCTACACA GTCAACAC ACACTCTTCCCTACACG
	F-8	AATGATACGGCGACCACCGAGATCTACACA GTCACTGA ACACTCTTCCCTACACG
	F-9	AATGATACGGCGACCACCGAGATCTACACT TCTCGTCA ACACTCTTCCCTACACG
	F-10	AATGATACGGCGACCACCGAGATCTACACT TTGGTACG ACACTCTTCCCTACACG
reverse	R-A	CAAGCAGAAGACGGCATA CGAGATAAACCGGA AGTGACTGGAGTTCAGACG
	R-B	CAAGCAGAAGACGGCATA CGAGATAGAGTGAC GTGACTGGAGTTCAGACG
	R-C	CAAGCAGAAGACGGCATA CGAGATCAACTGGT GTGACTGGAGTTCAGACG
	R-D	CAAGCAGAAGACGGCATA CGAGATCGTTCGTT GTGACTGGAGTTCAGACG
	R-E	CAAGCAGAAGACGGCATA CGAGATCTGTTAC GTGACTGGAGTTCAGACG
	R-F	CAAGCAGAAGACGGCATA CGAGATGCTTGCA AGTGACTGGAGTTCAGACG
	R-G	CAAGCAGAAGACGGCATA CGAGATGTCAACT GGTGACTGGAGTTCAGACG
	R-H	CAAGCAGAAGACGGCATA CGAGATTCCTCAT GGTGACTGGAGTTCAGACG
	R-I	CAAGCAGAAGACGGCATA CGAGATTCGACTAG GTGACTGGAGTTCAGACG
	R-J	CAAGCAGAAGACGGCATA CGAGATTTGCAAGC GTGACTGGAGTTCAGACG

Analysis of amplicon sequencing

The reads received from the Illumina Sequencing platform were quality-filtered with the software Trimmomatic 0.39 and subsequently aligned to the PA14 reference genome by using the Burrows-Wheeler Aligner^{252,258,267}. SAMtools was used to generate bam-files that were evaluated with the Integrative Genomics Viewer^{262,266}. The strain frequency was calculated via the SNP counts. Subsequently, the mean frequencies of two strains were calculated and plotted for every treatment and competition.

Statistics

All statistical analyses were performed with the R programming language and the R Studio software^{264,265}. In the upcoming text section of the results, p-values are presented in comparison to size thresholds (e.g. > 0.05 , < 0.005) instead of absolute values.

- To test the influence of treatment parameters on adaptive growth dynamics during evolution experiments, linear mixed effect models were constructed with yield as the response variable and growth period, inhibitory concentration (IC) and transfer size (TS) as predictors. Tukey's HSD was calculated for multiple pairwise comparisons of the group means to quantify the differences between the groups.
- Linear models and Tukey's HSD were also calculated for the influence of both IC and TS on evolved resistance. In this case, AUC was used as the resistance parameter.
- Pearson's product-moment correlation was calculated to test the association between individual mutation frequencies and total number of mutations per population.
- Pairwise t-tests were performed to compare the mean resistance between two groups of mutants. The same test was also applied to compare the mean frequencies of different genotypes in mixed populations after running competition assays.
- For the competition assays, one-way ANOVAs were calculated to compare frequencies and AUC of the same clonal variant between different treatment conditions. Tukey's HSD was calculated for multiple pairwise comparisons of the group means.

- Bartlett tests were applied to compare the size of treatment group variance.
- Shannon's diversity index H was calculated for each treatment group:

$$H = \sum_{i=1}^s - (P_i * \ln P_i)$$

with P_i representing the fraction of the treatment group made up of populations that carry mutation i and s representing the number of mutated genes found in each treatment group.

- Fixation indices (F_{ST}) were calculated for every treatment group of every sequenced transfer. For that, haplotypes were inferred from the frequency distribution of all individual mutations over the course of the experiment. Mutations were identified as being independent (and therefore representing different haplotypes) when their change in frequencies did not overlap over time. Haplotype diversity was calculated as:

$$H = 1 - \sum_{i=1}^j P_i^2$$

with P_i representing the fraction of a haplotype in the population and j representing the total number of haplotypes. Haplotype diversity was calculated within individual populations of the treatment group (H_S) and between the different replicates of the treatment group (H_T). F_{ST} was then calculated as:

$$F_{ST} = \frac{H_T - \overline{H_S}}{H_T}$$

Results

In the following sections, the results of the evolution experiments and of the subsequent analyses are sorted by the different analytical methods. Dose-response curves were obtained for PA14 against all treatment drugs. The individual treatment dosages (IC20, IC50 and IC80 for all three transfer sizes) as well as the MICs and their multiples are summarized in Supplementary Table S4 (page 164). Three separate evolution experiments were carried out successfully by applying the described experimental protocol. In all three cases, PA14 was challenged against three different ICs of a single antibiotic and for each drug concentration, three different transfer sizes were used. The experiments have been run for CAR, CIP and GEN. However, the results of the individual experiments for each drug vary in depth:

- For GEN, evolution experiments were performed, evolved resistance was assessed, the evolutionary allele dynamics were uncovered, and clones were selected to model specific dynamics in competition experiments.
- For CIP, evolution experiments were performed, evolved resistance was assessed, and the evolutionary allele dynamics were uncovered.
- For CAR, evolution experiments were performed, and evolved resistance was assessed.

The experimental complications of colistin will be discussed in greater detail in a separate chapter of the discussion.

To widen the focus on the impact of the parameters on the large number of treatment groups, the dataset was reduced to the maximum and minimum parameters of the treatment conditions. Therefore, the k500 transfer size and the IC50 drug concentration groups will not be discussed in the following sections of the thesis. Summary graphs that include the results of the removed treatment groups can be found in the supplementary data. Mean inhibition of all treatment groups over the course of the evolution experiments are summarized in Supplementary Figures S1 (CAR, page 148), S2 (CIP, page 149) and S3 (GEN, page 150). Dose Response Curves of surviving populations from all treatment groups after the evolution experiments are summarized in Supplementary Figures S4 (CAR, page 165), S5 (CIP, page 166) and S6 (GEN, page 167).

Evolutionary growth patterns

Populations of PA14 were allowed to evolve for a total of 16 growth periods under either high or low drug concentrations. At the end of each growth period, distinct numbers of cells were transferred. To demonstrate the growth dynamics of the evolving PA14 populations throughout the experiments, the cell concentrations obtained from the flow cytometry assays were used to calculate the mean yield of the treatment groups relative to the yield of the corresponding no-drug control treatment. To investigate to what degree the controlled experimental factors affected bacterial growth during the experiment, linear mixed effect models were constructed with yield as the response variable and growth period, inhibitory concentration (IC) and transfer size (TS) as predictors. Tukey's HSD was calculated for multiple pairwise comparisons of the groups means to find out which treatment groups differ from each other. A summary of average cell numbers from all treatment groups from all transfers can be found in Supplementary Tables S1 (CAR, page 151 ff), S2 (CIP, page 155 ff) and S3 (GEN, page 159 ff).

Large TS groups evolve higher yield in GEN evolution experiment

In the GEN experiment, most populations experienced a substantial decrease in growth after the second transfer, after which they rapidly recovered and reached their first fitness plateau (Figure 8). This effect occurred independently of both IC and TS. For most populations, the yield remained stable for most transfers after the recovery and only increased again towards the end of the experiment. While the large TS groups IC20-M5 and IC80-M5 reached the same yield as the controls at the end of the experiment, the small TS groups IC20-k50 and IC80-k50 remained inhibited. All treatment groups maintained variation in yield between their replicates throughout the experiment. Both IC and TS, as well as their interaction, showed a significant influence on yield (Table 9). Apart from the IC80-M5 and IC20-k50 pair and the IC80-M5 and IC80-k50 pair, all other pairs of treatment groups had different responses in overall yield from one another (Table 10).

In summary, all treatment groups adapted to GEN within the first few transfers, regardless of treatment regimen. Unlike the large TS groups, the small TS groups remained inhibited at the end of the experiment.

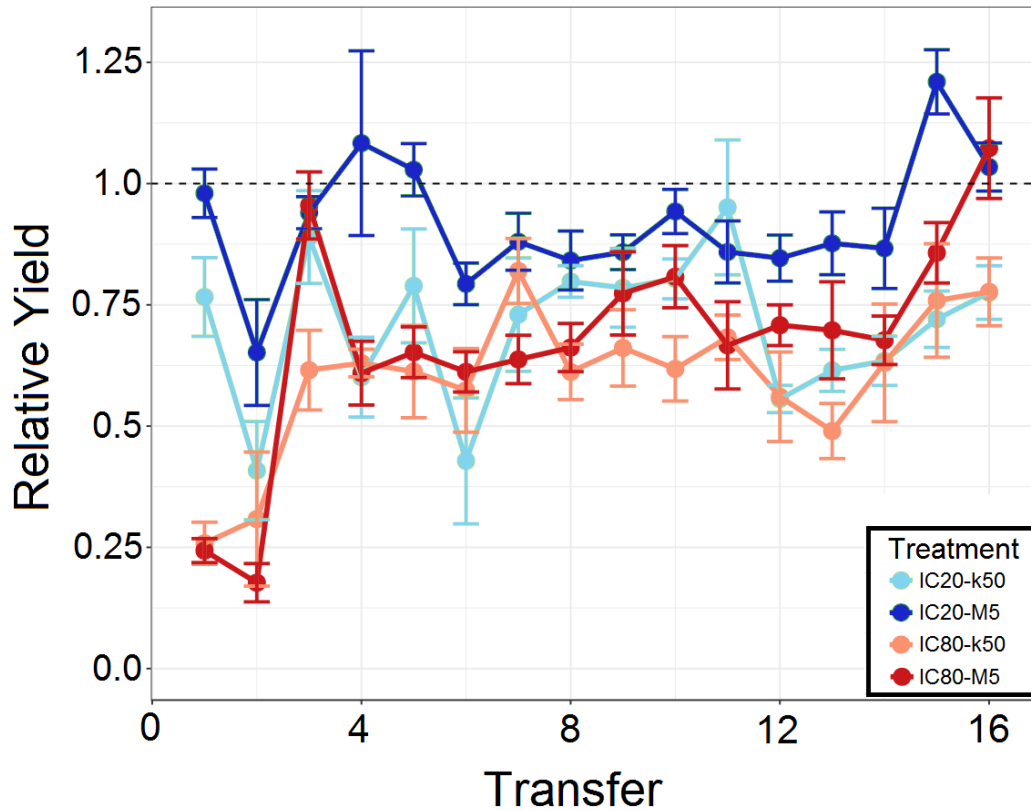


Figure 8: Large TS groups evolve higher yield in GEN evolution experiment. The X-axis represents the time series of the evolution experiment: every point represents the end of a growth period before the next transfer. The Y-axis represents the mean yield of the treatments based on the cell concentrations obtained from the flow cytometer readouts. Error bars represent standard error of mean (8 replicates). Blue: IC20 treatments; Red: IC80 treatments; light colors represent 50k transfers; dark colors represent 5M transfers.

Table 9: Yield over time: Linear mixed model results for gentamicin. The model tests the influence of IC, TS and time of transfer, as well as their individual interactions, on population yield. Formula: Yield ~ IC * TS * Transfer * (1 | Well). Asterisks represent significant difference between two treatment groups (* = $p < 0.05$, *** = $p < 0.005$, n.s. = $p > 0.05$).

Predictor	Chisq	p adj.	Significance
IC	31.3366	2.170e-08	***
TS	17.1945	3.374e-05	***
Transfer	21.4627	3.608e-06	***
IC:TS	4.4706	0.03448	*
IC:Transfer	15.3998	8.700e-05	***
TS:Transfer	5.97	0.01455	*
IC:TS:Transfer	0.7331	0.39187	n.s.

Table 10: Yield over time: TukeyHSD results for gentamicin. The test compares the difference in mean yield between the individual treatment groups. Yield ~ Treatment. Asterisks represent significant difference between two treatment groups (* = $p < 0.05$, *** = $p < 0.005$, n.s. = $p > 0.05$).

Comparison	diff	p adj.	Significance
IC20 M5-IC20 k50	0.19435357	0.0000001	***
IC80k50-IC20 k50	-0.11163962	0.0058367	*
IC80 M5-IC20 k50	-0.05015434	0.4816255	n.s.
IC80 k50-IC20 M5	-0.30599319	0.0000000	***
IC80 M5-IC20 M5	-0.24450791	0.0000000	***
IC80 M5-IC80 k50	0.06148528	0.2979427	n.s.

Yield improves faster under large TS in CIP evolution experiment

For the evolution experiment with CIP, a change in yield was observed in all treatment groups (Figure 9). For the IC20 treatments, the growth increased by two steps during the experiment, first in the beginning of the experiment and again in its second half. For the IC80 treatments, yield increased stronger and faster than for IC20 in the beginning but then reached its equilibrium at transfer four. Extinction events did not occur in populations of the other treatment groups, but all replicates but one went extinct for the IC80-k50 treatment. Apart from growth period, both IC and TS also showed significant influence on yield (Table 11). IC80-M5 and IC20-k50 were the only two treatment groups that did not show a significant difference in overall yield from one another (Table 12). The results indicate that bacterial populations generally adapted faster to CIP when the TS was large but may have adapted at slower rates and at a higher risk of extinction when they experienced stronger bottlenecks. Interestingly, the two large TS groups showed an even higher yield than the uninhibited controls at the final transfer (Figure 9), indicating a higher fitness for samples grown in the presence of CIP.

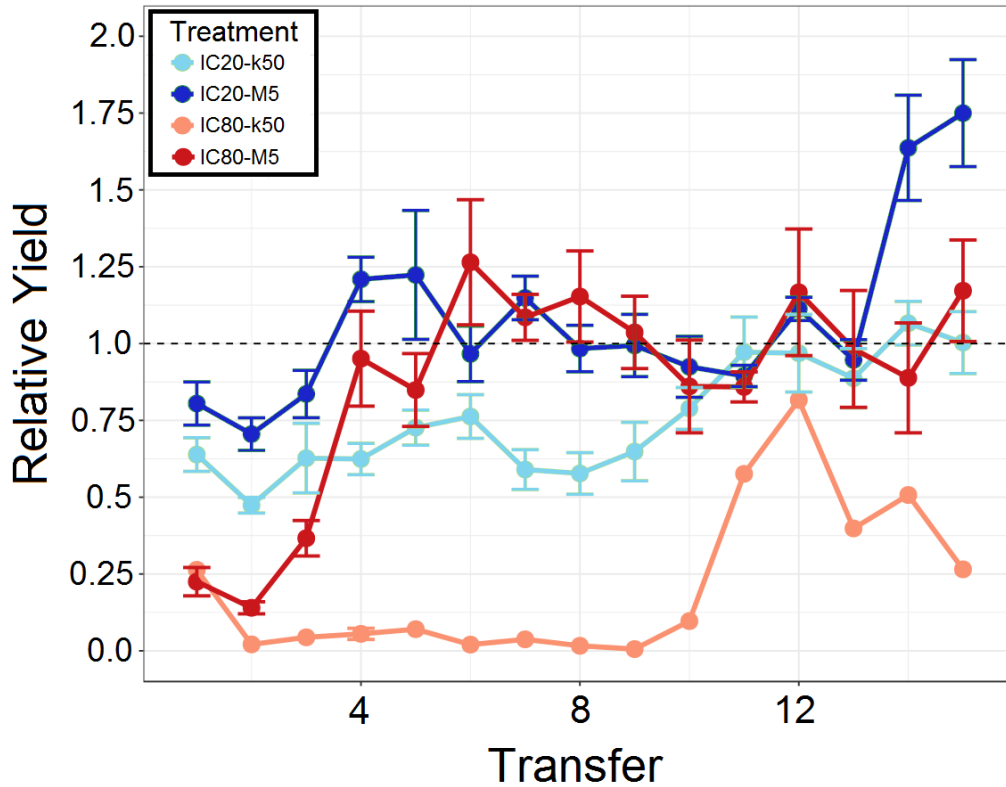


Figure 9: Yield improves faster under large TS in CIP evolution experiment. The X-axis represents the time series of the evolution experiment: Every point represents the end of a growth period before the next transfer. The Y-axis represents the mean yield of the treatments based on the cell concentrations obtained from the flow cytometer readouts. Error bars represent standard error of mean (8 replicates). Blue: IC20 treatments; Red: IC80 treatments; light colors represent 50k transfers; dark colors represent 5M transfers.

Table 11: Yield over time: Linear mixed model results for ciprofloxacin. The model tests the influence of IC, TS and time of transfer, as well as their individual interactions, on population yield. Formula: Yield ~ IC * TS * Transfer * (1 | Well). Asterisks represent significant difference between two treatment groups (* = $p < 0.05$, *** = $p < 0.005$, n.s. = $p > 0.05$).

Predictor	Chisq	p adj.	Significance
IC	16.0519	6.163e-05	***
TS	33.3524	7.688e-09	***
Transfer	48.4366	3.411e-12	***
IC:TS	1.5364	0.21516	n.s.
IC:Transfer	5.4547	0.01952	*
TS:Transfer	2.9815	0.08422	n.s.
IC:TS:Transfer	2.0076	0.15651	n.s.

Table 12: Yield over time: TukeyHSD results for ciprofloxacin. The test compares the difference in mean yield between the individual treatment groups. Yield ~ Treatment. Asterisks represent significant difference between two treatment groups (* = $p < 0.05$, *** = $p < 0.005$, n.s. = $p > 0.05$).

Comparison	diff	p adj.	Significance
IC20 M5-IC20 k50	0.431779	0.0000021	***
IC80k50-IC20 k50	-0.55585	0.0002649	***
IC80 M5-IC20 k50	0.154925	0.0974278	n.s.
IC80 k50-IC20 M5	-0.98763	0.0000000	***
IC80 M5-IC20 M5	-0.27686	0.000144	***
IC80 M5-IC80 k50	0.710774	0.0000011	n.s.

All treatment groups adapt gradually in CAR evolution experiment

In the case of the CAR experiment, all treatments remained inhibited to a certain degree over the course of evolution (Figure 10). They did not achieve similar yield like the uninhibited control during the experiment, as it was observed for the CIP treatments. However, there was a strong and quick increase in yield for the IC80 treatments at the beginning of the experiment after which yield fluctuated around its equilibrium. In the IC20 treatments, the k50 group showed a higher yield than the M5 group throughout the experiment. In contrast, there did not seem to be an influence of TS on yield for the IC80 groups. However, the replicates of the IC80 groups generally also showed high variance in yield. In contrast to the CIP experiment, the influence of the TS on the evolutionary dynamics was small. The linear mixed effect model revealed that only transfer and the interaction of transfer and IC were valuable predictors of yield, but not TS (Table 13). IC20-50 produced a higher yield than the other groups. No difference in yield was found between the remaining groups (Table 14). In general, the treatment regimens did not influence the growth of the populations to different degrees.

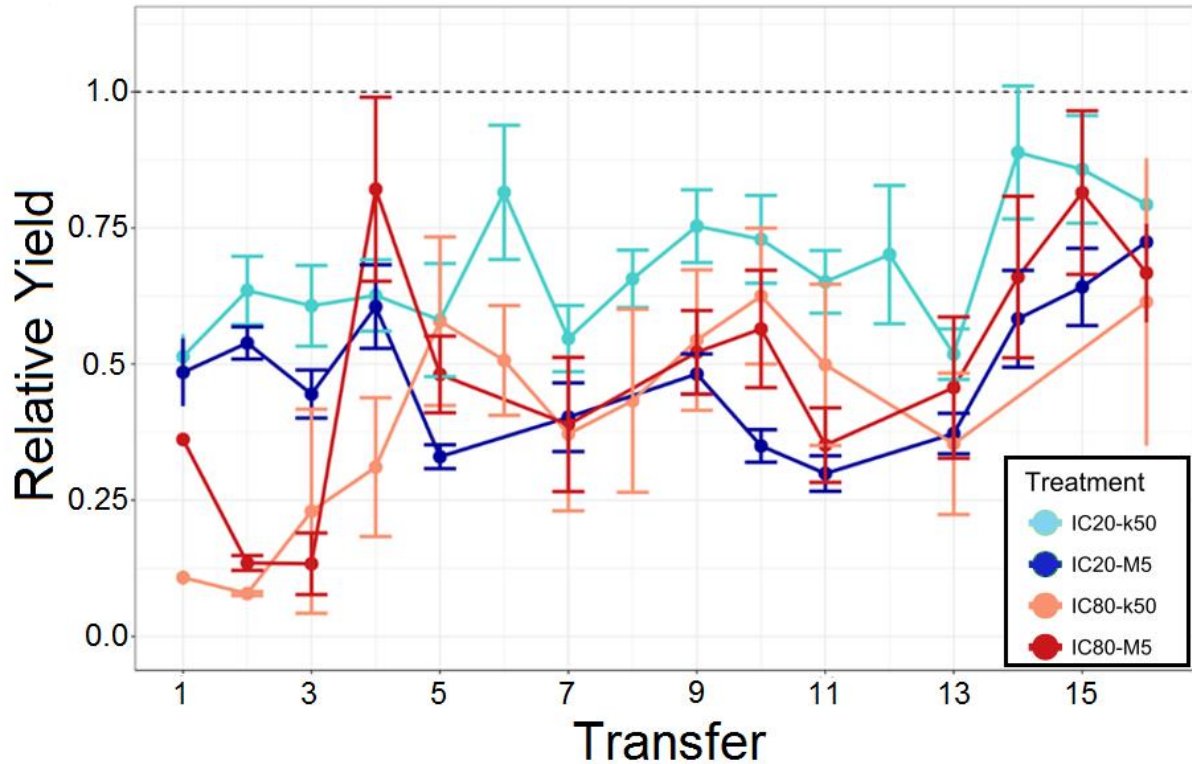


Figure 10: All treatment groups adapt slowly in CAR evolution experiment. The X-axis represents the time series of the evolution experiment: Every point represents the end of a growth period before the next transfer. The Y-axis represents the mean yield of the treatments based on the cell concentrations obtained from the flow cytometer readouts. Error bars represent standard error of mean (8 replicates). Blue: IC20 treatments; Red: IC80 treatments; light colors represent 50k transfers; dark colors represent 5M transfers.

Table 13: Yield over time: Linear mixed model results for carbenicillin. The model tests the influence of IC, TS and time of transfer, as well as their individual interactions, on population yield. Formula: Yield ~ IC * TS * Transfer * (1 | Well). Asterisks represent significant difference between two treatment groups (***) = $p < 0.005$, n.s. = $p > 0.05$.

Predictor	Chisq	p adj.	Significance
IC	2.6406	0.104162	n.s.
TS	0.7848	0.375689	n.s.
Transfer	61.5023	4.422e-15	***
IC:TS	2.3921	0.121949	n.s.
IC: Transfer	10.4923	0.001199	***
TS: Transfer	1.7042	0.191737	n.s.
IC:TS: Transfer	0.1616	0.687709	n.s.

Table 14: Yield over time: TukeyHSD results for carbenicillin. The test compares the difference in mean yield between the individual treatment groups. Formula: Yield ~ Treatment. Asterisks represent significant difference between two treatment groups (***) = $p < 0.005$, n.s. = $p > 0.05$).

Comparison	diff	p adj.	Significance
IC20 M5-IC20 k50	-0.17899935	0.0000363	***
IC80k50-IC20 k50	-0.25196649	0.0000000	***
IC80 M5-IC20 k50	-0.18731949	0.0000228	***
IC80 k50-IC20 M5	-0.07296714	0.3097091	n.s.
IC80 M5-IC20 M5	-0.00832014	0.9972808	n.s.
IC80 M5-IC80 k50	0.06464700	0.4374637	n.s.

Evolved resistance

As most populations improved their growth ability over the course of the evolution experiments, adaptation was expected to have evolved by the acquisition of resistance mutations. To test for evolved resistance, the individual populations that survived the final transfer period were challenged against several concentration levels of the applied antibiotic. Concentrations above and below the MIC of the wild type were tested to measure the resistance properties after evolution under the different treatments. The area under the curve (AUC) was calculated for each DRC to quantify resistance. To test the influence of different treatment factors on the intensity of resistance, linear mixed effect models were constructed that contained AUC as the response variable and IC, TS and their interaction as predictors. In addition to the resistance measurements, the endpoint populations were also grown in antibiotic free media to further characterize changes in growth behavior relative to the evolved no-drug controls. Continuous OD measurements were obtained to calculate the mean length of lag phase and mean maximum growth rate of the evolved populations to check for potential fitness trade-offs.

IC20-k50 and IC80-M5 evolve the highest resistance in GEN evolution experiment

In the GEN resistance assays, most treatments (even the low ICs) led to resistance to inhibition levels significantly higher than the MIC of the wild type (Figure 11A). However, the

highest resistance at the end of the experiment was observed for the IC20-k50 and the IC80-M5 treatment groups (Figure 11A). The effect of treatment on evolved resistance became more apparent when comparing the AUC of the obtained DRCs (Figure 11B). AUC was then used as the response variable for the construction of linear mixed effect models (Table 15).

For the GEN treatments, the model revealed a significant influence of the interaction between IC and TS on evolved GEN resistance ($p < 0.005$). For the IC20 treatments, populations that evolved under large TS acquired the lowest resistance and small TS acquired the highest resistance ($p < 0.05$). The reverse effect was observed for the IC80 treatments, although the difference in resistance between the two TS groups was not significant ($p = 0.28$). Variance in resistance was different between small and large TS for IC20 ($p < 0.05$), but it was not for IC80 ($p = 0.87$, Bartlett test). In all GEN treatments, the variance in OD increased at drug concentrations above the MIC of the wild type, indicating diverse adaptive responses within the treatment groups that led to different levels of resistance for the individual lineages. Interestingly, IC20-k50 lineages evolved as high resistance as the IC80 treatment groups ($p > 0.99$, Tukey HSD, Table 16).

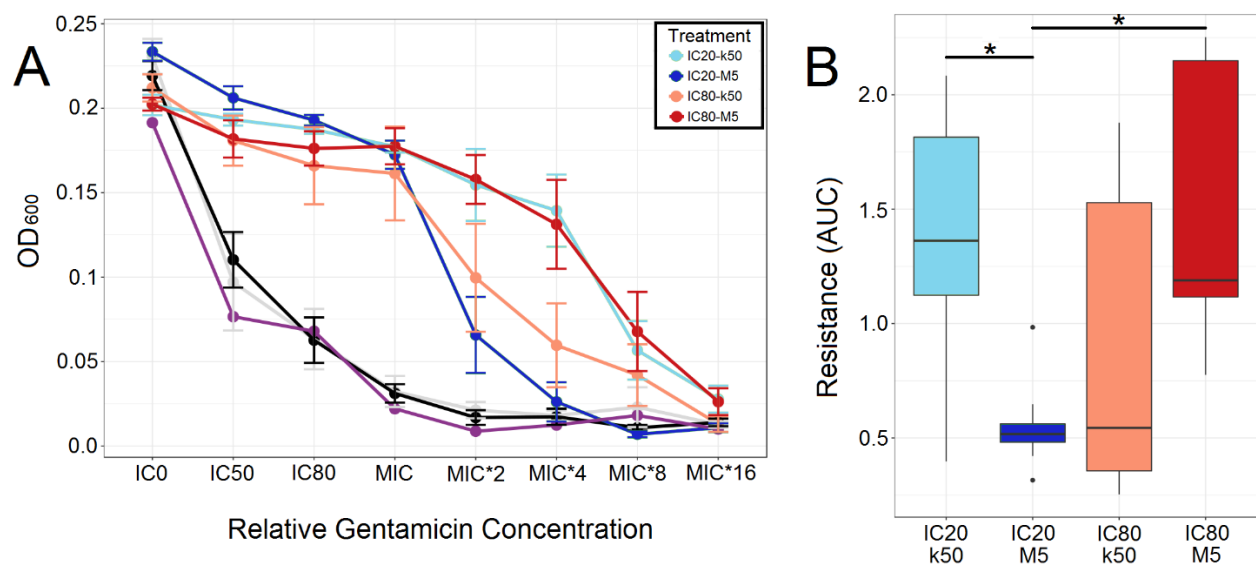


Figure 11: IC20-k50 and IC80-M5 evolve the highest resistance in GEN evolution experiment. **A:** The X-axis represents the relative levels of antibiotic concentrations against which the evolved PA14 populations were challenged. The Y-axis represents the final OD of the tested bacterial populations at a wavelength of 600 nm after 12 hours of incubation in presence of the respective drug concentration. Error bars represent standard error of mean (8 replicates). Blue: IC20 treatments; Red: IC80 treatments; Grey: IC0; Purple: unevolved PA14 control; light colors represent 50k transfers; dark colors represent 5M transfers. **B:** The X-axis and colors represent different treatment groups. The Y-axis represents AUC as a proxy for resistance to the treatment drug. Asterisks represent significant difference between two treatment groups ($* = p < 0.05$; TukeyHSD).

Table 15: Linear mixed effect model results for evolved gentamicin resistance. The model tests the influence of IC and TS, as well as their interaction, on evolved resistance (AUC) to the treatment drug. Formula: $AUC \sim IC * TS$. Asterisks represent significant difference between two treatment groups (***) = $p < 0.005$, n.s. = $p > 0.05$).

Predictor	Sum Sq	F	p adj.	Significance
IC	0.2180	0.7051	0.408450	n.s.
TS	0.2356	0.7622	0.390341	n.s.
IC:TS	3.5331	11.4288	0.002217	***

Table 16: TukeyHSD results for evolved gentamicin resistance. The test compares the difference in mean resistance (AUC) between the individual treatment groups. Formula: $AUC \sim Treatment$. Asterisks represent significant difference between two treatment groups (* = $p < 0.05$, n.s. = $p > 0.05$).

Comparison	diff	p adj.	Significance
IC20 M5-IC20 k50	-0.82755375	0.0291850	*
IC80k50-IC20 k50	-0.49102390	0.3109650	n.s.
IC80 M5-IC20 k50	0.03406569	0.9993913	n.s.
IC80 k50-IC20 M5	0.33652984	0.6256745	n.s.
IC80 M5-IC20 M5	0.86161944	0.0280381	*
IC80 M5-IC80 k50	0.52508959	0.2840705	n.s.

Growth measurements in drug-free medium revealed that those treatment groups that yielded the strongest resistance against the treatment drug also evolved a longer lag phase length than the less resistant groups (Figure 12B). All treatments showed great variation in maximum growth rate. Most of the populations that evolved a high level of resistance against the treatment drug also had a reduced maximum growth rate compared to the Wt (IC20-k50: mean = 0.0107, $t = -2.292$, $p = 0.056$; IC80-M5: mean = 0.0099, $t = -3.2045$, $p < 0.05$; one-sample t-test; Figure 12A). A negative correlation between resistance and maximum growth rate was identified (-0.494 Pearson's product-moment correlation; $p < 0.01$; see Figure 13). However, when considering the influence of treatment group, strong negative correlation between resistance and growth rate was only found in the IC80-k50 group (-0.765 Pearson's product-moment correlation; $p < 0.01$), but not in the other treatment groups. In general, evolved resistance did not correlate with length of lag phase.

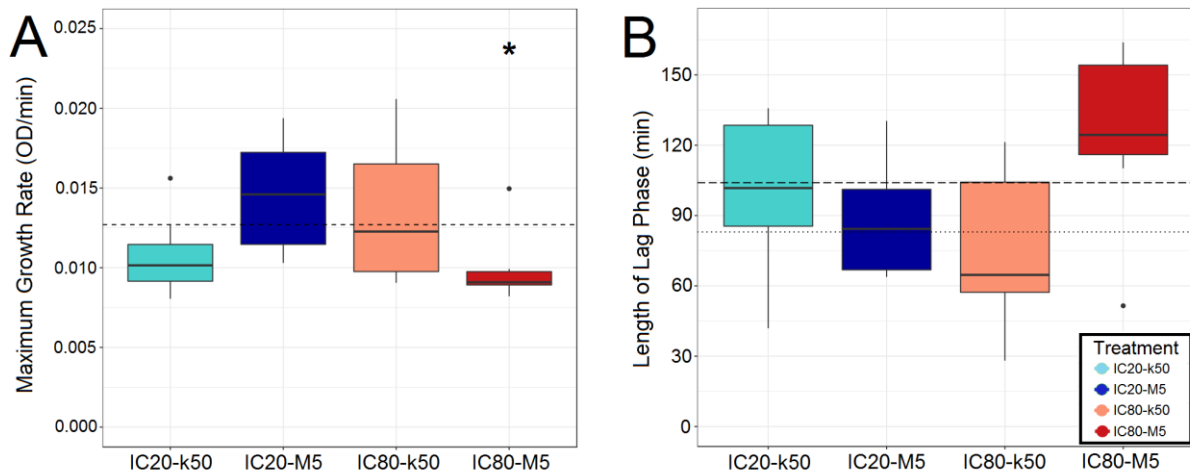


Figure 12: The most GEN-resistant group shows the lowest growth in drug-free medium. (A) maximum growth rate (OD/min); (B) length of lag phase (min). Measurements taken in absence of antibiotics. The X-axes and colors represent different treatment groups. The Y-axes represent the growth parameters of the treatment groups after the evolution experiment. 8 biological replicates. Mean fitness of control groups is represented by black horizontal lines: (A) dotted line represents both transfer sizes; (B) long-dashed line represents M5; short-dashed line represents k50. Asterisks represent significant difference of treatment group to control (* = $p < 0.05$; one-sample t-test).

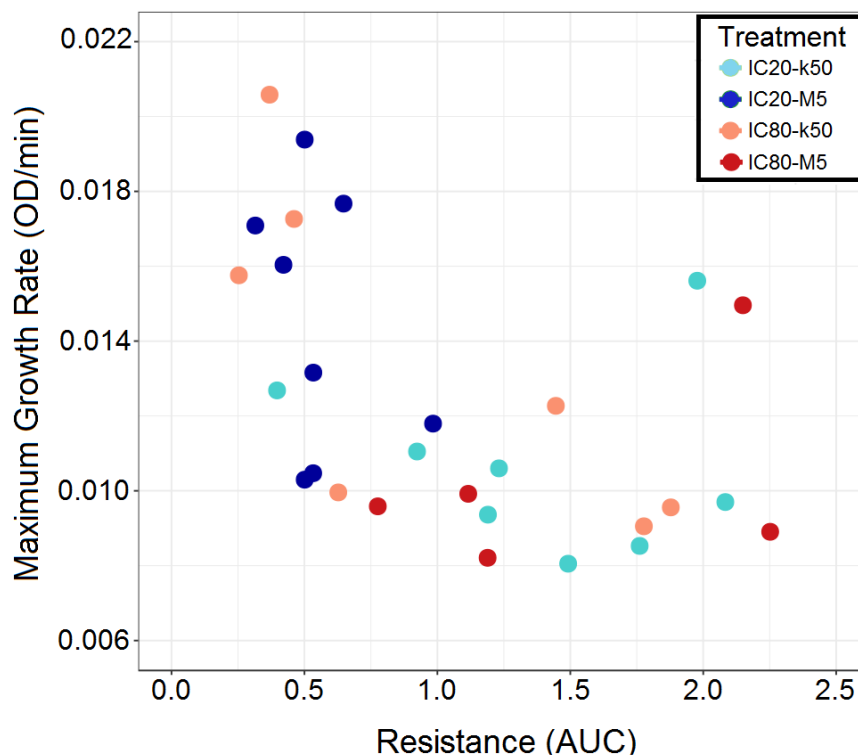


Figure 13: GEN resistance correlates negatively with maximum growth rate. The X-axis represents gentamicin resistance of evolved populations based on the AUC of the DRC of the resistance assay. The Y-axis represents the populations maximum growth rate (OD/min). Colors refer to different treatment groups: Light blue: IC20-k50, Dark blue: IC20-M5, Light red: IC80-k50, Dark red: IC80-M5.

In conclusion, evolved resistance against GEN was highest for the IC80-M5 and IC20-k50 groups. The resistance observed in the IC80-M5 populations is also associated with a decreased growth rate in drug-free medium.

IC20-k50 and IC80-M5 evolve the highest resistance in CIP evolution experiment

For CIP, no evolved resistance was observed in the IC20-M5 treatment group (dark blue line in Figure 14A). All other treatment conditions provoked evolution of resistance as high as > 16xMIC of the wild type. The interaction of IC and TS had a significant influence on resistance ($p < 0.005$, LME; Table 17). For the IC20 treatments with CIP, resistance was the weakest for the large TS and the strongest for the small TS ($p < 0.01$, two sample t-test; Figure 14B; Table 18). The IC80 treatments had contrasting results: The large TS groups evolved a higher resistance than the single surviving population of the small TS. Variation in resistance was generally greater for small TS than for large TS ($p < 0.005$ for IC20, Bartlett test).

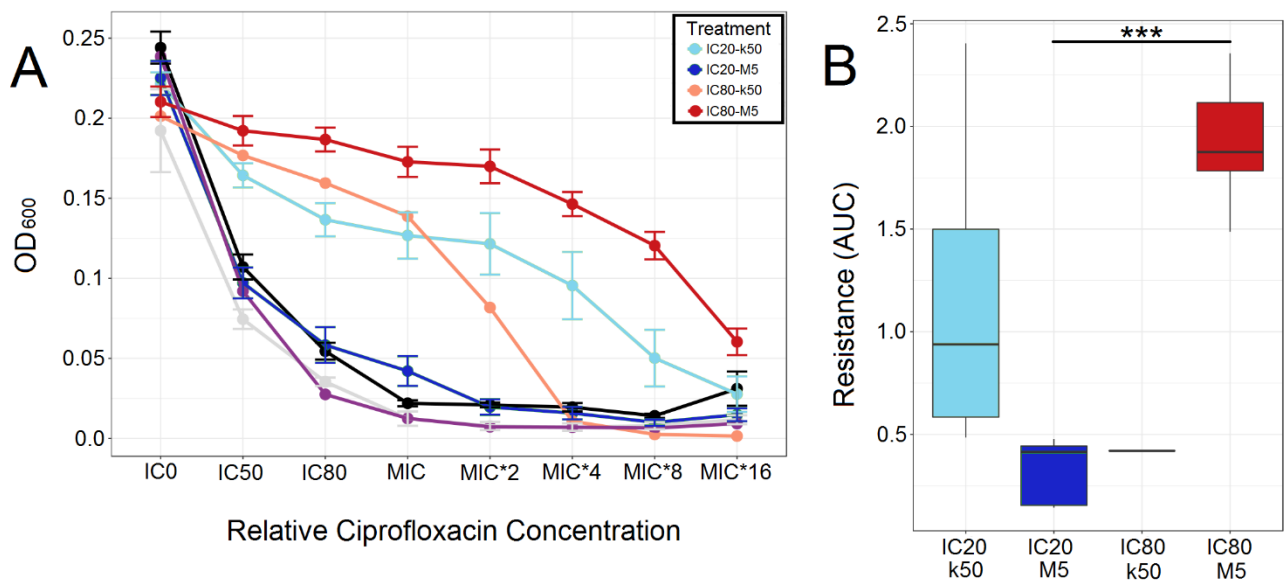


Figure 14: IC20-k50 and IC80-M5 evolve the highest resistance in CIP evolution experiment. **A:** The X-axis represents the relative levels of antibiotic concentrations against which the evolved populations were challenged. The Y-axis represents the final OD of the tested bacterial populations after 12 hours of incubation in presence of the respective drug concentration. Error bars represent standard error of mean (8 replicates). Blue: IC20 treatments; Red: IC80 treatments; Black/Grey: IC0; Purple: unevolved PA14 control; light colors represent 50k transfers; dark colors represent 5M transfers. **B:** The X-axis and colors represent different treatment groups. The Y-axis represents AUC as a proxy for resistance to the treatment drug. Asterisks represent significant difference between two treatment groups (***) = $p < 0.005$; TukeyHSD).

Table 17: Linear model results for evolved ciprofloxacin resistance. The model tests the influence of IC and TS, as well as their interaction, on evolved resistance (AUC) to the treatment drug. Formula: $AUC \sim IC * TS$. Asterisks represent significant difference between two treatment groups (***) = $p < 0.005$, n.s. = $p > 0.05$).

Predictor	Sum Sq	F	p adj.	Significance
IC	6.3214	32.705	1.122e-05	***
TS	0.6435	3.329	0.0823252	n.s.
IC:TS	3.8414	19.874	0.0002173	***

Table 18: TukeyHSD results for evolved ciprofloxacin resistance. The test compares the difference in mean resistance (AUC) between the individual treatment groups. Formula: $AUC \sim Treatment$. Asterisks represent significant difference between two treatment groups (***) = $p < 0.005$, n.s. = $p > 0.05$).

Comparison	diff	p adj.	Significance
IC20 M5-IC20 k50	-0.780653	0.0094321	n.s.
IC80k50-IC20 k50	-0.691694	0.4646439	n.s.
IC80 M5-IC20 k50	0.8258906	0.0058931	n.s.
IC80 k50-IC20 M5	0.0889594	0.9974583	n.s.
IC80 M5-IC20 M5	1.6065437	0.0000019	***
IC80 M5-IC80 k50	1.5175844	0.0183543	n.s.

The endpoint populations were also grown in absence of the antibiotics to calculate the mean length of lag phase and mean maximum growth rate of the evolved populations (see Figure 15). On average, the different CIP treatment groups showed a higher growth rate and shorter lag phase than the ancestor. However, these differences were not statistically significant. There did not appear to be an association between maximum growth rate and resistance and neither between length of lag phase and resistance.

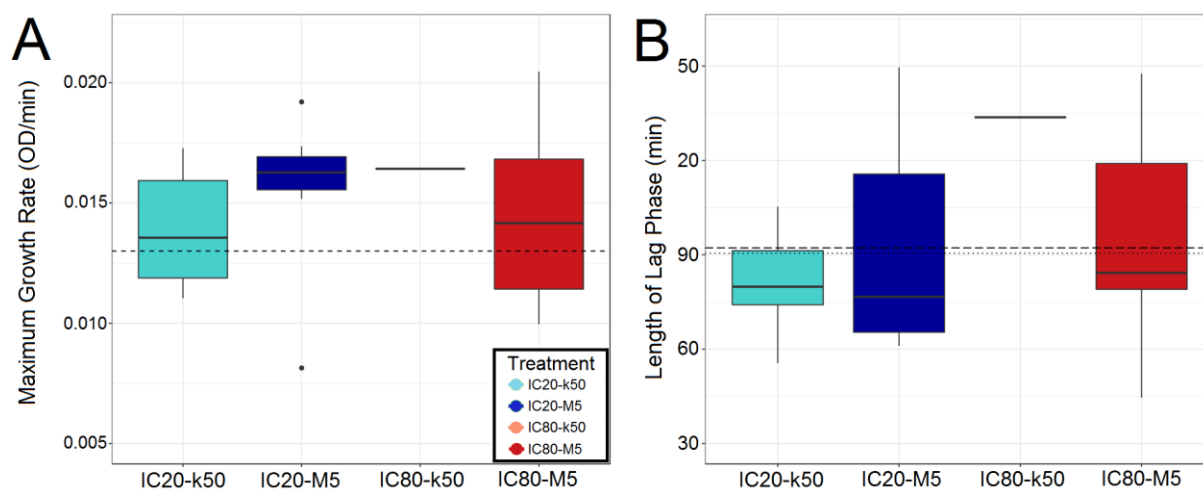


Figure 15: Adaptation to CIP does not affect growth in drug-free medium for all treatment groups. (A) maximum growth rate (OD/min); (B) length of lag phase (min). Measurements taken in absence of antibiotics. The X-axes and colors represent different treatment groups. The Y-axes represent the growth parameters of the treatment groups after the evolution experiment. 8 biological replicates for all treatment groups but IC80-k50 (one replicate). Mean fitness of control groups is represented by black horizontal lines: (A) dotted line represents both transfer sizes; (B) long-dashed line represents M5; short-dashed line represents k50.

In summary, the highest CIP resistance evolved in the IC80-M5 treatment group and the second highest in the IC20-k50 treatment group. CIP resistance did not appear to be associated with a fitness cost in drug-free medium.

IC80-treated groups evolve highest resistance in CAR evolution experiment

In case of the CAR resistance properties, the high IC adapted lineages showed a high average growth at concentration levels below the MIC but reduced growth at levels above the MIC (Figure 16). The low IC adapted lineages did not have higher yield than the evolved no-drug control lineages. In addition, only IC could be identified as a valuable predictor of resistance AUC ($p < 0.005$), but not TS ($p = 0.41$, GLMM; see Table 19). This indicates that the applied bottleneck sizes did not affect evolvability of resistance differently. Additionally, these observations indicate that the bacteria did not acquire mutations that confer high-level resistance against CAR but primarily adapted to drug concentrations that they originally encountered in the experiment. Otherwise, increased fitness levels would have been expected for higher concentrations than those they had been treated with. All treatment groups evolved a

slightly, but not significantly lower growth rate compared to the ancestor (Figure 17A). There did not seem to be an association between length of lag phase and relative resistance of the population (Figure 17B).

In general, no difference in CAR resistance was observed between the two M5 treatment groups and the two k50 groups. Higher resistance evolved under IC80 treatment than under IC20 treatment, but growth remained limited in all treatment groups at CAR concentration levels > MIC. All treatment groups evolved a slightly lower growth rate in drug-free medium compared to the control groups.

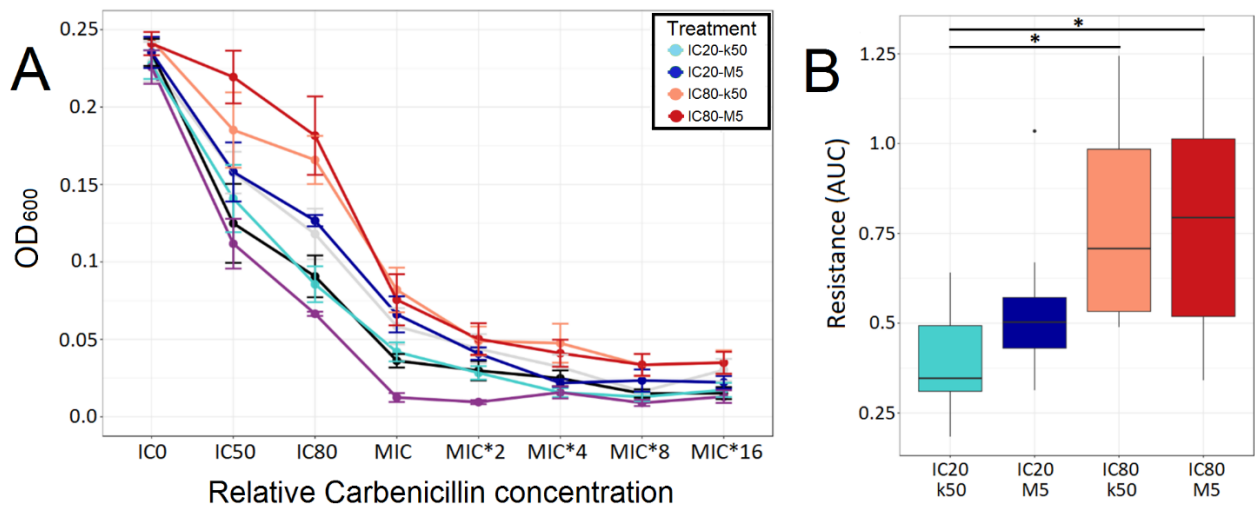


Figure 16: IC80-treated groups evolved higher resistance than IC20-treated groups in CAR evolution experiment. A: The X-axis represents the relative levels of antibiotic concentrations against which the evolved PA14 populations were challenged. The Y-axis represents the final OD of the tested bacterial populations after 12 hours of incubation in presence of the respective drug concentration. Error bars represent standard error of mean (8 replicates). Blue: IC20 treatments; Red: IC80 treatments; Grey: IC0; Purple: unevolved PA14 control; light colors represent 50k transfers; dark colors represent 5M transfers. **B:** The X-axis and colors represent different treatment groups. The Y-axis represents AUC as a proxy for resistance to the treatment drug. Asterisks represent significant difference between two treatment groups (* = $p < 0.05$; TukeyHSD).

Table 19: Linear model results for evolved carbenicillin resistance. The model tests the influence of IC and TS, as well as their interaction, on evolved resistance (AUC) to the treatment drug. Formula: $AUC \sim IC * TS$. Asterisks represent significant difference between two treatment groups (***) = $p < 0.005$, n.s. = $p > 0.05$).

Predictor	Sum Sq	F	p adj.	Significance
IC	0.71895	10.4350	0.003243	***
TS	0.04688	0.6804	0.416668	n.s.
IC:TS	0.04784	0.6944	0.411998	n.s.

Table 20: TukeyHSD results for evolved carbenicillin resistance. The test compares the difference in mean resistance (AUC) between the individual treatment groups. Formula: $AUC \sim Treatment$. Asterisks represent significant difference between two treatment groups (* = $p < 0.05$, n.s. = $p > 0.05$).

Comparison	diff	p adj.	Significance
IC20 M5-IC20 k50	0.153843750	0.6490516	n.s.
IC80k50-IC20 k50	0.386317411	0.0394518	*
IC80 M5-IC20 k50	0.382764063	0.0334898	*
IC80 k50-IC20 M5	0.232473661	0.3376358	n.s.
IC80 M5-IC20 M5	0.228920313	0.3214733	n.s.
IC80 M5-IC80 k50	-0.003553348	0.999993	n.s.

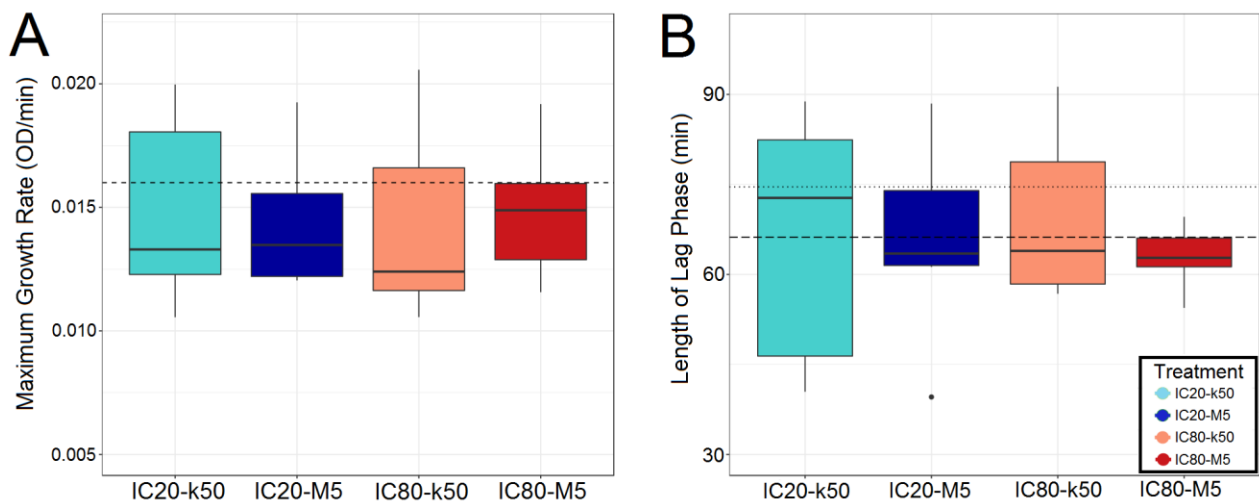


Figure 17: CAR-adapted lineages have slightly lower growth in drug-free medium. (A) maximum growth rate (OD/min); (B) length of lag phase (min). Measurements were taken in absence of antibiotics. The X-axes and colors represent different treatment groups. 8 biological replicates. The Y-axes represent the growth parameters of the treatment groups after the evolution experiment. Mean fitness of control groups is represented by black horizontal lines: (A) dotted line represents both transfer sizes; (B) long-dashed line represents M5; short-dashed line represents k50.

Evolutionary genomics

WGS was performed for lineages from the final transfer of the evolution experiments to identify mutations that have occurred during the experiment and that may have caused changes in fitness and resistance. In addition, DNA was also extracted and sequenced from an earlier time point of the evolution experiment, transfer 3. At that time point, the bacteria had already overcome the strongest fitness deficit, but fixation of specific beneficial mutations would not have been expected yet. The genomic analyses of the additional early time point were done to investigate if early adaptation is due to genetic change and – if so – whether early adaptation was caused by the same beneficial mutations that can be found at the final time point or by different mutations.

Mutations in two-component regulators and *ptsP* dominate populations of GEN evolution experiment

A detailed summary of all mutations that were found in the endpoint populations of the GEN experiment is provided in Supplementary Table S7 (page 179). In the genomic dataset of the GEN evolution experiment, an overall high diversity of genes was found to be mutated. More than a dozen genes from different classes were found to be mutated, of which the two-component regulatory systems PmrAB, ParRS and PhoPQ were the most affected genes (see Figure 18).

In the IC20-M5 treatment group, mutations in *ptsP* were found in all replicate populations at high frequencies (dark blue box in Figure 18). For IC80-M5, mutations in either *pmrB* (4/7) or *ptsP* (3/7) were dominant at transfer 16 (dark red box in Figure 18). Interestingly, all three replicate populations with mutations in *ptsP* at transfer 16 showed mutations in *pmrB* at transfer 3. This indicates that *pmrB* mutations were replaced by more advantageous mutations in *ptsP* over the course of the experiment. This was especially remarkable since populations dominated by *ptsP* mutations showed a lower resistance than populations in which *pmrB* mutations were most frequent (Figure 20). For IC20-k50, a higher mutational diversity was observed, with most genes affected by mutations belonging to two-component regulators (light blue box in Figure 18). *pmrB* and *parR* mutations (each 3/8) were present in several replicates. In addition, unique mutations in *envZ* and the uncharacterized *PA14_08640* were found in single replicate populations. Single populations of the IC80-k50 treatment also carried unique

mutations in *fusA1*, *cysJ* and *waaL*. Again, most mutations in this treatment group also were found in two-component regulators (*parS* 3/8, *phoQ* 2/8, *pmrB* 1/8) and *ptsP* (2/8) (light red box in Figure 18).

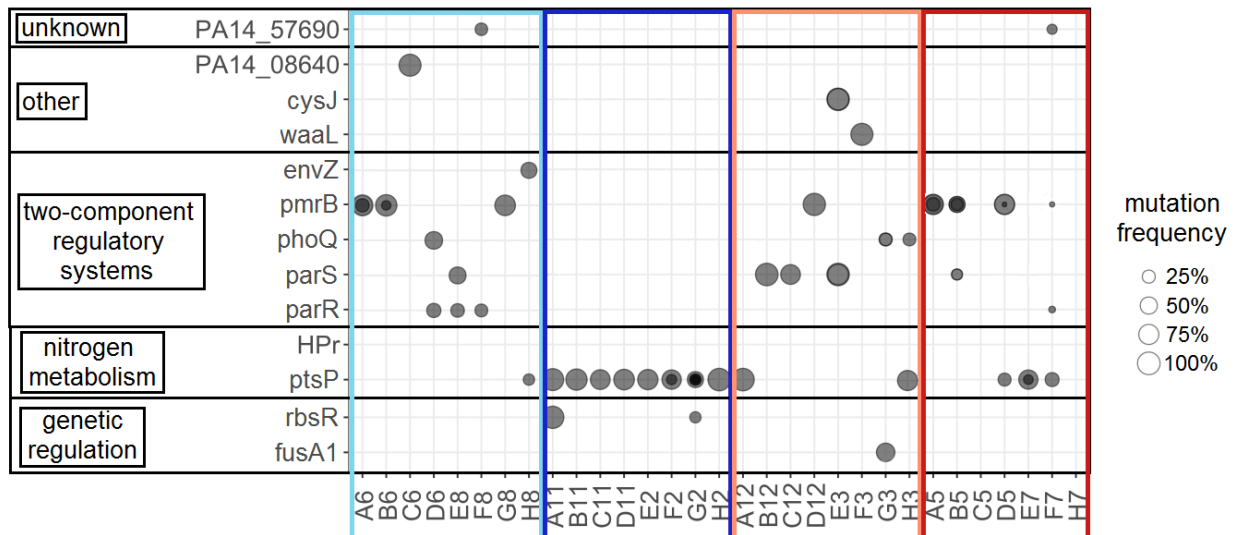


Figure 18: Most mutations in evolved populations of GEN evolution experiment found in two-component regulators and *ptsP*. The X-axis represents replicate populations. The Y-axis represents mutated genes. Dots represent mutations found in respective gene/population. The size of dots corresponds with the frequency of mutations within a population. Grey dots represent mutations found at transfer 16 of the evolution experiment. Dark dots represent multiple mutations found in the same gene at transfer 16. Black boxes represent gene function. Colored boxes represent treatment group of populations: Light blue: IC20-k50, Dark blue: IC20-M5, Light red: IC80-k50, Dark red: IC80-M5.

Overall, genetic diversity based on Shannon’s diversity indices was higher in the small TS groups than in the large TS groups (see Table 21). Not only were a high number and a high diversity of mutated genes found in the GEN dataset, but also multiple mutations in the same gene were often found in several replicates. Many mutations occurred at high frequencies. However, only two mutations were found at such high frequencies in two respective populations that they unquestionably qualify as double mutants (A11: *ptsP* + *rbsR*; E3: *parS* + *cysJ*). For most other populations, an increase in the total number of mutations was associated with a decrease in frequency of the most dominant mutation (-0.677 Pearson's product-moment correlation, $p < 0.005$; see Figure 19). This result does not prove clonal interference. Nevertheless, this trend indicates that multiple mutations in a population were more likely to occur in several different genetic variants than in only one.

Table 21: Gentamicin: Shannon’s diversity indices H and Hmax for each treatment group.

Antibiotic	Treatment	Shannon’s H	Hmax
GEN	IC20-k50	3.273	3.459
GEN	IC20-M5	2.040	2.585
GEN	IC80-k50	2.855	3
GEN	IC80-M5	2.046	2.322

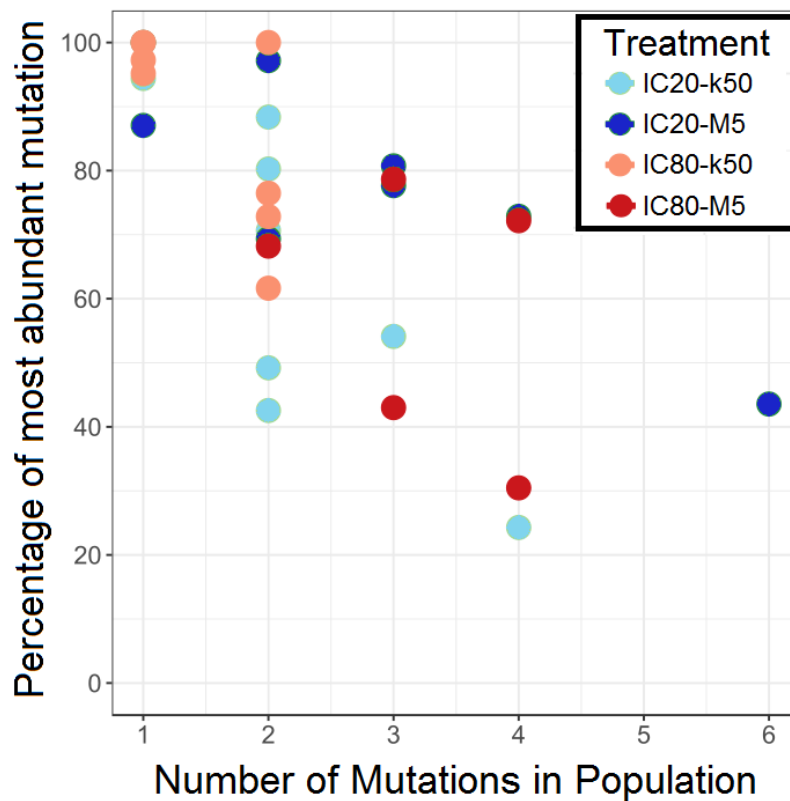


Figure 19: Frequency of the most common mutation in a population decreases with the total number of mutations in GEN evolution experiment. The X-axis represents total number of mutations found in each population. The Y-axis represents frequency of most frequent mutation in population. Colors refer to different treatment groups: Light blue: IC20-k50, Dark blue: IC20-M5, Light red: IC80-k50, Dark red: IC80-M5.

As *pmrB* and *ptsP* were the most commonly mutated genes across all treatment groups, the resistance of the populations dominated by mutations in either gene was compared. Overall, populations with dominant mutations in *pmrB* had higher resistance than populations dominated by *ptsP* mutations ($p < 0.005$, Welch's t-test; see Figure 20). *pmrB* did not occur in IC20-M5. Instead, all replicate populations of that group were dominated by *ptsP* mutations. This potentially indicates that *ptsP* mutants were selectively favored in the IC20-M5 treatment, which may have introduced a bias to the statistical test. However, a higher resistance in *pmrB* mutants was also observed in treatment groups where either genetic variant was dominating at least one population.

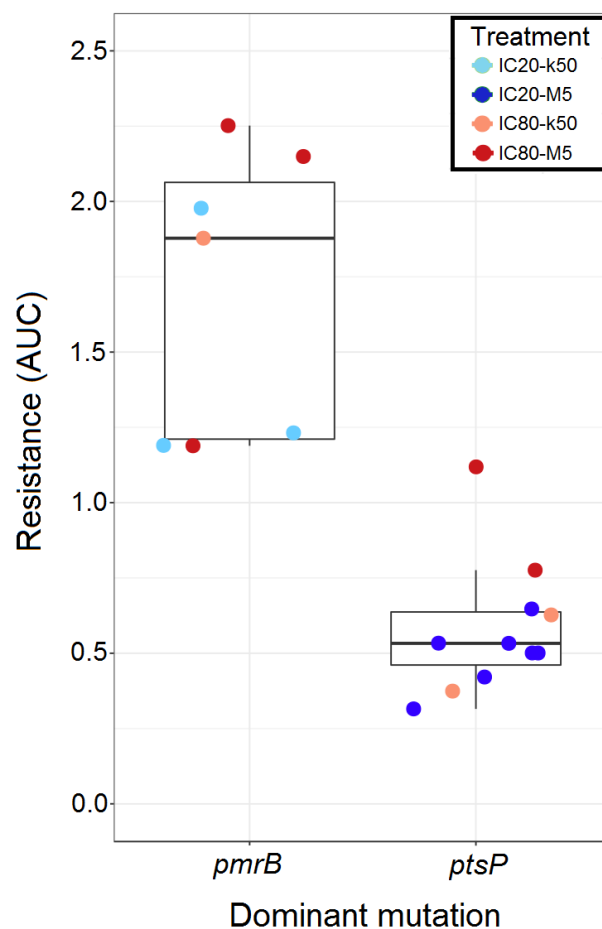


Figure 20: Populations with the most frequent mutation in *ptsP* show lower resistance than populations with the most frequent mutation in *pmrB*. The X-axis represents genes affected by most frequent mutations. The Y-axis represents AUC as a proxy for resistance to GEN. Colors refer to different treatment groups: Light blue: IC20-k50, Dark blue: IC20-M5, Light red: IC80-k50, Dark red: IC80-M5. Asterisks represent significant difference between two treatment groups ($* = p < 0.05$; Welch's t-test).

In summary, mutations in either one of two genes dominated populations of large TS: *pmrB* mutants were most common in IC80-M5 populations and *ptsP* mutants dominated IC20-M5 populations. Alteration of *pmrB* seems to be associated with high GEN resistance whereas *ptsP* mutations conferred lower resistance. A higher diversity of genes was affected by mutations under strong bottleneck regimens, with most mutated genes being functionally associated with two-component regulatory systems. There was only little proof of fixed genotypes carrying multiple mutations.

Mutations in multidrug efflux regulators dominate populations of CIP evolution experiment

A detailed summary of all mutations that were found in the endpoint populations of the CIP experiment is provided in Supplementary Table S5 (page 169). For CIP, mutations were identified primarily in genes that are associated with multidrug efflux pumps, especially negative regulators of efflux pumps (Figure 21). Based on population genomics of the sequencing data, Shannon's H was calculated as a measure of genetic diversity within the treatment groups (Table 22). Compared to GEN (Table 21), most treatment groups that evolved under CIP treatment displayed low genetic diversity, with only IC20-k50 displaying high H by the end of the experiment.

Table 22: Ciprofloxacin: Shannon's diversity indices H and Hmax for each treatment group.

Antibiotic	Treatment	Shannon's H	Hmax
CIP	IC20-k50	2.436	2.807
CIP	IC20-M5	1.585	1.585
CIP	IC80-k50	1	1
CIP	IC80-M5	0.971	1

Highly frequent mutations were not discovered in the IC20-M5 treatment group. This was interesting because populations of this group showed a much higher yield than the control group at the end of the experiment despite evolving no resistance. Based on the genomic data, this response had no genetic foundation. In four IC80-M5 populations, mutations in an uncharacterized ABC transporter gene (*PA14_09300*) were present at transfer 3 at intermediate

frequencies. At transfer 16, these mutations were no longer present and instead had been replaced by mutations in *nfxB* (4/8 populations) and *mexS* (6/8). For IC20-k50, a higher mutational diversity (Shannon's H 2.436) could be observed, with most mutations occurring in *mexZ* (6/8, including 3 with additional mutations in *tetR*) and *mexS* (3/8). Mutations in *nalC*, *nfxB* and *PA14_09300* were found in different single populations. For the IC80-k50 treatment, only one replicate population survived until the end of the experiment. This population showed a mutation in *PA14_09300*, the same ABC transporter that was found to be mutated at transfer 3 for some IC80-M5 populations but later outcompeted by mutations in RND efflux systems.

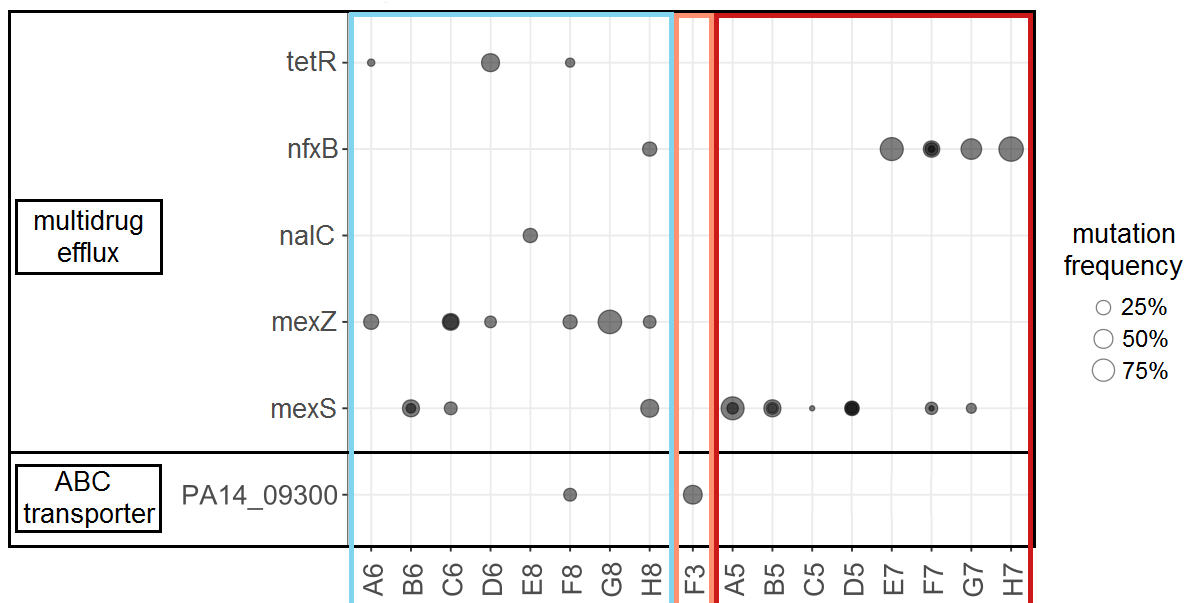


Figure 21: Most mutations in evolved populations of CIP evolution experiment found in multidrug efflux regulators. The X-axis represents replicate populations. The Y-axis represents mutated genes. Dots represent mutations found in respective gene/population. The size of dots corresponds with the frequency of mutations within a population. Grey dots represent mutations found at transfer 16 of the evolution experiment. Dark dots represent multiple mutations found in the same gene at transfer 16. Black boxes represent gene function. Colored boxes represent treatment group of populations: Light blue: IC20-k50, Light red: IC80-k50, Dark red: IC80-M5.

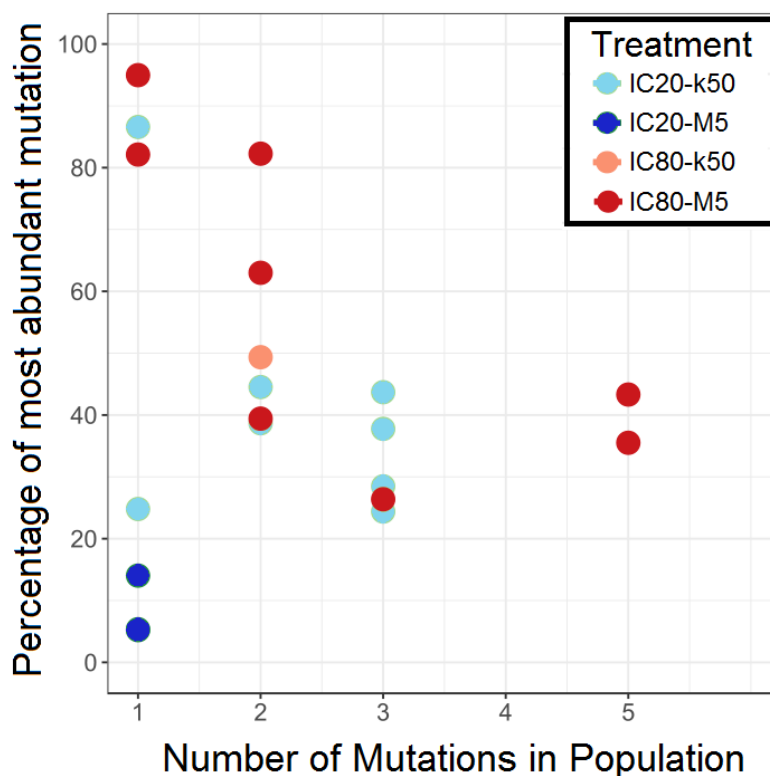


Figure 22: Frequency of the most common mutation in a population decreases with the total number of mutations in CIP evolution experiment. The X-axis represents total number of mutations found in each population. The Y-axis represents frequency of most frequent mutation in population. Colors refer to different treatment groups: Light blue: IC20-k50, Dark blue: IC20-M5, Light red: IC80-k50, Dark red: IC80-M5.

In general, only few mutations were found to have completely fixed by the last growth period and most mutations only occur at low frequencies $< 50\%$. This may indicate that fitness benefits of the detected mutations were rather small, and that selection of mutated alleles was rather weak. In addition, very few mutations were already present at transfer 3. This indicates that a phenotypic response to the selective pressure occurred first and that mutants with high efflux occurred only at later stages of the experiment. As previously observed in the GEN dataset, an increase in the total number of mutations per population was associated with a decrease in frequency of the most dominant mutation also in the CIP dataset (Figure 22).

In conclusion, no resistance mutations could be detected under IC20-M5. In those treatment groups that did evolve resistance, all mutated genes were associated with drug efflux. A higher diversity of mutated genes was identified for small TS than for large TS, with only *nfxB* and *mexS* mutants dominating the IC80-M5 treatment. No evidence of double mutants could be found.

Evolutionary allele dynamics

To uncover and reconstruct the underlying adaptive dynamics of the evolving populations over the course of the experiment, frozen populations from intermediate transfer periods were regrown in 2 ml M9 and DNA was extracted according to the CTAB protocol. WGS was performed and genetic variants were identified with the previously described approach. A detailed overview of the frequencies of all high-frequency mutations that were identified in the evolution experiments at different transfers is provided in Supplementary Tables S6 (CIP, page 171 ff) and S8 (GEN, page 182 ff).

Populations adapt faster under large TS in GEN evolution experiment

The different treatment groups of the GEN evolution experiment are summarized in Figures 23-26 and show distinct adaptive allele dynamics. Both small TS groups acquired a high variation of mutated genes. However, populations of the IC80 group adapted much faster. Mutations first appeared at transfer 3 or 5 and subsequently increased in frequency at a high rate (Figure 25). In contrast, populations of the IC20 population adapted slowly. With replicate population A6 as the lone exception, first mutations commonly occurred at around transfer period 7 or 9 and reached high frequencies only during the second half of the experiment (Figure 23). In addition, I observed more competitive dynamics in the IC20 group. In populations C6, D6, E8 and H8, mutations that were found to dominate the population at an intermediate time point decreased in frequency by the end of the experiment while the frequencies of other mutations increased (Figure 23). In contrast, single clones dominated the allele dynamics in the IC80 group (e.g. replicates A12, B12, D12, E3, F3; figure 25). Mutations were selected early and had outcompeted others by the end of the experiment.

Unlike the small TS populations (k50), populations of the large TS treatment groups (M5) showed a clear trend towards few mutated genes. In the IC20-M5 group, all populations carried dominant mutations in the gene *ptsP*, with most populations carrying more than one *ptsP* mutation. In most populations, the first *ptsP* mutations occurred by transfer 5 or 7 and slowly took over the population (Figure 24). In the replicates A11, E2 and F2, competitive dynamics between *ptsP* and *pmrB* mutations took place. In all cases, *ptsP* won the competition and *pmrB* was lost from the population by transfer 11 (Figure 24). In the IC80-M5 group,

mutations in *pmrB* achieved high frequencies by transfer 3 (Figure 26). In most replicates, the frequencies of the early mutations remained on the same level for most transfer periods of the evolution experiment. However, in several populations (D5, E7, F7, H7) mutations in *ptsP* occurred and rose in frequencies towards the end of the experiment. In all replicates, clonal interference was observed between at least two different mutations (Figure 26).

In conclusion, the antibiotic concentrations primarily seemed to influence the speed of adaptation. Mutants took many generations to increase in frequency under low IC regimens. In contrast, mutants found in high IC treatments increased in frequency comparatively quickly. On the other hand, bottleneck size also influenced the speed of adaptation under high IC but primarily influenced which mutants were selected. Under large TS, the dominant mutants of *pmrB* and *ptsP* were always selected early. In contrast, allele selection was less specific under low TS.

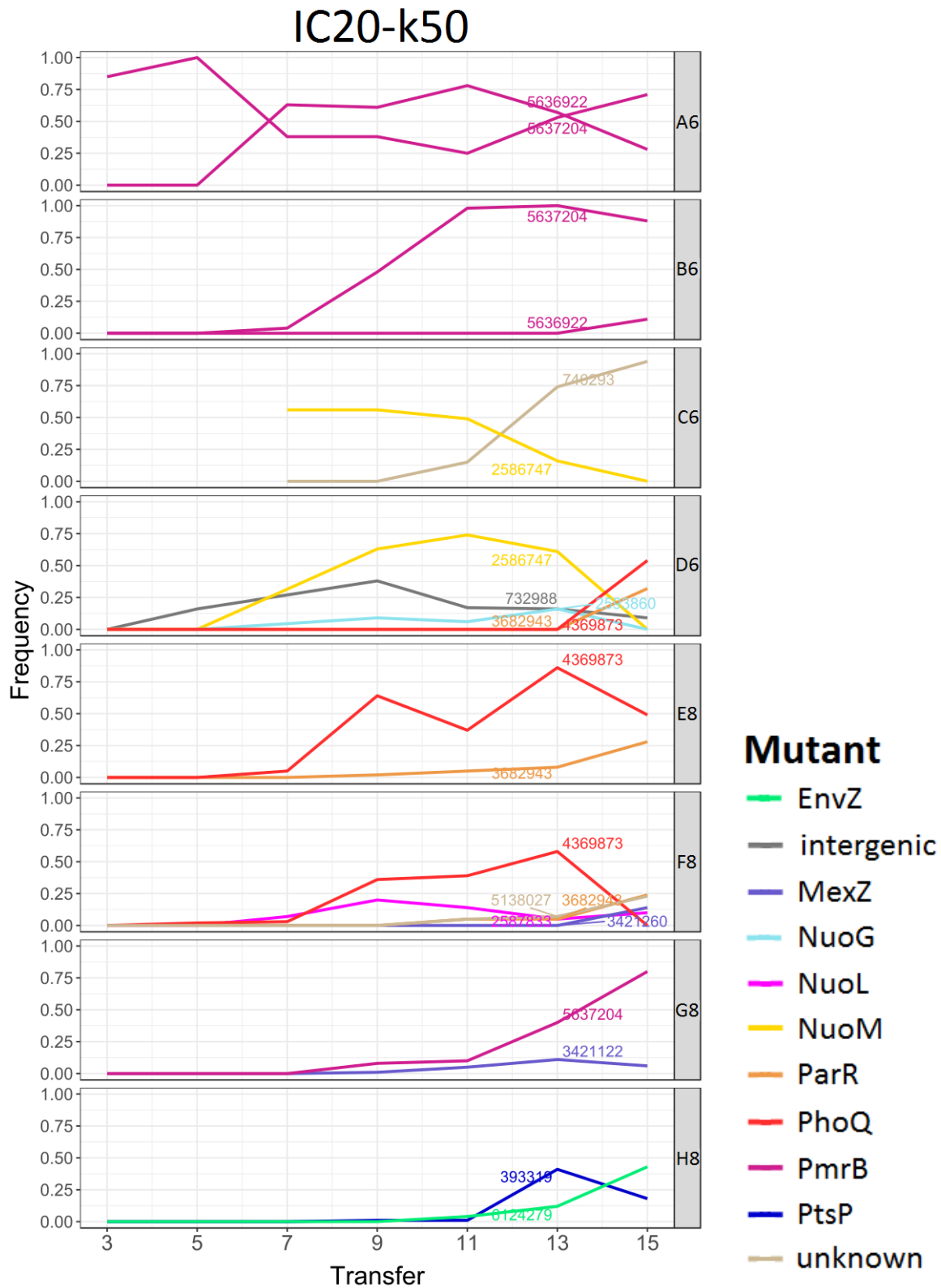


Figure 23: Complex evolutionary allele dynamics between mutations in various genes found in IC20-k50 populations of GEN evolution experiment. Population names are given in the boxes right of the graphs. The X-axis represents transfer. The Y-axis represents frequency of mutation in population. Colors refer to different genes that the mutations appear in (see legend on right). Line annotations refer to the position of the mutation in the PA14 genome.

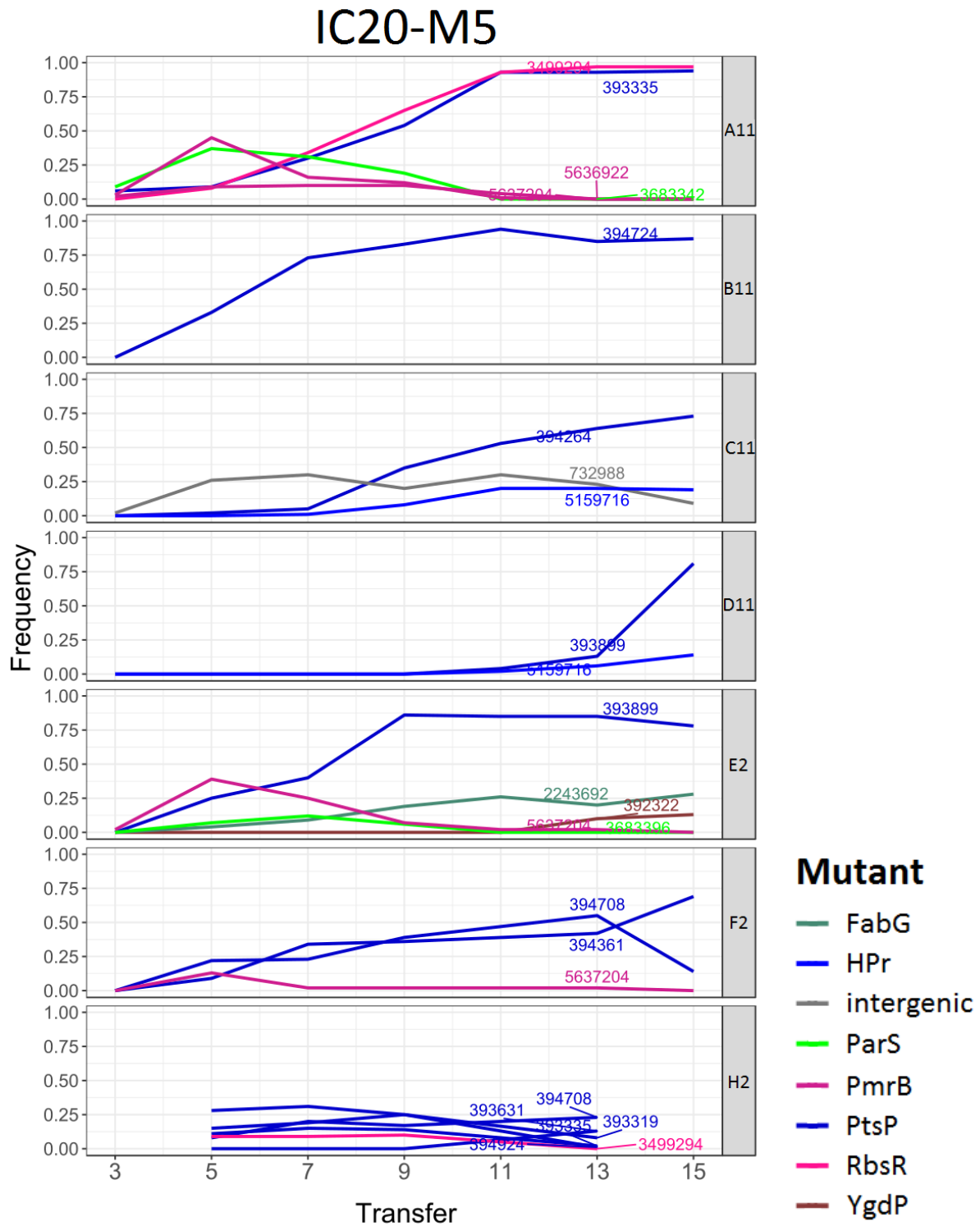


Figure 24: Mutations in *ptsP* dominate evolutionary allele dynamics in IC20-M5 populations of GEN evolution experiment. Population names are given in the boxes right of the graphs. The X-axis represents transfer. The Y-axes represent frequency of mutation in population. Colors refer to different genes that the mutations appear in (see legend on right). Line annotations refer to the position of the mutation in the PA14 genome.

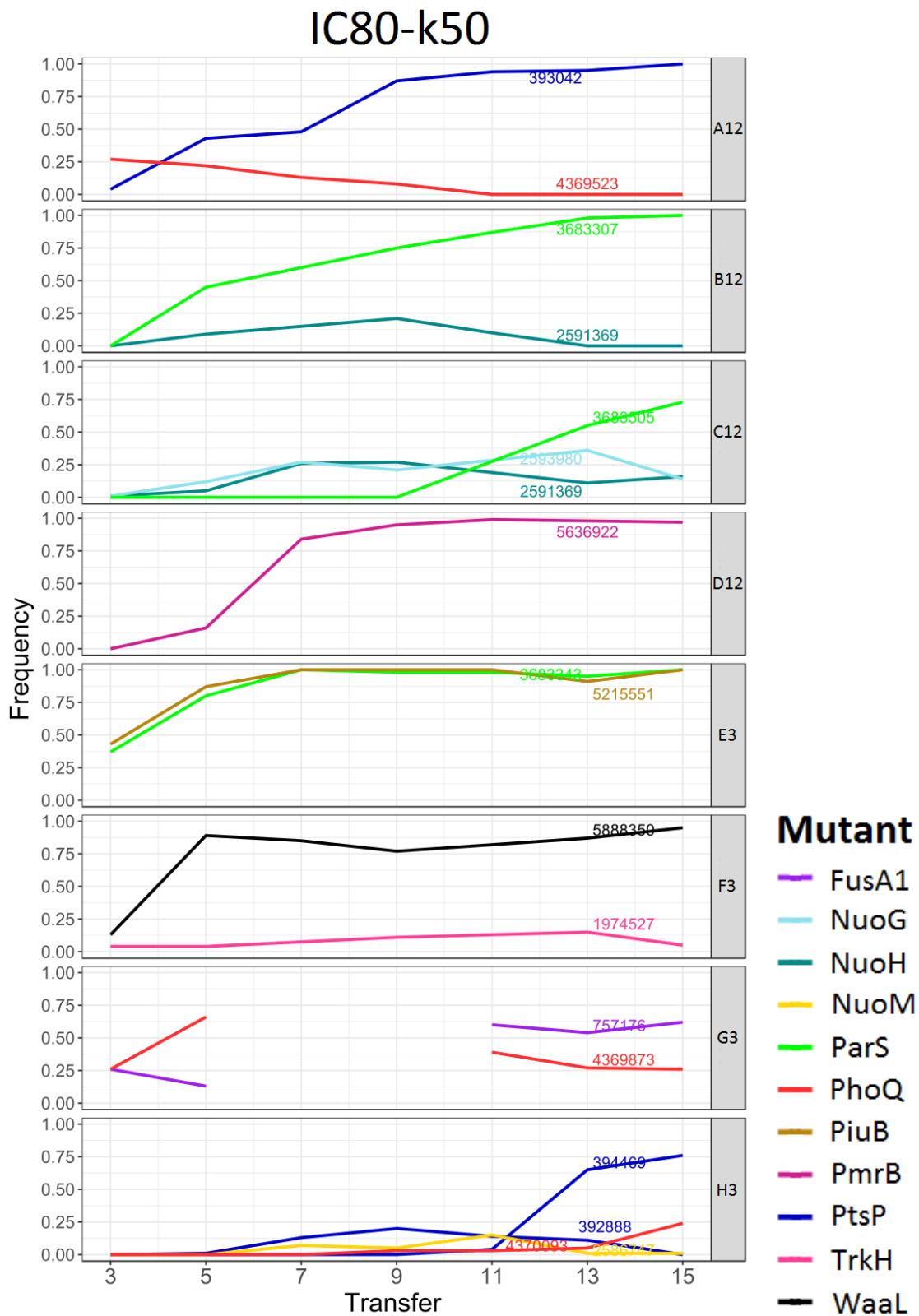


Figure 25: Single mutations in different genes dominate evolutionary allele dynamics in IC80-k50 populations of GEN evolution experiment. Population names are given in the boxes right of the graphs. The X-axis represents transfer. The Y-axis represents frequency of mutation in population. Colors refer to different genes that the mutations appear in (see legend on right). Line annotations refer to the position of the mutation in the PA14 genome.

IC80-M5

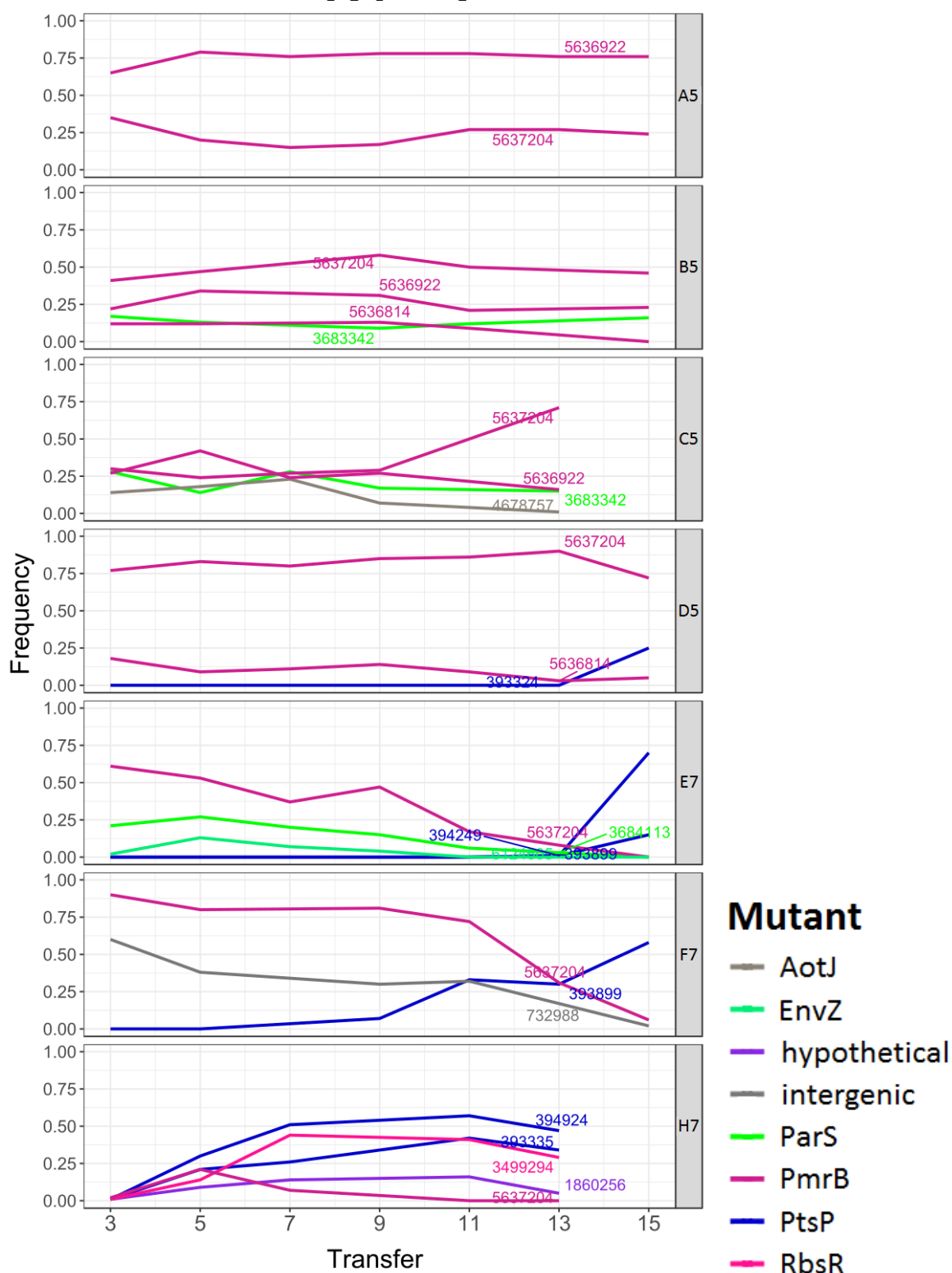


Figure 26: Mutations in *pmrB* dominate evolutionary allele dynamics in IC80-M5 populations of GEN evolution experiment. Population names are given in the boxes right of the graphs. The X-axis represents transfer. The Y-axes represent frequency of mutation in population. Colors refer to different genes that the mutations appear in (see legend on right). Line annotations refer to the position of the mutation in the PA14 genome.

Increased clonal competition during CIP evolution experiment

Some aspects of the evolutionary genomics of the CIP-adapted populations were similar to the results of the GEN experiment. However, there were also some important differences to point out. First, most replicate populations for the IC80-k50 group went extinct early in the experiment which did not allow me to quantify aspects of adaptation of that treatment. The only surviving population carried a mutation in the ABC transporter gene *PA14_09300*, which also occurred in early transfers of some replicates of other treatment groups. In addition, no genetic variants could be detected in the IC20-M5 group at significant frequencies. Potential reasons for the deviating evolutionary genomics of these two treatment groups will be addressed in the discussion part of the thesis. In the following segment, the results of the evolutionary allele dynamics of the IC20-k50 (Figure 27) and the IC80-M5 (Figure 28) groups will be presented, as only these groups showed signs of evolutionary adaptation (i.e., manifestation and selection of mutations). The two different treatment groups showed different adaptive dynamics, with a higher number of mutated genes found in the small TS group. Both groups showed a similar degree of clonal interference, with multiple clones arising in most populations at the same time. Competitive dynamics were rare in both two groups.

Populations of the IC20-k50 group adapted slowly (Figure 27). The first mutations occurred only after transfer 5 in all populations and – with replicate population G8 as the lone exception – did not reach high frequencies of >50% by the end of the experiment. Despite the high degree of clonal interference, adding up the frequencies of the individual mutations never resulted in a total mutant frequency of 100%, meaning that the Wt was still present by the end of the experiment at substantial frequencies. *mexZ* was the most frequently mutated gene of the group (found in 6 out of 8 populations), followed by *mexS* (5).

Populations of the IC80-M5 treatment group had only few mutated genes (Figure 28). *nfxB* mutants were the most frequent genotype in 5 out of 8 populations, with *mexS* dominating the remaining three. Four populations (A5, B5, D5, F7) also had two or more mutations in the same gene. The first mutations occurred by transfer 5 and subsequently increased in frequency. The total mutant frequency was higher than in the IC20-k50 group by the end of the experiment, but it never reached 100% either.

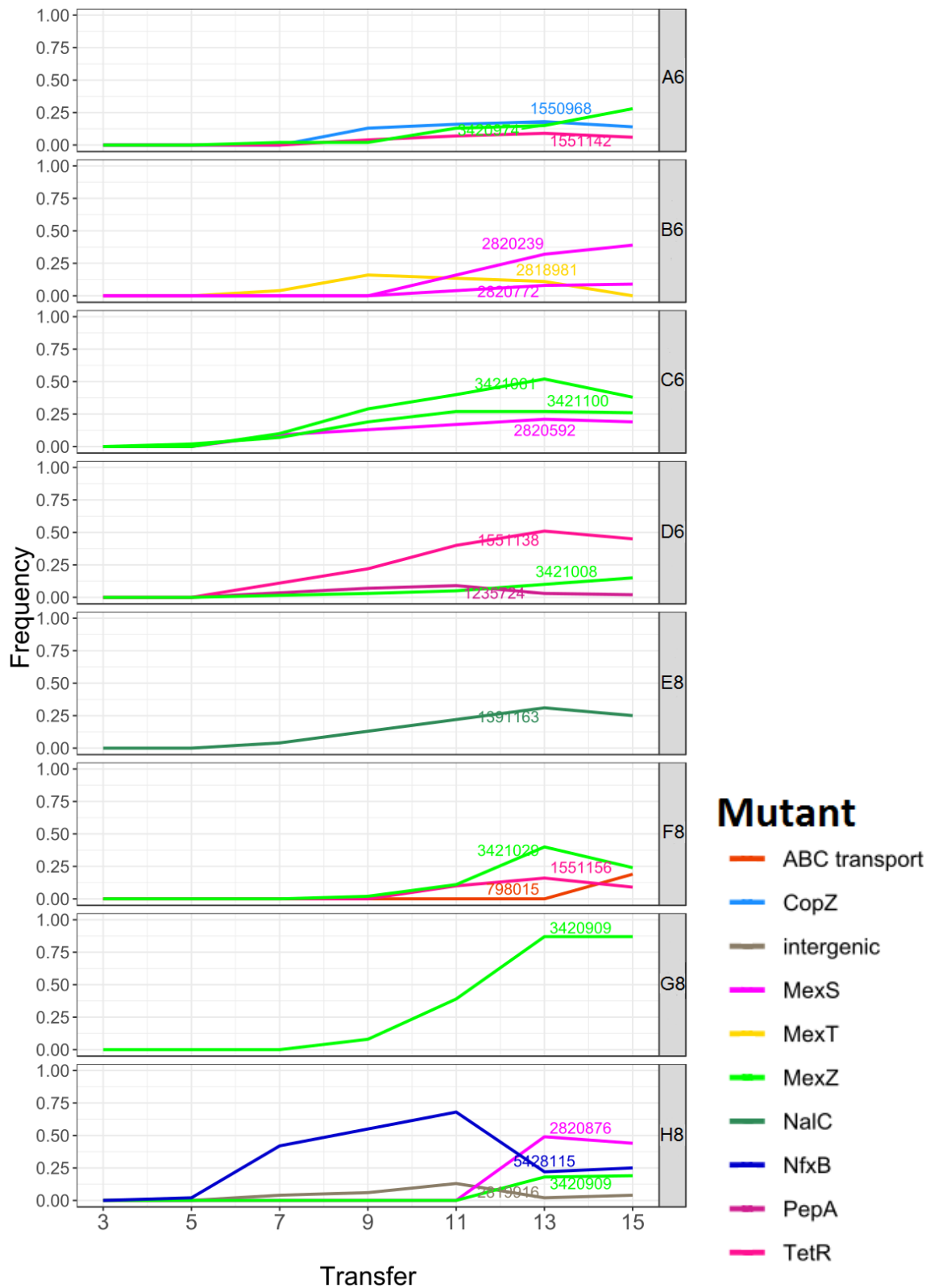


Figure 27: Clonal interference between mutations in different genes shapes evolutionary allele dynamics in IC20-k50 populations of CIP evolution experiment. Population names are given in the boxes right of the graphs. The X-axis represents transfer. The Y-axis represents frequency of mutation in population. Colors refer to different genes that the mutations appear in (see legend on right). Line annotations refer to the position of the mutation in the PA14 genome.

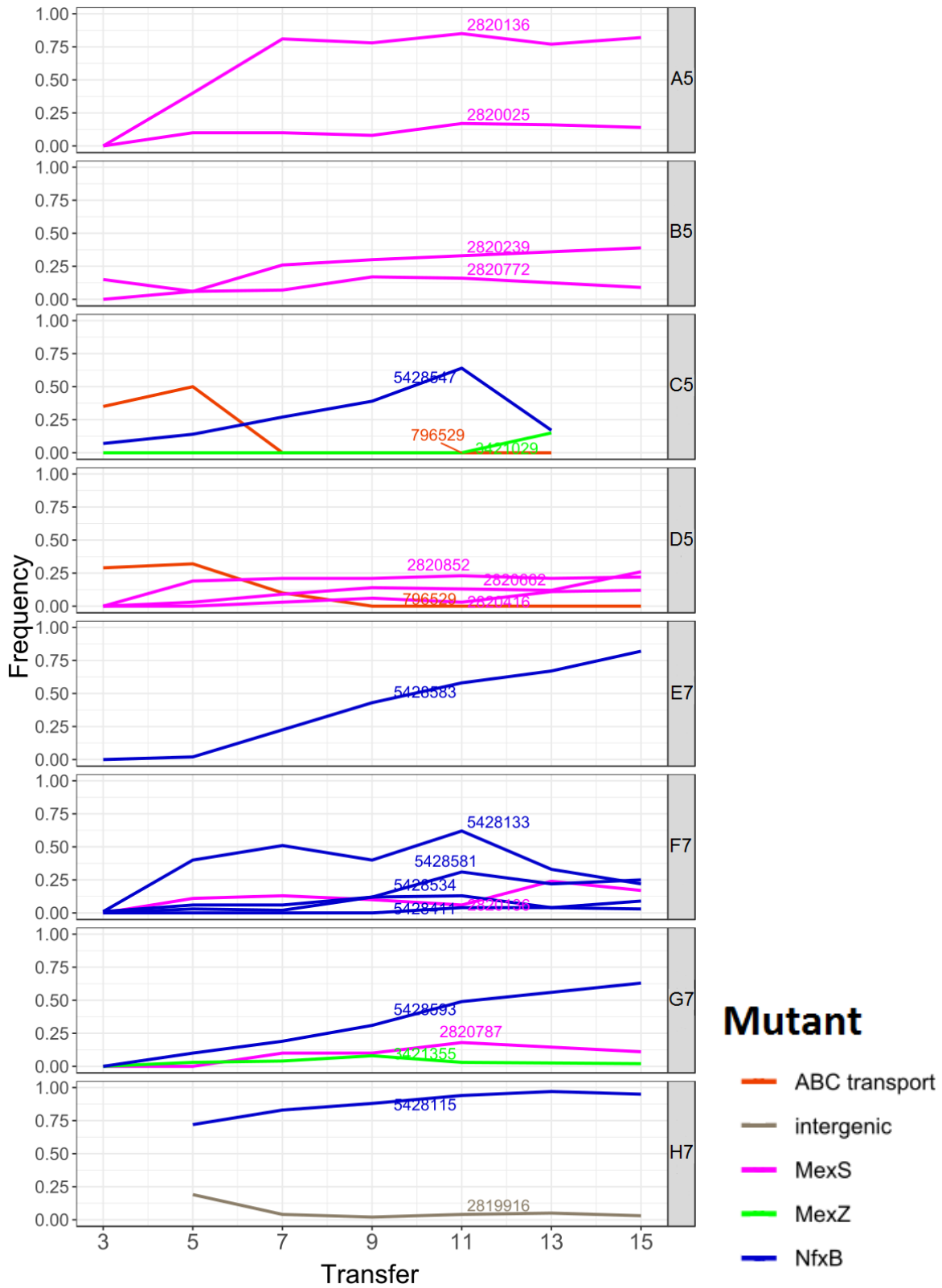


Figure 28: Mutations in *mexS* and *nfxB* dominate evolutionary allele dynamics in IC80-M5 populations of CIP evolution experiment. Population names are given in the boxes right of the graphs. The X-axis represents transfer. The Y-axis represents frequency of mutation in population. Colors refer to different genes that the mutations appear in (see legend on right). Line annotations refer to the position of the mutation in the PA14 genome.

Fixation indices (FST)

Treatment groups show unique changes in diversity metrics during the GEN evolution experiment

To evaluate the allele dynamics of the evolving populations statistically, the population genomic dataset was used to calculate the fixation index (FST) for each treatment group and time point. FST is a commonly used metric to assess genetic differentiation of populations. The FST calculations used in this thesis were based on the haplotype diversity within populations (HS) and the haplotype diversity between populations (HT). HS was calculated as the mean of haplotype diversity of all individual replicate populations in a treatment group. HT was calculated by summing up the frequencies of all haplotypes in the entire treatment group.

HT dynamics could be described by an asymptotic increase in all treatment groups apart from IC80-M5 (see Figure 29A). In the beginning, IC80-M5 had the highest HT (~ 0.8) which fluctuated slightly but did not substantially change over the course of the experiment. In contrast, the other treatment groups had a low initial HT of < 0.4 with IC80-k50 showing the highest and IC20-M5 the lowest initial HT. The initial increase of HT was faster in IC80-k50 and IC20-M5 than in IC20-k50. Eventually, all groups reached very close HT of ~ 0.85 by the end of the experiment, with IC80-k50 reaching a slightly higher HT of ~ 0.9. All curves were flattening after transfer 9. It is critical to emphasize that HT was calculated based on frequencies of individual SNPs and not their affected genes. All populations of the IC20-M5 group carried (often multiple) mutations in *ptsP*. However, the diversity of the variants was quite substantial, with only 5 out of 13 variants occurring more than once in the dataset. This high diversity of alleles explains the high HT.

HS was generally small compared to HT and had very different dynamics (Figure 29B). In summary, HS increased initially and decreased again after having reached its maximum. IC80-k50, IC20-M5 and IC80-M5 all reached their respective HS maxima by transfer 7 while IC20-k50 reached its maximum at the last transfer. Both IC80 groups had much higher initial HS at transfer 3 than the IC20 groups. This indicates that the first variants had already occurred in the IC80 treatments but not in IC20 treatments. IC80-M5 showed the highest HS over the course of the entire experiment with slightly below 0.6. IC80-k50 on the other hand had the second-highest HS at the beginning of the experiment but the lowest by its end (~ 0.19), as well as the lowest peak of all treatment groups (~ 0.38). IC20-M5 showed the strongest increase of all groups with ~ 0.5 between transfer 3 and transfer 7.

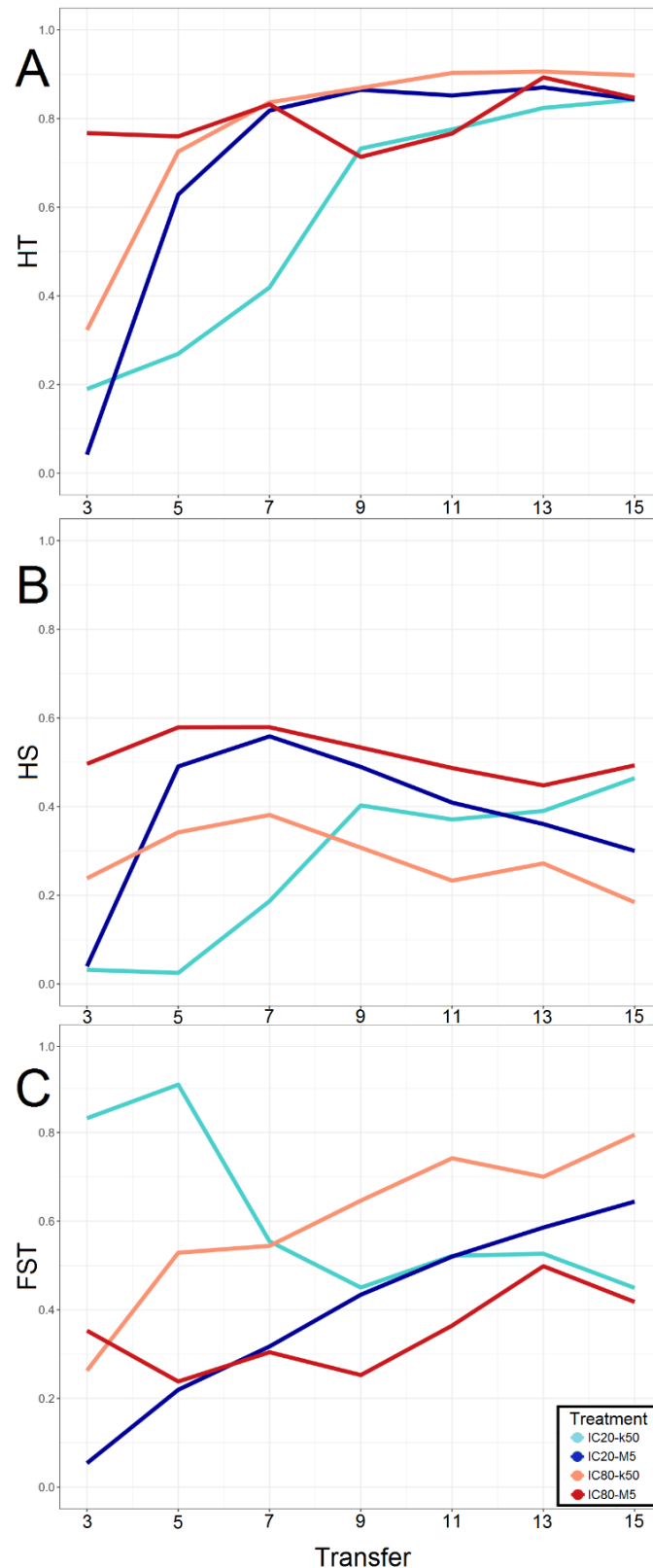


Figure 29: Treatment groups show unique changes in diversity metrics during the GEN evolution experiment. **A:** HT dynamics (haplotype diversity between populations); **B:** HS dynamics (haplotype diversity within populations); **C:** FST dynamics (genetic differentiation of populations). The X-axis represents transfer. The Y-axes represent the respective diversity metric. Colors refer to different treatment groups: Light blue: IC20-k50, Dark blue: IC20-M5, Light red: IC80-k50, Dark red: IC80-M5.

Taken together, these results translated to the following dynamics of the FST (Figure 29C): Initially, the FST was low in all treatment groups (< 0.4), with IC80-50 being the only exception (~ 0.83). The cause for the high initial FST in IC80-50 is the extremely low HS in season 3. As a mutation in *pmrB* was already dominating population A6, HT was substantially higher than HS, resulting in a high FST. Thus, the high FST could be explained by a single population being substantially different from the others. On the other hand, all populations in IC80-M5 had already acquired multiple mutations at increased frequencies by season 3, resulting in an intermediate initial FST. After the first couple of transfers, the FST also increased in the IC20-M5 and IC80-k50 groups. This was caused by the first couple of mutants establishing themselves in the populations. In both groups, the FST gradually increased throughout the experiment, translating to the increasing fixation of different mutations in the populations. As the diversity of alleles in the dataset was high and different variants became dominant in individual populations, the FST increased. In contrast, the FST in the IC20-k50 and IC80-M5 groups leveled off at intermediate values in the second half of the experiment. These dynamics underline the clonal interference between different alleles in populations of both treatment groups. In IC80-M5, clonal interference between the same alleles was observed in several populations. Thus, the overall FST only changed slightly throughout the experiment. In IC20-k50 on the other hand, multiple mutations increased to relevant frequencies only in the second half of the experiment which translated to an intermediate FST. Overall, the FST dynamics further highlight observations made for the allele dynamics data: Under large TS, several mutants replaced the Wt quickly, but the population diversified rather slowly afterwards. Under IC80-k50, Wt was quickly replaced by a single haplotype. Under IC20-k50 on the other hand, Wt was maintained for the longest stretch of the experiment.

Competition Assays

Growth advantage of *ptsP* over *pmrB* decreases under high IC

Note: The results in this section were obtained in collaboration with Alexandra Tietze as part of her BSc thesis.

The outcome of the evolutionary allele dynamics of the GEN evolution experiment showed that *ptsP* and *pmrB* are the most commonly mutated genes in the two most selective groups of the large TS, IC20-M5 and IC80-M5. Several cases of competitive dynamics between

ptsP and *pmrB* mutants were also found in the allele dynamics dataset. Thus, three evolved clones of each genetic variant were selected from different treatment groups to model competitive dynamics of different genotypes under the applied experimental conditions. The relative fitness of the selected clones was determined by performing three competition experiments under the same treatment conditions that were applied for the evolution experiment. Three sets of pairwise competition experiments were performed, in which evolved clones with mutations in either *pmrB* or *ptsP* competed against one another or against the ancestral clone PA14 (Table 23). After competition, the individual SNP regions were amplified by PCR and Illumina sequencing was performed on the amplicons. The obtained Illumina sequencing reads were used to calculate the SNP frequencies of the two competing strains after the competition. The relative frequencies of the different strains for each treatment condition are summarized in Figure 30.

The first pair of mutants included the clones *pmrB*-D12 and *ptsP*-A12 which evolved in the IC80-k50 treatment group (Figure 30A). Both clones were the only *ptsP* and *pmrB* mutants that occurred in this treatment group of the evolution experiment. The second mutant pair consisted of clones that evolved in the IC20 treatment groups (Figure 30B). *PmrB*-A6-6 evolved under IC20-k50 treatment where low antibiotic concentration and small TS led to diverse fixation of mutations. However, no mutations in *ptsP* were fixed in the IC20-k50 group. In contrast, mutations in *ptsP* were almost exclusively selected in the evolution experiment of the IC20-M5 group, with *ptsP*-B11 being one of the clones. Since *pmrB* mutants only occurred in IC20-k50 and in *ptsP* mutants only in IC20-M5, clones from both treatment groups were combined in the respective competition experiments. The third mutant pair included the clones *pmrB*-A5-4 and *ptsP*-E7-8 which evolved in the IC80-M5 treatment group of the evolution experiment (Figure 30C).

Table 23: Clones used in the three competition experiments.

Experiment	Previous treatment group	<i>pmrB</i> mutant	<i>ptsP</i> mutant	control
1	IC80-k50	D12	A12	PA14
2	IC20	A6-6 (k50)	B11 (M5)	PA14
3	IC80-M5	A5-4	E7-8	PA14

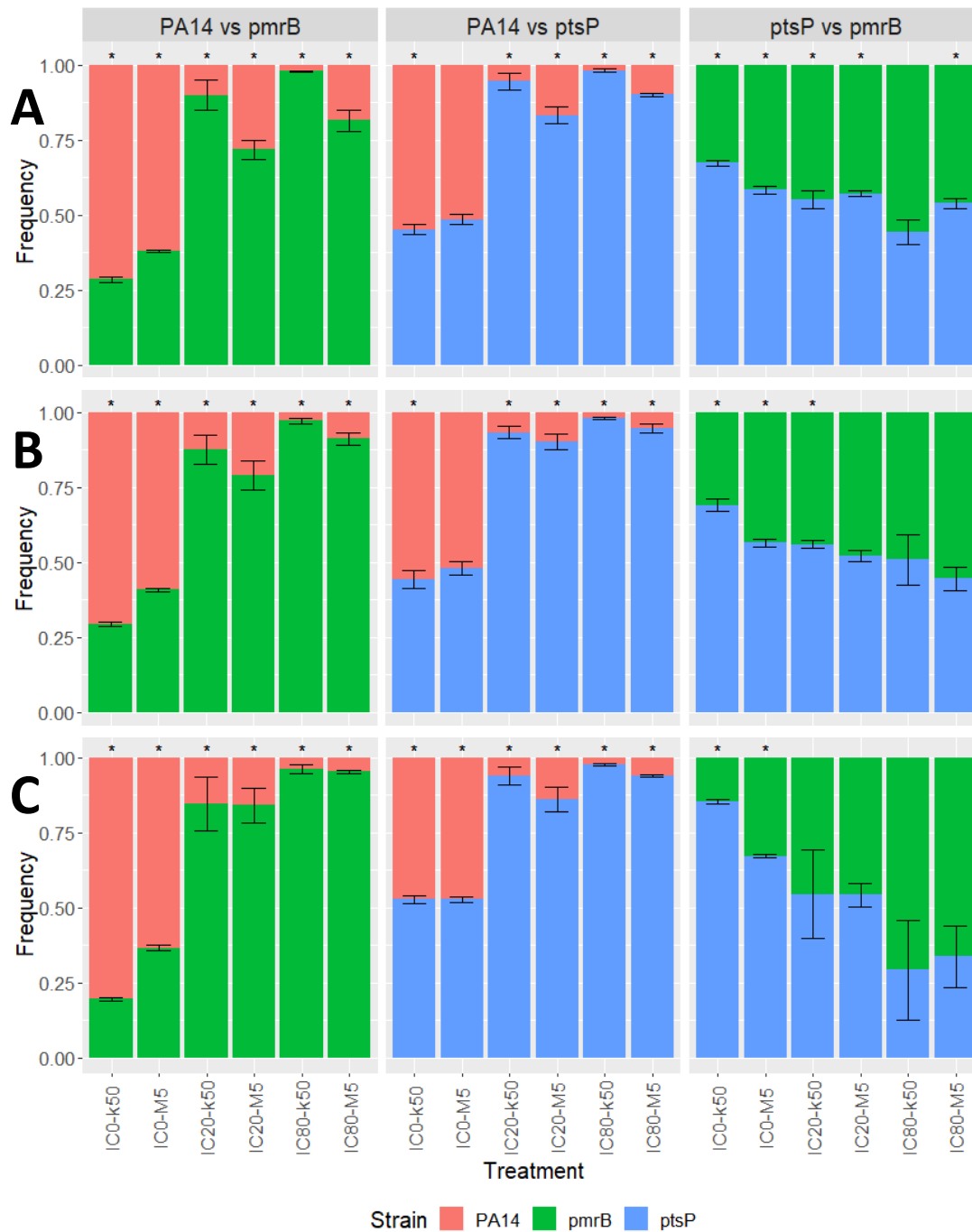


Figure 30: *ptsP* shows a growth advantage over *pmrB* in competitions under low IC.

Different mutant clones which evolved in the previous serial transfer evolution experiment competed against one another. 8 Technical replicates for every treatment condition. A: Clones evolved under high GEN treatment and small transfer size (IC80-k50). B: Clones evolved under low GEN concentration (IC20-k50 & IC20-M5). C: Clones evolved under high GEN concentration and large transfer size (IC80-M5). The X-axis represents the different treatment conditions. The Y-axis represents the relative frequency of the clones. Colors refer to different clonal variants: Red = Wt, Green = *pmrB*, Blue = *ptsP*. Error bars represent the standard error based on five technical replicates for each treatment. Asterisks represent significant difference in frequency between two strains (* = p < 0.05; two sample t-test).

For the competition between the two mutant clones, all three competition experiments resulted in a significantly higher frequency of *ptsP* mutants in the IC0-k50 treatment. In the first experiment, the frequency for *ptsP* mutants was slightly higher in the treatment groups IC0-M5, IC20-k50, IC20-M5 and IC80-M5. In the second experiment, *ptsP* mutant frequency was slightly higher in only the IC0-M5 and IC20-k50 treatment. The third experiment led to the highest frequency of the *ptsP* mutant in the IC0-k50 treatment as well as the IC0-M5 treatment. No significant difference in frequency between *pmrB* and *ptsP* mutants was detected in the IC80-k50 treatment of all three competition experiments, and neither in the IC80-M5 nor the IC20-M5 treatment of the second experiment. The outcome of the third experiment showed greater variance under GEN treatment, which did not allow to detect a clear winner of the competition.

When competing against PA14, *ptsP* mutants displayed about equal frequencies in the drug-free environment whereas the frequency of *pmrB* mutants was lower than the PA14 frequency. The resistant strains dominated in the treatment groups with antibiotic and always outcompeted PA14. The frequencies of the mutant clones were especially high in the k50 groups. No significant difference in frequency of the resistant mutant was detected between the IC20 and IC80 treatment groups.

Since the general outcome of the three competition experiments was similar, their data were combined in one dataset (Figure 31). The competition against PA14 in drug-free environments showed an equal frequency of *ptsP* and lower frequency of *pmrB* compared to the ancestor. The resistant strain outcompeted PA14 in the treatment groups with antibiotics. In the competition of the two mutated strains, the *ptsP* frequency was significantly higher in the IC0 and IC20 treatment groups (Figure 31). No difference in frequency of *pmrB* and *ptsP* was detected in the IC80 treatment groups. In total, *ptsP* frequency decreased with increasing antibiotic concentration (Figure 32, Table 24, Table 25).

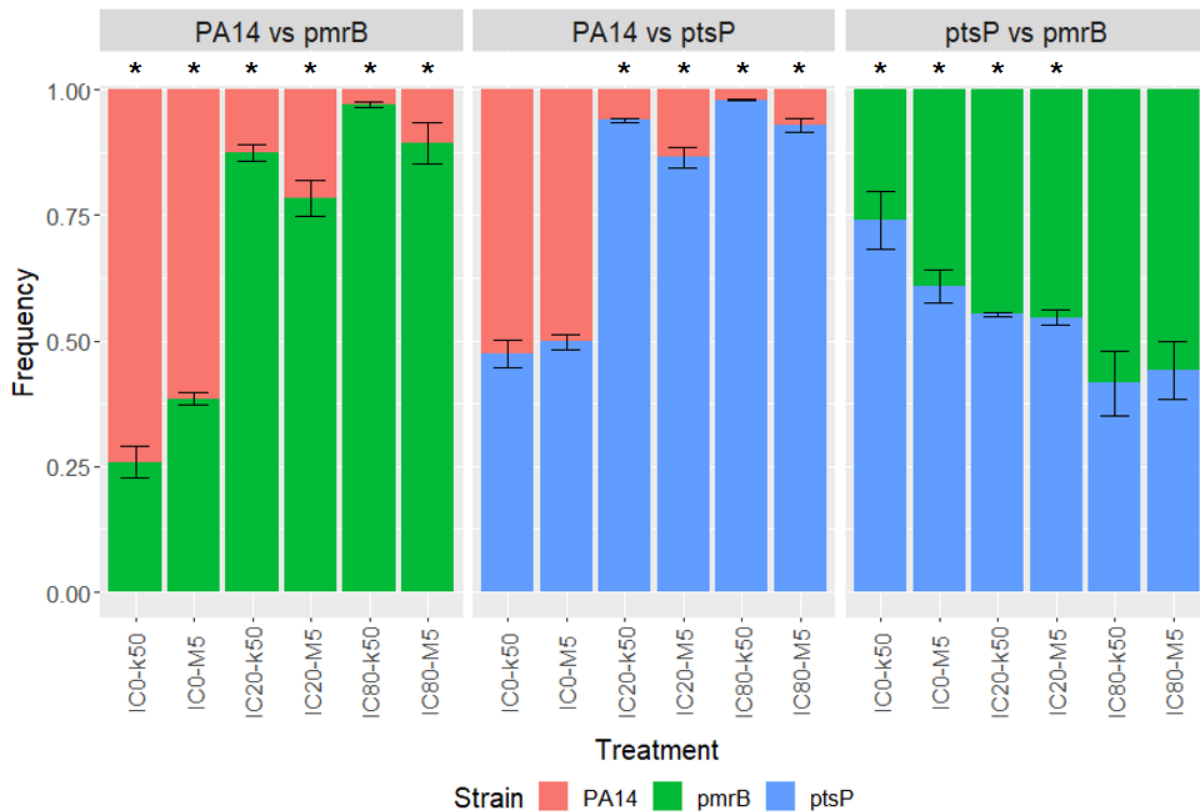


Figure 31: Combined results of the three competition experiments. The mean frequencies of the three biological replicates (each with 8 technical replicates) are plotted for each treatment condition. The X-axis represent the different treatment conditions. The Y-axis represent the relative frequency of the clones. Colors refer to different clonal variants: Red = Wt, Green = *pmrB*, Blue = *ptsP*. Error bars represent the standard error based on three biological replicates for each treatment. Asterisks represent significant difference in frequency between two strains (* = $p < 0.05$; two sample t-test).

Table 24: One-way ANOVA of frequency of *ptsP* mutants in competition against *pmrB* mutants based on treatment group. Asterisks represent significant difference between two treatment groups (* = $p < 0.05$, *** = $p < 0.005$).

Source	Df	Sum Sq	Mean Sq	F value	p adj.	Significance
Treatment	5	1.1197	0.2239	11.7633	2.669E-08	***
Residuals	83	1.8064	0.0706			

Table 25: Tukey HSD for multiple pairwise-comparison of frequency of *ptsP* mutants in competition against *pmrB* mutants and treatment group. Asterisks represent significant difference between two treatment groups (* = $p < 0.05$, *** = $p < 0.005$, n.s. = $p > 0.05$).

Treatment	Diff	lwr	upr	p adj.	Significance
IC20-k50-IC0-k50	-0.1871	-0.3488	-0.0255	0.0138	*
IC80-k50-IC0-k50	-0.3239	-0.4827	-0.1650	0.0000009	***
IC20-M5-IC0-M5	-0.0616	-0.2204	0.0973	0.8671	n.s.
IC80-M5-IC0-M5	-0.1660	-0.3249	-0.0072	0.0352	*
IC80-k50-IC20-k50	-0.1367	-0.2984	0.0249	0.1457	n.s.
IC80-M5-IC20-M5	-0.1045	-0.2633	0.0544	0.3983	n.s.

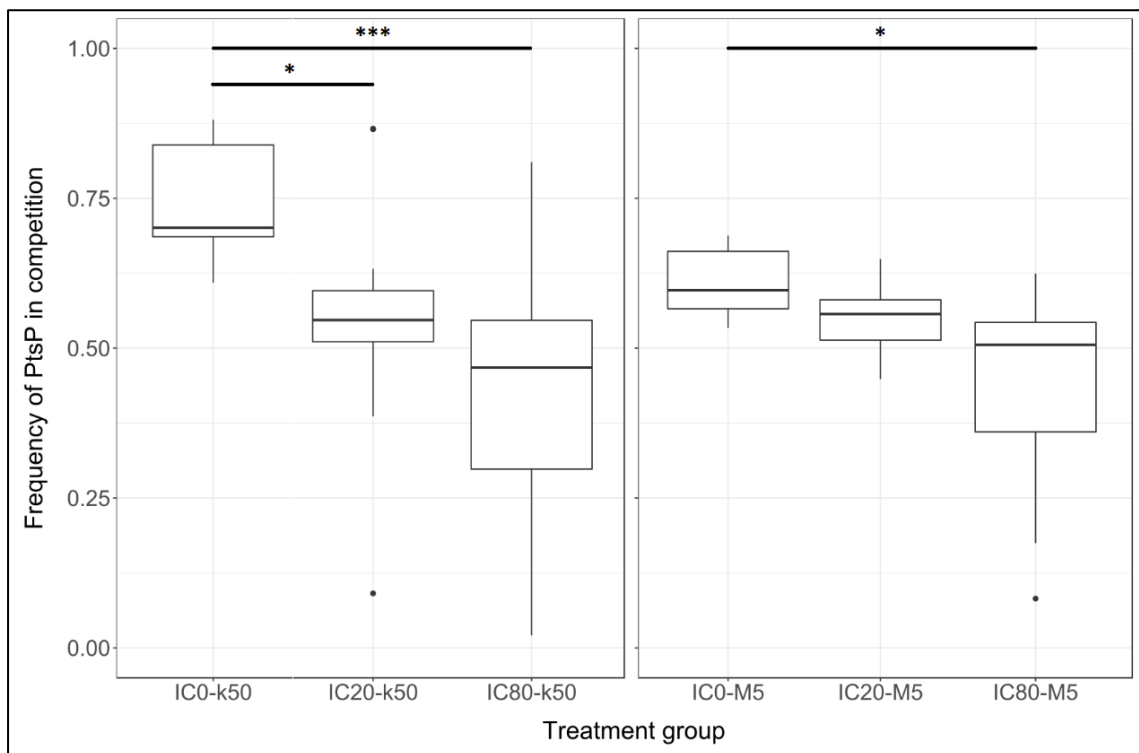


Figure 32: Frequencies of *ptsP* mutants decrease when competing against *pmrB* mutants under high GEN concentrations. The frequencies of 15 technical replicates are plotted for each treatment condition. The X-axis represents the different treatment groups. The Y-axis represents *ptsP* frequency in competition. Asterisks represent significant difference between two treatment groups (* = $p < 0.05$, *** = $p < 0.005$; one-way ANOVA).

Growth characteristics under drug-free conditions

ptsP shows better growth than *pmrB* under drug-free conditions

The final OD of the control plates of the GEN competition assays (see previous section) was used to infer growth characteristics under drug-free conditions for the single strains as a proxy for a possible cost of drug resistance. Linear models were calculated to detect whether a growth parameter of the single strains has an influence on the competition outcome (Table 26). The competition outcome was compared separately to the following fitness parameters of single strain growth: AUC, growth rate, length of lag phase and final OD₆₀₀.

25 % of the competition outcome could be explained by AUC alone. Nonetheless, this was only true for the competitions that included PA14. No significant influence could be detected when the dataset was reduced to the competitions between *pmrB* and *ptsP*. There was also no correlation between the competition outcome (both with or without PA14) and growth rate, length of lag phase or the final OD₆₀₀ of the single strains (Table 26). Significant difference in AUC could be observed between all three clones at all GEN concentrations for k50 (Figure 33). However, under either GEN concentrations, no difference in AUC was observed between *pmrB* and *ptsP* for M5 (Figure 34).

Table 26: Linear models to detect influence of single strain growth characteristics on the competition outcome. AUC = area under curve; GR = growth rate; OD = maximum OD; LT = length of lag phase. Asterisks represent significant difference between two strains (***) = $p < 0.005$, n.s. = $p > 0.05$; one-way ANOVA).

	Source	Sum Sq	Mean Sq	F value	p adj.	Significance
all competition results	AUC	0.252683	0.252683	18.108900	0.0006	***
	GR	0.015547	0.015547	1.114200	0.3069	n.s.
	OD	0.001778	0.001778	0.127400	0.7258	n.s.
	LT	0.001300	0.001300	0.093200	0.7641	n.s.
only <i>ptsP</i> vs. <i>pmrB</i>	AUC	0.001880	0.001880	0.142500	0.7119	n.s.
	GR	0.016380	0.016380	1.241900	0.2853	n.s.
	OD	0.000128	0.000128	0.009700	0.9231	n.s.
	LT	0.000078	0.000078	0.005900	0.9400	n.s.

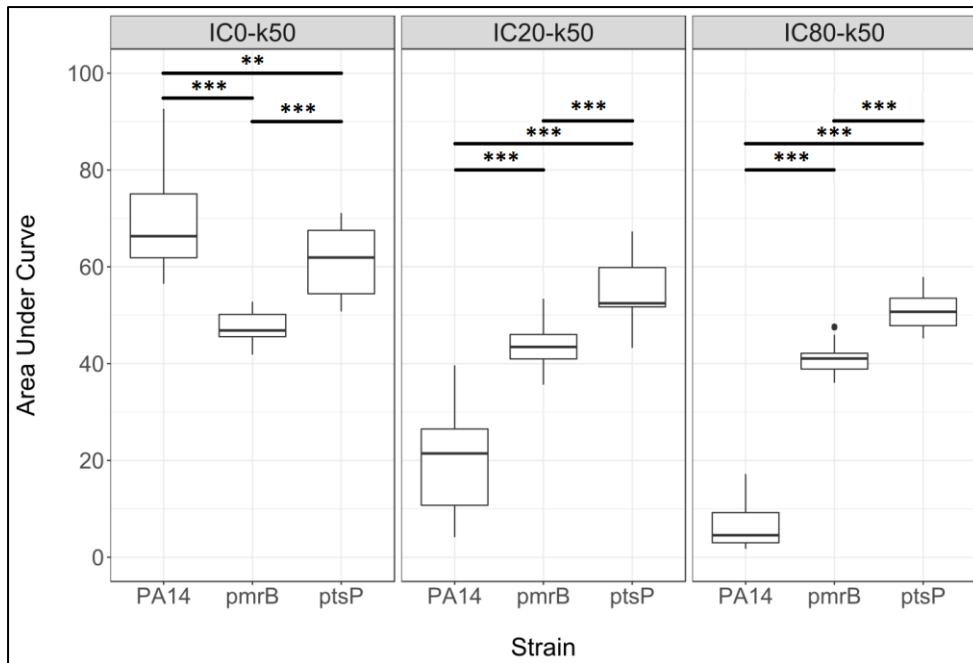


Figure 33: AUC of single strain growth (k50). Boxes represent different treatment conditions. The X axes represent the different genotypes. The Y axis represents the AUC size. Asterisks represent significant difference between two strains (** = $p < 0.01$, *** = $p < 0.005$, n.s. = $p > 0.05$; one-way ANOVA). $n = 15$

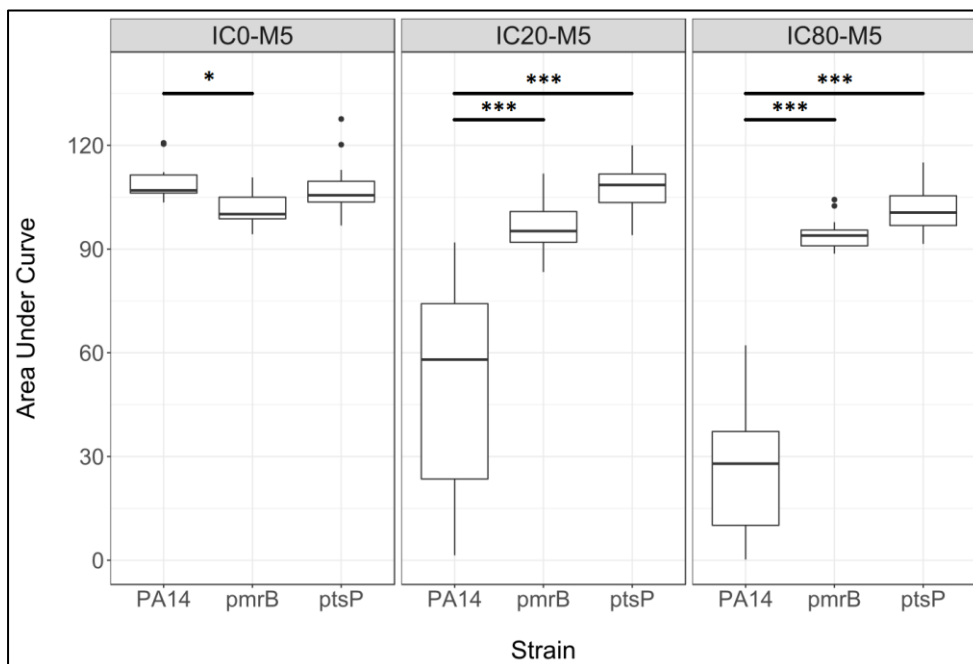


Figure 34: AUC of single strain growth (M5). Boxes represent different treatment conditions. The X-axis represents the different genotypes. The Y-axis represents the AUC size. Asterisks represent significant difference between two strains (* = $p < 0.05$, *** = $p < 0.005$; one-way ANOVA). $n = 15$

Discussion

Over the past decades, the spread of antibiotic resistance among nosocomial bacterial pathogens has developed into a global problem ²⁷⁶. It has been prognosed that by 2050, infections by antibiotic-resistant bacteria will be the leading cause of death in Africa and Asia ²⁷⁷. New approaches in the fight against antibiotic resistance are thus desperately needed. Experimental evolution has shown to be a promising approach to investigate evolutionary dynamics associated with drug resistance and has led to several important discoveries ⁸². However, the influence of population biological factors on drug resistance has been neglected for the most part ⁹³. Population bottlenecks play a particularly significant role in the evolutionary history of bacterial populations. Bacterial populations can evolve resistance by various adaptive paths. The serial bottlenecks that they experience both in nature and in experimental evolution have important consequences on their chance to adapt to selective environments by certain mutational steps ^{144,175}. The strength of population bottlenecks influences the likelihood to acquire specific beneficial mutations and therefore can constrain the adaptive path of the population by secondary mutations. In this thesis, I validated the influence of different bottleneck sizes at different levels of selective pressure on the evolvability of resistance in populations of the *Pseudomonas aeruginosa* PA14. Three different evolution experiments have been successfully completed that simulate single drug treatments with CAR (beta-lactam), CIP (quinolone) and GEN (aminoglycoside), for approximately 100 generations. In the evolution experiments, two population sizes of PA14 (50 000 and 5 000 000 cells) were transferred between growth periods of 9.5 hours in the presence of the respective antibiotics at concentrations that inhibit growth by either 20% or 80%. Based on this experimental design, the influence of serial population bottlenecks on resistance evolution was systematically studied and compared to empirical hypotheses.

For the discussion, I will first summarize, interpret and compare the main results of the different evolution experiments and their follow-up analyses. Although the individual drugs share certain adaptational patterns, there are also some important differences between the three drugs that must be discussed in greater detail. Afterwards, I will compare the main findings of my thesis to previously published literature on the issue of population bottlenecks in bacterial populations and their influence on adaptive allele dynamics. At last, an outlook of additional research will be provided that may advance the insights that have been made so far.

Table 27: Summary of results.

Result	Gentamicin	Ciprofloxacin	Carbenicillin
Evolutionary growth patterns	<ul style="list-style-type: none"> • Large TS groups evolved higher yield than small TS groups • Yield dropped in the beginning of the experiment, but then quickly reached its peak in all treatment groups 	<ul style="list-style-type: none"> • Large TS groups evolved max. yield faster than small TS groups • All but one replicate went extinct under IC80-k50 	<ul style="list-style-type: none"> • Neither TS nor IC influenced yield recovery • All treatment groups remained inhibited
Evolved resistance + growth	<ul style="list-style-type: none"> • Large TS populations evolved high resistance under high IC • Small TS populations evolved high resistance under low IC • All treatment groups evolved resistance > MIC • Most resistant populations have decreased growth rate 	<ul style="list-style-type: none"> • IC80-M5 populations evolved highest resistance • IC20-M5 populations evolved no resistance • Small TS populations with high variation in strength of resistance • Growth rate and length of lag phase not affected by resistance 	<ul style="list-style-type: none"> • High IC populations evolved higher resistance than low IC populations • TS had no effect on strength of evolved resistance • Generally, only little resistance gained across all treatment groups • Growth rate and length of lag phase not compromised
Evolutionary genomics	<ul style="list-style-type: none"> • Higher diversity of genes affected by mutations under large TS than under small TS treatment • Two-component regulator sensor kinases and <i>ptsP</i> primarily affected by mutations • Faster occurrence of mutants and increase in frequency under larger TS and higher IC • Clonal interference in all treatment groups 	<ul style="list-style-type: none"> • Higher diversity of genes affected by mutations under large TS than under small TS treatment • Multidrug efflux regulators primarily affected by mutations • IC20-M5 populations did not acquire mutations • Faster spread of mutants under IC80-M5 than under small TS • Clonals interference common 	
Clonal competition	<ul style="list-style-type: none"> • Competitive advantage of <i>ptsP</i> over <i>pmrB</i> decreases with increasing IC • Single strain growth not a good predictor of competition outcome 		

Synthesis of different evolution experiments

Bottleneck strength and selection strength cause contrasting yield dynamics

In all evolution experiments, both the IC and the TS had an influence on the evolutionary dynamics of the bacterial populations, albeit to different degrees. In the CIP evolution experiment, the TS had a two-fold stronger influence on yield than IC, with large TS groups generally growing to a higher yield than small TS groups (Figure 9, page 60). The opposite effect was observed for the GEN experiment, where low IC populations reached a higher yield than high IC populations towards the end of the experiment (Figure 8, page 58). In the CAR experiment, only IC20-k50 achieved a higher yield than the other groups (Figure 10, page 62). In either experiment, the combined effect of both factors on yield was either small (GEN) or not significant. The effect of bottleneck size on yield was low in the GEN experiment, as all treatment groups experienced a strong reduction in yield after the second transfer (Table 9, page 58). In the CAR treatment, TS did not affect adaptive dynamics of yield, either (Table 13, page 62). For CIP, both strong bottleneck treatments reached their maximum fitness much later than the groups with wide bottlenecks, indicating that populations adapt faster when the TS is large (Table 11, page 60). In this case, the wide bottleneck potentially allowed for a larger variety of mutants to occur in the populations and consequently for selection to act earlier on the larger set of mutants ^{278,279}.

Combined effects of bottleneck and selective strength on resistance evolution

Resistance and growth measurements of the evolved lineages revealed distinct patterns for different antibiotics: Populations that experienced large TS during evolution showed high levels of resistance when the IC was high, while low levels of resistance evolved when the IC was low. However, for the populations that experienced small TS during the experiment, the opposite effect occurred: Populations evolved higher resistance at low IC than at high IC. This dichotomous combined influence of bottleneck size and selective strength was observed for both GEN (Figure 11, page 64) and CIP (Figure 14, page 67). In either case, the largest difference in resistance evolved between the two groups that evolved under large TS (wide bottleneck).

The result for the large TS could be attributed to a larger genetic diversity within the populations. This would increase the chance of parallel evolution since the likelihood of the most beneficial mutation to occur in every replicate population is high. The selective pressure imposed by the drug concentration favors mutations of different fitness properties: Low selective pressure (IC20) selects for mutations that confer high fitness under low drug concentrations. In contrast, high selective pressure (IC80) is more likely to select for mutations that also confer high resistance. Furthermore, genetic drift is expected to play a more pivotal role for the fixation of beneficial alleles when the TS is small (strong bottlenecks)¹³⁶. Thus, the selective strength is expected to have only little influence. Because of the lack of clonal competition, any mutation with a beneficial fitness effect will have a stronger fitness advantage early on. High resistance was able to evolve under low drug concentration. However, the mutations likely fixed due to stochasticity of mutation supply rate and their resistance properties were therefore selected randomly^{55,279}. An alternative explanation would be that only high selective pressure causes early selection of random beneficial mutations. In contrast, comparatively low selective pressure would allow for clonal competition which eventually favors mutations that confer both increased fitness and resistance²⁸⁰.

The endpoint populations were grown in the absence of the antibiotics to further characterize changes in growth behavior relative to the ancestral PA14 wild type. Continuous OD measurements were obtained to calculate the mean length of lag phase and mean maximum growth rate of the evolved populations. In general, most evolved populations of all treatment types have a slightly shorter lag phase than the ancestor, which is a common signature of media adaptation²⁸¹. For both GEN and CIP, treatment groups that evolved the highest resistance also show the lowest overall fitness in absence of the treatment drug. For the CIP dataset, the most resistant treatment groups IC20-k50 and IC80-M5 have a maximum growth rate that is not different from the evolved no-drug control (Figure 15, page 69). On the contrary, the least resistant treatment group IC20-M5 shows a higher maximum growth rate than the control. For the GEN dataset on the other hand, the least resistant treatment groups IC20-M5 and IC80-k50 do not differ in maximum growth rate from the evolved no-drug controls and the two more resistant groups IC20-k50 and IC80-M5 have a lower maximum growth rate (Figure 12, page 66). For either drug, resistance is strongly associated with a substantial fitness cost^{38,90}.

Contrary to the results of CIP and GEN, bottleneck strength did not influence resistance evolution under CAR treatment. The high IC treatment groups evolved higher resistance than

the low IC groups. However, there was no difference in resistance between either group of pairs of the same IC (Figure 16, page 70). In addition, no difference in maximum growth rate and length of lag phase could be found between the different CAR treatment groups (Figure 17, page 71). The results could indicate that the adaptations observed in the evolutionary data are due to mutations of small effect. Alternatively, phenotypic effects rather than genetic mutations have been shown to be responsible for the observed adaptive pattern ²⁸². However, it must be noted that PA14 is naturally better equipped to withstand high concentrations of CAR compared to other PA strains as their AmpC beta-lactamase can hydrolyze beta-lactam antibiotics ²⁸³. Since multifold concentrations of the MIC are already very high (for comparison, the concentrations used for the tests with CIP are 1000-fold lower than for CAR) and CAR must be dissolved in ethanol, it is likely that ethanol contributed to increased killing at higher concentration levels. More delicate testing for evolved resistance would need to be done to provide us with a result that can be interpreted more clearly.

Different treatment groups show distinct genomic signatures

WGS of entire populations from the last transfer point revealed distinct signatures of genetic adaptation for each treatment group. Populations that experienced large TS acquired a lower diversity of mutations than populations of small TS. In the IC80-M5 populations of both GEN (Figure 18, page 73) and CIP (Figure 21, page 77), mutations were found in only two genes among all treatment replicates. In the IC20-M5 populations, all replicates had mutations in only one gene (GEN) or no mutations were found (CIP). For individual populations of small TS, mutations were also found in genes that did not occur in any other population within the dataset. Overall, the genomics of the end point populations confirm my hypothesis that strong bottlenecks lead to more variation among replicates. The identified mutations are associated with different levels of resistance and fitness effects. In addition, most mutations found in each respective dataset are associated with a distinct gene function (CIP: multidrug efflux, GEN: two-component regulatory systems). Several populations had acquired more than one mutation by the end of the experiment. However, fixation of two mutations in the same background could only be confidently identified in two individual cases, hinting at the possibility of increased clonal interference.

For GEN, mutations in sensor kinases of two-component regulatory systems were most commonly selected. Two-component regulatory systems are molecular signal transduction systems that sense different environmental stimuli and regulate physiological responses upon environmental changes²⁶⁸⁻²⁷⁰. They typically consist of two proteins: A membrane-associated histidine kinase that senses environmental stimuli and a corresponding response regulator that regulates the differential expression of larger sets of target genes of the cellular response. Function-altering mutations in the kinase would cause a change in stimulus sensing and consequently also in the expression of environmentally linked genes^{269,270}. The two-component systems found to be affected by mutations in this dataset are PmrAB, ParSR and PhoPQ. Among other cellular responses, all three systems regulate LPS modifications of the bacterial outer cell membrane, specifically lipid A²⁸⁴⁻²⁸⁶. Unlike most other groups of antibiotics, aminoglycosides can enter bacterial cells by binding to the negatively charged components of the bacterial membrane^{287,288}. By binding to lipid A, aminoglycosides can influence the membrane composition and increase its permeability, therefore also increasing the uptake rate of other aminoglycoside molecules^{86,247}. Modification of lipid A that is conferred by mutations in two-component regulatory systems would prevent the self-regulated uptake of aminoglycosides and therefore increase resistance^{84,87,289}. Lipid A modification is a commonly cited resistance mechanism against polypeptide antibiotics but is also often found in aminoglycoside-resistant bacteria^{211,290}. Mutations in *pmrB* and *phoQ* are regularly observed as adaptational responses that confer resistance against both aminoglycosides and polymyxins^{84,291}. *ParS/parR* mutations have been reported to down-regulate the regulatory gene *mexS* of the *mexEF-oprN* operon and up-regulate the quorum sensing (QS) genes *lasI* and *rhlI*, the main regulators of the two QS systems of PA²⁹².

Apart from two-component systems, most mutations are found in the gene *ptsP*. *ptsP* is a phosphoenolpyruvate-dependent phosphotransferase that transfers the phosphoryl group from phosphoenolpyruvate (PEP) to the phosphoryl carrier protein (NPr)²⁷⁴. It is known as an important player for the nitrogen cycle and glucose transport in bacteria^{293,293}. Deletions of *ptsP* have previously been described to cause overproduction of pyocyanin in PA, a toxin and virulence factor produced by PA to oxidize other molecules²⁹⁵. However, the role of *ptsP* in aminoglycoside resistance has not yet been characterized properly²⁹⁶. Previous studies have identified an increased resistance of *ptsP* mutants of *E. coli* against antimicrobial peptides²⁹⁷. Furthermore, loss of *ptsP* renders PA susceptible to membrane permeabilization by human opsonin SP-A²⁹⁸. It has also been revealed that the disruption of *ptsP* causes a significant

increase in the expression of the major QS regulators *lasI* and *rhlI* ²⁹⁵. QS controls many cellular functions like motility, polysaccharide synthesis, biofilm formation and activation of virulence factors ^{88,299}. Thus, *ptsP* may mediate GEN resistance through QS-associated adaptation.

PtsP and *pmrB* are the two most frequently mutated genes across all treatment groups and all replicates with a TS of M5 carry dominant mutations in either *ptsP* or *pmrB*. While 5 of 7 replicates in the IC80-M5 group are dominated by *pmrB* mutations (the remaining two by *ptsP* mutants), all replicates in the IC20-M5 group carry their dominant mutation in *ptsP*. This agrees with the original expectation that a higher degree of parallel evolution takes place under large TS because of the increased likelihood of the fittest mutant to occur ³⁰⁰. Any additional dominant mutations that achieve high frequencies within populations were only found once in populations of the k50 treatment groups. A mutation in *cysJ*, a member of the sulfite reductase complex, occurs in population IC80-k50-E3 at a frequency of 100% that likely is hitchhiking along with the selected *ptsP* mutation. Mutations in *waaL* (in population IC80-k50-F3), a ligase involved in LPS synthesis ³⁰¹, and *fusA1* (in population IC80-k50-G3), the regulator of ribosomal translocation during translation elongation, also dominate single populations ³⁰². The resistance tests indicate that only mild resistance is conferred by the latter two mutations. Thus, they may have been selected early in the experiment and were able to rise in frequency due to the lack of influx of fitter mutations. In addition, a mutation in the yet uncharacterized gene PA14_08640 conferred high resistance for population IC20-k50-C6. Gene ontology provides a peptidoglycan binding function for the gene. Orthologs found in other *Pseudomonas* species are characterized as sporulation proteins. In addition, no genes involved with multidrug efflux systems were found to be mutated in the GEN dataset. This is interesting as overexpression of MexXY-OprM is associated with aminoglycoside resistance in clinical PA isolates ^{69,211}.

Mutations in *pmrB* and *parR* of PA14 were also discovered in other evolution experiments that were done in association with different projects of the lab. *pmrB* and *parR* mutants were among the most commonly selected genotypes in an evolution experiment in which the concentration of GEN as the single treatment drug was gradually increased ⁸⁰. These clones evolved resistance against GEN concentrations of ~ 30x the MIC of the ancestor. *pmrB* mutants also established themselves in populations that were treated with GEN for more than 1000 generations at a constant dose of IC75 or in a cycling treatment of three drugs (including GEN) that were switched at every fourth transfer ¹¹⁷. Interestingly, all SNPs or short Indels found in

said experiments occurred at different nucleotide positions of *pmrB* than the variants discovered in this thesis. This might provide more evidence that the variants discovered in this thesis could have stemmed from standing genetic variation in the original starting culture. *ptsP* mutations were not found in the end point populations of the experiment in which treatment concentrations of GEN were increased. This corroborates my finding that *ptsP* mutations confer mild but not high resistance against GEN (Figure 20, page 75). However, *ptsP* variants were identified at high frequencies in two populations of CAR-resistant PA14 clones that were treated with GEN at MIC-level concentrations for ~ 300 generations⁸³. This finding shows that PA14 might commonly evolve low-level resistance against GEN by acquiring *ptsP* mutations.

For CIP, the mutant distributions are a crucial caveat for the results of the resistance assays. In the IC80-k50 treatment group, all but one replicate went extinct. This indicates that the combination of selective pressure and bottleneck strength did not allow for the appearance of beneficial mutations in time for the populations to survive the treatment conditions and that they could neither survive by physiological adaptation alone. In contrast, no mutations were observed in the IC20-M5 treatment group. One explanation for this result is that physiological adaptation was enough to improve fitness without mutations in regulatory regions providing additional fitness benefits. Alternatively, no mutations occurred that improved the fitness of the population to levels above the wild type. Ultimately, drift was not strong enough to elevate any mutations to relevant frequencies. Therefore, evolutionary genomics and the allele dynamics could only be analyzed for the two remaining treatment groups IC20-k50 and IC80-M5. However, these results provide clear implications for the resistance tests: Resistance primarily evolves by acquisition of beneficial mutations and populations go extinct when said mutations do not occur in time.

Most identified mutations were found in negative regulators of efflux pumps. Efflux pumps are active transporters localized in the cytoplasmic membrane that remove substances like antibiotics, xenobiotics and metal ions from the cytoplasm and periplasm and transport them out of the cell^{303,304}. Efflux pumps affected by mutations in the CIP dataset are MexCD-OprJ (repressed by *nfxB*), MexEF-OprN (*mexS*), MexAB-OprM (*nalC*) and MexXY-OprM (*mexZ*). All different efflux systems are members of the resistance-nodulation-division (RND) superfamily^{304,305}. Deletion of the repressor compromises the activity of negative regulators. The efflux systems would be expressed at a higher rate and thus antibiotics would be removed from the cells at an increased frequency^{303,305}. The most commonly mutated efflux systems in

the dataset, MexCD-OprJ and MexEF-OprN, are associated with high clinical resistance to CIP and other fluoroquinolones. Mutational overexpression of MexAB-OprM and MexXY-OprM on the other hand causes rather modest fluoroquinolone resistance and is a less common adaptive response^{305,306}. In addition to the removal of drug molecules from the cell, multidrug efflux pumps are also known to extrude different QS autoinducers^{88,299}. It has been demonstrated that overexpression of the MexCD-OprJ multidrug efflux pump represses the QS response of PA³⁰⁷. Furthermore, the expression of QS-regulated genes is impaired, and the production of QS-regulated virulence factors strongly decreases when MexEF-OprN is overexpressed³⁰⁷. In contrast, the shut-down of MexEF-OprN selects for increased QS cooperation in PA³⁰⁸. Thus, resistance against CIP through the observed pathways likely comes at the cost of compromising QS efficiency.

Mutations for IC80-M5 were primarily found in either *nfxB* or *mexS*, two clinically relevant genes that confer high CIP resistance³⁰⁴. A higher diversity of genes was mutated in the IC20-k50 group. Missense mutations in the drug targets DNA gyrase and topoisomerase IV are commonly associated with high fluoroquinolone resistance in clinical PA isolates²¹¹. Mutations in the corresponding genes were not found in the dataset. However, since those mutations are commonly associated with high fitness costs, they likely only fix when the selective pressure is sufficiently high³⁰⁶. IC80-k50 was the only treatment group that showed significant extinction and may have benefitted the most by mutations that affect the drug target sites. Mutations in *nfxB* and *mexS* were also found in a different evolution experiment of the lab in which CIP was applied as the lone treatment drug against PA14¹¹⁷. However, at higher dosages of CIP, mutations in either *gyrA/gyrB* or *oprD* became more significant for the evolution of high resistance⁸⁰.

The effects of genetic drift differ substantially between high and low TS and have very likely contributed to the outcome of the evolution experiments. However, it is important to note that the adaptive regimens may also have selected for cell density dependent fitness effects. Transferring different cell numbers to the same total volume results in different cell concentrations at the beginning of a growth phase. Implicating the possible importance of QS for our evolved lineages, mutations that improve growth under low cell densities would likely be selected for in the small TS groups. The results of the CIP evolution experiment did not confirm this hypothesis, as the affected efflux pump systems commonly also remove QS autoinducers at increased rate when upregulated. However, this activity was most likely not under direct

selection but rather an evolved trade-off for increased excretion of antibiotics. In the GEN dataset, mutations in *ptsP* and ParR/ParS positively influence QS activity. This finding may indicate a potential association between QS activity and GEN resistance. However, its selection probability did not depend on cell density, as mutations in *ptsP* and PaR/ParS occurred and in most treatment groups of both small and large TS. *PtsP* mutants did occur more often under large TS than under small TS. Instead, we would have expected *ptsP* mutations to have an even more beneficial effect under small TS than under large TS. Thus, genetic drift rather than cell density appears to have played the more pivotal role for the selection of mutations with potentially increased QS.

Allele dynamics are influenced by bottleneck strength

To uncover the evolutionary dynamics of resistance on a genomic level, WGS was performed on the populations at intermediate transfer periods of the evolution experiment. For the GEN evolution experiment, rates of adaptation differ for the treatment groups (Figures 23-26, pages 81-84). Unsurprisingly, populations adapt faster under strong selection in both bottleneck regimens with beneficial mutations occurring earlier under wide bottlenecks. In contrast, low selective pressure allows for more competitive allele dynamics over time, even under strong bottlenecks. In addition, clonal interference occurs in every treatment group except for IC80-k50. This highlights that drift primarily drives adaptation only under the combination of high selective pressure and strong bottlenecks. Surprisingly, populations evolved a higher mean resistance under IC20-k50 than under IC80-k50. The allele dynamics offer a potential explanation for this outcome. The diversity of selected mutants between the populations was high in both treatment groups, indicating that drift played an important role for the selection of alleles under strong bottlenecks. Under strong bottlenecks and high selectivity (IC80-k50), the first beneficial variants were selected more rapidly. By season 7, most populations of the IC80-k50 group had acquired one mutation at elevated frequencies which went on to become fixed. This left the populations with a low proportion of Wt cells from which other beneficial mutants could arise. In contrast, most populations under low selectivity (IC20-k50) had not acquired a single mutation by season 7. The slow rise of mutants under IC20-k50 enabled multiple mutations to occur and compete before the fixation of one. The slower selection of beneficial variants therefore also increased the likelihood that an even fitter mutation might establish itself in the population and confer higher resistance before the first mutation was fixed.

Overall, only three different variants of *pmrB* mutants are found in the entire dataset. On the other hand, 15 different *ptsP* mutants were found. This may indicate that either the few *pmrB* mutations are subjected more strongly to standing genetic variation than the individual *ptsP* mutations or that beneficial phenotypic effects of mutations are restricted to fewer nucleotides in *pmrB* than for *ptsP*. To test the latter hypothesis, additional functional genetic tests would be necessary. At least two of the three *pmrB* variants achieve high frequencies by transfer three in the IC80-M5 group. In the IC20-M5 treatment, the three *pmrB* mutations first occur simultaneously to the first *ptsP* variants. Even if the *pmrB* variants were subjected to standing genetic variation, they must occur at such low frequencies in the starting population that they are removed from the small TS populations early by dilution during transfers.

In the CIP evolution experiment, clonal interference took place in most replicates of both relevant treatment groups, independent of bottleneck strength. For the IC20-k50 treatment group, mutations occurred late in the experiment and some populations evolved only little resistance (Figure 27, page 86). But also, in the IC80-M5 treatment group, mutants occurred only by transfer 5 and thus required a lot more time to rise to high frequencies than mutations in the IC80-M5 populations of the GEN experiment (Figure 28, page 87). The results highlight that the first mutants with a fitness advantage required several dozen generations to establish themselves in the CIP treated populations and subsequently be selected. Two or more beneficial mutations were selected early in the IC80-M5 group and clonal interference took place for most of the experiment. For the IC20-k50 group, second mutants occurred only in the second half of the evolution experiment after which increased clonal interference could occur. In four IC80-M5 populations, mutations in an uncharacterized ABC transporter gene (PA14_09300) had occurred by transfer 3. ABC transporters can contribute to the removal of antibiotics from the cell lumen^{309,310}. Thus, the identified mutations may have been adaptive, although they went on to be outcompeted by likely fitter mutations that modulate RND efflux activity, the more significant efflux protein family regarding antibiotic resistance in *Pseudomonas aeruginosa*^{311–313}. Only one mutation in PA14_09300 could be found among IC20-k50 populations. The only surviving IC80-k50 population also acquired a mutation in PA14_09300 during the second half of the experiment.

Clonal competition influenced by selective regimen

Within the GEN dataset, *ptsP* and *pmrB* are the most commonly mutated genes. Mutations in either gene dominate the two large TS groups which theoretically allow for the highest diversity of mutants to occur. This led me to hypothesize that *pmrB* and *ptsP* are the mutations with the highest competitive ability under the applied experimental conditions. For a simplified model of evolutionary dynamics, competition experiments with mutant clones of *ptsP* and *pmrB* were designed (Figure 30, page 92). In those experiments, *ptsP* mutants showed a generally but not universally higher competitive ability than *pmrB* mutants. More specifically, the competitive benefit of *ptsP* mutants was higher under low IC conditions but faded under high IC conditions (Figure 32, page 95). The high growth advantage of *ptsP* mutants under low GEN concentration is represented by the competition outcome as well as by the evolution experiment. However, the competition experiments could not explain why *ptsP* mutants were able to establish themselves in some replicate populations at late stages of the evolution experiment. There does not seem to be a general fitness advantage of these clones. *pmrB* mutants generally dominated in the IC80-M5 group of the evolution experiment but did not outcompete *ptsP* under IC80-M5 conditions in the competition experiment. Large standard errors of the competitions indicate a certain stochastic effect of clonal fitness that can allow either genetic variant to win the competition.

The results of the competition assays demonstrate an evolutionary trade-off for *pmrB* mutants, as they carry a higher resistance than *ptsP* mutants but also a higher fitness cost at low GEN concentrations. The decreased growth of *pmrB* mutants is a fitness disadvantage in drug-free environments. The less resistant *ptsP* mutants on the other hand do not show any significant fitness cost when competing against the wild type. *ptsP* is the most dominant mutation in the IC20-M5 treatment group because it provides resistance against sufficiently high inhibitory levels of the treatment drug. At the same time, *ptsP* mutants maintain the ancestral growth characteristics. Low IC and wide bottleneck do not select for high resistance, because only a low fitness burden needs to be overcome, and high resistance is less favorable when it is associated with an increased fitness cost. In contrast, *ptsP* does not have a growth advantage over *pmrB* at IC80. Since *pmrB* is established as the dominant mutant early in the evolution experiment, other factors than resistance must influence the competitive dynamics between both mutants. One possible explanation would be that those specific *ptsP* mutations that arose

in the IC80-M5 group at later stages of the evolution experiment confer higher growth benefits than other *ptsP* variants and therefore were able to establish themselves late.

Findings of the evolution experiment and the summary of the competition treatments indicate that the *ptsP* mutants should outcompete both Wt and the *pmrB* mutants under all experimental conditions. Although *pmrB* mutations confer a higher resistance, *ptsP* mutations provide a higher growth rate at all treatment concentrations. Thus, the question remains: Why does *ptsP* not dominate all treatments of the main evolution experiments? As previously stated, a possible explanation could be that the selected *pmrB* mutants have already been present at very low initial frequencies in the starting culture of the experiment. Early selection of *pmrB* mutants could then have prevented or postponed the establishment of independent *ptsP* mutants in the IC80-M5 populations. WGS of the starting culture could not confirm this hypothesis. However, the coverage size of 10^3 reads for the WGS is drastically lower than the inoculum size of 5×10^6 and any clonal frequency $< 1\%$ could easily go undetected. Alternatively, growth rate alone might not be the decisive factor for competition outcome but other effects of the selected mutations. In this context, the potential upregulation of QS systems in *ptsP* mutants might be a beneficial factor to consider in future functional analyses of the mutants. The performed competition experiments ran only for a single growth period, which was not enough to comprehend the complex fitness dynamics between *ptsP* and *pmrB* under IC80 conditions. Thus, additional competition experiments that enable competitive dynamics over longer periods of time will likely provide a more in-depth understanding of whether each mutant can establish itself in a population that is dominated by the other.

The growth advantage of the evolved mutant clones over PA14 was remarkably higher than expected from the evolution experiment. The mutant clones dominated the competitions and grew at a faster pace than they did in the evolution experiment, where it took the mutants up to nine transfers to dominate a population. The higher fitness of PA14 in the evolution experiment can be explained due to the physiological adaptation to the GEN concentration before the mutations emerged^{314,315}. To control for this effect, PA14 can be incubated in GEN medium before the competition to reconstruct the experimental conditions. However, this would also risk the emergence of new mutations in the Wt background that could compromise the interpretation of competition outcomes. Another explanation for the difference in growth of the resistant clones between the evolution experiment and the competition assay is the starting populations size. In the evolution experiment, mutations first occurred in single cells

and only slowly increased in frequency as the population was dominated by the wild type or other variants. In contrast, mutants started the competition experiments at a relative initial frequency of 50%, allowing for a faster spread through the population.

The growth measurements of single strains in drug-free medium did not show significant influence on the competition outcome. No influence was found for either the growth rate, final OD and length of lag phase. The only significant correlation was obtained for the AUC in competitions involving PA14. In those competitions, the mutant strains were highly dominant due to their GEN resistance. The smaller growth differences between *pmrB* and *ptsP* mutants in competition with each other could not be linked to their single strain growth. Those findings do not imply a lack of correlation between single strain growth and growth in competition, but rather emphasize the difficulties of comparing different growth parameters. Growth characteristics of individual strains can result in different effects in fitness measurements. Consequently, results of competition assays and growth curves cannot be expected to generally show correlation³¹⁶.

Distinct evolutionary dynamics for individual drugs

Generally, PA14 shows similar adaptive dynamics to the individual treatment regimens across different antibiotics. However, there are also some important differences to point out between the experimental datasets. High resistance evolved in all treatment groups of the GEN experiment. In contrast, resistance did not evolve in two treatment groups of the CIP experiment. On one hand, the IC20-M5 group could survive without acquiring any mutations at high frequencies. On the other hand, the IC80-k50 group almost went completely extinct early in the experiment. In addition, resistance only seemed to increase for the high IC groups of the CAR experiment, but not for the low IC groups. Apart from different adaptational dynamics, resistance to the respective treatment drugs is conferred by modification of target genes of different functions. It is therefore essential to discuss the potential influence of pharmacodynamic effects of the individual drugs on adaptive dynamics of the PA14 populations.

CAR is a carboxypenicillin that inhibits DD-transpeptidase, thereby preventing transpeptidation that crosslinks the peptide side chains of peptidoglycan strands³¹⁷. Carboxypenicillins provide *in vitro* activity against a variety of Gram-negative bacteria. Their medicinal

relevance focusses primarily on their activity against *Pseudomonas aeruginosa* and some proteobacteria³¹⁷. Their superior activity against *P. aeruginosa* may be due to better penetration characteristics or greater affinity for penicillin binding proteins. However, strains producing elevated amounts of beta-lactamase are commonly resistant against carboxy-penicillins³¹⁸. As PA14 produces the AmpC beta-lactamase and no beta-lactamase blocker like tazobactam was added to the treatment, adaptation may likely have been conferred by increased expression of AmpC²⁸³. In this case of phenotypic adaptation, the IC of the treatment drug would most likely have a stronger influence on expression levels than bottleneck size.

CIP is a second-generation fluoroquinolone that inhibits the bacterial DNA gyrase and topoisomerase IV which eventually causes single and double-strand breaks in the DNA²⁴⁶. Common clinical resistance mechanisms include target-altering mutations and deleterious mutations of porins that reduce drug permeability²¹¹. However, the increased drug efflux primarily observed in this study has also been commonly described for CIP resistance³⁰⁴. A possible explanation for the increased extinction in the IC80-k50 treatment group could be a likely inoculum effect that is further enabled by increased drug efflux^{319,320}. As 100-fold less bacteria are challenged against the same amount of drug molecules in the small TS treatment compared to the large TS treatment, the drug-to-cell ratio is larger under small TS. In either scenario, cells will take up drug molecules either temporarily (in case of successful efflux) or long-term (if the drug binds to its target) during drug exposure. In case of cell death, drug molecules would be released by the dead cell and become available again to be taken up by other cells³²¹. However, the selective pressure on individual cells will always be stronger in small populations than in larger populations because the number of available drug molecules will always be higher³²². Cells with increased drug efflux will thereby increase the selective pressure on their neighbouring cells by making secreted molecules available again at a fast rate³²³. On the other hand, increased drug efflux alone may not be enough to resist the high selective pressure of available drug molecules in a small population. Consequently, additional mutations would be required to either restrict the drug uptake or to reduce the cost of efflux. In contrast to the high extinction levels in IC80-k50, the populations evolved under IC20-M5 did not acquire any mutations at relevant frequencies. In this case, a large population was used as an inoculum against fewer drug molecules. As the amount of available drug molecules would not be enough to kill the entire population, the surviving cells likely adapted by increasing their fitness when not compromised by ciprofloxacin molecules instead of acquiring costly and potentially unnecessary resistance mutations^{28,324}.

The inoculum effect was especially strong in preliminary experiments for MIC determination of GEN. Previous tests revealed that drug efficacy is strongly dependent on inoculum size. Thus, IC concentrations were adjusted to reach a similar level of inhibition in the different treatment groups. As aminoglycosides are very small molecules compared to most other antibiotic classes, they do not require porins or other transport channels for uptake. Therefore, apart from increased drug efflux and enzymatic deactivation, common resistance mechanisms are associated with processes that affect the cell wall as a barrier against drug uptake ²¹¹. Mutations that appeared under strong bottlenecks did not appear under wide bottlenecks. Treatments under both bottleneck sizes primarily selected for mutations in two-component regulatory systems that cause lipid-A modifications which ultimately change the outer membrane structure ⁸⁴. However, even before the first set of mutants could be identified in individual populations, the fitness increased drastically in all treatment groups after the third transfer. A possible explanation for the spontaneous spike in population yield would be a reduction of membrane potential that reduced the uptake of GEN and thereby drug-induced cell death ^{325,326}. In addition, the population size itself also influences the adaptation rate. Populations quickly recovered their yield in the GEN experiment and acquired mutations afterwards. In contrast, the slower, more gradual increase in population yield in the CIP and CAR experiments indicate that growth remains limited until the first mutations rise in frequency. The early recovery likely contributes to earlier selection of beneficial variants in the GEN experiment by allowing more replication events to occur during the early transfer periods ¹¹¹.

Overall, the results highlight that the mode of selection is an important factor of influence on the evolutionary dynamics of experimental populations. Therefore, the selective conditions themselves may have an even greater effect on adaptive dynamics than the absolute bottleneck strength. However, bottlenecks may further potentiate selectivity.

Revisiting the original hypotheses

The main conclusions of the work presented in this thesis, related to the objectives and hypotheses stated in the first introduction of the thesis, are the following:

H_{1,1}: Wide rather than small bottleneck size reduces treatment efficacy in terms of strength and speed of resistance evolution.

While the bottleneck size must not necessarily have a significant effect on the degree of resistance that evolves in the long term (as shown for the CAR data), it certainly affects the adaptive dynamics that take place along the way. Resistance alleles required more time to first occur in populations of smaller TS than under large TS in all treatments for which allele dynamics were investigated. The mean resistance of the IC80 treatments was always higher for the large transfer groups than for the small transfer groups. In contrast, the mean evolved resistance of the IC20 treatments was higher for the small transfer groups than for the large transfer groups for two out of three antibiotics (CIP and GEN). The highest amount of extinction events was observed for the high IC and low TS combination of the CIP evolution experiment. This indicates that – depending on the treatment drug – populations might struggle more to adapt under strong bottlenecks than under weak bottlenecks.

H_{1,2}: High rather than low antibiotic selection strength reduces treatment efficacy in terms of strength and speed of resistance evolution.

When ignoring the influence of TS on resistance evolution, this hypothesis can be accepted for both GEN and CIP treatments, as the highest resistance evolved the fastest under high IC treatments. However, resistance was higher under low IC treatments when the TS was small, but not when it was large. In contrast, high IC treatments produced higher and faster resistance for large TS than for small TS. For CAR, however, high IC provoked higher resistance under both large and small TS. The selective strength conferred by the antibiotic concentration generally had a stronger impact on the speed of resistance evolution than bottleneck size. Bacteria always survived high IC treatments by acquiring mutations that confer high resistance, regardless of bottleneck size. In contrast, low IC treatments were not always survived due to high resistance. Instead, adaptation was often driven by low-resistance mutations or even

without mutations. In addition, the first mutants only slowly rose to relevant frequencies under low IC treatment, whereas resistance evolved in less than half of the time under high IC.

H_{1,3}: Small rather than wide bottleneck size increases variation in accumulation of selectively favored mutations.

In terms of quantity of beneficial alleles, similar numbers of mutations were able to establish themselves in populations of both bottleneck sizes. However, the types of mutations that were selected differed substantially between the two groups. A higher redundancy of selected genes and a higher degree of parallel evolution were found in the large TS groups than in the small TS groups. In addition, clonal interference was more prevalent in large TS groups than in small TS groups. In contrast, a larger diversity in affected genes was found for mutants in the small TS groups. Furthermore, the allele dynamics of small TS groups rather showed signatures of short-term competitions instead of mutual co-existence or clonal interference in the evolving populations.

H_{1,4}: High rather than low antibiotic selection strength increases parallel evolution.

Only the results of the GEN experiment can be used to address this hypothesis, as most replicates from all treatment groups survived and evolved in only this experiment. Under high IC, a higher degree of parallel evolution took place under large TS than under small TS. All surviving populations of large TS acquired mutations in *pmrB*, whereas selection was more random under small TS. The same was true for the low IC treatments, as all populations acquired *ptsP* mutations under large TS, but a much higher variation of genes was under selection under small TS. Thus, bottleneck size had a more pronounced influence on parallel evolution than selection strength.

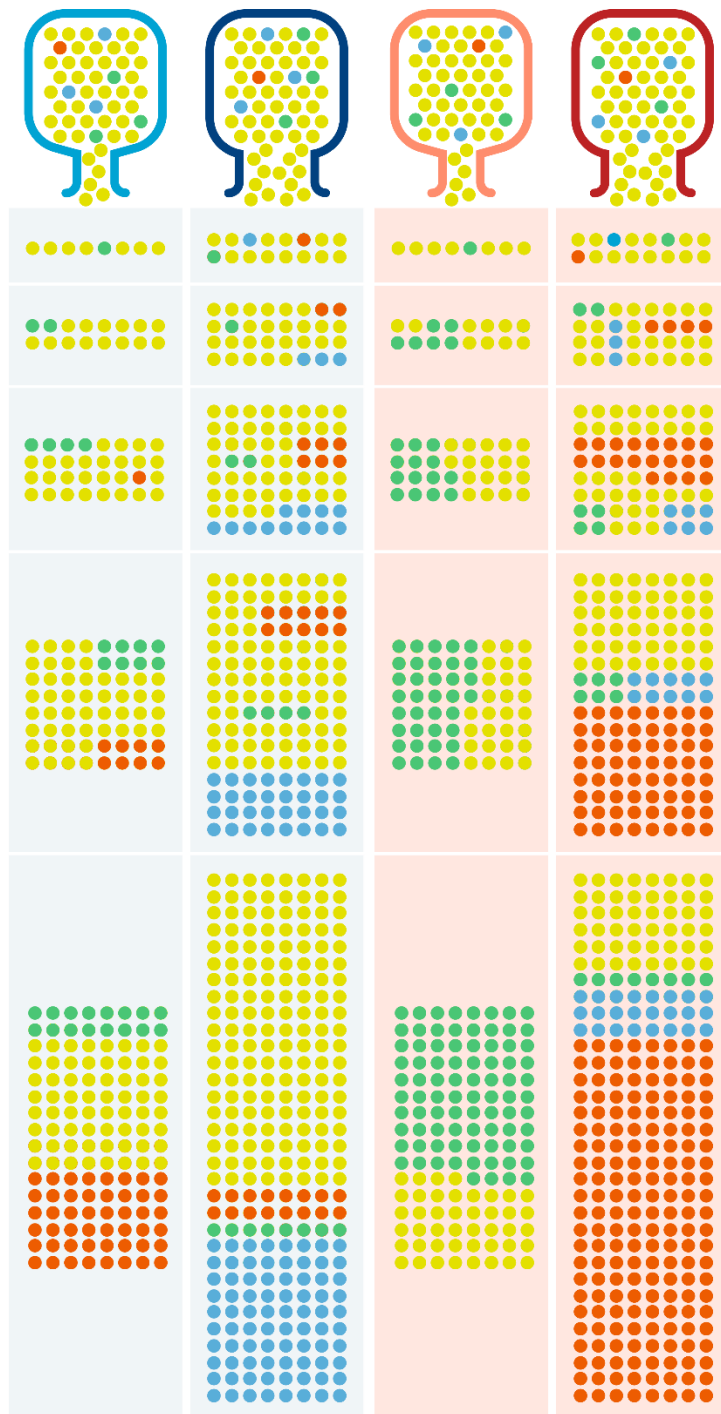


Figure 35: Schematic interpretation of the results. The four bottles in the upper layer represent different populations that undergo either a strong or a weak bottleneck. Blue bottles are treated with low IC and red bottles with high IC. Yellow dots represent wild type cells and dots of other colors represent different mutants. The lower layers illustrate the distribution of mutants after several rounds of cell division. A higher genetic diversity is maintained under weak bottlenecks which leads to selection of the fittest variant. Fitness of variants and strength of selection depend on IC: Blue variants are favoured under low IC and red variants under high IC. Under strong bottlenecks, lower diversity is maintained and selection of first mutants is random. Rapid selection of mutants under high IC might prevent the occurrence of even fitter mutations, which is more likely to play out under low IC. Note: This graph was designed in collaboration with Heike Mahrt (www.grafikdesign-mahrt.de).

Comparing this thesis to the state of the art

The results demonstrate a strong influence of bottleneck strength on the adaptive dynamics of bacterial populations. The combined effect of bottleneck size and selectivity provides mutations of certain effect with different likelihoods to occur and to fix in the population at high frequencies. In general, the results support the original theoretical predictions that a stronger reduction of the effective population size due to population bottlenecks favors the loss of low-frequency beneficial mutations by genetic drift and decreases the chance of parallel evolution. To discuss the results of the GEN experiment as a representative, wide bottlenecks produced a larger starting population size that increased the probability of multiple beneficial mutations being present in each population. This situation enabled the competition between independent beneficial mutations in *pmrB* and *ptsP* which eventually favored one variant over the other, depending on GEN concentration. In contrast, strong bottlenecks were less likely to select for one of two variants but enabled additional mutations of lower fitness effect to eventually dominate. *pmrB* and *ptsP* mutations were also selected in some replicate populations under strong bottlenecks. However, the degree of parallel evolution is far lower than in the wide bottleneck groups.

These results contrast with previously published experimental work by Vogwill *et al.* (2016) that reported a high likelihood of parallel evolution under both strong and wide bottlenecks³²⁷. However, certain aspects of experimental design need to be considered when comparing the results of both studies. First, only a single antibiotic, rifampicin, with a narrow resistance spectrum was used at a single, high concentration in the study by Vogwill *et al.* Second, even though the bottleneck sizes are comparable to the experiments performed for this thesis, relative bottlenecks were applied rather than absolute bottlenecks. These two factors may favor a bias towards a small number of mutations of high fitness effect that enable adaptation to the antibiotic of choice. In addition, a higher carrying capacity was used in the study by Vogwill *et al.* which increases the number of generations over the course of a growth period and can give preexisting mutations another selective advantage^{97,175}.

The results of this thesis agree in principle with previous findings by Lachapelle *et al.* (2015). They found that population size influences the impact of selection, chance and history on evolutionary trajectories of algae populations under high salt concentrations¹⁶⁵. Their findings indicate that lineages that evolve under strong bottlenecks reach different local fitness

peaks while wide bottlenecks lead to increased parallel evolution. They also found that lineages were more likely to reach the global fitness peak under wide bottlenecks. Lachapelle *et al.* used a different experimental model for their experiments and maintained relative bottlenecks of populations of different end point size. Yet, I can draw the same conclusions from my data as the same observations were made for the PA14 lineages that evolved in the GEN and CIP experiments.

In 2020, Garoff *et al.* published the results of an evolution experiment where populations of *Escherichia coli* adapted to increasing concentrations of ciprofloxacin while undergoing three different bottleneck sizes (single cells, 3×10^8 cells and 3×10^{10} cells) ³²⁸. They reported that very large bottlenecks (3×10^{10} cells) led to both highest resistance and highest fitness by selectively favoring target-altering mutations. In contrast, the smaller bottlenecks also selected for many mutations in genes of different function that conferred low fitness and/or resistance. They also found that bottlenecks smaller than the average nucleotide substitution rate of *E. coli* resulted in genotypes that are less similar to genotypes observed in resistant clinical isolates. It is important to note the main difference in the experimental approach compared to my thesis: Instead of maintaining steady antibiotic concentrations of different size $< \text{MIC}$, a single drug concentration was increased at regular intervals to concentration levels $\gg \text{MIC}$. Although this approach favored different mutations of specific effect, the reported results underline the main findings of my thesis: Large bottlenecks maintain a higher genetic diversity that maximizes the chance of parallel evolution driven by the fittest mutants. The results also highlight that large population sizes should be considered when translation of experimental findings to large natural populations of pathogens is desired.

Furthermore, my findings partially agree with recent findings by Wein & Dagan (2019), who found that population bottleneck size impacts genetic diversity regardless of the selective pressure of the treatment regimen ¹⁹⁸. Although the same observation was made for the GEN experiment, it was not for the CIP experiment, highlighting the importance of the spectrum of possible adaptive paths under the respective stressor. Wein and Dagan observed the highest genetic diversity to evolve under optimal growth conditions. To allow for selection of beneficial alleles in the control lineages of this thesis, the number of generations that the populations evolved for was ultimately too low. However, Wein & Dagan also reported that wide population bottlenecks enabled the highest degree of parallel evolution and that clonal

interference was less common under strong bottlenecks and high selectivity. The latter two observations could be confirmed in this thesis.

I also found that multiple variants of *pmrB* and *ptsP* mutations are showing clonal interference in the wide bottleneck treatment groups. This observation contrasts with previously reported findings that mutations of identical effect are less likely to be selected once a beneficial variant is established within the population¹⁸⁴. However, a simple explanation could be that the natural bottlenecks that occur during an infection of a host are much more severe than the wide bottlenecks applied in this thesis. Even stronger bottlenecks would be more likely to favor the selection of a single allele¹³⁸.

ptsP mutations show a very low fitness cost in the absence of selective pressure, which is especially apparent in the 1:1 competition experiment. Here, *ptsP* mutants show the same fitness as the PA14 Wt under IC0 conditions. There is no difference in exponential growth rate and length of lag phase between the two genotypes either, which are common fitness parameters under selection in serial transfer experiments. As mutations that confer high fitness and low-cost adaptation are positively selected for, their allele dynamics likely mask other low-frequency variants that emerged during the experiment. In the wide bottleneck treatment groups, the selection of fast growing *ptsP* variants therefore likely reduces the overall genetic diversity of the replicate populations. By the end of a growth period, the population bottleneck will remove low-frequency variants from the population which further benefits the high-frequency variants. Thus, my findings support earlier predictions by Wahl et al. (2001) on the survival probability of mutations in bacterial populations, which state that mutations that occur at an early point in a growth period have a higher chance of being fixed than mutations that emerge at a later time point¹⁷⁸. The growth dynamics of the large TS populations are characterized by the number of generations of the bottlenecked populations as well as their mutational patterns. Therefore, they have different effects on allele fixation probabilities, depending on bottleneck strength. These are likely complemented by the effects of genetic drift.

Bacterial populations experience parallel evolution both in natural and laboratory environments^{92,300,329,330}. A commonly cited reason for increased parallel evolution in populations of large size is the high chance of clonal interference to occur and to influence allele dynamics^{133,153}. Parallel evolution could be observed in the wide bottleneck populations with larger initial population size, but not for strong bottleneck populations. However, it was

mainly observed on the gene level and less commonly on the nucleotide level. Apart from a small set of *pmrB* variants in the GEN dataset, there was little to no effect of bottlenecks on the frequency of individual SNPs within genes under selection. This implies that SNPs at different sites in the gene likely confer a similar fitness effect. Consequently, selection will be more evident between genes than within them. However, there can be considerable diversity in the phenotypic effects of different single nucleotide variants within the same gene, as it may very well be the case for *pmrB* and *ptsP*^{331,332}.

Overall, I can report that high resistance can evolve even under low IC of antibiotics when the bacterial populations are subjected to strong bottlenecks. The GEN evolution experiment shows that costly mutations that confer high resistance are less likely to be out-competed by less costly mutations that confer lower resistance under strong periodic bottlenecks. However, low selective pressure also increases the likelihood of genetic diversity to be maintained in the population that can give rise to even fitter variants. In contrast, fast fixation of single variants is more likely to occur under high selectivity. Strong population bottlenecks under high selection favor mutations of high effect, but they simultaneously reduce the population's genetic diversity. This also means that the population's potential to adapt to additional selective stressors and to other environments is limited by the evolved fitness trade-offs³³³. In the context of antibiotic resistance evolution, this may provide a window of opportunity for adaptive antibiotic therapy. Collateral sensitivity that has been conferred by the acquired resistance mutation could then be exploited by switching the treatment drug^{77,80}. As large populations have a higher chance of parallel evolution, they are also more likely to repeatedly evolve the same fitness trade-offs³³⁴. Thus, the efficacy of adaptive therapy may be even more predictable in large bacterial populations that undergo strong selection. On the other hand, adaptive therapy of small bacterial populations might require a more individualized approach as the selection of specific mutations and their associated fitness trade-offs is less predictable.

Some experimental lineages already show complex allele dynamics over a rather short evolutionary timescale of about 100 generations. Ultimately, the length of the evolution experiments was too short for secondary mutations to establish themselves and further drive evolutionary dynamics. Thus, the results are difficult to relate to a clinical setting like the adaptation of PA to the CF lung, which takes place over decades of years and tens of thousands of generations. The spreading of different PA sub-lineages within the lung is likely

accompanied by population bottlenecks of unknown size. The high clonal diversity of PA isolates within a patient can either be a result of increased clonal interference (wide bottleneck) or of the spread of a clone to a previously uninhabited patch within the lung after a strong bottleneck^{231,335}. However, assumptions about bottleneck strength are impossible to be drawn when the spatial structure that is provided by the lung environment is ignored as a factor that can contribute to increased clonal diversification. It is therefore crucial not to ignore the influence of spatial structure if future experiments were to be desired for greater understanding of bacterial adaptation to the CF lung.

For the experiments, only drug concentrations below the MIC were used. The reasoning for this choice was to maintain the relatively low number of replicates of evolving populations per treatment group for long periods without risking the extinction of most. Thus, the drug efficacy was expected to be insufficient for population eradication by design. Indeed, most populations used in this thesis did not only survive but also adapted to their respective treatments. However, the high extinction rate in the high IC and low TS treatment of the CIP evolution experiment indicates that extinction is possible at sub-MIC concentrations when the selective pressure is high and the population size is too small for resistance mutations to occur in time. If higher concentrations had been used, it is likely that parallel evolution would have been more common across all bottleneck treatments as high antibiotic resistance is commonly conferred by large-effect mutations in only few genes³³⁶.

In addition, the three applied bottleneck intensities represent only a small fraction of potential bottleneck sizes which bacteria can experience in natural environments. Thus, even the weakest and strongest population bottlenecks applied in this work cannot capture the spectrum of naturally occurring population bottlenecks of pathogenic bacteria. Some infecting populations can be very large (e.g. $\sim 10^9$ CFU/bladder in urinary tract infections), while bacterial populations of lung infections tend to divide into very small compartments⁹⁶. As the extinction levels for the IC80-k50 group of the CIP experiment show, the bottleneck strength was already too severe to allow for evolutionary adaptation to take place. Thus, the impact of bottleneck strength on evolvability of resistance also depends on the mode of action of the applied antibiotic and the mode by which resistance is conferred.

Colistin experiments

In addition to the three completed experiments, test runs have been performed for another drug, colistin (also known as polymyxin E). Polymyxins are polypeptides that are used as antibiotics for the treatment of Gram-negative bacteria. They disrupt the cell membranes of bacteria after binding to lipopolysaccharides of the outer membrane³³⁷. Colistin was commonly used in hospitals against PA infections until the 1980s, after which its use was discontinued because of strong nephrotoxic side effects. It was later re-introduced in the 1990s as a last resort antibiotic after infections caused by multidrug-resistant Gram-negative bacteria had become more prevalent in hospitals³³⁷. It has since also been routinely used for the regular treatment of CF patients. It has proven to be a valuable treatment drug, as it shows a very high effectivity against PA and resistance is observed only rarely in clinical environments³³⁷⁻³³⁹. Resistance against colistin and other polymyxins is usually conferred by modifications of lipid A in the cell membrane, like most GEN resistance observed in this thesis^{340,341}. One of the better described resistance mutations is *mcr-1* (mobilized colistin resistance) which is encoded on a plasmid and mediated by acquisition via horizontal gene transfer between different bacterial strains³⁴³. *Mcr-1* encodes for an enzyme that transfers a phosphoethanolamine residue to the lipid A^{344,345}. Its high clinical relevancy makes colistin an attractive drug to study with my experimental system. It is a last resort antibiotic that may become even more important in the upcoming decades due to the spread of multidrug resistance among pathogenic bacteria. Fortunately, clinical resistance is still rare. However, it is on the rise, as increased transfer of *mcr-1* between different pathogenic strains and species has been observed globally over the last couple of years³⁴⁶.

However, due to its properties as a polypeptide, colistin also commonly imposes technical difficulties for lab research that make it very challenging to incorporate into my evolution experiments³⁴⁷. Colistin has polycationic features that make it bind to different materials, including polystyrene³⁴⁸. Thus, measurements in commonly used polystyrene plates and tubes tend to yield unreliable results. Not only do DRCs in polystyrene plates show high variation among technical replicates of the same treatment during one run, but the results of one DRC are difficult to reproduce. To be able to run experiments more reliably, the chance of colistin randomly binding to surfaces and molecules needs to be reduced. My strategy to achieve this goal was to exchange 96-well polystyrene plates with polypropylene or glass-coated plates which have a lower affinity for colistin than polystyrene. In addition, magnesium

was removed from M9 growth medium as colistin has a high affinity to its ions³³⁷. I performed trial runs with the altered setup and concluded that exchanging the plates and medium had a positive effect on reproducibility of colistin measurements. The DRCs produced smaller variation among technical replicates and measurements could be repeated more reliably between different dates than it had previously been the case with the original setup. However, even though variation could be reduced by removing magnesium from the M9 medium, it could not be eliminated. In addition, the absence of magnesium proved to be a stressor that reduced the growth rate of PA14 quite substantially. Uninhibited PA14 reached stationary phase within 12-16 hours in a culture with normal M9 medium, but it did not reach stationary phase after 24 hours in magnesium depleted M9. Thus, I decided not to continue working with M9 for experiments with colistin but instead continue to look for a different complex medium that works out more reliably. A first trial run revealed that LB medium might have a high potential for colistin experiments, as DRC measurements could be reproduced more reliably than with MP (see Supplementary Figure S7, page 168)

It is important to note that a different growth medium may likely provoke different adaptive patterns and that other medium-specific mutations could occur. If this has any implications on potential epistatic effects of beneficial mutations with mutations that confer adaptation to the medium remains to be seen. The pending colistin experiment should therefore not be directly compared to the other experiments. However, the changes to the setup will most likely allow us to study the evolutionary dynamics of colistin adaptation more reliably than it would have been possible with the original setup.

Outlook

Future work will hopefully enable us to measure the intensity of population bottlenecks that bacteria experience *in vivo* due to transmission and host immune responses more precisely than before. Immediate steps to follow up on the results of this thesis should rather focus on the completion of the current dataset.

The competition experiments done for individual clones from the GEN dataset produced important insights into the competitive dynamics that played out between different genetic variants during evolutionary adaptation. However, the time span used in the assays was not long enough to uncover definite trends under some experimental conditions. These include

the change of competitive dynamics between *pmrB* and *ptsP* mutants under high GEN concentrations and a stronger, but not significantly different competitive outcome under strong bottlenecks compared to wide bottlenecks. Thus, additional competition assays should be performed, in which the duration of competition is extended to several transfers to reliably determine any real differences in power dynamics under different treatment conditions. In addition, the treatment groups should be extended to different starting ratios (e.g. 1:100 and 100:1 instead of 1:1) to simulate whether one genetic variant is able to establish itself in a population dominated by another variant. These conditions would also be closer to and more comparable with those that played out during the evolution experiments.

The insights gained by the improved competition assays would then also be of great use to develop population genetic models that simulate allele dynamics of evolving populations under different bottleneck strengths. As the data obtained in this thesis is very complex, it would be a valuable approach to use mathematical modelling to reduce the complexity of the conditions down to the most relevant parameters. By applying mathematical models to understand the dynamics observed in the evolution experiments, the effect of other bottleneck sizes could ideally also be reliably predicted.

In addition, a more in-depth functional validation of the *ptsP* mutants would be an important step to better understand the role of *ptsP* for resistance evolution of GEN. The gene is known as an important player in the nitrogen cycle, but it has so far not been studied in detail for its role in antibiotic resistance. The conferred resistance against GEN is not particularly strong and most likely not clinically relevant. Nevertheless, *ptsP* likely is an important steppingstone for lower levels of resistance and might be an interesting candidate to potentially be involved in other types of lower level stress responses.

Eventually, additional experiments with colistin should be performed with an improved experimental setup. Colistin is of great clinical importance for the treatment of CF patients. As it remains one of the most valuable last-resort antibiotics, colistin will likely become of even greater relevance in the upcoming years after the writing of this thesis.

Instead of following up on the results of the CAR experiment, I would rather propose to repeat the experiment with a more clinically relevant beta-lactam antibiotic and include a commonly associated beta-lactamase blocker that forces additional resistance mechanisms to evolve. One important candidate would be piperacillin in combination with tazobactam.

References

1. Williams KJ. The introduction of “chemotherapy” using arsphenamine - The first magic bullet. *J R Soc Med.* 2009;102(8):343-348. doi:10.1258/jrsm.2009.09k036
2. Ehrlich P. Diskussionsbemerkungen zum Vortrag von Wechselmann (Chemotherapie der Syphilis). *Bericht ueber die Tagung der Freien Vereinigung fuer Mikrobiol.* 1910;47:223-224.
3. Lloyd NC, Morgan HW, Nicholson BK, Ronimus RS. The composition of Ehrlich’s Salvarsan: Resolution of a century-old debate. *Angew Chemie - Int Ed.* 2005;44(6):941-944. doi:10.1002/anie.200461471
4. Bosch F, Rosich L. The contributions of paul ehrlich to pharmacology: A tribute on the occasion of the centenary of his nobel prize. *Pharmacology.* 2008;82(3):171-179. doi:10.1159/000149583
5. Zaffiri L, Gardner J, Toledo-Pereyra LH. History of antibiotics. from salvarsan to cephalosporins. *J Investig Surg.* 2012;25(2):67-77. doi:10.3109/08941939.2012.664099
6. Davies J, Davies D. Origins and evolution of antibiotic resistance. *Microbiol Mol Biol Rev.* 2010;74(3):417-433. doi:10.1128/MMBR.00016-10
7. Aminov RI. A brief history of the antibiotic era: Lessons learned and challenges for the future. *Front Microbiol.* 2010;1(DEC):1-7. doi:10.3389/fmicb.2010.00134
8. Gould K. Antibiotics: From prehistory to the present day. *J Antimicrob Chemother.* 2016;71(3):572-575. doi:10.1093/jac/dkv484
9. Ventola CL. [Review] The antibiotic resistance crisis: part 1: causes and threats. *Pharm Ther.* 2015;40(4):277-283. doi:Article
10. Kohanski MA, Dwyer DJ, Collins JJ. How antibiotics kill bacteria: From targets to networks. *Nat Rev Microbiol.* 2010;8(6):423-435. doi:10.1038/nrmicro2333
11. van der Meij A, Worsley SF, Hutchings MI, van Wezel GP. Chemical ecology of antibiotic production by actinomycetes. *FEMS Microbiol Rev.* 2017;41(3):392-416. doi:10.1093/femsre/fux005
12. Hibbing ME, Fuqua C, Parsek MR, Peterson SB. Bacterial competition: surviving and thriving in the microbial jungle. *Nat Rev Microbiol.* 2010;8(1):15-25. doi:10.1038/nrmicro2259.Bacterial
13. Yim G, Wang HH, Davies J. Antibiotics as signalling molecules. *Philos Trans R Soc B Biol Sci.* 2007;362(1483):1195-1200. doi:10.1098/rstb.2007.2044
14. Romero D, Traxler MF, López D, Kolter R. Antibiotics as signal molecules. *Chem Rev.* 2011;111(9):5492-5505. doi:10.1021/cr2000509
15. Rémy B, Mion S, Plener L, Elias M, Chabrière E, Daudé D. Interference in bacterial quorum sensing: A biopharmaceutical perspective. *Front Pharmacol.* 2018;9(MAR). doi:10.3389/fphar.2018.00203
16. Beceiro A, Tomás M, Bou G. Antimicrobial resistance and virulence: A successful or deleterious association in the bacterial world? *Clin Microbiol Rev.* 2013;26(2):185-230.

doi:10.1128/CMR.00059-12

17. Kohanski M a, DePristo M a, Collins JJ. Sublethal antibiotic treatment leads to multidrug resistance via radical-induced mutagenesis. *Mol Cell*. 2010;37(3):311-320. doi:10.1016/j.molcel.2010.01.003
18. Andersson DI, Hughes D, Kubicek-Sutherland JZ. Mechanisms and consequences of bacterial resistance to antimicrobial peptides. *Drug Resist Updat*. 2016;26:43-57. doi:10.1016/j.drug.2016.04.002
19. World Health Organization, ed. *Antimicrobial Resistance: Global Report on Surveillance*. Geneva, Switzerland: World Health Organization; 2014.
20. Enzler MJ, Berbari E, Osmon DR. Antimicrobial prophylaxis in adults. *Mayo Clin Proc*. 2011;86(7):686-701. doi:10.4065/mcp.2011.0012
21. Munckhof W. Antibiotics for surgical prophylaxis. *Aust Prescr*. 2005;28(2):38-40. doi:10.18773/austprescr.2005.030
22. Landers TF, Cohen B, Wittum TE, Larson EL. A review of antibiotic use in food animals: Perspective, policy, and potential. *Public Health Rep*. 2012;127(1):4-22. doi:10.1177/003335491212700103
23. Manyi-Loh C, Mamphweli S, Meyer E, Okoh A. *Antibiotic Use in Agriculture and Its Consequential Resistance in Environmental Sources: Potential Public Health Implications*. Vol 23.; 2018. doi:10.3390/molecules23040795
24. Van Boeckel TP, Brower C, Gilbert M, et al. Global trends in antimicrobial use in food animals. *Proc Natl Acad Sci U S A*. 2015;112(18):5649-5654. doi:10.1073/pnas.1503141112
25. Heuer H, Schmitt H, Smalla K. Antibiotic resistance gene spread due to manure application on agricultural fields. *Curr Opin Microbiol*. 2011;14(3):236-243. doi:10.1016/j.mib.2011.04.009
26. Grenni P, Ancona V, Barra Caracciolo A. Ecological effects of antibiotics on natural ecosystems: A review. *Microchem J*. 2018;136:25-39. doi:10.1016/j.microc.2017.02.006
27. Danner MC, Robertson A, Behrends V, Reiss J. Antibiotic pollution in surface fresh waters: Occurrence and effects. *Sci Total Environ*. 2019;664:793-804. doi:10.1016/j.scitotenv.2019.01.406
28. Gullberg E, Cao S, Berg OG, et al. Selection of resistant bacteria at very low antibiotic concentrations. *PLoS Pathog*. 2011;7(7):1-9. doi:10.1371/journal.ppat.1002158
29. Wistrand-Yuen E, Knopp M, Hjort K, Koskiniemi S, Berg OG, Andersson DI. Evolution of high-level resistance during low-level antibiotic exposure. *Nat Commun*. 2018;9(1). doi:10.1038/s41467-018-04059-1
30. Alanis AJ. Resistance to Antibiotics: Are We in the Post-Antibiotic Era? *Arch Med Res*. 2005;36(6):697-705. doi:10.1016/j.arcmed.2005.06.009
31. Falagas ME, Bliziotis IA. Pandrug-resistant Gram-negative bacteria: the dawn of the post-antibiotic era? *Int J Antimicrob Agents*. 2007;29(6):630-636. doi:10.1016/j.ijantimicag.2006.12.012

32. Dcosta VM, King CE, Kalan L, et al. Antibiotic resistance is ancient. *Nature*. 2011;477(7365):457-461. doi:10.1038/nature10388
33. Fisher RA. *The Genetical Theory of Natural Selection by R.A. Fisher ; Edited with a Foreword and Notes by J.H. Bennett*. A complete. Oxford: Oxford University Press; 1999.
34. Laxminarayan R, Mills AJ, Breman JG, et al. Advancement of global health: key messages from the Disease Control Priorities Project. *Lancet*. 2006;367(9517):1193-1208. doi:10.1016/S0140-6736(06)68440-7
35. Lynch M, Ackerman MS, Gout JF, et al. Genetic drift, selection and the evolution of the mutation rate. *Nat Rev Genet*. 2016;17(11):704-714. doi:10.1038/nrg.2016.104
36. Foster PL. Stress-Induced Mutagenesis in Bacteria. *Crit Rev Biochem Mol Biol*. 2007;42(5):373–397. doi:doi:10.1080/10409230701648494
37. Eliopoulos GM, Blazquez J. Hypermutation as a Factor Contributing to the Acquisition of Antimicrobial Resistance. *Clin Infect Dis*. 2003;37(9):1201-1209. doi:10.1086/378810
38. Andersson DI, Levin BR. The biological cost of antibiotic resistance. *Curr Opin Microbiol*. 1999;2(5):489-493. doi:10.1016/S1369-5274(99)00005-3
39. McArthur AG, Wagleichner N, Nizam F, et al. The comprehensive antibiotic resistance database. *Antimicrob Agents Chemother*. 2013;57(7):3348-3357. doi:10.1128/AAC.00419-13
40. Blair JMA, Webber MA, Baylay AJ, Ogbolu DO, Piddock LJ V. Molecular mechanisms of antibiotic resistance. *Nat Rev Microbiol*. 2015;13(1):42-51. doi:10.1038/nrmicro3380
41. Alekshun MN, Levy SB. Molecular mechanisms of antibacterial multidrug resistance. *Cell*. 2007;128(6):1037-1050. doi:10.1016/j.cell.2007.03.004
42. Depardieu F, Podglajen I, Leclercq R, Collatz E, Courvalin P. Modes and modulations of antibiotic resistance gene expression. *Clin Microbiol Rev*. 2007;20(1):79-114. doi:10.1128/CMR.00015-06
43. Lambert PA. Mechanisms of antibiotic resistance in *Pseudomonas aeruginosa*. *J R Soc Med Suppl*. 2002;95(41):22-26.
44. Webber MA, Piddock LJ V. The importance of efflux pumps in bacterial antibiotic resistance. *J Antimicrob Chemother*. 2003;51(1):9-11. doi:10.1093/jac/dkg050
45. Sandegren L, Andersson DI. Bacterial gene amplification: Implications for the evolution of antibiotic resistance. *Nat Rev Microbiol*. 2009;7(8):578-588. doi:10.1038/nrmicro2174
46. Kondrashov FA. Gene duplication as a mechanism of genomic adaptation to a changing environment. *Proc R Soc B Biol Sci*. 2012;279(1749):5048-5057. doi:10.1098/rspb.2012.1108
47. Band VI, Weiss DS. Heteroresistance: A cause of unexplained antibiotic treatment failure? *PLoS Pathog*. 2019;15(6):e1007726. doi:10.1371/journal.ppat.1007726
48. Nicoloff H, Hjort K, Levin BR, Andersson DI. The high prevalence of antibiotic heteroresistance in pathogenic bacteria is mainly caused by gene amplification. *Nat Microbiol*. 2019;4(3):504-514. doi:10.1038/s41564-018-0342-0

49. Crofts TS, Gasparri AJ, Dantas G. Next-generation approaches to understand and combat the antibiotic resistome. *Nat Rev Microbiol.* 2017;15(7):422-434. doi:10.1038/nrmicro.2017.28
50. Beardmore RE, Peña-Miller R, Gori F, Iredell J, Barlow M. Antibiotic cycling and antibiotic mixing: Which one best mitigates antibiotic resistance? *Mol Biol Evol.* 2017;34(4):802-817. doi:10.1093/molbev/msw292
51. Skippington E, Ragan MA. Lateral genetic transfer and the construction of genetic exchange communities. *FEMS Microbiol Rev.* 2011;35(5):707-735. doi:10.1111/j.1574-6976.2010.00261.x
52. Cabezón E, de la Cruz F, Arechaga I. Conjugation inhibitors and their potential use to prevent dissemination of antibiotic resistance genes in bacteria. *Front Microbiol.* 2017;8(NOV):1-7. doi:10.3389/fmicb.2017.02329
53. Brown-Jaque M, Calero-Cáceres W, Muniesa M. Transfer of antibiotic-resistance genes via phage-related mobile elements. *Plasmid.* 2015;79:1-7. doi:10.1016/j.plasmid.2015.01.001
54. Sniegowski PD, Gerrish PJ. Beneficial mutations and the dynamics of adaptation in asexual populations. *Philos Trans R Soc B Biol Sci.* 2010;365(1544):1255-1263. doi:10.1098/rstb.2009.0290
55. Hall AR, Griffiths VF, MacLean RC, Colegrave N. Mutational neighbourhood and mutation supply rate constrain adaptation in *Pseudomonas aeruginosa*. *Proc R Soc B Biol Sci.* 2010;277(1681):643-650. doi:10.1098/rspb.2009.1630
56. Amato SM, Fazen CH, Henry TC, et al. The role of metabolism in bacterial persistence. *Front Microbiol.* 2014;5(MAR):1-9. doi:10.3389/fmicb.2014.00070
57. Harms A, Maisonneuve E, Gerdes K. Mechanisms of bacterial persistence during stress and antibiotic exposure. *Science (80-).* 2016;354(6318). doi:10.1126/science.aaf4268
58. Barrett TC, Mok WWK, Murawski AM, Brynildsen MP. Enhanced antibiotic resistance development from fluoroquinolone persisters after a single exposure to antibiotic. *Nat Commun.* 2019;10(1):1-11. doi:10.1038/s41467-019-09058-4
59. Windels EM, Michiels JE, Fauvart M, Wenseleers T, Van den Bergh B, Michiels J. Bacterial persistence promotes the evolution of antibiotic resistance by increasing survival and mutation rates. *ISME J.* 2019;13(5):1239-1251. doi:10.1038/s41396-019-0344-9
60. Frieden T. Antibiotic Resistance Threats. *CDC.* 2013:22-50. doi:CS239559-B
61. Levy SB. Factors impacting on the problem of antibiotic resistance. *J Antimicrob Chemother.* 2002;49(1):25-30. doi:10.1093/jac/49.1.25
62. Nikaido H. Multidrug Resistance in Bacteria. *Annu Rev Biochem.* 2009;78(1):119-146. doi:10.1146/annurev.biochem.78.082907.145923
63. Spellberg B, Guidos R, Gilbert D, et al. The Epidemic of Antibiotic-Resistant Infections: A Call to Action for the Medical Community from the Infectious Diseases Society of America. *Clin Infect Dis.* 2008;46(2):155-164. doi:10.1086/524891

64. Conly JM, Johnston BL. Where are all the new antibiotics? The new antibiotic paradox. *Can J Infect Dis Med Microbiol.* 2005;16(3):159-160.
65. Laxminarayan R. Antibiotic effectiveness: Balancing conservation against innovation. *Science (80-).* 2014;345(6202):1299-1301. doi:10.1126/science.1254163
66. Renwick MJ, Simpkin V, Mossialos E. International and European Initiatives Targeting Innovation in Antibiotic Drug Discovery and Development. 2016;44(0).
67. Kupferschmidt K. Resistance fighters. *Sci.* 2016;352(6287):758–761. doi:10.1126/science.352.6287.758
68. Clatworthy AE, Pierson E, Hung DT. Targeting virulence: a new paradigm for antimicrobial therapy. *Nat Chem Biol.* 2007;3(9):541-548. doi:10.1038/nchembio.2007.24
69. Li B, Webster TJ. Bacteria antibiotic resistance: New challenges and opportunities for implant-associated orthopedic infections. *J Orthop Res.* 2018;36(1):22-32. doi:10.1002/jor.23656
70. Furfaro LL, Payne MS, Chang BJ. Bacteriophage Therapy: Clinical Trials and Regulatory Hurdles. *Front Cell Infect Microbiol.* 2018;8(October):376. doi:10.3389/fcimb.2018.00376
71. Kortright KE, Chan BK, Koff JL, Turner PE. Phage Therapy: A Renewed Approach to Combat Antibiotic-Resistant Bacteria. *Cell Host Microbe.* 2019;25(2):219-232. doi:10.1016/j.chom.2019.01.014
72. Lázár V, Martins A, Spohn R, et al. Antibiotic-resistant bacteria show widespread collateral sensitivity to antimicrobial peptides. *Nat Microbiol.* 2018;3(6):718-731. doi:10.1038/s41564-018-0164-0
73. Lipsitch M, Siber GR. How can vaccines contribute to solving the antimicrobial resistance problem? *MBio.* 2016;7(3):1-8. doi:10.1128/mBio.00428-16
74. Hoelzer K, Bielke L, Blake DP, et al. Vaccines as alternatives to antibiotics for food producing animals. Part 2: New approaches and potential solutions. *Vet Res.* 2018;49(1):1-15. doi:10.1186/s13567-018-0561-7
75. Bikard D, Barrangou R. Using CRISPR-Cas systems as antimicrobials. *Curr Opin Microbiol.* 2017;37:155-160. doi:10.1016/j.mib.2017.08.005
76. Worthington RJ, Melander C. Combination approaches to combat multidrug-resistant bacteria. *Trends Biotechnol.* 2013;31(3):177-184. doi:10.1016/j.tibtech.2012.12.006
77. Imamovic L, Sommer MO a. Use of collateral sensitivity networks to design drug cycling protocols that avoid resistance development. *Sci Transl Med.* 2013;5(204):204ra132. doi:10.1126/scitranslmed.3006609
78. Lázár V, Pal Singh G, Spohn R, et al. Bacterial evolution of antibiotic hypersensitivity. *Mol Syst Biol.* 2013;9(700):700. doi:10.1038/msb.2013.57
79. Imamovic L, Ellabaan MMH, Dantas Machado AM, et al. Drug-Driven Phenotypic Convergence Supports Rational Treatment Strategies of Chronic Infections. *Cell.* 2018;172(1-2):121-134.e14. doi:10.1016/j.cell.2017.12.012

80. Barbosa C, Trebosc V, Kemmer C, et al. Alternative Evolutionary Paths to Bacterial Antibiotic Resistance Cause Distinct Collateral Effects. *2017*;34(November):2229-2244. doi:10.1093/molbev/msx158
81. Pál C, Papp B, Lázár V. Collateral sensitivity of antibiotic-resistant microbes. *Trends Microbiol.* 2015;23(7):401-407. doi:10.1016/j.tim.2015.02.009
82. Jansen G, Barbosa C, Schulenburg H. Experimental evolution as an efficient tool to dissect adaptive paths to antibiotic resistance. *Drug Resist Updat.* 2013;16(6):96-107. doi:10.1016/j.drug.2014.02.002
83. C Barbosa, R Römhild, P Rosenstiel HS. Evolutionary stability of collateral sensitivity to antibiotics in the model pathogen *Pseudomonas aeruginosa*. *Elife.* 2019. doi:10.7554/eLife.51481
84. Poole K. Aminoglycoside Resistance in. *Antimicrob Agents Chemother.* 2005;49(2):479-487. doi:10.1128/AAC.49.2.479
85. Sylvie Garneau-Tsodikova KJL. Mechanisms of Resistance to Aminoglycoside Antibiotics: Overview and Perspectives. *Med Chem Comm.* 2016;7(1):11-27. doi:10.1039/C5MD00344J
86. Hancock REW, Farmer SW, Li Z, Poole K. Interaction of aminoglycosides with the outer membranes and purified lipopolysaccharide and OmpF porin of *Escherichia coli*. *Antimicrob Agents Chemother.* 1991;35(7):1309-1314. doi:10.1128/AAC.35.7.1309
87. Delcour AH. Delcour, A. H. (2010). NIH Public Access, 1794(5), 808–816. <http://doi.org/10.1016/j.bbapap.2008.11.005.Outer>. 2010;1794(5):808-816. doi:10.1016/j.bbapap.2008.11.005.Outer
88. Blanco P, Hernando-Amado S, Reales-Calderon J, et al. Bacterial Multidrug Efflux Pumps: Much More Than Antibiotic Resistance Determinants. *Microorganisms.* 2016;4(1):14. doi:10.3390/microorganisms4010014
89. Lenski RE. Bacterial evolution and the cost of antibiotic resistance. *Int Microbiol.* 1998;1(4):265-270. doi:10.2436/im.v1i4.27
90. Melnyk AH, Wong A, Kassen R. The fitness costs of antibiotic resistance mutations. *Evol Appl.* 2015;8(3):273-283. doi:10.1111/eva.12196
91. Zur Wiesch PS, Engelstädter J, Bonhoeffer S. Compensation of fitness costs and reversibility of antibiotic resistance mutations. *Antimicrob Agents Chemother.* 2010;54(5):2085-2095. doi:10.1128/AAC.01460-09
92. Gerrish PJ, Lenski RE. The fate of competing beneficial mutations in an asexual population. *Genetica.* 1998;102-103(1-6):127-144. doi:10.1023/A:1017067816551
93. MacLean RC, Hall AR, Perron GG, Buckling A. The population genetics of antibiotic resistance: integrating molecular mechanisms and treatment contexts. *Nat Rev Genet.* 2010;11(6):405-414. doi:10.1038/nrg2778
94. Wilson DJ, Hernandez RD, Andolfatto P, Przeworski M. A population genetics-phylogenetics approach to inferring natural selection in coding sequences. *PLoS Genet.* 2011;7(12). doi:10.1371/journal.pgen.1002395

95. Hughes D, Andersson DI. Evolutionary consequences of drug resistance: shared principles across diverse targets and organisms. *Nat Rev Genet.* 2015;16(8):459-471. doi:10.1038/nrg3922
96. Hughes D, Andersson DI. Evolutionary Trajectories to Antibiotic Resistance. *Annu Rev Microbiol.* 2017;71(1):579-596. doi:10.1146/annurev-micro-090816-093813
97. Levin BR, Perrot V, Walker N. Compensatory mutations, antibiotic resistance and the population genetics of adaptive evolution in bacteria. *Genetics.* 2000;154(3):985-997.
98. MacLean RC, Vogwill T. Limits to compensatory adaptation and the persistence of antibiotic resistance in pathogenic bacteria. *Evol Med Public Heal.* 2015;2015(1):4-12. doi:10.1093/emph/eou032
99. Blount ZD, Borland CZ, Lenski RE. Historical contingency and the evolution of a key innovation in an experimental population of *Escherichia coli*. 2008;105(23):7899-7906.
100. Barrick JE, Lenski RE. Genome dynamics during experimental evolution. *Nat Rev Genet.* 2013;14(12):827-839. doi:10.1038/nrg3564
101. Baym M, Stone LK, Kishony R. Multidrug evolutionary strategies to reverse antibiotic resistance. *Science (80-).* 2015;351(6268):aad3292-aad3292. doi:10.1126/science.aad3292
102. Cvijović I, Nguyen Ba AN, Desai MM. Experimental Studies of Evolutionary Dynamics in Microbes. *Trends Genet.* 2018;34(9):693-703. doi:10.1016/j.tig.2018.06.004
103. Bram Van den Bergh, Toon Swings, Maarten Fauvart JM. Experimental Design, Population Dynamics, and Diversity in Microbial Experimental Evolution. *Microbiol Mol Biol Rev.* 2018;82(3):1-54.
104. Buermans HPJ, Dunnen JT Den. Biochimica et Biophysica Acta Next generation sequencing technology : Advances and applications ☆. *BBA - Mol Basis Dis.* 2014;1842(10):1932-1941. doi:10.1016/j.bbadis.2014.06.015
105. Jaszczyszyn Y, Thermes C, Dijk EL Van. Ten years of next-generation sequencing technology. 2014:1-9. doi:10.1016/j.tig.2014.07.001
106. Brockhurst MA, Colegrave N, Rozen DE. Next-generation sequencing as a tool to study microbial evolution. *Mol Ecol.* 2011;20(5):972-980. doi:10.1111/j.1365-294X.2010.04835.x
107. Dettman JR, Rodrigue N, Melnyk AH, Wong A, Bailey SF, Kassen R. Evolutionary insight from whole-genome sequencing of experimentally evolved microbes. *Mol Ecol.* 2012;21(9):2058-2077. doi:10.1111/j.1365-294X.2012.05484.x
108. Perron GG, Gonzalez A, Buckling A. Source-sink dynamics shape the evolution of antibiotic resistance and its pleiotropic fitness cost. *Proc Biol Sci.* 2007;274(1623):2351-2356. doi:10.1098/rspb.2007.0640
109. Kim S, Lieberman TD, Kishony R. Alternating antibiotic treatments constrain evolutionary paths to multidrug resistance. *Proc Natl Acad Sci U S A.* September 2014. doi:10.1073/pnas.1409800111
110. Hegreness M, Shores N, Damian D, Hartl D, Kishony R. Accelerated evolution of resistance in multidrug environments. *Proc Natl Acad Sci U S A.* 2008;105(37):13977-13981. doi:10.1073/pnas.0805965105

111. Levin-Reisman I, Ronin I, Gefen O, Braniss I, Shoresh N, Balaban NQ. Antibiotic tolerance facilitates the evolution of resistance. *Science* (80-). 2017;355(6327):826-830. doi:10.1126/science.aaj2191
112. Hegreness M, Shoresh N, Damian D, Hartl D, Kishony R. Accelerated evolution of resistance in multidrug environments. *Proc Natl Acad Sci U S A*. 2008;105(37):13977-13981.
113. Perron GG, Gonzalez A, Buckling A. Source–sink dynamics shape the evolution of antibiotic resistance and its pleiotropic fitness cost. *Proc R Soc B Biol Sci*. 2007;274(1623):2351-2356. doi:10.1098/rspb.2007.0640
114. Toprak E, Veres A, Michel JB, Chait R, Hartl DL, Kishony R. Evolutionary paths to antibiotic resistance under dynamically sustained drug selection. *Nat Genet*. 2012;44(1):101-105. doi:10.1038/ng.1034
115. Wong A, Rodrigue N, Kassen R. Genomics of adaptation during experimental evolution of the opportunistic pathogen *Pseudomonas aeruginosa*. *PLoS Genet*. 2012;8(9):e1002928. doi:10.1371/journal.pgen.1002928
116. Barbosa C, Beardmore R, Schulenburg H, Jansen G. Antibiotic combination efficacy (ACE) networks for a *Pseudomonas aeruginosa* model. *PLoS Biol*. 2018;16(4):1-25. doi:10.1371/journal.pbio.2004356
117. Roemhild R, Gokhale CS, Dirksen P, et al. Cellular hysteresis as a principle to maximize the efficacy of antibiotic therapy. *Proc Natl Acad Sci U S A*. 2018;115(39):9767-9772. doi:10.1073/pnas.1810004115
118. Levin B, Lipsitch M, Perrot V, et al. The population genetics of antibiotic resistance. *Clin Infect Dis*. 1997;24:S9--S16.
119. Stewart FM, Antia R, Levin BR, Lipsitch M, Mittler JE. The Population Genetics of Antibiotic Resistance II: Analytic theory for sustained populations of bacteria in a community of hosts. *Theor Popul Biol*. 1998;53(2):152-165. doi:10.1006/tpbi.1997.1352
120. Baquero F, Coque TM. Multilevel population genetics in antibiotic resistance. *FEMS Microbiol Rev*. 2011;35(5):705-706. doi:10.1111/j.1574-6976.2011.00293.x
121. Zur Wiesch PA, Kouyos R, Engelstädter J, Regoes RR, Bonhoeffer S. Population biological principles of drug-resistance evolution in infectious diseases. *Lancet Infect Dis*. 2011;11(3):236-247.
122. Jiao YJ, Baym M, Veres A, Kishony R. Population diversity jeopardizes the efficacy of antibiotic cycling. *bioRxiv*. 2016:1-15.
123. Klockgether J, Cramer N, Wiehlmann L, Davenport CF, Tümmler B. *Pseudomonas aeruginosa* Genomic Structure and Diversity. *Front Microbiol*. 2011;2(July):150. doi:10.3389/fmicb.2011.00150
124. Mowat E, Paterson S, Fothergill JL, et al. *Pseudomonas aeruginosa* population diversity and turnover in cystic fibrosis chronic infections. *Am J Respir Crit Care Med*. 2011;183(12):1674-1679. doi:10.1164/rccm.201009-1430OC
125. Tai AS, Bell SC, Kidd TJ, et al. Genotypic diversity within a single *Pseudomonas aeruginosa* strain commonly shared by Australian patients with cystic fibrosis. *PLoS*

- One*. 2015;10(12):1-17. doi:10.1371/journal.pone.0144022
126. Clemente JC, Pehrsson EC, Blaser MJ, et al. The microbiome of uncontacted Amerindians. *Sci Adv*. 2015;1(3):e1500183-e1500183. doi:10.1126/sciadv.1500183
 127. Worby CJ, Lipsitch M, Hanage WP. Within-host bacterial diversity hinders accurate reconstruction of transmission networks from genomic distance data. *PLoS Comput Biol*. 2014;10(3):e1003549. doi:10.1371/journal.pcbi.1003549
 128. Lively CM. The effect of host genetic diversity on disease spread. *Am Nat*. 2010;175(6). doi:10.1086/652430
 129. Van Houte S, Ekroth AKE, Broniewski JM, et al. The diversity-generating benefits of a prokaryotic adaptive immune system. *Nature*. 2016;532(7599):385-388. doi:10.1038/nature17436
 130. Gandon S, Michalakis Y. Local adaptation, evolutionary potential and host-parasite coevolution: Interactions between migration, mutation, population size and generation time. *J Evol Biol*. 2002;15(3):451-462. doi:10.1046/j.1420-9101.2002.00402.x
 131. Wright ES, Vetsigian KH. Inhibitory interactions promote frequent bistability among competing bacteria. *Nat Commun*. 2016;7:11274. doi:10.1038/ncomms11274
 132. Conlin PL, Chandler JR, Kerr B. Games of life and death: antibiotic resistance and production through the lens of evolutionary game theory. *Curr Opin Microbiol*. 2014;21:35-44. doi:10.1016/j.mib.2014.09.004
 133. Maddamsetti R, Lenski RE, Barrick JE. Adaptation, Clonal Interference, and Frequency-Dependent Interactions in a Long-Term Evolution Experiment with *Escherichia coli*. *Genetics*. 2015;200(2):619-631. doi:10.1534/genetics.115.176677
 134. Patwa Z, Wahl LM. The fixation probability of beneficial mutations. *J R Soc Interface*. 2008;5(28):1279-1289. doi:10.1098/rsif.2008.0248
 135. Ellegren H, Galtier N. Determinants of genetic diversity. *Nat Rev Genet*. 2016;17(7):422-433. doi:10.1038/nrg.2016.58
 136. Nei M, Maruyama T, Chakraborty R. The Bottleneck Effect and Genetic Variability in Populations. *Evolution (N Y)*. 1975;29(1):1-10.
 137. Bohannan BJM, Lenski RE. Linking genetic change to community evolution: Insights from studies of bacteria and bacteriophage. *Ecol Lett*. 2000;3(4):362-377. doi:10.1046/j.1461-0248.2000.00161.x
 138. Abel S, Abel zur Wiesch P, Davis BM, Waldor MK. Analysis of Bottlenecks in Experimental Models of Infection. *PLoS Pathog*. 2015;11(6):1-7. doi:10.1371/journal.ppat.1004823
 139. Bull RA, Luciani F, McElroy K, et al. Sequential bottlenecks drive viral evolution in early acute hepatitis c virus infection. *PLoS Pathog*. 2011;7(9). doi:10.1371/journal.ppat.1002243
 140. Hannan TJ, Totsika M, Mansfield KJ, Moore KH, Schembri MA, Hultgren SJ. Host-pathogen checkpoints and population bottlenecks in persistent and intracellular uropathogenic *Escherichia coli* bladder infection. *FEMS Microbiol Rev*. 2012;36(3):616-

648. doi:10.1111/j.1574-6976.2012.00339.x
141. Rego ROM, Bestor A, Štefka J, Rosa PA. Population bottlenecks during the infectious cycle of the lyme disease spirochete *Borrelia burgdorferi*. *PLoS One*. 2014;9(6). doi:10.1371/journal.pone.0101009
 142. Geoghegan JL, Senior AM, Holmes EC. Pathogen population bottlenecks and adaptive landscapes: Overcoming the barriers to disease emergence. *Proc R Soc B Biol Sci*. 2016;283(1837). doi:10.1098/rspb.2016.0727
 143. Flanagan JL, Brodie EL, Weng L, et al. Loss of bacterial diversity during antibiotic treatment of intubated patients colonized with *Pseudomonas aeruginosa*. *J Clin Microbiol*. 2007;45(6):1954-1962. doi:10.1128/JCM.02187-06
 144. Szendro IG, Franke J, de Visser JAGM, Krug J. Predictability of evolution depends nonmonotonically on population size. *Proc Natl Acad Sci U S A*. 2013;110(2):571-576. doi:10.1073/pnas.1213613110
 145. Woolfit M. Effective population size and the rate and pattern of nucleotide substitutions. *Biol Lett*. 2009;5(April):417-420. doi:10.1098/rsbl.2009.0155
 146. Handel A, Rozen DE. The impact of population size on the evolution of asexual microbes on smooth versus rugged fitness landscapes. *BMC Evol Biol*. 2009;9:236. doi:10.1186/1471-2148-9-236
 147. De Visser JAGM, Rozen DE. Limits to adaptation in asexual populations. *J Evol Biol*. 2005;18(4):779-788. doi:10.1111/j.1420-9101.2005.00879.x
 148. Elena SF, Lenski RE. Evolution experiments with microorganisms: the dynamics and genetic bases of adaptation. *Nat Rev Genet*. 2003;4(6):457-469. doi:10.1038/nrg1088
 149. Hill WG, Robertson A. The effect of linkage on limits to artificial selection. *Genet Res (Camb)*. 1966;8(1):269-294. doi:10.1017/S001667230800949X
 150. Desai MM, Fisher DS, Murray AW. The Speed of Evolution and Maintenance of Variation in Asexual Populations. *Curr Biol*. 2007;17(5):385-394. doi:10.1016/j.cub.2007.01.072
 151. Campos PRA, Wahl LM. The adaptation rate of asexuals: Deleterious mutations, clonal interference and population bottlenecks. *Evolution (N Y)*. 2010;64(7):1973-1983. doi:10.1111/j.1558-5646.2010.00981.x
 152. Bollback JP, Huelsenbeck JP. Clonal interference is alleviated by high mutation rates in large populations. *Mol Biol Evol*. 2007;24(6):1397-1406. doi:10.1093/molbev/msm056
 153. Fogle CA, Nagle JL, Desai MM. Clonal interference, multiple mutations and adaptation in large asexual populations. *Genetics*. 2008;180(4):2163-2173. doi:10.1534/genetics.108.090019
 154. Park SC, Krug J. Clonal interference in large populations. *Proc Natl Acad Sci U S A*. 2007;104(46):18135-18140. doi:10.1073/pnas.0705778104
 155. De Visser JAGM, Rozen DE. Clonal interference and the periodic selection of new beneficial mutations in *Escherichia coli*. *Genetics*. 2006;172(4):2093-2100. doi:10.1534/genetics.105.052373

156. de Visser J a. GM, Cooper TF, Elena SF. The causes of epistasis. *Proc R Soc B Biol Sci.* 2011;278(1725):3617-3624. doi:10.1098/rspb.2011.1537
157. Borrell S, Teo Y, Giardina F, et al. Epistasis between antibiotic resistance mutations drives the evolution of extensively drug-resistant tuberculosis. *Evol Med public Heal.* 2013;2013(1):65-74. doi:10.1093/emph/eot003
158. Maisnier-Patin S, Roth JR, Fredriksson A, Nyström T, Berg OG, Andersson DI. Genomic buffering mitigates the effects of deleterious mutations in bacteria. *Nat Genet.* 2005;37(12):1376-1379. doi:10.1038/ng1676
159. Lang GI, Desai MM. The spectrum of adaptive mutations in experimental evolution. *Genomics.* 2014;104(6):412-416. doi:10.1016/j.ygeno.2014.09.011
160. Khan AI, Dinh DM, Schneider D, Lenski RE, Cooper TF. Negative epistasis between beneficial mutations in an evolving bacterial population. *Science.* 2011;332(6034):1193-1196. doi:10.1126/science.1203801
161. Vogwill T, Kojadinovic M, MacLean RC. Epistasis between antibiotic resistance mutations and genetic background shape the fitness effect of resistance across species of *Pseudomonas*. *Proc R Soc B Biol Sci.* 2016;283(1830):20160151. doi:10.1098/rspb.2016.0151
162. Kvittek DJ, Sherlock G. Reciprocal sign epistasis between frequently experimentally evolved adaptive mutations causes a rugged fitness landscape. *PLoS Genet.* 2011;7(4). doi:10.1371/journal.pgen.1002056
163. Palmer AC, Toprak E, Baym M, et al. Delayed commitment to evolutionary fate in antibiotic resistance fitness landscapes. *Nat Commun.* 2015;6(May 2014):1-8. doi:10.1038/ncomms8385
164. Wu NC, Dai L, Olson CA, Lloyd-Smith JO, Sun R. Adaptation in protein fitness landscapes is facilitated by indirect paths. *Elife.* 2016;5(JULY):1-21. doi:10.7554/eLife.16965
165. Lachapelle J, Reid J, Colegrave N. Repeatability of adaptation in experimental populations of different sizes. *Proc R Soc B Biol Sci.* 2015;282(1805). doi:10.1098/rspb.2014.3033
166. Motoo Kimura TO. The average number of generations until fixation of a mutant gene in a finite population. *Genetics.* 1969;(61):763-771.
167. Kuo CH, Moran NA, Ochman H. The consequences of genetic drift for bacterial genome complexity. *Genome Res.* 2009;19(8):1450-1454. doi:10.1101/gr.091785.109
168. LACY RC. Loss of Genetic Diversity from Managed Populations: Interacting Effects of Drift, Mutation, Immigration, Selection, and Population Subdivision. *Conserv Biol.* 1987;1(2):143-158. doi:10.1111/j.1523-1739.1987.tb00023.x
169. Moxon R, Kussell E. The impact of bottlenecks on microbial survival, adaptation, and phenotypic switching in host–pathogen interactions. *Evolution (N Y).* 2017;71(12):2803-2816. doi:10.1111/evo.13370
170. Vogwill T, Comfort AC, Furió V, MacLean RC. Persistence and resistance as complementary bacterial adaptations to antibiotics. *J Evol Biol.* 2016;29(6):1223-1233.

doi:10.1111/jeb.12864

171. Vuilleumier S, Yearsley JM, Perrin N. The fixation of locally beneficial alleles in a metapopulation. *Genetics*. 2008;178(1):467-475. doi:10.1534/genetics.107.081166
172. Brandvain Y, Wright SI. The Limits of Natural Selection in a Nonequilibrium World. *Trends Genet*. 2016;32(4):201-210. doi:10.1016/j.tig.2016.01.004
173. Otto SP, Whitlock MC. Probability of Fixation in Populations of Changing Size. *Genetics*. 1997;146(1967):723-733.
174. Wahl LM, Zhu AD. Survival probability of beneficial mutations in bacterial batch culture. *Genetics*. 2015;200(1):309-320. doi:10.1534/genetics.114.172890
175. Wahl LM, Gerrish PJ, Saika-Voivod I. Evaluating the impact of population bottlenecks in experimental evolution. *Genetics*. 2002;162(2):961-971.
176. Lynch M, Butcher D, Bürger R, Gabriel W. The mutational meltdown in asexual populations. *J Hered*. 1993;84(5):339-344. doi:10.1093/oxfordjournals.jhered.a111354
177. Herron MD, Doebeli M. Parallel Evolutionary Dynamics of Adaptive Diversification in *Escherichia coli*. *PLoS Biol*. 2013;11(2). doi:10.1371/journal.pbio.1001490
178. Wahl LM, Gerrish PJ. The probability that beneficial mutations are lost in populations with periodic bottlenecks. *Evolution (N Y)*. 2001;55(12):2606-2610. doi:10.1111/j.0014-3820.2001.tb00772.x
179. Handel A, Bennett MR. Surviving the bottleneck: Transmission mutants and the evolution of microbial populations. *Genetics*. 2008;180(4):2193-2200. doi:10.1534/genetics.108.093013
180. Raynes Y, Halstead AL, Sniegowski PD. The effect of population bottlenecks on mutation rate evolution in asexual populations. *J Evol Biol*. 2014;27(1):161-169. doi:10.1111/jeb.12284
181. Aardema ML, von Loewenich FD. Varying influences of selection and demography in host-adapted populations of the tick-transmitted bacterium, *Anaplasma phagocytophilum*. *BMC Evol Biol*. 2015;15:58. doi:10.1186/s12862-015-0335-z
182. Coyne JA. Ernst Mayr and the Origin of Species. *Evolution (N Y)*. 1994;48(1):19. doi:10.2307/2409999
183. Olson-Manning F, Wagner, M. R., Mitchell-Olds T. Adaptive evolution: evaluating empirical support for theoretical predictions. *Nat Rev Genet*. 2013;13(12):867-877. doi:10.1038/nrg3322.Adaptive
184. Martinez JL. General principles of antibiotic resistance in bacteria. *Drug Discov Today Technol*. 2014;11(1):33-39. doi:10.1016/j.ddtec.2014.02.001
185. Bergstrom CT, Mcelhany P, Real LA. Transmission bottlenecks as determinants of virulence in rapidly evolving pathogens. *Proc Natl Acad Sci U S A*. 1999;96(9):5095-5100. doi:10.1073/pnas.96.9.5095
186. Martínez L, Baquero F. Interactions among Strategies Associated with Bacterial Infection: Pathogenicity, Epidemicity, and Antibiotic Resistance. *Clin Microbiol Rev*.

- 2002;15(4):647-679. doi:10.1128/CMR.15.4.647
187. Forrester NL, Guerbois M, Seymour RL, Spratt H, Weaver SC. Vector-Borne Transmission Imposes a Severe Bottleneck on an RNA Virus Population. *PLoS Pathog.* 2012;8(9). doi:10.1371/journal.ppat.1002897
 188. Gutiérrez S, Michalakis Y, Blanc S. Virus population bottlenecks during within-host progression and host-to-host transmission. *Curr Opin Virol.* 2012;2(5):546-555. doi:10.1016/j.coviro.2012.08.001
 189. LeClair JS, Wahl LM. The Impact of Population Bottlenecks on Microbial Adaptation. *J Stat Phys.* 2018;172(1):114-125. doi:10.1007/s10955-017-1924-6
 190. Obadia B, Güvener ZT, Zhang V, et al. Probabilistic Invasion Underlies Natural Gut Microbiome Stability. *Curr Biol.* 2017;27(13):1999-2006.e8. doi:10.1016/j.cub.2017.05.034
 191. Vaishampayan PA, Kuehl J V., Froula JL, Morgan JL, Ochman H, Francino MP. Comparative metagenomics and population dynamics of the gut microbiota in mother and infant. *Genome Biol Evol.* 2010;2(1):53-66. doi:10.1093/gbe/evp057
 192. McCutcheon JP, Moran NA. Extreme genome reduction in symbiotic bacteria. *Nat Rev Microbiol.* 2012;10(1):13-26. doi:10.1038/nrmicro2670
 193. Stephens WZ, Wiles TJ, Martinez ES, et al. Identification of population bottlenecks and colonization factors during assembly of bacterial communities within the zebrafish intestine. *MBio.* 2015;6(6):1-11. doi:10.1128/mBio.01163-15
 194. Kim S, Covington A, Pamer EG. The intestinal microbiota: Antibiotics, colonization resistance, and enteric pathogens. *Immunol Rev.* 2017;279(1):90-105. doi:10.1111/imr.12563
 195. Sorbara MT, Pamer EG. Interbacterial mechanisms of colonization resistance and the strategies pathogens use to overcome them. *Mucosal Immunol.* 2019;12(1):1-9. doi:10.1038/s41385-018-0053-0
 196. Campos PRA, Wahl LM. The effects of population bottlenecks on clonal interference, and the adaptation effective population size. *Evolution (N Y).* 2009;63(4):950-958. doi:10.1111/j.1558-5646.2008.00595.x
 197. Elena SF, Wilke CO, Ofria C, Lenski RE. Effects of population size and mutation rate on the evolution of mutational robustness. *Evolution (N Y).* 2007;61(3):666-674. doi:10.1111/j.1558-5646.2007.00064.x
 198. Wein T, Dagan T. The effect of population bottleneck size and selective regime on genetic diversity and evolvability in bacteria. *bioRxiv.* 2019:726158. doi:10.1101/726158
 199. Tortora GJ, Funke BR, Case CL. *Microbiology: An Introduction.* Twelfth ed. Boston: Pearson; 2016.
 200. Vasil ML. *Pseudomonas aeruginosa: Biology, mechanisms of virulence, epidemiology.* *J Pediatr.* 1986;108(5 PART 2):800-805. doi:10.1016/S0022-3476(86)80748-X
 201. Cornelis P, Matthijs S. *Pseudomonas Siderophores and their Biological Significance.* *Microb Siderophores.* 2007;12:193-203. doi:10.1007/978-3-540-71160-5_9

202. Moradali MF, Ghods S, Rehm BHA. *Pseudomonas aeruginosa* lifestyle: A paradigm for adaptation, survival, and persistence. *Front Cell Infect Microbiol.* 2017;7(FEB). doi:10.3389/fcimb.2017.00039
203. Stover CK, Erwin AL, Mizoguchi SD, et al. Complete genome sequence of *Pseudomonas aeruginosa* PAO1 , an opportunistic pathogen. *Nature.* 2000;406(August):959-964.
204. Mathee K, Narasimhan G, Valdes C, et al. Dynamics of *Pseudomonas aeruginosa* genome evolution. *Proc Natl Acad Sci.* 2008;105(8):3100-3105. doi:10.1073/pnas.0711982105
205. Looft C, Reinsch N, Rudat I, et al. High Frequency of Hypermutable *Pseudomonas aeruginosa* in Cystic Fibrosis Lung Infection. 2000;288(May):1251-1253.
206. Saucier M, Zhang Q, Liberati NT, et al. The broad host range pathogen *Pseudomonas aeruginosa* strain PA14 carries two pathogenicity islands harboring plant and animal virulence genes. 2004;101(8).
207. Aloush V, Navon-Venezia S, Seigman-Igra Y, Cabili S, Carmeli Y. Multidrug-resistant *Pseudomonas aeruginosa*: Risk factors and clinical impact. *Antimicrob Agents Chemother.* 2006;50(1):43-48. doi:10.1128/AAC.50.1.43-48.2006
208. Obritsch MD, Fish DN, MacLaren R, Jung R. Nosocomial infections due to multidrug-resistant *Pseudomonas aeruginosa*: Epidemiology and treatment options. *Pharmacotherapy.* 2005;25(10 I):1353-1364. doi:10.1592/phco.2005.25.10.1353
209. WHO | WHO publishes list of bacteria for which new antibiotics are urgently needed. WHO. 2017. <http://www.who.int/mediacentre/news/releases/2017/bacteria-antibiotics-needed/en/#.Wh3JO7fsjHE.mendeley>. Accessed November 28, 2017.
210. Kos VN, Déraspe M, McLaughlin RE, et al. The resistome of *Pseudomonas aeruginosa* in relationship to phenotypic susceptibility. *Antimicrob Agents Chemother.* 2015;59(1):427-436. doi:10.1128/AAC.03954-14
211. López-Causapé C, Cabot G, del Barrio-Tofiño E, Oliver A. The versatile mutational resistome of *Pseudomonas aeruginosa*. *Front Microbiol.* 2018;9(APR):1-9. doi:10.3389/fmicb.2018.00685
212. Breidenstein EBM, de la Fuente-Núñez C, Hancock REW. *Pseudomonas aeruginosa*: All roads lead to resistance. *Trends Microbiol.* 2011;19(8):419-426. doi:10.1016/j.tim.2011.04.005
213. Li G, Shen M, Le S, et al. Genomic analyses of multidrug resistant *Pseudomonas aeruginosa* PA1 resequenced by single-molecule real-time sequencing. *Biosci Rep.* 2016;36(6):1-15. doi:10.1042/BSR20160282
214. Garau J, Gomez L. *Pseudomonas aeruginosa* pneumonia. *Curr Opin Infect Dis.* 2003;16(2):135-143. doi:10.1097/00001432-200304000-00010
215. Fujitani S, Sun HY, Yu VL, Weingarten JA. Pneumonia due to *pseudomonas aeruginosa*: Part I: Epidemiology, clinical diagnosis, and source. *Chest.* 2011;139(4):909-919. doi:10.1378/chest.10-0166
216. Fothergill JL, Walshaw MJ, Winstanley C. Transmissible strains of *Pseudomonas aeruginosa* in cystic fibrosis lung infections. *Eur Respir J.* 2012;40(1):227-238. doi:10.1183/09031936.00204411

217. Bhagirath AY, Li Y, Somayajula D, Dadashi M, Badr S, Duan K. Cystic fibrosis lung environment and *Pseudomonas aeruginosa* infection. *BMC Pulm Med.* 2016;16(1):1-22. doi:10.1186/s12890-016-0339-5
218. Riordan JR, Rommens JM, Kerem B, et al. Identification of the cystic fibrosis gene: cloning and characterization of complementary {DNA}. *Science.* 1989;245(4922):1066-1073.
219. Rommens J, Iannuzzi M, Kerem B, et al. Identification of the cystic fibrosis gene: chromosome walking and jumping. *Science (80-).* 1989;245(4922):1059-1065. doi:10.1126/science.2772657
220. Vankeerberghen A, Cuppens H, Cassiman J-J. The cystic fibrosis transmembrane conductance regulator: an intriguing protein with pleiotropic functions. *J Cyst Fibros.* 2002;1(1):13-29. doi:10.1016/S1569-1993(01)00003-0
221. Verkman AS, Song Y, Thiagarajah JR. Role of airway surface liquid and submucosal glands in cystic fibrosis lung disease. *AJP Cell Physiol.* 2003;284(1):C2--C15. doi:10.1152/ajpcell.00417.2002
222. Derichs N. Targeting a genetic defect: cystic fibrosis transmembrane conductance regulator modulators in cystic fibrosis. *Eur Respir Rev.* 2013;22(127):58-65. doi:10.1183/09059180.00008412
223. Zabner J, Smith JJ, Karp PH, Widdicombe JH, Welsh MJ. Loss of CFTR Chloride Channels Alters Salt Absorption by Cystic Fibrosis Airway Epithelia In Vitro. 1998;2:397-403.
224. Hull J. Cystic fibrosis transmembrane conductance regulator dysfunction and its treatment. *JRSM.* 2012;105(Supplement 2):S2--S8. doi:10.1258/jrsm.2012.12s001
225. Rowe SM, Miller S, Sorscher EJ. Cystic Fibrosis. *N Engl J Med.* 2005;352(19):1992-2001. doi:10.1056/NEJMra043184
226. Davis PB. Cystic fibrosis since 1938. *Am J Respir Crit Care Med.* 2006;173(5):475-482. doi:10.1164/rccm.200505-840OE
227. UK Cystic Fibrosis Trust Antibiotic Working Group. *Antibiotic Treatment for Cystic Fibrosis.*; 2009.
228. Carmody LA, Zhao J, Kalikin LM, et al. The daily dynamics of cystic fibrosis airway microbiota during clinical stability and at exacerbation. *Microbiome.* 2015;3(1):12. doi:10.1186/s40168-015-0074-9
229. Jelsbak L, Johansen HK, Frost AL, et al. Molecular epidemiology and dynamics of *Pseudomonas aeruginosa* populations in lungs of cystic fibrosis patients. *Infect Immun.* 2007;75(5):2214-2224. doi:10.1128/IAI.01282-06
230. Schobert M, Jahn D. Anaerobic physiology of {*Pseudomonas*} *aeruginosa* in the cystic fibrosis lung. *Int J Med Microbiol.* 2010;300(8):549-556. doi:10.1016/j.ijmm.2010.08.007
231. Marvig RL, Johansen HK, Molin S, Jelsbak L. Genome analysis of a transmissible lineage of *Pseudomonas aeruginosa* reveals pathoadaptive mutations and distinct evolutionary paths of hypermutators. *PLoS Genet.* 2013;9(9):e1003741. doi:10.1371/journal.pgen.1003741

232. Oliver a, Mena a. Bacterial hypermutation in cystic fibrosis, not only for antibiotic resistance. *Clin Microbiol Infect.* 2010;16(7):798-808. doi:10.1111/j.1469-0691.2010.03250.x
233. Drenkard E, Ausubel FM. Pseudomonas biofilm formation and antibiotic resistance are linked to phenotypic variation. 2002;416(April):200-203.
234. Hurley MN, Cámara M, Smyth AR. Novel approaches to the treatment of Pseudomonas aeruginosa infections in cystic fibrosis. *Eur Respir J.* 2012;40(4):1014-1023. doi:10.1183/09031936.00042012
235. Wood DM, Smyth AR. Antibiotic strategies for eradicating Pseudomonas aeruginosa in people with cystic fibrosis. In: *Cochrane Database of Systematic Reviews.* ; 2006. <http://doi.wiley.com/10.1002/14651858.CD004197.pub2>.
236. Chmiel JF, Aksamit TR, Chotirmall SH, et al. Antibiotic management of lung infections in cystic fibrosis: I. The microbiome, methicillin-resistant Staphylococcus aureus, gram-negative bacteria, and multiple infections. *Ann Am Thorac Soc.* 2014;11(7):1120-1129. doi:10.1513/AnnalsATS.201402-050AS
237. Bhatt JM. Treatment of pulmonary exacerbations in cystic fibrosis. *Eur Respir Rev.* 2013;22(129):205-216. doi:10.1183/09059180.00006512
238. Waters V, Stanojevic S, Klingel M, et al. Prolongation of antibiotic treatment for cystic fibrosis pulmonary exacerbations. *J Cyst Fibros.* 2015;14(6):770-776. doi:10.1016/j.jcf.2015.07.010
239. Thomas J, Cook DJ, Brooks D. Chest physical therapy management of patients with cystic fibrosis: A meta-analysis. *Am J Respir Crit Care Med.* 1995;151(3 I):846-850. doi:10.1164/ajrccm/151.3_pt_1.846
240. Tueffers L, Barbosa C, Bobis I, et al. Pseudomonas aeruginosa populations in the cystic fibrosis lung lose susceptibility to newly applied β -lactams within 3 days. *J Antimicrob Chemother.* 2019;74(10):2916-2925. doi:10.1093/jac/dkz297
241. Winstanley C, O'Brien S, Brockhurst MA. Pseudomonas aeruginosa Evolutionary Adaptation and Diversification in Cystic Fibrosis Chronic Lung Infections. *Trends Microbiol.* 2016;24(5):327-337. doi:10.1016/j.tim.2016.01.008
242. Lucca F, Guarneri M, Ros M, Muffato G, Rigoli R, Da Dalt L. Antibiotic resistance evolution of pseudomonas aeruginosa in cystic fibrosis patients (2010-2013). *Clin Respir J.* 2018;12(7):2189-2196. doi:10.1111/crj.12787
243. Roemhild R, Barbosa C, Beardmore RE, Jansen G, Schulenburg H. Temporal variation in antibiotic environments slows down resistance evolution in pathogenic Pseudomonas aeruginosa. *Evol Appl.* 2015;8(10):945-955. doi:10.1111/eva.12330
244. Barbosa C, Beardmore R, Schulenburg H, Jansen G. Antibiotic combination efficacy (ACE) networks for a Pseudomonas aeruginosa model. *PLoS Biol.* 2018;16(4):1-25. doi:10.1371/journal.pbio.2004356
245. Neu HC. Carbenicillin and ticarcillin. *Med Clin North Am.* 1982;66(1):61-77. doi:10.1016/S0025-7125(16)31442-0
246. Oliphant CM, Pharm D, Hershey MS. Quinolones : A Comprehensive Review. *Clin*

- Pharmacol.* 2002;65(3):455-464.
247. Krause KM, Serio AW, Kane TR, Connolly LE. Aminoglycosides : An Overview. *Cold Spring Harb Perspect Med.* 2016:1-18.
 248. Hayward RS, Harding J, Molloy R, et al. Adverse effects of a single dose of gentamicin in adults: a systematic review. *Br J Clin Pharmacol.* 2018;84(2):223-238. doi:10.1111/bcp.13439
 249. Lim LM, Pharm D, Ly N, et al. Resurgence of Colistin: A Review of Resistance, Toxicity, Pharmacodynamics, and Dosing. *Pharmacotherapy.* 2010;30(12):1279-1291. doi:10.1592/phco.30.12.1279.Resurgence
 250. Wang R, Van Dorp L, Shaw LP, et al. The global distribution and spread of the mobilized colistin resistance gene *mer-1*. *Nat Commun.* 2018;9(1):1-9. doi:10.1038/s41467-018-03205-z
 251. Mikkelsen H, McMullan R, Filloux A. The *Pseudomonas aeruginosa* reference strain PA14 displays increased virulence due to a mutation in *ladS*. *PLoS One.* 2011;6(12):e29113. doi:10.1371/journal.pone.0029113
 252. Lee DG, Urbach JM, Wu G, et al. Genomic analysis reveals that *Pseudomonas aeruginosa* virulence is combinatorial. *Genome Biol.* 2006;7(10). doi:10.1186/gb-2006-7-10-r90
 253. Wiehlmann L, Wagner G, Cramer N, et al. Population structure of {*Pseudomonas*} *aeruginosa*. *Proc Natl Acad Sci.* 2007;104(19):8101-8106. doi:10.1073/pnas.0609213104
 254. Wong A, Rodrigue N, Kassen R. Genomics of Adaptation during Experimental Evolution of the Opportunistic Pathogen *Pseudomonas aeruginosa*. *PLoS Genet.* 2012;8(9). doi:10.1371/journal.pgen.1002928
 255. van Ditmarsch D, Xavier JB. Seeing is believing: What experiments with microbes reveal about evolution. *Trends Microbiol.* 2014;22(1):2-4. doi:10.1016/j.tim.2013.11.004
 256. Madsen JS, Lin YC, Squyres GR, et al. Facultative control of matrix production optimizes competitive fitness in *Pseudomonas aeruginosa* PA14 biofilm models. *Appl Environ Microbiol.* 2015;81(24):8414-8426. doi:10.1128/AEM.02628-15
 257. Alseth EO, Pursey E, Luján AM, McLeod I, Rollie C, Westra ER. Bacterial biodiversity drives the evolution of CRISPR-based phage resistance. *Nature.* 2019;574(7779):549-552. doi:10.1038/s41586-019-1662-9
 258. Li H, Durbin R. Fast and accurate short read alignment with Burrows–Wheeler transform. *bioinformatics.* 2009;25(14):1754-1760.
 259. Andrews S. FastQC: a quality control tool for high throughput sequence data. <http://www.bioinformatics.babraham.ac.uk/projects/fastqc>. 2010.
 260. Garrison E, Marth G. Haplotype-based variant detection from short-read sequencing. 2012:1-9. <http://arxiv.org/abs/1207.3907>.
 261. Hall BG, Acar H, Nandipati A, Barlow M. Growth Rates Made Easy. *Mol Biol Evol.* 2013;31(1):232-238. doi:10.1093/molbev/mst187

262. Robinson JT, Thorvaldsdóttir H, Winckler W, et al. Integrative genomics viewer. *Nat Biotechnol.* 2011;29:24.
263. Ye K, Schulz MH, Long Q, Apweiler R, Ning Z. Pindel: A pattern growth approach to detect break points of large deletions and medium sized insertions from paired-end short reads. *Bioinformatics.* 2009;25(21):2865-2871. doi:10.1093/bioinformatics/btp394
264. R Development Core Team. *R: A Language and Environment for Statistical Computing.*; 2008. <http://www.r-project.org>.
265. RStudio Team. *RStudio: Integrated Development for R.* URL. RStudio, Inc., Boston, MA; 2015. <http://www.rstudio.com>.
266. Li H, Handsaker B, Wysoker A, et al. The Sequence Alignment/Map format and SAMtools. *Bioinformatics.* 2009;25(16):2078-2079. doi:10.1093/bioinformatics/btp352
267. Bolger, A. M., Lohse, M., & Usadel B. Trimmomatic: A flexible trimmer for Illumina Sequence Data. 2014.
268. Okonechnikov K, Golosova O, Fursov M, team the U. Unipro UGENE: a unified bioinformatics toolkit. *Bioinformatics.* 2012;28(8):1166-1167. doi:10.1093/bioinformatics/bts091
269. Koboldt DC, Zhang Q, Larson DE, et al. VarScan 2: Somatic mutation and copy number alteration discovery in cancer by exome sequencing. *Genome Res.* 2012;22(3):568-576. doi:10.1101/gr.129684.111
270. Bentley DR, Balasubramanian S, Swerdlow HP, et al. Accurate whole human genome sequencing using reversible terminator chemistry. - Supplement. *Nature.* 2008;456(7218):53-59. doi:10.1038/nature07517
271. Cock PJA, Fields CJ, Goto N, Heuer ML, Rice PM. The Sanger FASTQ file format for sequences with quality scores, and the Solexa/Illumina FASTQ variants. *Nucleic Acids Res.* 2009;38(6):1767-1771. doi:10.1093/nar/gkp1137
272. Garrison E, Marth G. Haplotype-based variant detection from short-read sequencing. 2012:1-9.
273. Cingolani P, Platts A, Wang LL, et al. A program for annotating and predicting the effects of single nucleotide polymorphisms, SnpEff: SNPs in the genome of *Drosophila melanogaster* strain w1118; iso-2; iso-3. *Fly (Austin).* 2012;6(2):80-92. doi:10.4161/fly.19695
274. Sanger F, Nicklen S, Coulson AR. DNA sequencing with chain-terminating inhibitors. *Proc Natl Acad Sci U S A.* 1977;74(12):5463-5467. doi:10.1073/pnas.74.12.5463
275. Heather JM, Chain B. The sequence of sequencers: The history of sequencing DNA. *Genomics.* 2016;107(1):1-8. doi:10.1016/j.ygeno.2015.11.003
276. Aslam B, Wang W, Arshad MI, et al. Antibiotic resistance: a rundown of a global crisis. *Infect Drug Resist.* 2018;11:1645-1658. doi:10.2147/IDR.S173867
277. O' Neil J. *Antimicrobial Resistance : Tackling a Crisis for the Health and Wealth of Nations.*; 2014. [https://amr-review.org/sites/default/files/AMR Review Paper - Tackling a crisis for the health and wealth of nations_1.pdf](https://amr-review.org/sites/default/files/AMR%20Review%20Paper%20-%20Tackling%20a%20crisis%20for%20the%20health%20and%20wealth%20of%20nations_1.pdf).

278. Samani P, Bell G. Adaptation of experimental yeast populations to stressful conditions in relation to population size. *J Evol Biol.* 2010;23(4):791-796. doi:10.1111/j.1420-9101.2010.01945.x
279. Bell G. Evolutionary rescue and the limits of adaptation. *Philos Trans R Soc Lond B Biol Sci.* 2013;368(1610):20120080. doi:10.1098/rstb.2012.0080
280. Greaves M, Maley CC. Clonal evolution in cancer. *Nature.* 2012;481(7381):306-313. doi:10.1038/nature10762
281. Bharat V, Adkar, Michael Manhart, Sanchari Bhattacharyya, Jian Tian MM and EIS. Optimization of lag phase shapes the evolution of a bacterial enzyme. *Nat Ecol Evol.* 2017;1(6):1-18. doi:10.1038/s41559-017-0149.
282. Ho WC, Zhang J. Evolutionary adaptations to new environments generally reverse plastic phenotypic changes. *Nat Commun.* 2018;9(1):1-11. doi:10.1038/s41467-017-02724-5
283. Berrazeg M, Jeannot K, Ntsogo Enguéné VY, et al. Mutations in β -lactamase AmpC increase resistance of *Pseudomonas aeruginosa* isolates to antipseudomonal cephalosporins. *Antimicrob Agents Chemother.* 2015;59(10):6248-6255. doi:10.1128/AAC.00825-15
284. Barrow K, Kwon DH. Alterations in two-component regulatory systems of phoPQ and pmrAB are associated with polymyxin B resistance in clinical isolates of *Pseudomonas aeruginosa*. *Antimicrob Agents Chemother.* 2009;53(12):5150-5154. doi:10.1128/AAC.00893-09
285. Groisman, Eduardo A. The pleiotropic two-component regulatory system PhoP-PhoQ. *J Bacteriol.* 2001;183(6):1835-1842. doi:10.1128/JB.183.6.1835
286. Fernández L, Gooderham WJ, Bains M, McPhee JB, Wiegand I, Hancock REW. Adaptive resistance to the “last hope” antibiotics polymyxin B and colistin in *Pseudomonas aeruginosa* is mediated by the novel two-component regulatory system ParR-ParS. *Antimicrob Agents Chemother.* 2010;54(8):3372-3382. doi:10.1128/AAC.00242-10
287. Hancock REW, Raffle VJ, Nicas TI. Involvement of the outer membrane in gentamicin and streptomycin uptake and killing in *Pseudomonas aeruginosa*. *Antimicrob Agents Chemother.* 1981;19(5):777-785. doi:10.1128/AAC.19.5.777
288. Taber HW, Mueller JP, Miller PF, Arrow AS. Bacterial uptake of aminoglycoside antibiotics. *Microbiol Rev.* 1987;51(4):439-457.
289. Beceiro A, Llobet E, Aranda J, et al. Phosphoethanolamine modification of lipid A in colistin-resistant variants of *Acinetobacter baumannii* mediated by the pmrAB two-component regulatory system. *Antimicrob Agents Chemother.* 2011;55(7):3370-3379. doi:10.1128/AAC.00079-11
290. Lee JY, Ko KS. Mutations and expression of PmrAB and PhoPQ related with colistin resistance in *Pseudomonas aeruginosa* clinical isolates. *Diagn Microbiol Infect Dis.* 2014;78(3):271-276. doi:10.1016/j.diagmicrobio.2013.11.027
291. Gooderham WJ, Hancock REW. Regulation of virulence and antibiotic resistance by two-component regulatory systems in *Pseudomonas aeruginosa*. *FEMS Microbiol Rev.*

- 2009;33(2):279-294. doi:10.1111/j.1574-6976.2008.00135.x
292. Wang D, Seeve C, Pierson LS, Pierson EA. Transcriptome profiling reveals links between ParS/ParR, MexEF-OprN, and quorum sensing in the regulation of adaptation and virulence in *Pseudomonas aeruginosa*. *BMC Genomics*. 2013;14(1). doi:10.1186/1471-2164-14-618
293. Reizer J, Reizer A, Merrick MJ, Plunkett G, Rose DJ, Saier MH. Novel phosphotransferase-encoding genes revealed by analysis of the *Escherichia coli* genome: A chimeric gene encoding an Enzyme I homologue that possesses a putative sensory transduction domain. *Gene*. 1996;181(1-2):103-108. doi:10.1016/S0378-1119(96)00481-7
294. Rabus R, Reizer J, Paulsen I, Saier MH. Enzyme I Ntr from *Escherichia coli*. *J Biol Chem*. 1999;274(37):26185-26191. doi:10.1074/jbc.274.37.26185
295. Xu H, Lin W, Xia H, et al. Influence of ptsP gene on pyocyanin production in *Pseudomonas aeruginosa*. *FEMS Microbiol Lett*. 2005;253(1):103-109. doi:10.1016/j.femsle.2005.09.027
296. Sanz-García F, Hernando-Amado S, Martínez JL. Mutational evolution of *Pseudomonas aeruginosa* resistance to ribosome-targeting antibiotics. *Front Genet*. 2018;9(OCT):1-13. doi:10.3389/fgene.2018.00451
297. Lee CR, Koo BM, Cho SH, et al. Requirement of the dephospho-form of enzyme IINtr for derepression of *Escherichia coli* K-12 *ilvBN* expression. *Mol Microbiol*. 2005;58(1):334-344. doi:10.1111/j.1365-2958.2005.04834.x
298. Zhang S, Chen Y, Potvin E, et al. Comparative signature-tagged mutagenesis identifies *Pseudomonas* factors conferring resistance to the pulmonary collectin SP-A. *PLoS Pathog*. 2005;1(3):0259-0268. doi:10.1371/journal.ppat.0010031
299. Sun J, Deng Z, Yan A. Bacterial multidrug efflux pumps: Mechanisms, physiology and pharmacological exploitations. *Biochem Biophys Res Commun*. 2014;453(2):254-267. doi:10.1016/j.bbrc.2014.05.090
300. Bailey SF, Blanquart F, Bataillon T, Kassen R. What drives parallel evolution?: How population size and mutational variation contribute to repeated evolution. *BioEssays*. 2017;39(1):1-9. doi:10.1002/bies.201600176
301. Abeyrathne PD, Lam JS. WaaL of *Pseudomonas aeruginosa* utilizes ATP in in vitro ligation of O antigen onto lipid A-core. *Mol Microbiol*. 2007;65(5):1345-1359. doi:10.1111/j.1365-2958.2007.05875.x
302. Bolard A, Plésiat P, Jeannot K. Mutations in gene *fusA1* as a novel mechanism of aminoglycoside resistance in clinical strains of *Pseudomonas aeruginosa*. *Antimicrob Agents Chemother*. 2018;62(2):1-10. doi:10.1128/AAC.01835-17
303. Mesaros N, Nordmann P, Plésiat P, et al. *Pseudomonas aeruginosa*: Resistance and therapeutic options at the dawn of the 2d millenium. *Antibiotiques*. 2007;9(3):189-198. doi:10.1016/S1294-5501(07)91378-3
304. Jeannot K, Elsen S, Köhler T, Attree I, Van Delden C, Plésiat P. Resistance and virulence of *Pseudomonas aeruginosa* clinical strains overproducing the MexCD-OprJ efflux pump. *Antimicrob Agents Chemother*. 2008;52(7):2455-2462. doi:10.1128/AAC.01107-07

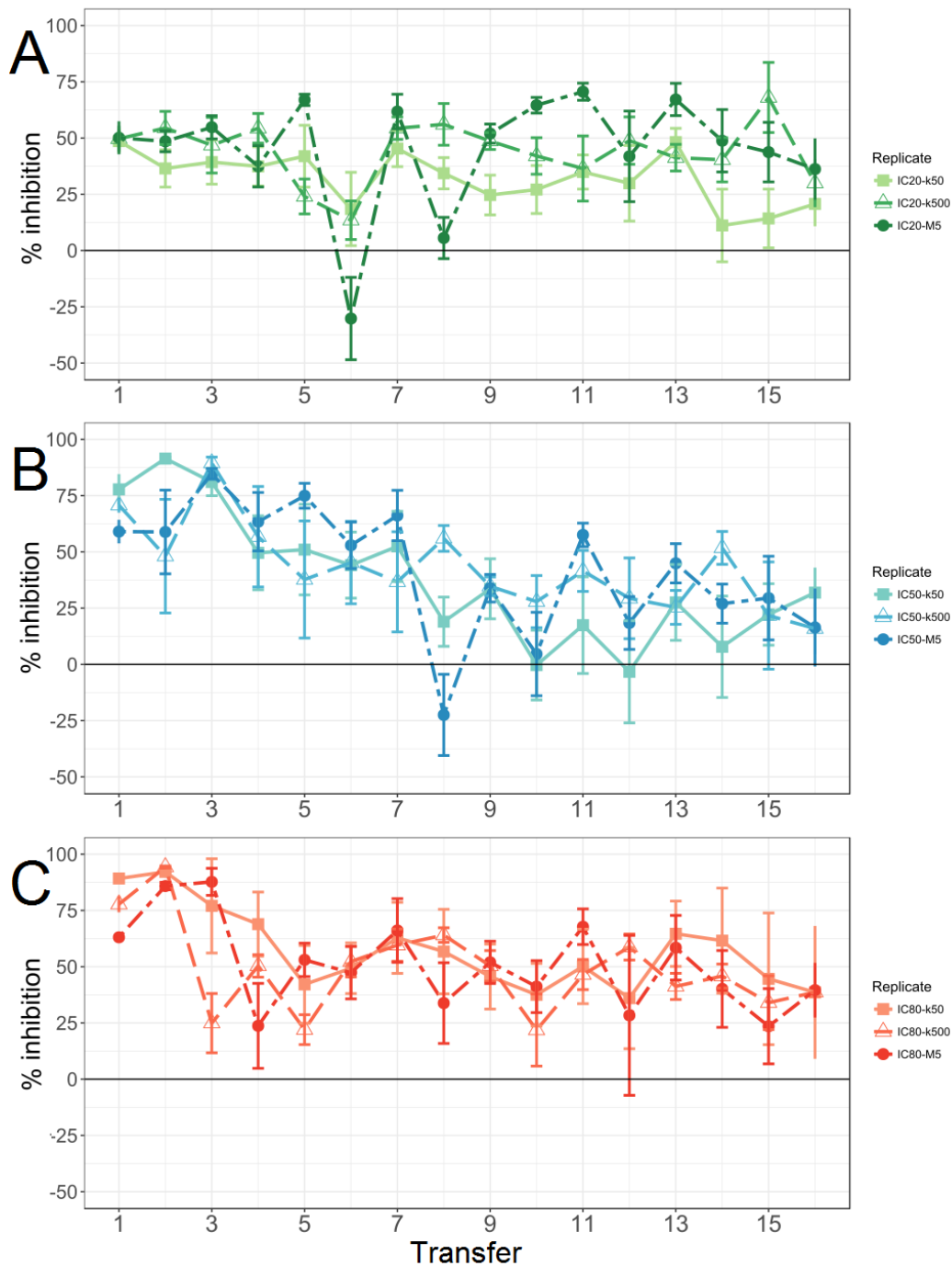
305. Su HC, Ramkissoon K, Doolittle J, et al. The development of ciprofloxacin resistance in *Pseudomonas aeruginosa* involves multiple response stages and multiple proteins. *Antimicrob Agents Chemother.* 2010;54(11):4626-4635. doi:10.1128/AAC.00762-10
306. Nilsson AI, Koskiniemi S, Eriksson S, Kugelberg E, Hinton JCD, Andersson DI. Bacterial genome size reduction by experimental evolution. *Proc Natl Acad Sci U S A.* 2005;102(34):12112-12116. doi:0503654102 [pii]r10.1073/pnas.0503654102
307. Alcalde-Rico M, Olivares-Pacheco J, Alvarez-Ortega C, Cámara M, Martínez JL. Role of the multidrug resistance efflux pump MexCD-OprJ in the *Pseudomonas aeruginosa* quorum sensing response. *Front Microbiol.* 2018;9(NOV):1-16. doi:10.3389/fmicb.2018.02752
308. Oshri RD, Zrihen KS, Shner I, Omer Bendori S, Eldar A. Selection for increased quorum-sensing cooperation in *Pseudomonas aeruginosa* through the shut-down of a drug resistance pump. *ISME J.* 2018;12(10):2458-2469. doi:10.1038/s41396-018-0205-y
309. Choi Y, Yu A-M. ABC Transporters in Multidrug Resistance and Pharmacokinetics, and Strategies for Drug Development. *Curr Pharm Des.* 2014;20(5):793-807. doi:10.2174/138161282005140214165212
310. Greene NP, Kaplan E, Crow A, Koronakis V. Antibiotic resistance mediated by the MacB ABC transporter family: A structural and functional perspective. *Front Microbiol.* 2018;9(MAY). doi:10.3389/fmicb.2018.00950
311. Poole K. Efflux-mediated multiresistance in Gram-negative bacteria. *Clin Microbiol Infect.* 2004;10(1):12-26. doi:10.1111/j.1469-0691.2004.00763.x
312. Zgurskaya HI, Nikaido H. Multidrug resistance mechanisms: Drug efflux across two membranes. *Mol Microbiol.* 2000;37(2):219-225. doi:10.1046/j.1365-2958.2000.01926.x
313. Zgurskaya HI. Multicomponent drug efflux complexes: architecture and mechanism of assembly. *Future Microbiol.* 2009;4:919-932. doi:10.2217/fmb.09.62.
314. Viveiros M, Dupont M, Rodrigues L, et al. Antibiotic stress, genetic response and altered permeability of *E. coli*. *PLoS One.* 2007;2(4). doi:10.1371/journal.pone.0000365
315. Ashish A. Malik, Bruce C. Thomson, Andrew S. Whiteley, Mark Bailey RIG. Bacterial Physiological Adaptations to Contrasting Edaphic Conditions Identified Using Landscape Scale Metagenomics. *MBio.* 2017;8(4):1-13.
316. Chevin LM. On measuring selection in experimental evolution. *Biol Lett.* 2011;7(2):210-213. doi:10.1098/rsbl.2010.0580
317. WRIGHT AJ, WILKOWSKE CJ. The Penicillins. *Mayo Clin Proc.* 1991;66(10):1047-1063. doi:10.1016/S0025-6196(12)61730-3
318. Giovanni Bonfiglio, Younes Laksai, Luigi Franchino GA and GN. Mechanisms of beta-lactam resistance amongst *Pseudomonas aeruginosa* isolated in an Italian survey. *J Antimicrob Chemother.* 1998;42:697-702.
319. Brook I. Inoculum Effect. *Rev Infect Dis.* 1989;11(3):361-368. doi:10.1093/clinids/11.3.361
320. Tan C, Phillip Smith R, Srimani JK, et al. The inoculum effect and band-pass bacterial response to periodic antibiotic treatment. *Mol Syst Biol.* 2012;8(617):1-11.

doi:10.1038/msb.2012.49

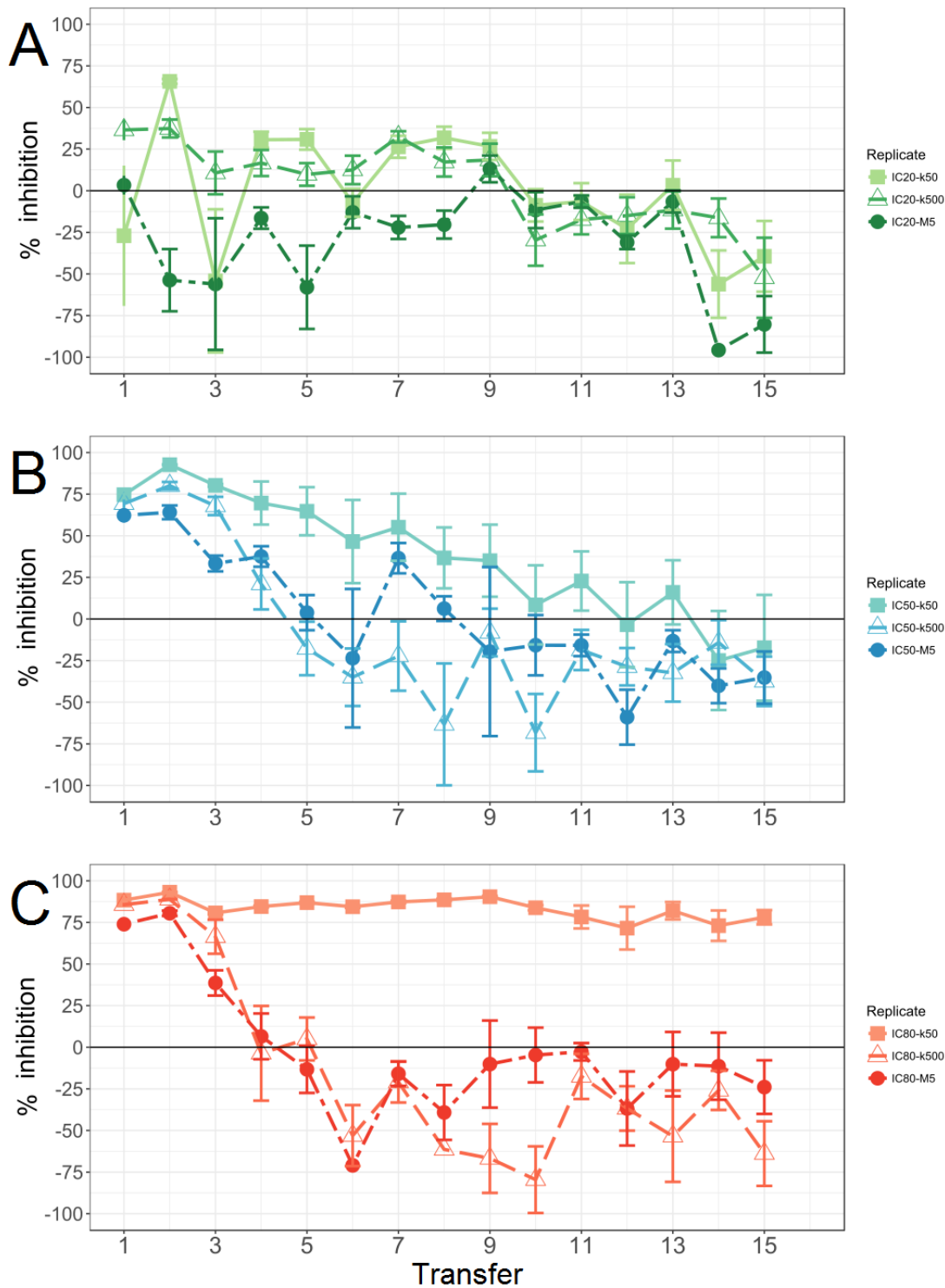
321. Baeder DY, Regoes RR. Pharmacodynamic inoculum effect from the perspective of bacterial population modeling. *bioRxiv*. 2019:550368. doi:10.1101/550368
322. Oz T, Guvenek A, Yildiz S, Karaboga E, Talha Y. Strength of selection pressure is an important parameter contributing to the complexity of antibiotic resistance evolution. 2014:1-33.
323. Wen X, Langevin AM, Dunlop MJ. Antibiotic export by efflux pumps affects growth of neighboring bacteria. *Sci Rep*. 2018;8(1):1-9. doi:10.1038/s41598-018-33275-4
324. Ge B, Domesle KJ, Yang Q, et al. Effects of low concentrations of erythromycin, penicillin, and virginiamycin on bacterial resistance development in vitro. *Sci Rep*. 2017;7(1):1-11. doi:10.1038/s41598-017-09593-4
325. Damper PD, Epstein W. Role of the membrane potential in bacterial resistance to aminoglycoside antibiotics. *Antimicrob Agents Chemother*. 1981;20(6):803-808. doi:10.1128/AAC.20.6.803
326. Vestergaard M, Nøhr-Meldgaard K, Ingmer H. Multiple pathways towards reduced membrane potential and concomitant reduction in aminoglycoside susceptibility in *Staphylococcus aureus*. *Int J Antimicrob Agents*. 2018;51(1):132-135. doi:10.1016/j.ijantimicag.2017.08.024
327. Vogwill T, Phillips RL, Gifford DR, Maclean RC. Divergent evolution peaks under intermediate population bottlenecks during bacterial experimental evolution. *Proc R Soc B Biol Sci*. 2016;283(1835). doi:10.1098/rspb.2016.0749
328. Garoff L, Pietsch F, Huseby DL, Lilja T, Brandis G. Population bottlenecks strongly influence the evolutionary trajectory to fluoroquinolone resistance in *Escherichia coli*. *Mol Biol Evol*. 2020:1-30.
329. Fraune S, Bosch TCG. Why bacteria matter in animal development and evolution. *BioEssays*. 2010;32(7):571-580. doi:10.1002/bies.200900192
330. Lieberman TD, Michel JB, Aingaran M, et al. Parallel bacterial evolution within multiple patients identifies candidate pathogenicity genes. *Nat Genet*. 2011;43(12):1275-1280. doi:10.1038/ng.997
331. Kassen R, Bataillon T. Distribution of fitness effects among beneficial mutations before selection in experimental populations of bacteria. *Nat Genet*. 2006;38(4):484-488. doi:10.1038/ng1751
332. MacLean RC, Buckling A. The distribution of fitness effects of beneficial mutations in *Pseudomonas aeruginosa*. *PLoS Genet*. 2009;5(3). doi:10.1371/journal.pgen.1000406
333. Yvonne Willi, Josh Van Buskirk AAH. Limits to the Adaptive Potential of Small Populations. *Annu Rev Ecol Syst*. 2006;37:433-458. doi:10.2307/annurev.ecolsys.37.091305.300
334. Chavhan Y, Malusare S, Dey S. Larger bacterial populations evolve heavier fitness trade-offs and undergo greater ecological specialization Author contributions. 2020;5697. doi:10.1101/2020.02.02.930883

335. Feliziani S, Marvig RL, Luján AM, et al. Coexistence and within-host evolution of diversified lineages of hypermutable *Pseudomonas aeruginosa* in long-term cystic fibrosis infections. *PLoS Genet.* 2014;10(10):e1004651. doi:10.1371/journal.pgen.1004651
336. Sommer MOA, Munck C, Toft-Kehler RV, Andersson DI. Prediction of antibiotic resistance: Time for a new preclinical paradigm? *Nat Rev Microbiol.* 2017;15(11):689-696. doi:10.1038/nrmicro.2017.75
337. Falagas ME, Kasiakou SK. Colistin : The Revival of Polymyxins for the Management of Multidrug-Resistant Gram-Negative Bacterial Infections. *Rev Antinfective Agents.* 2005;40:1333-1342.
338. Hindler J a, Humphries RM. Colistin MIC variability by method for contemporary clinical isolates of multidrug-resistant Gram-negative bacilli. *J Clin Microbiol.* 2013;51(6):1678-1684. doi:10.1128/JCM.03385-12
339. Jansen G, Mahrt N, Tueffers L, et al. Association between clinical antibiotic resistance and susceptibility of *Pseudomonas* in the cystic fibrosis lung. *Evol Med public Heal.* 2016:eow016. doi:10.1093/emph/eow016
340. Blair JM a., Webber M a., Baylay AJ, Ogbolu DO, Piddock LJ V. Molecular mechanisms of antibiotic resistance. *Nat Rev Microbiol.* 2014;(December):1-10. doi:10.1038/nrmicro3380
341. Cai Y, Chai D, Wang R, Liang B, Bai N. Colistin resistance of *Acinetobacter baumannii*: clinical reports, mechanisms and antimicrobial strategies. *J Antimicrob Chemother.* 2012;67(7):1607-1615. doi:10.1093/jac/dks084
342. Guyonnet J, Manco B, Baduel L, Kaltsatos V, Aliabadi MHFS, Lees P. Determination of a dosage regimen of colistin by pharmacokinetic/pharmacodynamic integration and modeling for treatment of G.I.T. disease in pigs. *Res Vet Sci.* 2010;88(2):307-314. doi:10.1016/j.rvsc.2009.09.001
343. Liu YY, Wang Y, Walsh TR, et al. Emergence of plasmid-mediated colistin resistance mechanism MCR-1 in animals and human beings in China: A microbiological and molecular biological study. *Lancet Infect Dis.* 2016;16(2):161-168. doi:10.1016/S1473-3099(15)00424-7
344. Hinchliffe P, Yang QE, Portal E, et al. Insights into the Mechanistic Basis of Plasmid-Mediated Colistin Resistance from Crystal Structures of the Catalytic Domain of MCR-1. *Nat Publ Gr.* 2017;(November 2016):1-10. doi:10.1038/srep39392
345. Gao R, Hu Y, Li Z, et al. Dissemination and Mechanism for the MCR-1 Colistin Resistance. 2016:1-19. doi:10.1371/journal.ppat.1005957
346. Yi L, Wang J, Gao Y, et al. mcr-1–Harboring *Salmonella enterica* Serovar Typhimurium Sequence Type 34 in Pigs, China. *Emerg Infect Dis.* 2017;23(2):291-295.
347. Vasoo S. crossm Susceptibility Testing for the Polymyxins : Two Steps Back , Three Steps Forward ? 2017;55(9):2573-2582.
348. Karvanen M, Malmberg C, Friberg LE, Cars O. crossm Colistin Is Extensively Lost during. 2017;61(11):1-9.

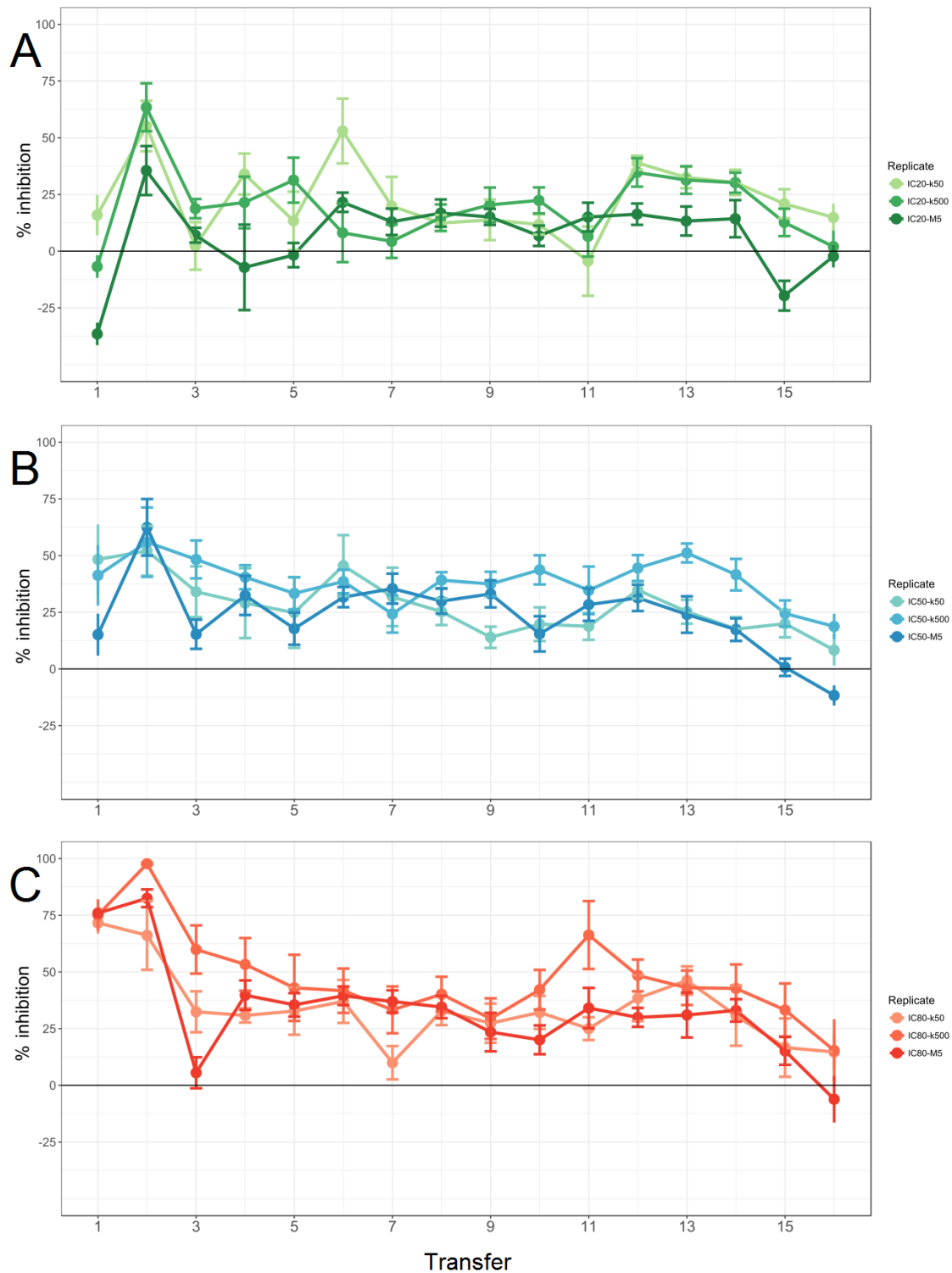
Supplementary data



Supplementary Figure S1: Graphs of inhibition dynamics for the CAR evolution experiment, including the IC50 and k500-TS groups. A: IC20 treatment groups. B: IC50 treatment groups. C: IC80 treatment groups. The X-axis represents the time series of the evolution experiment: every point represents the end of a growth period before the next transfer. The Y-axis represents the mean growth inhibition of the populations relative to the evolving no-drug control, based on the cell concentrations. Error bars represent standard error of mean (8 replicates). Light squares represent small TS, dark dots represent large TS, intermediate rectangles represent intermediate transfer size.



Supplementary Figure S2: Graphs of inhibition dynamics for the CIP evolution experiment, including the IC50 and k500-TS groups. A: IC20 treatment groups. B: IC50 treatment groups. C: IC80 treatment groups. The X-axis represents the time series of the evolution experiment: every point represents the end of a growth period before the next transfer. The Y-axis represents the mean growth inhibition of the populations relative to the evolving no-drug control, based on the cell concentrations. Error bars represent standard error of mean (8 replicates). Light squares represent small TS, dark dots represent large TS, intermediate rectangles represent intermediate transfer size.



Supplementary Figure S3: Graphs of inhibition dynamics for the GEN evolution experiment, including the IC50 and k500-TS groups. A: IC20 treatment groups. B: IC50 treatment groups. C: IC80 treatment groups. The X-axis represents the time series of the evolution experiment: every point represents the end of a growth period before the next transfer. The Y-axis represents the mean growth inhibition of the populations relative to the evolving no-drug control, based on the cell concentrations. Error bars represent standard error of mean (8 replicates). Light colors represent small TS, dark colors represent large TS, intermediate colors represent intermediate transfer size.

Supplementary Table S1: Cell counts of every transfer obtained from flow cytometry for CAR evolution experiment.

Treatment group	Transfer	Mean Cell Count	SD Cell Count
IC0-k50	1	276.946331	67.3855073
IC0-k50	2	241.774943	48.7532248
IC0-k50	3	255.965438	77.4930451
IC0-k50	4	331.316192	65.4718563
IC0-k50	5	260.56582	112.646024
IC0-k50	6	320.488319	57.9876193
IC0-k50	7	404.768278	139.758822
IC0-k50	8	289.884155	66.2110298
IC0-k50	9	285.647322	79.6611377
IC0-k50	10	360.003891	91.0430213
IC0-k50	11	256.578168	123.878903
IC0-k50	12	334.142949	133.533637
IC0-k50	13	398.032865	48.1718886
IC0-k50	14	344.958772	103.02192
IC0-k50	15	249.331345	64.1494956
IC0-k50	16	356.111328	112.310542
IC0-k500	1	325.091755	59.683695
IC0-k500	2	343.400636	142.359096
IC0-k500	3	221.455803	79.9719516
IC0-k500	4	379.282177	223.083399
IC0-k500	5	223.121174	162.841883
IC0-k500	6	371.891687	68.6805708
IC0-k500	7	413.039081	38.6490737
IC0-k500	8	450.286314	215.278455
IC0-k500	9	353.053462	117.455324
IC0-k500	10	409.830604	88.6561641
IC0-k500	11	361.665588	92.307046
IC0-k500	12	411.285003	128.149442
IC0-k500	13	347.208577	77.3783727
IC0-k500	14	400.830396	69.0635877
IC0-k500	15	395.287221	65.5867353
IC0-k500	16	366.729478	124.2502
IC0-M5	1	396.979844	82.3236561
IC0-M5	2	454.287496	172.314357
IC0-M5	3	350.101789	163.88227
IC0-M5	4	323.233959	90.6085925
IC0-M5	5	423.972066	161.826479
IC0-M5	6	338.692283	140.851094
IC0-M5	7	409.014308	177.994499
IC0-M5	8	281.183635	29.2387344
IC0-M5	9	358.513255	41.6739956

IC0-M5	10	428.645496	144.193091
IC0-M5	11	624.255813	175.615961
IC0-M5	12	381.115319	98.1754316
IC0-M5	13	508.27714	96.1700051
IC0-M5	14	397.604261	83.1187305
IC0-M5	15	392.291587	114.557448
IC0-M5	16	423.278604	116.906284
IC20-k50	1	142.255152	30.300197
IC20-k50	2	153.573076	40.0930066
IC20-k50	3	155.378366	50.1772489
IC20-k50	4	207.410623	57.4380412
IC20-k50	5	151.327318	71.6434679
IC20-k50	6	261.292038	104.489305
IC20-k50	7	221.351236	65.0766224
IC20-k50	8	190.314929	40.3539557
IC20-k50	9	215.175684	50.4875306
IC20-k50	10	262.426537	76.7036448
IC20-k50	11	167.033762	38.970924
IC20-k50	12	234.265217	112.312598
IC20-k50	13	206.252617	48.8221656
IC20-k50	14	306.506794	111.334634
IC20-k50	15	213.799089	65.116553
IC20-k50	16	282.359315	70.6582316
IC20-k500	1	163.656814	37.4693712
IC20-k500	2	156.340169	50.5805748
IC20-k500	3	117.785409	54.7288558
IC20-k500	4	173.176283	49.7931592
IC20-k500	5	169.51824	34.5847782
IC20-k500	6	321.75357	63.7532786
IC20-k500	7	188.474696	41.1039199
IC20-k500	8	197.82816	83.4859902
IC20-k500	9	181.262419	26.4485926
IC20-k500	10	237.569379	66.501328
IC20-k500	11	229.853382	104.683127
IC20-k500	12	210.314581	86.5121925
IC20-k500	13	203.90935	41.175698
IC20-k500	14	239.156797	78.7691597
IC20-k500	15	126.439018	123.175659
IC20-k500	16	256.882441	78.347822
IC20-M5	1	198.121582	58.2976068
IC20-M5	2	233.829629	42.1168261
IC20-M5	3	158.285948	36.0845711
IC20-M5	4	202.259544	59.4463982
IC20-M5	5	140.073761	21.3861311
IC20-M5	6	441.034389	124.01756
IC20-M5	7	156.40565	62.9599894

IC20-M5	8	265.50252	51.5880411
IC20-M5	9	172.175045	30.3754012
IC20-M5	10	151.832653	29.8658648
IC20-M5	11	183.593788	47.4754906
IC20-M5	12	221.623029	153.42486
IC20-M5	13	167.019852	72.9215213
IC20-M5	14	203.63278	110.189558
IC20-M5	15	220.739737	103.795754
IC20-M5	16	270.061762	115.522535
IC50-k50	1	61.5562866	37.5001279
IC50-k50	2	20.6251368	3.10989295
IC50-k50	3	48.4498632	31.2758885
IC50-k50	4	167.038319	108.879906
IC50-k50	5	127.622315	104.882608
IC50-k50	6	179.105964	94.1199247
IC50-k50	7	192.467452	126.441288
IC50-k50	8	234.850113	63.4276188
IC50-k50	9	189.675602	76.2140753
IC50-k50	10	361.088027	111.591456
IC50-k50	11	211.871579	110.159934
IC50-k50	12	345.127808	151.729801
IC50-k50	13	288.367936	134.259862
IC50-k50	14	317.946295	155.531922
IC50-k50	15	193.992011	68.1430047
IC50-k50	16	242.544752	79.2556178
IC50-k500	1	95.0863596	21.6853559
IC50-k500	2	178.170118	173.48209
IC50-k500	3	23.3331743	11.8276806
IC50-k500	4	164.086736	169.363525
IC50-k500	5	138.940128	116.127617
IC50-k500	6	203.589308	136.252655
IC50-k500	7	261.484154	183.875674
IC50-k500	8	198.144609	51.6562457
IC50-k500	9	230.554503	29.4762285
IC50-k500	10	295.480903	94.9621922
IC50-k500	11	211.414614	65.8487726
IC50-k500	12	290.522218	147.680011
IC50-k500	13	259.177188	52.2496128
IC50-k500	14	193.312609	58.4807319
IC50-k500	15	309.433575	188.373724
IC50-k500	16	308.362398	83.2393785
IC50-M5	1	162.633144	41.521759
IC50-M5	2	186.902312	169.033245
IC50-M5	3	53.5770021	16.6411494
IC50-M5	4	118.282444	83.9852832
IC50-M5	5	106.152016	46.9053221

IC50-M5	6	159.459928	70.1158965
IC50-M5	7	138.396048	91.6150396
IC50-M5	8	344.309512	101.485034
IC50-M5	9	237.173018	43.9606343
IC50-M5	10	408.838666	158.987442
IC50-M5	11	265.005671	65.3852712
IC50-M5	12	310.969734	89.3566199
IC50-M5	13	279.895628	88.6474846
IC50-M5	14	290.23342	69.0198818
IC50-M5	15	276.638591	145.847078
IC50-M5	16	353.889664	146.492745
IC80-k50	1	29.8913453	8.33128315
IC80-k50	2	18.9706495	1.96954026
IC80-k50	3	58.7970991	107.241534
IC80-k50	4	102.954762	94.429309
IC80-k50	5	150.816849	90.1980103
IC80-k50	6	162.424565	72.192164
IC80-k50	7	150.468402	127.814197
IC80-k50	8	125.428045	108.930102
IC80-k50	9	155.379448	82.4143923
IC80-k50	10	224.951002	100.386223
IC80-k50	11	127.955543	84.9913155
IC80-k50	12	213.75457	150.298481
IC80-k50	13	140.702171	115.449997
IC80-k50	14	132.566803	161.238388
IC80-k50	15	138.091733	145.925848
IC80-k50	16	218.734839	210.281345
IC80-k500	1	72.2827118	23.2344513
IC80-k500	2	19.5529948	3.18907374
IC80-k500	3	166.293456	58.3715734
IC80-k500	4	188.322205	37.8477913
IC80-k500	5	173.968444	29.565075
IC80-k500	6	177.486823	50.6664431
IC80-k500	7	166.975472	59.283559
IC80-k500	8	161.863313	29.2211216
IC80-k500	9	175.246916	48.1375491
IC80-k500	10	320.244734	131.278196
IC80-k500	11	193.498886	48.4542855
IC80-k500	12	169.676715	47.5010309
IC80-k500	13	203.965564	40.2674141
IC80-k500	14	217.121869	42.808901
IC80-k500	15	260.835357	94.5865603
IC80-k500	16	224.916838	78.3145096
IC80-M5	1	146.630707	11.6891872
IC80-M5	2	64.3802376	15.0898752
IC80-M5	3	43.0077556	41.9838324

IC80-M5	4	246.567352	122.05998
IC80-M5	5	199.074445	62.9686229
IC80-M5	6	178.375575	78.8440291
IC80-M5	7	138.660648	115.710109
IC80-M5	8	186.036676	100.821523
IC80-M5	9	172.259728	67.3419251
IC80-M5	10	252.28489	98.9198712
IC80-M5	11	201.216989	98.885759
IC80-M5	12	272.987208	270.851471
IC80-M5	13	211.233137	145.888746
IC80-M5	14	238.101548	135.757811
IC80-M5	15	299.964807	131.110918
IC80-M5	16	255.789483	102.838198

Supplementary Table S2: Cell counts of every transfer obtained from flow cytometry for CIP evolution experiment.

Treatment group	Transfer	Mean Cell Count	SD Cell Count
IC0-k50	1	221.914052	28.7119193
IC0-k50	2	452.151398	61.0461091
IC0-k50	3	191.366896	43.3002867
IC0-k50	4	277.995895	54.5824946
IC0-k50	5	308.624335	80.2204055
IC0-k50	6	214.807928	64.6156614
IC0-k50	7	249.454076	61.4705353
IC0-k50	8	262.271029	51.8089099
IC0-k50	9	289.259204	59.1879481
IC0-k50	10	212.416271	56.4138227
IC0-k50	11	265.883954	49.8632711
IC0-k50	12	212.764847	64.4683616
IC0-k50	13	249.789916	53.9890351
IC0-k50	14	183.80522	38.6572857
IC0-k50	15	193.316548	43.1123778
IC0-k500	1	350.469564	48.1663231
IC0-k500	2	315.132997	66.4194179
IC0-k500	3	286.018798	36.3845497
IC0-k500	4	382.037924	54.8865041
IC0-k500	5	319.574524	28.7184091
IC0-k500	6	304.730507	70.3408324
IC0-k500	7	290.821743	40.8371576

IC0-k500	8	265.055615	39.2008753
IC0-k500	9	283.995988	53.2441438
IC0-k500	10	197.932522	23.1314597
IC0-k500	11	287.116864	25.6101288
IC0-k500	12	275.124906	70.1162753
IC0-k500	13	266.957703	24.1748102
IC0-k500	14	300.525595	40.9326487
IC0-k500	15	250.849014	20.5388647
IC0-M5	1	389.666705	48.4270561
IC0-M5	2	384.834151	49.3501285
IC0-M5	3	237.515844	26.8894859
IC0-M5	4	351.427027	44.4804723
IC0-M5	5	261.775561	56.5484192
IC0-M5	6	295.135711	59.8184447
IC0-M5	7	319.66524	41.7694561
IC0-M5	8	281.423398	47.8161692
IC0-M5	9	393.522814	63.3698222
IC0-M5	10	286.806574	45.3237608
IC0-M5	11	291.797326	34.6040311
IC0-M5	12	289.448374	29.8182872
IC0-M5	13	307.219202	52.9842819
IC0-M5	14	277.341543	33.4873395
IC0-M5	15	320.731587	79.203413
IC20-k50	1	281.907464	93.5270761
IC20-k50	2	155.008824	6.54617179
IC20-k50	3	294.946468	82.2736502
IC20-k50	4	192.8702	13.5115505
IC20-k50	5	213.402237	19.0553345
IC20-k50	6	230.31295	18.0744151
IC20-k50	7	183.58704	16.4774183
IC20-k50	8	178.840427	17.5349175
IC20-k50	9	212.170506	23.5968997
IC20-k50	10	231.037592	20.6849412
IC20-k50	11	283.142851	29.3696951
IC20-k50	12	261.457354	43.754777
IC20-k50	13	241.593888	37.1990067
IC20-k50	14	286.919055	37.1843281
IC20-k50	15	269.466011	41.0604094
IC20-k500	1	222.399468	21.5090288
IC20-k500	2	197.337446	16.9887227
IC20-k500	3	255.400559	36.726021
IC20-k500	4	318.417329	29.9099487
IC20-k500	5	288.303191	21.7505144
IC20-k500	6	266.648204	26.1378801
IC20-k500	7	196.612062	9.84160607
IC20-k500	8	219.286644	23.2079554

IC20-k500	9	231.50126	27.8287817
IC20-k500	10	256.601859	30.5242417
IC20-k500	11	336.796567	25.62383
IC20-k500	12	316.246951	30.2541645
IC20-k500	13	297.933928	29.8586379
IC20-k500	14	349.435386	34.9153645
IC20-k500	15	381.985717	60.3598838
IC20-M5	1	376.561912	22.03499
IC20-M5	2	591.611558	71.9062446
IC20-M5	3	370.65747	93.9179431
IC20-M5	4	409.153933	22.6036035
IC20-M5	5	413.607303	65.4843949
IC20-M5	6	333.299437	28.2960622
IC20-M5	7	390.172352	22.1503297
IC20-M5	8	338.675544	23.6492933
IC20-M5	9	341.885529	31.667345
IC20-M5	10	320.170978	31.0284598
IC20-M5	11	310.843081	10.8150773
IC20-M5	12	379.156819	11.8321922
IC20-M5	13	327.139942	20.4658772
IC20-M5	14	542.882538	53.5687141
IC20-M5	15	578.168148	54.4284516
IC50-k50	1	56.1993707	2.58684057
IC50-k50	2	33.0932737	0.90735291
IC50-k50	3	37.7353258	1.57986897
IC50-k50	4	84.3713472	35.9590599
IC50-k50	5	108.852124	44.560041
IC50-k50	6	114.828132	53.6711035
IC50-k50	7	111.924919	50.2619611
IC50-k50	8	166.009097	47.9837458
IC50-k50	9	187.934008	62.6087204
IC50-k50	10	194.384567	50.4713137
IC50-k50	11	205.23689	47.3184827
IC50-k50	12	220.035706	54.3323526
IC50-k50	13	209.832307	48.1923808
IC50-k50	14	229.646406	54.7027243
IC50-k50	15	226.770147	61.4549883
IC50-k500	1	107.661637	9.02962372
IC50-k500	2	62.6498253	6.96428465
IC50-k500	3	91.8084818	15.741342
IC50-k500	4	301.62813	58.4590967
IC50-k500	5	376.104717	51.3802552
IC50-k500	6	411.337375	52.6056157
IC50-k500	7	355.524406	60.6349727
IC50-k500	8	432.84662	97.0000264
IC50-k500	9	306.994748	40.6699212

IC50-k500	10	333.05324	46.0205041
IC50-k500	11	340.525317	34.6839027
IC50-k500	12	353.996286	30.8938393
IC50-k500	13	353.37822	46.1482549
IC50-k500	14	342.906608	40.2800914
IC50-k500	15	344.784982	37.2362831
IC50-M5	1	146.943999	16.4461555
IC50-M5	2	138.149352	15.9653953
IC50-M5	3	158.28881	11.2510913
IC50-M5	4	219.45583	21.6600235
IC50-M5	5	251.76584	27.6292147
IC50-M5	6	364.65362	122.757482
IC50-M5	7	202.813218	29.0995073
IC50-M5	8	263.877701	20.8523075
IC50-M5	9	470.511335	199.868238
IC50-M5	10	331.968134	51.8888328
IC50-M5	11	338.012928	18.9039014
IC50-M5	12	460.186856	47.7470315
IC50-M5	13	347.955665	20.0458622
IC50-M5	14	388.620696	28.8960246
IC50-M5	15	433.571896	50.1895754
IC80-k50	1	227.174017	73.7459865
IC80-k50	2	31.0447649	0.72766911
IC80-k50	3	36.918216	1.63306323
IC80-k50	4	43.0084278	1.42020192
IC80-k50	5	40.4968748	1.55086367
IC80-k50	6	33.4470077	1.42282901
IC80-k50	7	31.6830073	1.83697332
IC80-k50	8	29.9744037	1.52425825
IC80-k50	9	27.691839	1.44638528
IC80-k50	10	34.3733835	3.27344373
IC80-k50	11	57.8060555	18.3338428
IC80-k50	12	60.5034691	27.3430903
IC80-k50	13	44.8638317	13.1646096
IC80-k50	14	49.5289308	16.7905415
IC80-k50	15	42.3335254	8.32644939
IC80-k500	1	50.2597459	3.7945767
IC80-k500	2	35.0788145	0.6327106
IC80-k500	3	96.0872387	29.2688597
IC80-k500	4	395.868271	108.689034
IC80-k500	5	303.639518	41.1419499
IC80-k500	6	466.424423	55.8510613
IC80-k500	7	351.483668	35.8488882
IC80-k500	8	427.70723	128.364935
IC80-k500	9	473.588789	58.8709582
IC80-k500	10	355.389357	39.6269202

IC80-k500	11	337.408447	38.9038311
IC80-k500	12	376.22966	36.6566555
IC80-k500	13	409.604196	73.2074618
IC80-k500	14	378.294636	35.3314993
IC80-k500	15	411.024576	48.7187601
IC80-M5	1	101.606488	14.40877
IC80-M5	2	75.0149371	6.12729496
IC80-M5	3	145.755904	18.033484
IC80-M5	4	328.449124	48.3066298
IC80-M5	5	296.559448	37.0202957
IC80-M5	6	504.608488	98.7811211
IC80-M5	7	370.451854	23.3912873
IC80-M5	8	391.652948	46.3433754
IC80-M5	9	433.316582	102.974007
IC80-M5	10	300.196391	47.1929751
IC80-M5	11	299.669934	15.2870857
IC80-M5	12	395.91714	64.3744236
IC80-M5	13	338.357588	59.4377944
IC80-M5	14	308.895579	55.9046187
IC80-M5	15	397.503088	51.6362625

Supplementary Table S3: Cell counts of every transfer obtained from flow cytometry for GEN evolution experiment.

Treatment group	Transfer	Mean Cell Count	SD Cell Count
IC0-k50	1	225.477276	44.9986345
IC0-k50	2	372.344918	58.4905965
IC0-k50	3	272.987813	30.1125126
IC0-k50	4	242.572895	39.6912698
IC0-k50	5	260.623676	60.8896978
IC0-k50	6	402.054419	35.0406552
IC0-k50	7	239.042974	46.4232176
IC0-k50	8	261.84903	44.7790678
IC0-k50	9	261.460818	55.0824994
IC0-k50	10	215.526544	35.6540515
IC0-k50	11	336.595085	55.6718814
IC0-k50	12	258.824261	55.729581
IC0-k50	13	224.058547	30.3091721
IC0-k50	14	214.830673	43.0233022
IC0-k50	15	379.718278	46.3420212

IC0-k50	16	458.408147	42.6109627
IC0-k500	1	444.3051	81.4608759
IC0-k500	2	350.193409	89.7039963
IC0-k500	3	249.270298	48.2693095
IC0-k500	4	337.844211	63.4175733
IC0-k500	5	264.787101	59.4158145
IC0-k500	6	208.558127	32.5286666
IC0-k500	7	223.962592	50.9950493
IC0-k500	8	246.322402	44.2636605
IC0-k500	9	237.812711	67.5894444
IC0-k500	10	269.349657	55.2094523
IC0-k500	11	333.299641	60.0715061
IC0-k500	12	234.171938	53.8823726
IC0-k500	13	197.987841	30.1291832
IC0-k500	14	208.15973	35.7055604
IC0-k500	15	302.450678	63.0442122
IC0-k500	16	355.879894	57.0842803
IC0-M5	1	300.407321	54.0830383
IC0-M5	2	277.506002	64.6456889
IC0-M5	3	345.087392	18.1304887
IC0-M5	4	187.234516	25.5915175
IC0-M5	5	330.512643	51.8755533
IC0-M5	6	228.773456	46.5078105
IC0-M5	7	365.378229	71.1253402
IC0-M5	8	330.25843	50.1095085
IC0-M5	9	241.410796	35.1152419
IC0-M5	10	258.968157	60.6153398
IC0-M5	11	179.459216	84.407918
IC0-M5	12	263.256033	27.9849239
IC0-M5	13	258.935476	37.0772014
IC0-M5	14	301.02335	58.724111
IC0-M5	15	311.119794	37.8417609
IC0-M5	16	376.751074	35.7497603
IC20-k50	1	206.104288	21.8102616
IC20-k50	2	109.789595	27.2531014
IC20-k50	3	239.358537	25.7098067
IC20-k50	4	161.65442	22.1207525
IC20-k50	5	212.286715	31.5903841
IC20-k50	6	115.188381	34.9182993
IC20-k50	7	196.320646	31.4863366
IC20-k50	8	214.694935	8.76086093
IC20-k50	9	211.190718	21.8718811
IC20-k50	10	216.171732	11.0396756
IC20-k50	11	255.817736	37.3987251
IC20-k50	12	149.531029	7.54677011
IC20-k50	13	165.392268	11.6479903

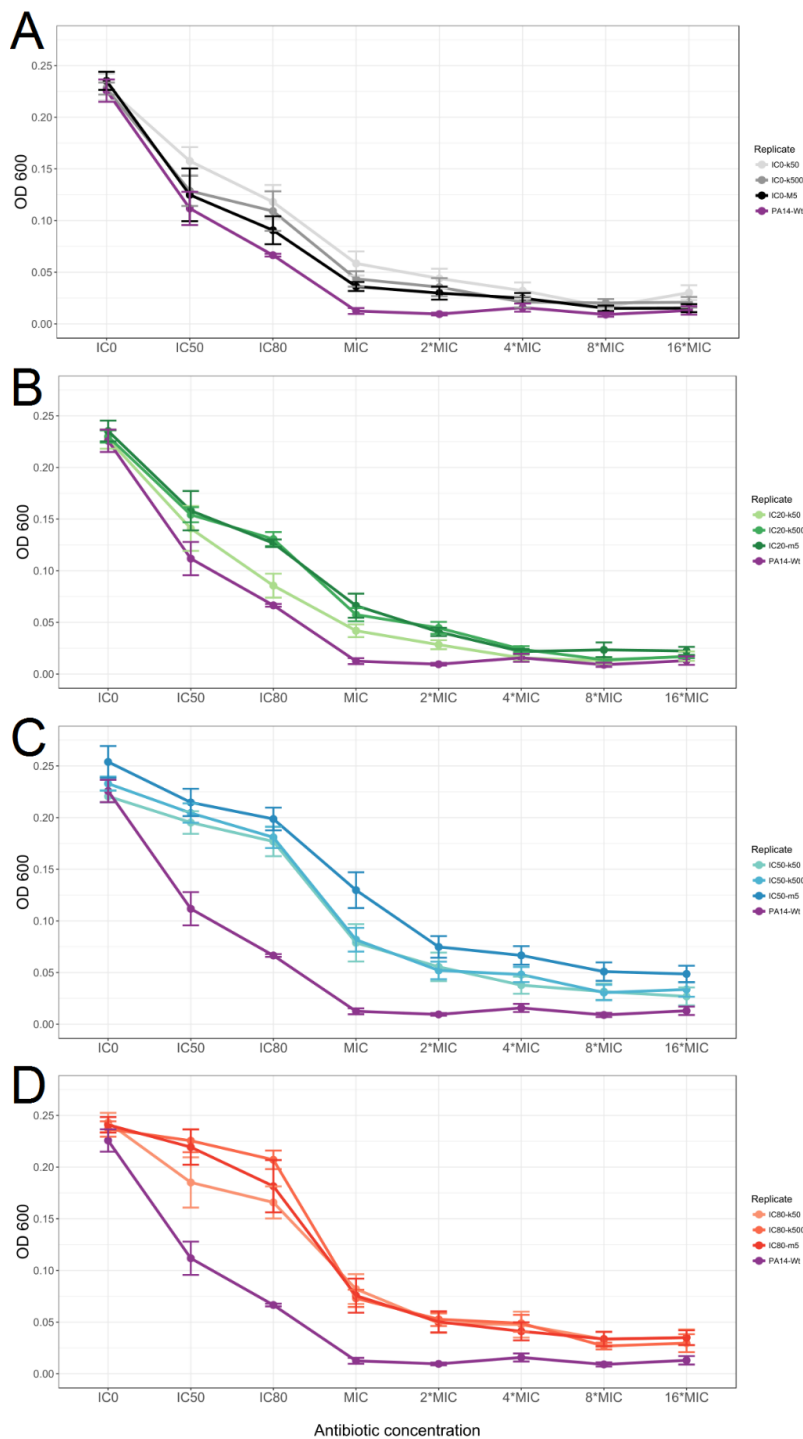
IC20-k50	14	170.715091	13.6592901
IC20-k50	15	193.780991	15.6655113
IC20-k50	16	208.553986	14.8528426
IC20-k500	1	293.708335	13.6925841
IC20-k500	2	100.504707	28.9999727
IC20-k500	3	223.468971	11.6356622
IC20-k500	4	215.946209	31.293201
IC20-k500	5	188.915519	27.3104519
IC20-k500	6	252.769678	35.5232692
IC20-k500	7	263.111654	20.1599509
IC20-k500	8	234.396646	16.0088738
IC20-k500	9	218.87973	21.0253166
IC20-k500	10	213.470328	15.765291
IC20-k500	11	257.04446	24.4790919
IC20-k500	12	179.581949	17.2749717
IC20-k500	13	188.771984	16.7307901
IC20-k500	14	192.007694	12.1886732
IC20-k500	15	240.17372	16.5759137
IC20-k500	16	269.520408	19.4490831
IC20-M5	1	402.64974	14.6074259
IC20-M5	2	190.162963	31.8271616
IC20-M5	3	274.251941	9.59086761
IC20-M5	4	316.106135	55.5666744
IC20-M5	5	300.108018	15.755755
IC20-M5	6	231.417665	12.5167603
IC20-M5	7	256.785563	17.16582
IC20-M5	8	245.496856	17.7274846
IC20-M5	9	250.473108	10.4299649
IC20-M5	10	274.999578	13.2493009
IC20-M5	11	250.650407	18.674871
IC20-M5	12	246.918688	13.8958235
IC20-M5	13	255.831092	18.9058124
IC20-M5	14	252.786158	24.1664842
IC20-M5	15	352.971222	19.3641889
IC20-M5	16	301.739371	14.4604923
IC50-k50	1	126.615949	37.8097801
IC50-k50	2	117.379258	26.8838199
IC50-k50	3	161.559533	27.4197629
IC50-k50	4	173.893362	37.6844726
IC50-k50	5	184.09743	38.0894761
IC50-k50	6	133.375376	32.9792673
IC50-k50	7	167.173793	31.6113096
IC50-k50	8	183.096967	14.4048892
IC50-k50	9	210.742147	11.4801499
IC50-k50	10	196.582295	18.2128487
IC50-k50	11	198.905868	14.5720453

IC50-k50	12	159.705284	9.25855637
IC50-k50	13	183.126832	12.941289
IC50-k50	14	201.905958	12.8923158
IC50-k50	15	196.023216	14.7954088
IC50-k50	16	224.616179	16.6721932
IC50-k500	1	161.443433	36.6370629
IC50-k500	2	121.231526	42.0474564
IC50-k500	3	142.151803	22.9957077
IC50-k500	4	163.726303	14.5909508
IC50-k500	5	183.303701	19.5012755
IC50-k500	6	168.95844	14.203235
IC50-k500	7	208.312119	22.5410912
IC50-k500	8	167.290963	9.63882803
IC50-k500	9	171.971255	14.851288
IC50-k500	10	154.828972	17.6859156
IC50-k500	11	179.653398	28.8482792
IC50-k500	12	152.59616	15.6780769
IC50-k500	13	134.326866	11.4902625
IC50-k500	14	160.667664	19.0927458
IC50-k500	15	207.707644	15.8241975
IC50-k500	16	223.425465	15.3466869
IC50-M5	1	250.336558	27.2383911
IC50-M5	2	110.796597	36.8427414
IC50-M5	3	249.817651	18.9779599
IC50-M5	4	199.334235	25.468553
IC50-M5	5	242.488027	20.9450338
IC50-M5	6	201.554615	13.1110279
IC50-M5	7	190.484767	19.4443336
IC50-M5	8	206.759315	16.2185672
IC50-M5	9	197.336213	17.5758222
IC50-M5	10	249.33679	22.9540567
IC50-M5	11	211.248921	21.1120359
IC50-M5	12	202.516304	17.0976643
IC50-M5	13	224.16511	23.7291589
IC50-M5	14	243.807213	14.6067135
IC50-M5	15	292.79641	11.2552936
IC50-M5	16	329.370632	13.1295305
IC80-k50	1	69.517246	11.6645995
IC80-k50	2	82.9326685	37.1832425
IC80-k50	3	165.533594	22.1133039
IC80-k50	4	169.474383	7.66081038
IC80-k50	5	164.730216	25.6180338
IC80-k50	6	154.31809	23.2060342
IC80-k50	7	220.557995	18.0012887
IC80-k50	8	164.57116	15.3584456
IC80-k50	9	177.854852	21.1804777

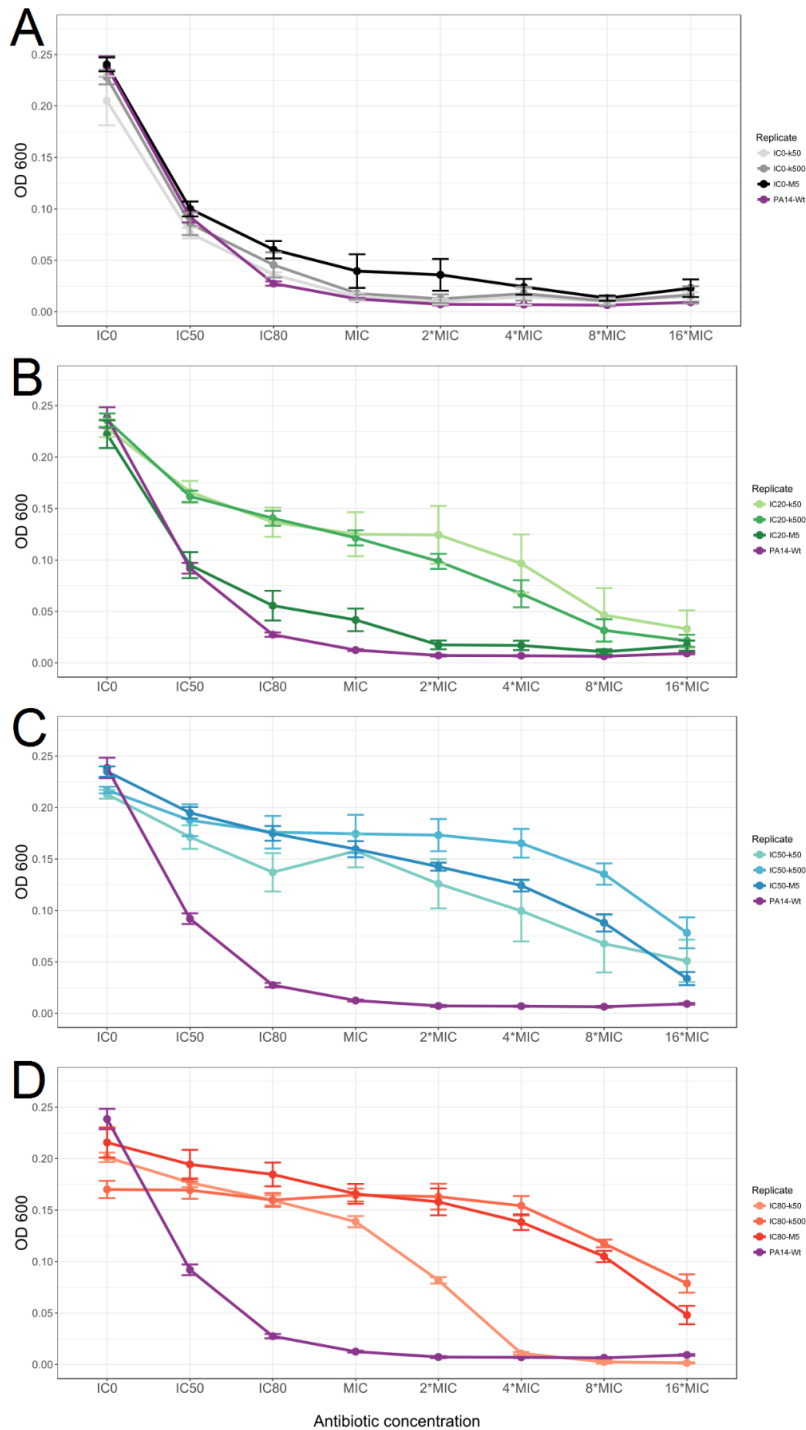
IC80-k50	10	166.247177	17.8514938
IC80-k50	11	183.754162	12.3160174
IC80-k50	12	150.788331	24.8099685
IC80-k50	13	131.769027	15.2853777
IC80-k50	14	169.581164	32.6215453
IC80-k50	15	204.195533	31.4758878
IC80-k50	16	208.962268	18.7915142
<hr/>			
IC80-k500	1	68.4863425	19.176526
IC80-k500	2	6.32062673	1.42720366
IC80-k500	3	110.287873	29.2419452
IC80-k500	4	128.364052	31.956976
IC80-k500	5	156.795036	40.084689
IC80-k500	6	160.259508	26.8375848
IC80-k500	7	183.469369	28.3861585
IC80-k500	8	164.515293	21.1754376
IC80-k500	9	194.077524	24.5690155
IC80-k500	10	158.99792	24.0360754
IC80-k500	11	92.7440267	41.1475318
IC80-k500	12	141.732028	19.2602753
IC80-k500	13	156.657785	20.8860236
IC80-k500	14	157.47478	29.1007777
IC80-k500	15	183.658244	32.1856609
IC80-k500	16	232.741612	37.9756764
<hr/>			
IC80-M5	1	70.9586259	7.20175156
IC80-M5	2	51.6492933	11.5261281
IC80-M5	3	278.639537	20.181287
IC80-M5	4	177.761326	19.2189745
IC80-M5	5	190.295179	15.2605293
IC80-M5	6	178.493653	12.0826955
IC80-M5	7	185.975008	14.5469704
IC80-M5	8	193.143444	14.5020189
IC80-M5	9	225.713872	25.032687
IC80-M5	10	235.767396	18.718247
IC80-M5	11	194.473062	26.2374033
IC80-M5	12	206.576206	12.2253772
IC80-M5	13	203.514476	29.2015369
IC80-M5	14	197.513509	14.5998297
IC80-M5	15	250.154352	18.1634063
IC80-M5	16	313.072455	30.2423769

Supplementary Table S4: Antibiotic concentrations used in resistance assays. All concentrations are given in ng/ml.

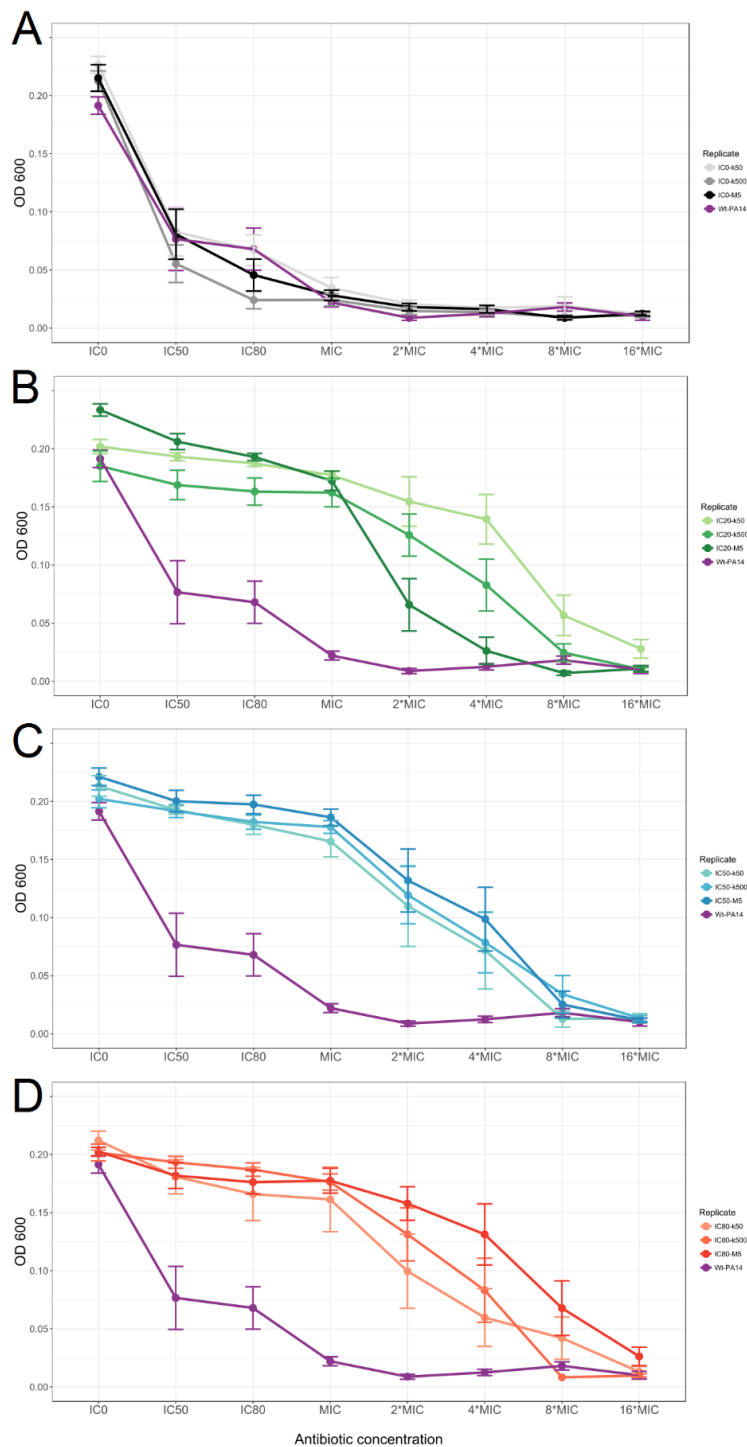
AB	Inoculum size	IC20	IC50	IC80	MIC	2x MIC	4x MIC	8x MIC	16x MIC
CAR	all	18000	26500	40000	52000	104000	208000	416000	832000
CIP	all	15	27.5	40	60	120	240	480	960
GEN	k50	300	330	380	440				
	k500	380	440	500	600	1200	2400	4800	9600
	M5	480	600	700	830				



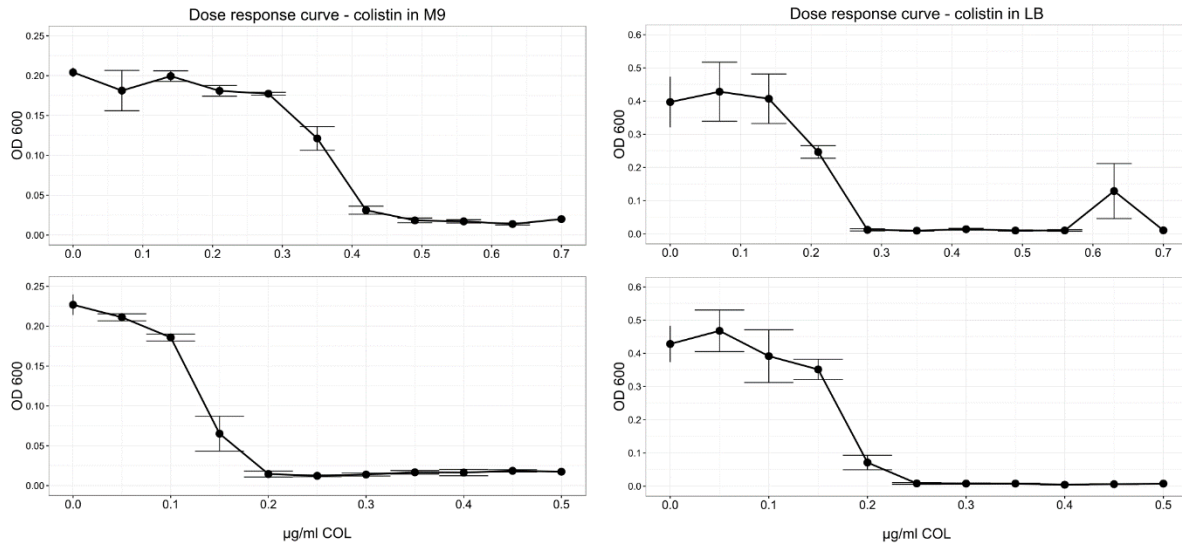
Supplementary Figure S4: Dose Response Curves of evolved populations of CAR experiment, including the IC50 and k500-TS groups. A: Evolved no-drug control treatment groups (grey). **B:** IC20 treatment groups (green). **C:** IC50 treatment groups (blue). **D:** IC80 treatment groups (red). The X-axis represents the relative levels of antibiotic concentrations against which the evolved PA14 populations were challenged; The Y-axis represents the final OD of the tested bacterial populations at a wavelength of 600 nm after 12 hours of incubation in presence of the respective drug concentration. Error bars represent standard error of mean (8 replicates). Purple: unevolved PA14 control; light colors represent 50k transfers, dark colors represent 5M transfers, intermediate colors represent 500k transfers.



Supplementary Figure S5: Dose Response Curves of evolved populations of CIP experiment, including the IC50 and k500-TS groups. **A:** Evolved no-drug control treatment groups (grey). **B:** IC20 treatment groups (green). **C:** IC50 treatment groups (blue). **D:** IC80 treatment groups (red). The X-axis represents the relative levels of antibiotic concentrations against which the evolved PA14 populations were challenged; The Y-axis represents the final OD of the tested bacterial populations at a wavelength of 600 nm after 12 hours of incubation in presence of the respective drug concentration. Error bars represent standard error of mean (8 replicates). Purple: unevolved PA14 control; light colors represent 50k transfers, dark colors represent 5M transfers, intermediate colors represent 500k transfers.



Supplementary Figure S6: Dose Response Curves of evolved populations of GEN experiment, including the IC50 and k500-TS groups. **A:** Evolved no-drug control treatment groups (grey). **B:** IC20 treatment groups (green). **C:** IC50 treatment groups (blue). **D:** IC80 treatment groups (red). The X-axis represents the relative levels of antibiotic concentrations against which the evolved PA14 populations were challenged; The Y-axis represents the final OD of the tested bacterial populations at a wavelength of 600 nm after 12 hours of incubation in presence of the respective drug concentration. Error bars represent standard error of mean (8 replicates). Purple: unevolved PA14 control; light colors represent 50k transfers, dark colors represent 5M transfers, intermediate colors represent 500k transfers.



Supplementary Figure S7: Dose Response Curves of PA14 against colistin in different growth media. Colistin shows stronger day-to-day variations in efficacy in M9 medium than in LB medium. Left: Colistin in M9 medium. Right: Colistin in LB medium. Top row: Measurements taken on 3 May 2017. Bottom row: Measurements taken on 5 May 2017. The X-axes represent the relative levels of antibiotic concentrations against which the evolved PA14 populations were challenged. The Y-axes represent the final OD of the tested bacterial populations at a wavelength of 600 nm after 12 hours of incubation in presence of the respective drug concentration. Error bars represent standard error of mean (8 replicates).

Supplementary Table S5: Mutations identified at transfer 16 of CIP evolution experiment.

IC	TS	Population	bp position	Wt sequence	Variant	Frequency	Annotation	Gene	Type	Consequence
IC20	k50	A6	1550968	T	*-/ CCGCGA GGAGG GCTA	13.71%	PA14_ 18070	CopZ	deletion	gene fusion
			1551142	TTGGGG TCATGC CCGGA	T	6.12%	PA14_ 18080	TetR	deletion	frameshift
			3420974	TCGTCG CGCAA G	T	28.47%	PA14_ 38380	MexZ	deletion	frameshift
IC20	k50	B6	2820239	T	*/+CCCC GCCCAT AC	38.67%	PA14_ 32420	MexS	insertion	inframe
			2820772	CGCCAC T	C	9.31%	PA14_ 32420	MexS	deletion	inframe
IC20	k50	C6	2820592	CGAGC GCTTCA CCGAG	C	19.11%	PA14_ 32420	MexS	deletion	inframe
			3421061	A	G	37.76%	PA14_ 38380	MexZ	SNP	missense
			3421100	GATCTG CCGTCG GCCGA AGC	G	26.37%	PA14_ 38380	MexZ	deletion	frameshift
IC20	k50	D6	1551138	ATCCTT GGGGTC ATGCC GGAT	A	44.52%	PA14_ 18080	TetR	deletion	inframe
			3421008	CGCAG ATGCCG TCCCAC A	C	15.23%	PA14_ 38380	MexZ	deletion	frameshift
IC20	k50	E8	1391163	T	*-/GGCA	24.80%	PA14_ 16280	NalC	deletion	frameshift
IC20	k50	F8	798015	GCGAA CGCGGC GGCGG CCGGAC CCGGGT GATCGT CGCCCA TCGTCT GGCCG AAGTCA GCGATG CCGACC	G	19.11%	PA14_ 09300	ABC transporter ATP- binding protein	deletion	inframe

				TGATCC TGGTGC TGGTCG CTGGCC GTCTGG T						
			1551156	GGATGC AGCCGC AC	G	8.86%	PA14_ 18080	TetR	deletion	frameshift
			3421029	A	*/-T	24.39%	PA14_ 38380	MexZ	deletion	frameshift
IC20	k50	G8	3420909	GGTAG GGAGA ACTGCG CA	G	86.58%	PA14_ 38380	MexZ	deletion	frameshift
IC20	k50	H8	2820876	T	*/+CGCC	43.69%	PA14_ 32420	MexS	deletion	frameshift
			3420909	GGTAG GGAGA ACTGCG CA	G	18.54%	PA14_ 38380	MexZ	deletion	frameshift
			5428115	T	W	24.70%	PA14_ 60860	NfxB	SNP	missense
IC20	M5	G2	96548	C	CTGGCT G	5.36%	PA14_ 00980	Fha1	insertion	inframe
IC80	k50	F3	796529	C	*/+GCTG GCG	49.35%	PA14_ 09300	ABC transporter ATP- binding protein	insertion	frameshift
			5836130	G	*/+C	8.41%	PA14_ 65520	molecular chaperone	insertion	frameshift
IC80	M5	A5	2820025	T	*/- GCGAA GAGCTG CCGACC CCG	14.13%	PA14_ 32420	MexS	deletion	frameshift
			2820136	C	T	82.26%	PA14_ 32420	MexS	SNP	stop gained
IC80	M5	B5	2820239	T	*/+CCCC GCCCAT AC	39.42%	PA14_ 32420	MexS	insertion	inframe
			2820772	CGCCAC T	C	9.23%	PA14_ 32420	MexS	deletion	inframe
IC80	M5	C5	PA14_32 420	diverse		PA14_3242 0	MexS			
IC80	M5	D5	2820416	CCGTGC TGATCA	C	11.84%	PA14_ 32420	MexS	deletion	frameshift
			2820662	TCGGCG ATGTCT C	T	26.38%	PA14_ 32420	MexS	deletion	inframe
			2820852	GCACAT CGAGC AA	G	21.05%	PA14_ 32420	MexS	deletion	inframe

IC80	M5	E7	5428583	C	*/- CGCGCT CCTGA	82.12%	PA14_ 60860	NfxB	deletion	stop lost
IC80	M5	F7	2820136	C	Y	17.48%	PA14_ 32420	MexS	SNP	stop gained
			2820239	T	TCCCCG CCCATA C	5	PA14_ 32420	MexS	insertion	inframe
			5428133	T	Y	35.51%	PA14_ 60860	NfxB	SNP	missense
			5428411	C	*/+GCG GACAG CAGA	5.41%	PA14_ 60860	NfxB	insertion	inframe
			5428581	G	*/-GC	18.89%	PA14_ 60860	NfxB	deletion	frameshift
IC80	M5	G7	2820787	G	A	10.52%	PA14_ 32420	MexS	SNP	missense
			5428593	C	A	63.00%	PA14_ 60860	NfxB	SNP	stop retained
IC80	M5	H7	5428115	T	A	94.96%	PA14_ 60860	NfxB	SNP	missense

Supplementary Table S6: Frequencies of all identified mutations during different transfers of CIP evolution experiment.

Treatment	Population	Transfer	bp position	Gene	Frequency
IC20-k50	A6	3	1550968	CopZ	0
IC20-k50	A6	5	1550968	CopZ	0
IC20-k50	A6	7	1550968	CopZ	0
IC20-k50	A6	9	1550968	CopZ	0.13
IC20-k50	A6	11	1550968	CopZ	0.16
IC20-k50	A6	13	1550968	CopZ	0.18
IC20-k50	A6	15	1550968	CopZ	0.14
IC20-k50	A6	3	1551142	TetR	0
IC20-k50	A6	5	1551142	TetR	0
IC20-k50	A6	7	1551142	TetR	0
IC20-k50	A6	9	1551142	TetR	0.04
IC20-k50	A6	11	1551142	TetR	0.07
IC20-k50	A6	13	1551142	TetR	0.09
IC20-k50	A6	15	1551142	TetR	0.06
IC20-k50	A6	3	3420974	MexZ	0
IC20-k50	A6	5	3420974	MexZ	0

IC20-k50	A6	7	3420974	MexZ	0.02
IC20-k50	A6	9	3420974	MexZ	0.02
IC20-k50	A6	11	3420974	MexZ	0.13
IC20-k50	A6	13	3420974	MexZ	0.15
IC20-k50	A6	15	3420974	MexZ	0.28
IC20-k50	B6	3	2818981	MexT	0
IC20-k50	B6	5	2818981	MexT	0
IC20-k50	B6	7	2818981	MexT	0.04
IC20-k50	B6	9	2818981	MexT	0.16
IC20-k50	B6	13	2818981	MexT	0.11
IC20-k50	B6	15	2818981	MexT	0
IC20-k50	B6	3	2820239	MexS	0
IC20-k50	B6	5	2820239	MexS	0
IC20-k50	B6	7	2820239	MexS	0
IC20-k50	B6	9	2820239	MexS	0
IC20-k50	B6	13	2820239	MexS	0.32
IC20-k50	B6	15	2820239	MexS	0.39
IC20-k50	B6	3	2820772	MexS	0
IC20-k50	B6	5	2820772	MexS	0
IC20-k50	B6	7	2820772	MexS	0
IC20-k50	B6	9	2820772	MexS	0
IC20-k50	B6	13	2820772	MexS	0.08
IC20-k50	B6	15	2820772	MexS	0.09
IC20-k50	C6	3	2820592	MexS	0
IC20-k50	C6	5	2820592	MexS	0
IC20-k50	C6	7	2820592	MexS	0.09
IC20-k50	C6	9	2820592	MexS	0.13
IC20-k50	C6	11	2820592	MexS	0.17
IC20-k50	C6	13	2820592	MexS	0.21
IC20-k50	C6	15	2820592	MexS	0.19
IC20-k50	C6	3	3421061	MexZ	0
IC20-k50	C6	5	3421061	MexZ	0
IC20-k50	C6	7	3421061	MexZ	0.1
IC20-k50	C6	9	3421061	MexZ	0.29
IC20-k50	C6	11	3421061	MexZ	0.4
IC20-k50	C6	13	3421061	MexZ	0.52
IC20-k50	C6	15	3421061	MexZ	0.38
IC20-k50	C6	3	3421100	MexZ	0
IC20-k50	C6	5	3421100	MexZ	0.02
IC20-k50	C6	7	3421100	MexZ	0.07
IC20-k50	C6	9	3421100	MexZ	0.19
IC20-k50	C6	11	3421100	MexZ	0.27
IC20-k50	C6	13	3421100	MexZ	0.27
IC20-k50	C6	15	3421100	MexZ	0.26
IC20-k50	D6	3	1551138	TetR	0
IC20-k50	D6	5	1551138	TetR	0

IC20-k50	D6	9	1551138	TetR	0.22
IC20-k50	D6	11	1551138	TetR	0.4
IC20-k50	D6	13	1551138	TetR	0.51
IC20-k50	D6	15	1551138	TetR	0.45
IC20-k50	D6	3	3421008	MexZ	0
IC20-k50	D6	5	3421008	MexZ	0
IC20-k50	D6	9	3421008	MexZ	0.03
IC20-k50	D6	11	3421008	MexZ	0.05
IC20-k50	D6	13	3421008	MexZ	0.1
IC20-k50	D6	15	3421008	MexZ	0.15
IC20-k50	D6	3	1235724	PepA	0
IC20-k50	D6	5	1235724	PepA	0
IC20-k50	D6	9	1235724	PepA	0.07
IC20-k50	D6	11	1235724	PepA	0.09
IC20-k50	D6	13	1235724	PepA	0.03
IC20-k50	D6	15	1235724	PepA	0.02
IC20-k50	E8	3	1391163	NalC	0
IC20-k50	E8	5	1391163	NalC	0
IC20-k50	E8	7	1391163	NalC	0.04
IC20-k50	E8	13	1391163	NalC	0.31
IC20-k50	E8	15	1391163	NalC	0.25
IC20-k50	F8	3	1551156	TetR	0
IC20-k50	F8	5	1551156	TetR	0
IC20-k50	F8	7	1551156	TetR	0
IC20-k50	F8	9	1551156	TetR	0
IC20-k50	F8	11	1551156	TetR	0.1
IC20-k50	F8	13	1551156	TetR	0.16
IC20-k50	F8	15	1551156	TetR	0.09
IC20-k50	F8	3	3421029	MexZ	0
IC20-k50	F8	5	3421029	MexZ	0
IC20-k50	F8	7	3421029	MexZ	0
IC20-k50	F8	9	3421029	MexZ	0.02
IC20-k50	F8	11	3421029	MexZ	0.11
IC20-k50	F8	13	3421029	MexZ	0.4
IC20-k50	F8	15	3421029	MexZ	0.24
IC20-k50	F8	3	798015	ABC transport	0
IC20-k50	F8	5	798015	ABC transport	0
IC20-k50	F8	7	798015	ABC transport	0
IC20-k50	F8	9	798015	ABC transport	0
IC20-k50	F8	11	798015	ABC transport	0
IC20-k50	F8	13	798015	ABC transport	0

IC20-k50	F8	15	798015	ABC transport	0.19
IC20-k50	G8	3	3420909	MexZ	0
IC20-k50	G8	5	3420909	MexZ	0
IC20-k50	G8	7	3420909	MexZ	0
IC20-k50	G8	9	3420909	MexZ	0.08
IC20-k50	G8	11	3420909	MexZ	0.39
IC20-k50	G8	13	3420909	MexZ	0.87
IC20-k50	G8	15	3420909	MexZ	0.87
IC20-k50	H8	3	3420909	MexZ	0
IC20-k50	H8	5	3420909	MexZ	0
IC20-k50	H8	7	3420909	MexZ	0
IC20-k50	H8	9	3420909	MexZ	0
IC20-k50	H8	11	3420909	MexZ	0
IC20-k50	H8	13	3420909	MexZ	0.18
IC20-k50	H8	15	3420909	MexZ	0.19
IC20-k50	H8	3	2820876	MexS	0
IC20-k50	H8	5	2820876	MexS	0
IC20-k50	H8	7	2820876	MexS	0
IC20-k50	H8	9	2820876	MexS	0
IC20-k50	H8	11	2820876	MexS	0
IC20-k50	H8	13	2820876	MexS	0.49
IC20-k50	H8	15	2820876	MexS	0.44
IC20-k50	H8	3	5428115	NfxB	0
IC20-k50	H8	5	5428115	NfxB	0.02
IC20-k50	H8	7	5428115	NfxB	0.42
IC20-k50	H8	9	5428115	NfxB	0.55
IC20-k50	H8	11	5428115	NfxB	0.68
IC20-k50	H8	13	5428115	NfxB	0.22
IC20-k50	H8	15	5428115	NfxB	0.25
IC20-k50	H8	3	2819916	intergenic	0
IC20-k50	H8	5	2819916	intergenic	0
IC20-k50	H8	7	2819916	intergenic	0.04
IC20-k50	H8	9	2819916	intergenic	0.06
IC20-k50	H8	11	2819916	intergenic	0.13
IC20-k50	H8	13	2819916	intergenic	0.02
IC20-k50	H8	15	2819916	intergenic	0.04
IC80-k50	F3	3	796529	ABC transport	0
IC80-k50	F3	5	796529	ABC transport	0
IC80-k50	F3	7	796529	ABC transport	0
IC80-k50	F3	9	796529	ABC transport	0
IC80-k50	F3	11	796529	ABC transport	0

IC80-k50	F3	13	796529	ABC transport	0
IC80-k50	F3	15	796529	ABC transport	0.47
IC80-k50	F3	3	6242627	CycB	0
IC80-k50	F3	5	6242627	CycB	0
IC80-k50	F3	7	6242627	CycB	0.03
IC80-k50	F3	9	6242627	CycB	1
IC80-k50	F3	11	6242627	CycB	1
IC80-k50	F3	13	6242627	CycB	1
IC80-k50	F3	15	6242627	CycB	0
IC80-M5	A5	3	2820025	MexS	0
IC80-M5	A5	5	2820025	MexS	0.1
IC80-M5	A5	7	2820025	MexS	0.1
IC80-M5	A5	9	2820025	MexS	0.08
IC80-M5	A5	11	2820025	MexS	0.17
IC80-M5	A5	13	2820025	MexS	0.16
IC80-M5	A5	15	2820025	MexS	0.14
IC80-M5	A5	3	2820136	MexS	0
IC80-M5	A5	5	2820136	MexS	0.4
IC80-M5	A5	7	2820136	MexS	0.81
IC80-M5	A5	9	2820136	MexS	0.78
IC80-M5	A5	11	2820136	MexS	0.85
IC80-M5	A5	13	2820136	MexS	0.77
IC80-M5	A5	15	2820136	MexS	0.82
IC80-M5	B5	3	2820239	MexS	0.15
IC80-M5	B5	5	2820239	MexS	0.06
IC80-M5	B5	7	2820239	MexS	0.26
IC80-M5	B5	9	2820239	MexS	0.3
IC80-M5	B5	11	2820239	MexS	0.33
IC80-M5	B5	15	2820239	MexS	0.39
IC80-M5	B5	3	2820772	MexS	0
IC80-M5	B5	5	2820772	MexS	0.06
IC80-M5	B5	7	2820772	MexS	0.07
IC80-M5	B5	9	2820772	MexS	0.17
IC80-M5	B5	11	2820772	MexS	0.16
IC80-M5	B5	15	2820772	MexS	0.09
IC80-M5	C5	3	796529	ABC transport	0.35
IC80-M5	C5	5	796529	ABC transport	0.5
IC80-M5	C5	7	796529	ABC transport	0
IC80-M5	C5	9	796529	ABC transport	0
IC80-M5	C5	11	796529	ABC transport	0

IC80-M5	C5	13	796529	ABC transport	0
IC80-M5	C5	15	796529	ABC transport	0
IC80-M5	C5	3	5428547	NfxB	0.07
IC80-M5	C5	5	5428547	NfxB	0.14
IC80-M5	C5	7	5428547	NfxB	0.27
IC80-M5	C5	9	5428547	NfxB	0.39
IC80-M5	C5	11	5428547	NfxB	0.64
IC80-M5	C5	13	5428547	NfxB	0.17
IC80-M5	C5	15	5428547	NfxB	0.05
IC80-M5	D5	3	796529	ABC transport	0.29
IC80-M5	D5	5	796529	ABC transport	0.32
IC80-M5	D5	7	796529	ABC transport	0.1
IC80-M5	D5	9	796529	ABC transport	0
IC80-M5	D5	11	796529	ABC transport	0
IC80-M5	D5	13	796529	ABC transport	0
IC80-M5	D5	15	796529	ABC transport	0
IC80-M5	D5	3	2820416	MexS	0
IC80-M5	D5	5	2820416	MexS	0
IC80-M5	D5	7	2820416	MexS	0.03
IC80-M5	D5	9	2820416	MexS	0.06
IC80-M5	D5	11	2820416	MexS	0.03
IC80-M5	D5	13	2820416	MexS	0.11
IC80-M5	D5	15	2820416	MexS	0.12
IC80-M5	D5	3	2820662	MexS	0
IC80-M5	D5	5	2820662	MexS	0.03
IC80-M5	D5	7	2820662	MexS	0.09
IC80-M5	D5	9	2820662	MexS	0.14
IC80-M5	D5	11	2820662	MexS	0.13
IC80-M5	D5	13	2820662	MexS	0.12
IC80-M5	D5	15	2820662	MexS	0.26
IC80-M5	D5	3	2820852	MexS	0
IC80-M5	D5	5	2820852	MexS	0.19
IC80-M5	D5	7	2820852	MexS	0.21
IC80-M5	D5	9	2820852	MexS	0.21
IC80-M5	D5	11	2820852	MexS	0.23
IC80-M5	D5	13	2820852	MexS	0.21
IC80-M5	D5	15	2820852	MexS	0.22
IC80-M5	E7	3	5428583	NfxB	0

IC80-M5	E7	5	5428583	NfxB	0.02
IC80-M5	E7	9	5428583	NfxB	0.43
IC80-M5	E7	11	5428583	NfxB	0.58
IC80-M5	E7	13	5428583	NfxB	0.67
IC80-M5	E7	15	5428583	NfxB	0.82
IC80-M5	F7	3	2820136	MexS	0
IC80-M5	F7	5	2820136	MexS	0.11
IC80-M5	F7	7	2820136	MexS	0.13
IC80-M5	F7	9	2820136	MexS	0.1
IC80-M5	F7	11	2820136	MexS	0.06
IC80-M5	F7	13	2820136	MexS	0.24
IC80-M5	F7	15	2820136	MexS	0.17
IC80-M5	F7	3	5428411	NfxB	0
IC80-M5	F7	5	5428411	NfxB	0
IC80-M5	F7	7	5428411	NfxB	0
IC80-M5	F7	9	5428411	NfxB	0
IC80-M5	F7	11	5428411	NfxB	0.04
IC80-M5	F7	13	5428411	NfxB	0.04
IC80-M5	F7	15	5428411	NfxB	0.09
IC80-M5	F7	3	5428581	NfxB	0
IC80-M5	F7	5	5428581	NfxB	0.03
IC80-M5	F7	7	5428581	NfxB	0.02
IC80-M5	F7	9	5428581	NfxB	0.12
IC80-M5	F7	11	5428581	NfxB	0.31
IC80-M5	F7	13	5428581	NfxB	0.22
IC80-M5	F7	15	5428581	NfxB	0.25
IC80-M5	F7	3	5428133	NfxB	0.01
IC80-M5	F7	5	5428133	NfxB	0.4
IC80-M5	F7	7	5428133	NfxB	0.51
IC80-M5	F7	9	5428133	NfxB	0.4
IC80-M5	F7	11	5428133	NfxB	0.62
IC80-M5	F7	13	5428133	NfxB	0.33
IC80-M5	F7	15	5428133	NfxB	0.22
IC80-M5	F7	3	5428534	NfxB	0.01
IC80-M5	F7	5	5428534	NfxB	0.06
IC80-M5	F7	7	5428534	NfxB	0.06
IC80-M5	F7	9	5428534	NfxB	0.12
IC80-M5	F7	11	5428534	NfxB	0.13
IC80-M5	F7	13	5428534	NfxB	0.04
IC80-M5	F7	15	5428534	NfxB	0.03
IC80-M5	G7	3	2820787	MexS	0
IC80-M5	G7	5	2820787	MexS	0
IC80-M5	G7	7	2820787	MexS	0.1
IC80-M5	G7	9	2820787	MexS	0.1
IC80-M5	G7	11	2820787	MexS	0.18
IC80-M5	G7	15	2820787	MexS	0.11

IC80-M5	G7	3	5428593	NfxB		0
IC80-M5	G7	5	5428593	NfxB		0.1
IC80-M5	G7	7	5428593	NfxB		0.19
IC80-M5	G7	9	5428593	NfxB		0.31
IC80-M5	G7	11	5428593	NfxB		0.49
IC80-M5	G7	15	5428593	NfxB		0.63
IC80-M5	G7	3	3421355	MexZ		0
IC80-M5	G7	5	3421355	MexZ		0.03
IC80-M5	G7	7	3421355	MexZ		0.04
IC80-M5	G7	9	3421355	MexZ		0.08
IC80-M5	G7	11	3421355	MexZ		0.03
IC80-M5	G7	15	3421355	MexZ		0.02
IC80-M5	H7	3	5428115	NfxB	NA	
IC80-M5	H7	5	5428115	NfxB		0.72
IC80-M5	H7	7	5428115	NfxB		0.83
IC80-M5	H7	9	5428115	NfxB		0.88
IC80-M5	H7	11	5428115	NfxB		0.94
IC80-M5	H7	13	5428115	NfxB		0.97
IC80-M5	H7	15	5428115	NfxB		0.95
IC80-M5	H7	3	2819916	intergenic	NA	
IC80-M5	H7	5	2819916	intergenic		0.19
IC80-M5	H7	7	2819916	intergenic		0.04
IC80-M5	H7	9	2819916	intergenic		0.02
IC80-M5	H7	11	2819916	intergenic		0.04
IC80-M5	H7	13	2819916	intergenic		0.05
IC80-M5	H7	15	2819916	intergenic		0.03

Supplementary Table S7: Mutations identified at transfer 16 of GEN evolution experiment.

IC	TS	Population	bp position	Wt sequence	Variant	Frequency	Annotation	Gene	Type	Consequence
IC20	k50	A6	5636922	G	R	27.92%	PA14_63160	PmrB	SNP	missense
			5637204	T	W	70.63%	PA14_63160	PmrB	SNP	missense
IC20	k50	B6	5636922	G	R	11.19%	PA14_63160	PmrB	SNP	missense
			5637204	T	A	88.36%	PA14_63160	PmrB	SNP	missense
IC20	k50	C6	740293	C	-CT/-CT	94.39%	PA14_08640	sporulation domain-containing protein	deletion	frameshift
IC20	k50	D6	732988	G	A	9.09%	-		SNP	non-genic
			3682943	G	R	31.51%	PA14_41260	ParR	SNP	missense
			4369873	A	M	54.12%	PA14_49170	PhoQ	SNP	missense
IC20	k50	E8	3682943	G	R	28.17%	PA14_41260	ParR	SNP	missense
			4369873	A	M	49.21%	PA14_49170	ParS	SNP	missense
IC20	k50	F8	2587833	T	*/-C	9.79%	PA14_29880	NuoL	deletion	frameshift
			3421260	CGCGCA GGAGG ATG	C	14.46%	PA14_38380	MexZ	deletion	frameshift
			3682943	G	R	24.29%	PA14_41260	ParR	SNP	missense
			5138027	CCCTGG ACGAA CAG	C	22.79%	PA14_57690	hypothetical protein	deletion	frameshift
IC20	k50	G8	5637204	T	A	80.25%	PA14_63160	PmrB	SNP	missense
			5673078	TGT	CGG	13.33%	PA14_63620	LipC	SNP	missense
IC20	k50	H8	393319	G	*/-C	17.86%	PA14_04410	PtsP	deletion	frameshift
			6124279	A	*/+GGC	42.55%	PA14_68680	EnvZ	insertion	inframe
IC20	M5	A11	393335	T	-G/-G	94%	PA14_04410	PtsP	deletion	frameshift
			3499294	G	T	97.17%	PA14_39300	RbsR	SNP	synonymous
IC20	M5	B11	394724	C	T	87.05%	PA14_04410	PtsP	SNP	missense
IC20	M5	C11	394264	C	*/- CACCCG	72.87%	PA14_04410	PtsP	deletion	inframe

			5159716	G	*/+C	19.27%	PA14_57980	phosphocarrier protein HPr	insertion	frameshift
			732988	G	R	8.76%	-		SNP	non-genic
			4842338	G	K	8.70%	PA14_54620	aldehyde dehydrogenase	SNP	missense
IC20	M5	D11	393899	T	-G/-G	80.74%	PA14_04410	PtsP	deletion	frameshift
			5159716	G	*/+C	14%	PA14_57980	phosphocarrier protein HPr	insertion	frameshift
			3590907	G	R	6.85%	PA14_40260	glycoprotein (quorum sensing)	SNP	synonymous
IC20	M5	E2	392322	GCGGG GCAGG	G	12.87%	PA14_04390	YgdP	deletion	gene fusion
			393899 T	-G/-G	77.65%	PA14_04410	PtsP	deletion	frameshift
			2243692	G	R	28.33%	PA14_25660	FabG	SNP	synonymous
IC20	M5	F2	394708	T	*/-ACG	13.84%	PA14_04410	PtsP	deletion	inframe deletion
			394361	G	S	69.36%	PA14_04410	PtsP	SNP	missense
IC20	M5	G2	393319	G	*/-C	43.56%	PA14_04410	PtsP	deletion	frameshift
			393335	T	*/-G	16.43%	PA14_04410	PtsP	deletion	frameshift
			394708	T	*/-ACG	6.73%	PA14_04410	PtsP	deletion	inframe deletion
			394924	C	*/-G	16.67%	PA14_04410	PtsP	deletion	frameshift
			3499294	G	K	17.48%	PA14_39300	RbsR	SNP	synonymous
			5452000	G	R	7.45%	PA14_61150	oxidoreductase	SNP	missense
IC20	M5	H2	393042	CGC	CC	100%	PA14_04410	PtsP	deletion	frameshift
IC80	k50	A12	393042	C	-G/-G	100%	PA14_04410	PtsP	deletion	frameshift
IC80	k50	B12	3683307	T	C	100%	PA14_41270	ParS	SNP	missense
IC80	k50	C12	2591369	C	*/+CAGC TGAG	15.56%	PA14_29930	NuoH	insertion	frameshift
			3683505	G	R	72.83%	PA14_41270	ParS	SNP	missense
IC80	k50	D12	5636922	G	A	97.25%	PA14_63160	PmrB	SNP	missense
IC80	k50	E3	3683343	C	G	100%	PA14_41270	ParS	SNP	missense
			5215551	G	A	100%	PA14_58560	PiuB	SNP	missense

IC80	k50	F3	5888350	C	T	95.16%	PA14_66100	WaaL	SNP	missense
IC80	k50	G3	757176	G	S	61.64%	PA14_08820	FusA1	SNP	missense
			4369873	A	M	26.02%	PA14_49170	PhoQ	SNP	missense
IC80	k50	H3	394469	T	C	76.47%	PA14_04410	PtsP	SNP	missense
			4370093	A	W	24.32%	PA14_49170	PhoQ	SNP	missense
IC80	M5	A5	732988	G	A	9.92%	-		SNP	non-genic
			5636922	G	A	78.64%	PA14_63160	PmrB	SNP	missense
			5637204	T	W	24.14%	PA14_63160	PmrB	SNP	missense
IC80	M5	B5	3683342	A	M	15.69%	PA14_41270	ParS	SNP	missense
			5636922	G	R	23.26%	PA14_63160	PmrB	SNP	missense
			5637204	T	W	43.00%	PA14_63160	PmrB	SNP	missense
IC80	M5	C5	2820052	G	GCC	5%	PA14_32420	MexS	insertion	frameshift
			2820244	G	*/-C	7.34%	PA14_32420	MexS	deletion	frameshift
			2820582	CCTGGA AGTCGA G	C	7%	PA14_32420	MexS	deletion	inframe
			5236486	T	*/+A	7.88%	PA14_58760	PilC	insertion	frameshift
			5428547	T	*/-GGA	43.31%	PA14_60860	NfxB	deletion	inframe
IC80	M5	D5	393324	C	*/-G	25%	PA14_04410	PtsP	deletion	frameshift
			3095099	AGGTG GCGCCG CTCGAA GGCGG CGCCAC CCC	A	7%	PA14_34820	AmbC	deletion	inframe
			5636814	T	*/-CGA	5%	PA14_63160	PmrB	deletion	inframe
			5637204	T	W	72.18%	PA14_63160	PmrB	SNP	missense
IC80	M5	E7	393899	T	*/-G	11.99%	PA14_04410	PtsP	deletion	frameshift
			394249	C	Y	68.21%	PA14_04410	PtsP	SNP	stop gained
IC80	M5	F7	393899	T	*/-G	30.47%	PA14_04410	PtsP	deletion	frameshift
			3682943	G	R	6.10%	PA14_41260	ParR	SNP	missense

			5138027	CCCTGG ACGAA CAG	C	13.25%	PA14_ 57690	hypothetica l protein	deletion	frameshift
			5637204	T	W	5.05%	PA14_ 63160	PmrB	SNP	missense
IC80	M5	H7	5428115	T	A	95.92%	PA14_ 60860	NfxB	SNP	missense

Table S8: Frequencies of all identified mutations during different transfers of GEN evolution experiment.

Treatment	Population	Transfer	bp position	Gene	Frequency
IC20-k50	A6	3	5637204	PmrB	0.85
IC20-k50	A6	5	5637204	PmrB	1
IC20-k50	A6	7	5637204	PmrB	0.38
IC20-k50	A6	9	5637204	PmrB	0.38
IC20-k50	A6	11	5637204	PmrB	0.25
IC20-k50	A6	13	5637204	PmrB	0.53
IC20-k50	A6	15	5637204	PmrB	0.71
IC20-k50	A6	3	5636922	PmrB	0
IC20-k50	A6	5	5636922	PmrB	0
IC20-k50	A6	7	5636922	PmrB	0.63
IC20-k50	A6	9	5636922	PmrB	0.61
IC20-k50	A6	11	5636922	PmrB	0.78
IC20-k50	A6	13	5636922	PmrB	0.57
IC20-k50	A6	15	5636922	PmrB	0.28
IC20-k50	B6	3	5637204	PmrB	0
IC20-k50	B6	5	5637204	PmrB	0
IC20-k50	B6	7	5637204	PmrB	0.04
IC20-k50	B6	9	5637204	PmrB	0.48
IC20-k50	B6	11	5637204	PmrB	0.98
IC20-k50	B6	13	5637204	PmrB	1
IC20-k50	B6	15	5637204	PmrB	0.88
IC20-k50	B6	3	5636922	PmrB	0
IC20-k50	B6	5	5636922	PmrB	0
IC20-k50	B6	7	5636922	PmrB	0
IC20-k50	B6	9	5636922	PmrB	0
IC20-k50	B6	11	5636922	PmrB	0
IC20-k50	B6	13	5636922	PmrB	0
IC20-k50	B6	15	5636922	PmrB	0.11
IC20-k50	C6	3	740293	unknown	0

IC20-k50	C6	5	740293	unknown	NA	
IC20-k50	C6	7	740293	unknown		0
IC20-k50	C6	9	740293	unknown		0
IC20-k50	C6	11	740293	unknown		0.15
IC20-k50	C6	13	740293	unknown		0.74
IC20-k50	C6	15	740293	unknown		0.94
IC20-k50	C6	3	2586747	NuoM		0
IC20-k50	C6	5	2586747	NuoM	NA	
IC20-k50	C6	7	2586747	NuoM		0.56
IC20-k50	C6	9	2586747	NuoM		0.56
IC20-k50	C6	11	2586747	NuoM		0.49
IC20-k50	C6	13	2586747	NuoM		0.16
IC20-k50	C6	15	2586747	NuoM		0
IC20-k50	D6	3	732988	intergenic		0
IC20-k50	D6	5	732988	intergenic		0.16
IC20-k50	D6	9	732988	intergenic		0.38
IC20-k50	D6	11	732988	intergenic		0.17
IC20-k50	D6	13	732988	intergenic		0.16
IC20-k50	D6	15	732988	intergenic		0.09
IC20-k50	D6	3	2593860	NuoG		0
IC20-k50	D6	5	2593860	NuoG		0
IC20-k50	D6	9	2593860	NuoG		0.09
IC20-k50	D6	11	2593860	NuoG		0.06
IC20-k50	D6	13	2593860	NuoG		0.16
IC20-k50	D6	15	2593860	NuoG		0
IC20-k50	D6	3	2586747	NuoM		0
IC20-k50	D6	5	2586747	NuoM		0
IC20-k50	D6	9	2586747	NuoM		0.63
IC20-k50	D6	11	2586747	NuoM		0.74
IC20-k50	D6	13	2586747	NuoM		0.61
IC20-k50	D6	15	2586747	NuoM		0
IC20-k50	D6	3	3682943	ParR		0
IC20-k50	D6	5	3682943	ParR		0
IC20-k50	D6	9	3682943	ParR		0
IC20-k50	D6	11	3682943	ParR		0
IC20-k50	D6	13	3682943	ParR		0
IC20-k50	D6	15	3682943	ParR		0.32
IC20-k50	D6	3	4369873	PhoQ		0
IC20-k50	D6	5	4369873	PhoQ		0
IC20-k50	D6	9	4369873	PhoQ		0
IC20-k50	D6	11	4369873	PhoQ		0
IC20-k50	D6	13	4369873	PhoQ		0
IC20-k50	D6	15	4369873	PhoQ		0.54
IC20-k50	E8	3	3682943	ParR		0
IC20-k50	E8	5	3682943	ParR		0
IC20-k50	E8	7	3682943	ParR		0

IC20-k50	E8	9	3682943	ParR	0.02
IC20-k50	E8	11	3682943	ParR	0.05
IC20-k50	E8	13	3682943	ParR	0.08
IC20-k50	E8	15	3682943	ParR	0.28
IC20-k50	E8	3	4369873	PhoQ	0
IC20-k50	E8	5	4369873	PhoQ	0
IC20-k50	E8	7	4369873	PhoQ	0.05
IC20-k50	E8	9	4369873	PhoQ	0.64
IC20-k50	E8	11	4369873	PhoQ	0.37
IC20-k50	E8	13	4369873	PhoQ	0.86
IC20-k50	E8	15	4369873	PhoQ	0.49
IC20-k50	F8	3	2587833	NuoL	0
IC20-k50	F8	5	2587833	NuoL	0
IC20-k50	F8	7	2587833	NuoL	0.07
IC20-k50	F8	9	2587833	NuoL	0.2
IC20-k50	F8	11	2587833	NuoL	0.14
IC20-k50	F8	13	2587833	NuoL	0.05
IC20-k50	F8	15	2587833	NuoL	0.1
IC20-k50	F8	3	3421260	MexZ	0
IC20-k50	F8	5	3421260	MexZ	0
IC20-k50	F8	7	3421260	MexZ	0
IC20-k50	F8	9	3421260	MexZ	0
IC20-k50	F8	11	3421260	MexZ	0
IC20-k50	F8	13	3421260	MexZ	0
IC20-k50	F8	15	3421260	MexZ	0.14
IC20-k50	F8	3	3682943	ParR	0
IC20-k50	F8	5	3682943	ParR	0
IC20-k50	F8	7	3682943	ParR	0
IC20-k50	F8	9	3682943	ParR	0
IC20-k50	F8	11	3682943	ParR	0.05
IC20-k50	F8	13	3682943	ParR	0.05
IC20-k50	F8	15	3682943	ParR	0.24
IC20-k50	F8	3	5138027	unknown	0
IC20-k50	F8	5	5138027	unknown	0
IC20-k50	F8	7	5138027	unknown	0
IC20-k50	F8	9	5138027	unknown	0
IC20-k50	F8	11	5138027	unknown	0.05
IC20-k50	F8	13	5138027	unknown	0.07
IC20-k50	F8	15	5138027	unknown	0.23
IC20-k50	F8	3	4369873	PhoQ	0
IC20-k50	F8	5	4369873	PhoQ	0.02
IC20-k50	F8	7	4369873	PhoQ	0.03
IC20-k50	F8	9	4369873	PhoQ	0.36
IC20-k50	F8	11	4369873	PhoQ	0.39
IC20-k50	F8	13	4369873	PhoQ	0.58
IC20-k50	F8	15	4369873	PhoQ	0

IC20-k50	G8	3	5637204	PmrB	0
IC20-k50	G8	5	5637204	PmrB	0
IC20-k50	G8	7	5637204	PmrB	0
IC20-k50	G8	9	5637204	PmrB	0.08
IC20-k50	G8	11	5637204	PmrB	0.1
IC20-k50	G8	13	5637204	PmrB	0.4
IC20-k50	G8	15	5637204	PmrB	0.8
IC20-k50	G8	3	3421122	MexZ	0
IC20-k50	G8	5	3421122	MexZ	0
IC20-k50	G8	7	3421122	MexZ	0
IC20-k50	G8	9	3421122	MexZ	0.01
IC20-k50	G8	11	3421122	MexZ	0.05
IC20-k50	G8	13	3421122	MexZ	0.11
IC20-k50	G8	15	3421122	MexZ	0.06
IC20-k50	H8	3	393319	PtsP	0
IC20-k50	H8	5	393319	PtsP	0
IC20-k50	H8	7	393319	PtsP	0
IC20-k50	H8	9	393319	PtsP	0.01
IC20-k50	H8	11	393319	PtsP	0.01
IC20-k50	H8	13	393319	PtsP	0.41
IC20-k50	H8	15	393319	PtsP	0.18
IC20-k50	H8	3	6124279	EnvZ	0
IC20-k50	H8	5	6124279	EnvZ	0
IC20-k50	H8	7	6124279	EnvZ	0
IC20-k50	H8	9	6124279	EnvZ	0
IC20-k50	H8	11	6124279	EnvZ	0.04
IC20-k50	H8	13	6124279	EnvZ	0.12
IC20-k50	H8	15	6124279	EnvZ	0.43
IC20-M5	A11	3	5636922	PmrB	0.03
IC20-M5	A11	5	5636922	PmrB	0.45
IC20-M5	A11	7	5636922	PmrB	0.16
IC20-M5	A11	9	5636922	PmrB	0.12
IC20-M5	A11	11	5636922	PmrB	0.01
IC20-M5	A11	13	5636922	PmrB	0
IC20-M5	A11	15	5636922	PmrB	0
IC20-M5	A11	3	5637204	PmrB	0.02
IC20-M5	A11	5	5637204	PmrB	0.09
IC20-M5	A11	7	5637204	PmrB	0.1
IC20-M5	A11	9	5637204	PmrB	0.1
IC20-M5	A11	11	5637204	PmrB	0.04
IC20-M5	A11	13	5637204	PmrB	0
IC20-M5	A11	15	5637204	PmrB	0
IC20-M5	A11	3	3683342	ParS	0.09
IC20-M5	A11	5	3683342	ParS	0.37
IC20-M5	A11	7	3683342	ParS	0.31
IC20-M5	A11	9	3683342	ParS	0.19

IC20-M5	A11	11	3683342	ParS	0
IC20-M5	A11	13	3683342	ParS	0
IC20-M5	A11	15	3683342	ParS	0
IC20-M5	A11	3	393335	PtsP	0.06
IC20-M5	A11	5	393335	PtsP	0.09
IC20-M5	A11	7	393335	PtsP	0.3
IC20-M5	A11	9	393335	PtsP	0.54
IC20-M5	A11	11	393335	PtsP	0.93
IC20-M5	A11	13	393335	PtsP	0.93
IC20-M5	A11	15	393335	PtsP	0.94
IC20-M5	A11	3	3499294	RbsR	0
IC20-M5	A11	5	3499294	RbsR	0.08
IC20-M5	A11	7	3499294	RbsR	0.34
IC20-M5	A11	9	3499294	RbsR	0.65
IC20-M5	A11	11	3499294	RbsR	0.93
IC20-M5	A11	13	3499294	RbsR	0.97
IC20-M5	A11	15	3499294	RbsR	0.97
IC20-M5	B11	3	394724	PtsP	0
IC20-M5	B11	5	394724	PtsP	0.33
IC20-M5	B11	7	394724	PtsP	0.73
IC20-M5	B11	9	394724	PtsP	0.83
IC20-M5	B11	11	394724	PtsP	0.94
IC20-M5	B11	13	394724	PtsP	0.85
IC20-M5	B11	15	394724	PtsP	0.87
IC20-M5	C11	3	394264	PtsP	0
IC20-M5	C11	5	394264	PtsP	0.02
IC20-M5	C11	7	394264	PtsP	0.05
IC20-M5	C11	9	394264	PtsP	0.35
IC20-M5	C11	11	394264	PtsP	0.53
IC20-M5	C11	13	394264	PtsP	0.64
IC20-M5	C11	15	394264	PtsP	0.73
IC20-M5	C11	3	5159716	HPr	0
IC20-M5	C11	5	5159716	HPr	0
IC20-M5	C11	7	5159716	HPr	0.01
IC20-M5	C11	9	5159716	HPr	0.08
IC20-M5	C11	11	5159716	HPr	0.2
IC20-M5	C11	13	5159716	HPr	0.2
IC20-M5	C11	15	5159716	HPr	0.19
IC20-M5	C11	3	732988	intergenic	0.02
IC20-M5	C11	5	732988	intergenic	0.26
IC20-M5	C11	7	732988	intergenic	0.3
IC20-M5	C11	9	732988	intergenic	0.2
IC20-M5	C11	11	732988	intergenic	0.3
IC20-M5	C11	13	732988	intergenic	0.23
IC20-M5	C11	15	732988	intergenic	0.09
IC20-M5	D11	3	393899	PtsP	0

IC20-M5	D11	5	393899	PtsP	0
IC20-M5	D11	7	393899	PtsP	0
IC20-M5	D11	9	393899	PtsP	0
IC20-M5	D11	11	393899	PtsP	0.04
IC20-M5	D11	13	393899	PtsP	0.13
IC20-M5	D11	15	393899	PtsP	0.81
IC20-M5	D11	3	5159716	HPr	0
IC20-M5	D11	5	5159716	HPr	0
IC20-M5	D11	7	5159716	HPr	0
IC20-M5	D11	9	5159716	HPr	0
IC20-M5	D11	11	5159716	HPr	0.02
IC20-M5	D11	13	5159716	HPr	0.06
IC20-M5	D11	15	5159716	HPr	0.14
IC20-M5	E2	3	5637204	PmrB	0.02
IC20-M5	E2	5	5637204	PmrB	0.39
IC20-M5	E2	7	5637204	PmrB	0.25
IC20-M5	E2	9	5637204	PmrB	0.07
IC20-M5	E2	11	5637204	PmrB	0.02
IC20-M5	E2	13	5637204	PmrB	0.02
IC20-M5	E2	15	5637204	PmrB	0
IC20-M5	E2	3	393899	PtsP	0
IC20-M5	E2	5	393899	PtsP	0.25
IC20-M5	E2	7	393899	PtsP	0.4
IC20-M5	E2	9	393899	PtsP	0.86
IC20-M5	E2	11	393899	PtsP	0.85
IC20-M5	E2	13	393899	PtsP	0.85
IC20-M5	E2	15	393899	PtsP	0.78
IC20-M5	E2	3	2243692	FabG	0
IC20-M5	E2	5	2243692	FabG	0.04
IC20-M5	E2	7	2243692	FabG	0.09
IC20-M5	E2	9	2243692	FabG	0.19
IC20-M5	E2	11	2243692	FabG	0.26
IC20-M5	E2	13	2243692	FabG	0.2
IC20-M5	E2	15	2243692	FabG	0.28
IC20-M5	E2	3	3683396	ParS	0
IC20-M5	E2	5	3683396	ParS	0.07
IC20-M5	E2	7	3683396	ParS	0.12
IC20-M5	E2	9	3683396	ParS	0.06
IC20-M5	E2	11	3683396	ParS	0
IC20-M5	E2	13	3683396	ParS	0
IC20-M5	E2	15	3683396	ParS	0
IC20-M5	E2	3	392322	YgdP	0
IC20-M5	E2	5	392322	YgdP	0
IC20-M5	E2	7	392322	YgdP	0
IC20-M5	E2	9	392322	YgdP	0
IC20-M5	E2	11	392322	YgdP	0

IC20-M5	E2	13	392322	YgdP		0.1
IC20-M5	E2	15	392322	YgdP		0.13
IC20-M5	F2	3	5637204	PmrB		0
IC20-M5	F2	5	5637204	PmrB		0.13
IC20-M5	F2	7	5637204	PmrB		0.02
IC20-M5	F2	9	5637204	PmrB		0.02
IC20-M5	F2	13	5637204	PmrB		0.02
IC20-M5	F2	15	5637204	PmrB		0
IC20-M5	F2	3	394708	PtsP		0
IC20-M5	F2	5	394708	PtsP		0.22
IC20-M5	F2	7	394708	PtsP		0.23
IC20-M5	F2	9	394708	PtsP		0.39
IC20-M5	F2	13	394708	PtsP		0.55
IC20-M5	F2	15	394708	PtsP		0.14
IC20-M5	F2	3	394361	PtsP		0
IC20-M5	F2	5	394361	PtsP		0.09
IC20-M5	F2	7	394361	PtsP		0.34
IC20-M5	F2	9	394361	PtsP		0.36
IC20-M5	F2	13	394361	PtsP		0.42
IC20-M5	F2	15	394361	PtsP		0.69
IC20-M5	G2	3	5947518	PilQ		0
IC20-M5	G2	5	5947518	PilQ		0.17
IC20-M5	G2	7	5947518	PilQ		0.46
IC20-M5	G2	9	5947518	PilQ		0.24
IC20-M5	G2	11	5947518	PilQ		0.4
IC20-M5	G2	13	5947518	PilQ	NA	
IC20-M5	G2	15	5947518	PilQ	NA	
IC20-M5	G2	3	393899	PtsP		0
IC20-M5	G2	5	393899	PtsP		0.02
IC20-M5	G2	7	393899	PtsP		0.17
IC20-M5	G2	9	393899	PtsP		0.27
IC20-M5	G2	11	393899	PtsP		0.17
IC20-M5	G2	13	393899	PtsP	NA	
IC20-M5	G2	15	393899	PtsP	NA	
IC20-M5	G2	3	393631	PtsP		0
IC20-M5	G2	5	393631	PtsP		0
IC20-M5	G2	7	393631	PtsP		0.08
IC20-M5	G2	9	393631	PtsP		0.13
IC20-M5	G2	11	393631	PtsP		0.13
IC20-M5	G2	13	393631	PtsP	NA	
IC20-M5	G2	15	393631	PtsP	NA	
IC20-M5	H2	3	393319	PtsP	NA	
IC20-M5	H2	5	393319	PtsP		0.28
IC20-M5	H2	7	393319	PtsP		0.31
IC20-M5	H2	9	393319	PtsP		0.25
IC20-M5	H2	13	393319	PtsP		0.08

IC20-M5	H2	15	393319	PtsP	NA	
IC20-M5	H2	3	393335	PtsP	NA	
IC20-M5	H2	5	393335	PtsP		0.11
IC20-M5	H2	7	393335	PtsP		0.15
IC20-M5	H2	9	393335	PtsP		0.14
IC20-M5	H2	13	393335	PtsP		0.02
IC20-M5	H2	15	393335	PtsP	NA	
IC20-M5	H2	3	394708	PtsP	NA	
IC20-M5	H2	5	394708	PtsP		0.08
IC20-M5	H2	7	394708	PtsP		0.2
IC20-M5	H2	9	394708	PtsP		0.17
IC20-M5	H2	13	394708	PtsP		0.23
IC20-M5	H2	15	394708	PtsP	NA	
IC20-M5	H2	3	394924	PtsP	NA	
IC20-M5	H2	5	394924	PtsP		0.15
IC20-M5	H2	7	394924	PtsP		0.19
IC20-M5	H2	9	394924	PtsP		0.25
IC20-M5	H2	13	394924	PtsP		0.01
IC20-M5	H2	15	394924	PtsP	NA	
IC20-M5	H2	3	3499294	RbsR		0
IC20-M5	H2	5	3499294	RbsR		0.09
IC20-M5	H2	7	3499294	RbsR		0.09
IC20-M5	H2	9	3499294	RbsR		0.1
IC20-M5	H2	13	3499294	RbsR		0
IC20-M5	H2	15	3499294	RbsR		0
IC20-M5	H2	3	393631	PtsP	NA	
IC20-M5	H2	5	393631	PtsP		0
IC20-M5	H2	7	393631	PtsP		0
IC20-M5	H2	9	393631	PtsP		0
IC20-M5	H2	13	393631	PtsP		0.13
IC20-M5	H2	15	393631	PtsP	NA	
IC80-k50	A12	3	4369523	PhoQ		0.27
IC80-k50	A12	5	4369523	PhoQ		0.22
IC80-k50	A12	7	4369523	PhoQ		0.13
IC80-k50	A12	9	4369523	PhoQ		0.08
IC80-k50	A12	11	4369523	PhoQ		0
IC80-k50	A12	13	4369523	PhoQ		0
IC80-k50	A12	15	4369523	PhoQ		0
IC80-k50	A12	3	393042	PtsP		0.04
IC80-k50	A12	5	393042	PtsP		0.43
IC80-k50	A12	7	393042	PtsP		0.48
IC80-k50	A12	9	393042	PtsP		0.87
IC80-k50	A12	11	393042	PtsP		0.94
IC80-k50	A12	13	393042	PtsP		0.95
IC80-k50	A12	15	393042	PtsP		1
IC80-k50	B12	3	3683307	ParS		0

IC80-k50	B12	5	3683307	ParS	0.45
IC80-k50	B12	7	3683307	ParS	0.6
IC80-k50	B12	9	3683307	ParS	0.75
IC80-k50	B12	11	3683307	ParS	0.87
IC80-k50	B12	13	3683307	ParS	0.98
IC80-k50	B12	15	3683307	ParS	1
IC80-k50	B12	3	2591369	NuoH	0
IC80-k50	B12	5	2591369	NuoH	0.09
IC80-k50	B12	7	2591369	NuoH	0.15
IC80-k50	B12	9	2591369	NuoH	0.21
IC80-k50	B12	11	2591369	NuoH	0.1
IC80-k50	B12	13	2591369	NuoH	0
IC80-k50	B12	15	2591369	NuoH	0
IC80-k50	C12	3	2591369	NuoH	0.01
IC80-k50	C12	5	2591369	NuoH	0.05
IC80-k50	C12	7	2591369	NuoH	0.26
IC80-k50	C12	9	2591369	NuoH	0.27
IC80-k50	C12	13	2591369	NuoH	0.11
IC80-k50	C12	15	2591369	NuoH	0.16
IC80-k50	C12	3	2593980	NuoG	0.01
IC80-k50	C12	5	2593980	NuoG	0.12
IC80-k50	C12	7	2593980	NuoG	0.27
IC80-k50	C12	9	2593980	NuoG	0.21
IC80-k50	C12	13	2593980	NuoG	0.36
IC80-k50	C12	15	2593980	NuoG	0.14
IC80-k50	C12	3	3683505	ParS	0
IC80-k50	C12	5	3683505	ParS	0
IC80-k50	C12	7	3683505	ParS	0
IC80-k50	C12	9	3683505	ParS	0
IC80-k50	C12	13	3683505	ParS	0.55
IC80-k50	C12	15	3683505	ParS	0.73
IC80-k50	D12	3	5636922	PmrB	0
IC80-k50	D12	5	5636922	PmrB	0.16
IC80-k50	D12	7	5636922	PmrB	0.84
IC80-k50	D12	9	5636922	PmrB	0.95
IC80-k50	D12	11	5636922	PmrB	0.99
IC80-k50	D12	13	5636922	PmrB	0.98
IC80-k50	D12	15	5636922	PmrB	0.97
IC80-k50	E3	3	3683343	ParS	0.37
IC80-k50	E3	5	3683343	ParS	0.8
IC80-k50	E3	7	3683343	ParS	1
IC80-k50	E3	9	3683343	ParS	0.98
IC80-k50	E3	11	3683343	ParS	0.98
IC80-k50	E3	13	3683343	ParS	0.95
IC80-k50	E3	15	3683343	ParS	1
IC80-k50	E3	3	5215551	PiuB	0.43

IC80-k50	E3	5	5215551	PiuB		0.87
IC80-k50	E3	7	5215551	PiuB		1
IC80-k50	E3	9	5215551	PiuB		1
IC80-k50	E3	11	5215551	PiuB		1
IC80-k50	E3	13	5215551	PiuB		0.91
IC80-k50	E3	15	5215551	PiuB		1
IC80-k50	F3	3	5888350	WaaL		0.13
IC80-k50	F3	5	5888350	WaaL		0.89
IC80-k50	F3	7	5888350	WaaL		0.85
IC80-k50	F3	9	5888350	WaaL		0.77
IC80-k50	F3	13	5888350	WaaL		0.87
IC80-k50	F3	15	5888350	WaaL		0.95
IC80-k50	F3	3	1974527	TrkH		0.04
IC80-k50	F3	5	1974527	TrkH		0.04
IC80-k50	F3	9	1974527	TrkH		0.11
IC80-k50	F3	13	1974527	TrkH		0.15
IC80-k50	F3	15	1974527	TrkH		0.05
IC80-k50	G3	3	757176	FusA1		0.26
IC80-k50	G3	5	757176	FusA1		0.13
IC80-k50	G3	7	757176	FusA1	NA	
IC80-k50	G3	9	757176	FusA1	NA	
IC80-k50	G3	11	757176	FusA1		0.6
IC80-k50	G3	13	757176	FusA1		0.54
IC80-k50	G3	15	757176	FusA1		0.62
IC80-k50	G3	3	4369873	PhoQ		0.26
IC80-k50	G3	5	4369873	PhoQ		0.66
IC80-k50	G3	7	4369873	PhoQ	NA	
IC80-k50	G3	9	4369873	PhoQ	NA	
IC80-k50	G3	11	4369873	PhoQ		0.39
IC80-k50	G3	13	4369873	PhoQ		0.27
IC80-k50	G3	15	4369873	PhoQ		0.26
IC80-k50	H3	3	392888	PtsP		0
IC80-k50	H3	5	392888	PtsP		0.01
IC80-k50	H3	7	392888	PtsP		0.13
IC80-k50	H3	9	392888	PtsP		0.2
IC80-k50	H3	11	392888	PtsP		0.14
IC80-k50	H3	13	392888	PtsP		0.11
IC80-k50	H3	15	392888	PtsP		0
IC80-k50	H3	3	4370093	PhoQ		0
IC80-k50	H3	5	4370093	PhoQ		0
IC80-k50	H3	7	4370093	PhoQ		0
IC80-k50	H3	9	4370093	PhoQ		0.03
IC80-k50	H3	11	4370093	PhoQ		0.03
IC80-k50	H3	13	4370093	PhoQ		0.05
IC80-k50	H3	15	4370093	PhoQ		0.24
IC80-k50	H3	3	394469	PtsP		0

IC80-k50	H3	5	394469	PtsP	0
IC80-k50	H3	7	394469	PtsP	0
IC80-k50	H3	9	394469	PtsP	0
IC80-k50	H3	11	394469	PtsP	0.04
IC80-k50	H3	13	394469	PtsP	0.65
IC80-k50	H3	15	394469	PtsP	0.76
IC80-k50	H3	3	2586747	NuoM	0
IC80-k50	H3	5	2586747	NuoM	0
IC80-k50	H3	7	2586747	NuoM	0.07
IC80-k50	H3	9	2586747	NuoM	0.05
IC80-k50	H3	11	2586747	NuoM	0.15
IC80-k50	H3	13	2586747	NuoM	0.01
IC80-k50	H3	15	2586747	NuoM	0.01
IC80-M5	A5	3	5637204	PmrB	0.35
IC80-M5	A5	5	5637204	PmrB	0.2
IC80-M5	A5	7	5637204	PmrB	0.15
IC80-M5	A5	9	5637204	PmrB	0.17
IC80-M5	A5	11	5637204	PmrB	0.27
IC80-M5	A5	13	5637204	PmrB	0.27
IC80-M5	A5	15	5637204	PmrB	0.24
IC80-M5	A5	3	5636922	PmrB	0.65
IC80-M5	A5	5	5636922	PmrB	0.79
IC80-M5	A5	7	5636922	PmrB	0.76
IC80-M5	A5	9	5636922	PmrB	0.78
IC80-M5	A5	11	5636922	PmrB	0.78
IC80-M5	A5	13	5636922	PmrB	0.76
IC80-M5	A5	15	5636922	PmrB	0.76
IC80-M5	B5	3	5636814	PmrB	0.12
IC80-M5	B5	5	5636814	PmrB	0.12
IC80-M5	B5	9	5636814	PmrB	0.13
IC80-M5	B5	11	5636814	PmrB	0.09
IC80-M5	B5	15	5636814	PmrB	0
IC80-M5	B5	3	3683342	ParS	0.17
IC80-M5	B5	5	3683342	ParS	0.13
IC80-M5	B5	9	3683342	ParS	0.09
IC80-M5	B5	11	3683342	ParS	0.12
IC80-M5	B5	15	3683342	ParS	0.16
IC80-M5	B5	3	5636922	PmrB	0.22
IC80-M5	B5	5	5636922	PmrB	0.34
IC80-M5	B5	9	5636922	PmrB	0.31
IC80-M5	B5	11	5636922	PmrB	0.21
IC80-M5	B5	15	5636922	PmrB	0.23
IC80-M5	B5	3	5637204	PmrB	0.41
IC80-M5	B5	5	5637204	PmrB	0.47
IC80-M5	B5	9	5637204	PmrB	0.58
IC80-M5	B5	11	5637204	PmrB	0.5

IC80-M5	B5	15	5637204	PmrB		0.46
IC80-M5	C5	3	5637204	PmrB		0.3
IC80-M5	C5	5	5637204	PmrB		0.24
IC80-M5	C5	7	5637204	PmrB		0.27
IC80-M5	C5	9	5637204	PmrB		0.29
IC80-M5	C5	13	5637204	PmrB		0.71
IC80-M5	C5	15	5637204	PmrB	NA	
IC80-M5	C5	3	5636922	PmrB		0.27
IC80-M5	C5	5	5636922	PmrB		0.42
IC80-M5	C5	7	5636922	PmrB		0.24
IC80-M5	C5	9	5636922	PmrB		0.27
IC80-M5	C5	13	5636922	PmrB		0.16
IC80-M5	C5	15	5636922	PmrB	NA	
IC80-M5	C5	3	4678757	AotJ		0.14
IC80-M5	C5	5	4678757	AotJ		0.18
IC80-M5	C5	7	4678757	AotJ		0.23
IC80-M5	C5	9	4678757	AotJ		0.07
IC80-M5	C5	13	4678757	AotJ		0.01
IC80-M5	C5	15	4678757	AotJ	NA	
IC80-M5	C5	3	3683342	ParS		0.28
IC80-M5	C5	5	3683342	ParS		0.14
IC80-M5	C5	7	3683342	ParS		0.28
IC80-M5	C5	9	3683342	ParS		0.17
IC80-M5	C5	13	3683342	ParS		0.15
IC80-M5	C5	15	3683342	ParS	NA	
IC80-M5	D5	3	5636814	PmrB		0.18
IC80-M5	D5	5	5636814	PmrB		0.09
IC80-M5	D5	7	5636814	PmrB		0.11
IC80-M5	D5	9	5636814	PmrB		0.14
IC80-M5	D5	11	5636814	PmrB		0.09
IC80-M5	D5	13	5636814	PmrB		0.03
IC80-M5	D5	15	5636814	PmrB		0.05
IC80-M5	D5	3	5637204	PmrB		0.77
IC80-M5	D5	5	5637204	PmrB		0.83
IC80-M5	D5	7	5637204	PmrB		0.8
IC80-M5	D5	9	5637204	PmrB		0.85
IC80-M5	D5	11	5637204	PmrB		0.86
IC80-M5	D5	13	5637204	PmrB		0.9
IC80-M5	D5	15	5637204	PmrB		0.72
IC80-M5	D5	3	393324	PtsP		0
IC80-M5	D5	5	393324	PtsP		0
IC80-M5	D5	7	393324	PtsP		0
IC80-M5	D5	9	393324	PtsP		0
IC80-M5	D5	11	393324	PtsP		0
IC80-M5	D5	13	393324	PtsP		0

IC80-M5	D5	15	393324	PtsP	0.25
IC80-M5	E7	3	3684113	ParS	0.21
IC80-M5	E7	5	3684113	ParS	0.27
IC80-M5	E7	7	3684113	ParS	0.2
IC80-M5	E7	9	3684113	ParS	0.15
IC80-M5	E7	11	3684113	ParS	0.06
IC80-M5	E7	13	3684113	ParS	0.03
IC80-M5	E7	15	3684113	ParS	0
IC80-M5	E7	3	5637204	PmrB	0.61
IC80-M5	E7	5	5637204	PmrB	0.53
IC80-M5	E7	7	5637204	PmrB	0.37
IC80-M5	E7	9	5637204	PmrB	0.47
IC80-M5	E7	11	5637204	PmrB	0.17
IC80-M5	E7	13	5637204	PmrB	0.08
IC80-M5	E7	15	5637204	PmrB	0
IC80-M5	E7	3	6124605	EnvZ	0.02
IC80-M5	E7	5	6124605	EnvZ	0.13
IC80-M5	E7	7	6124605	EnvZ	0.07
IC80-M5	E7	9	6124605	EnvZ	0.04
IC80-M5	E7	11	6124605	EnvZ	0
IC80-M5	E7	13	6124605	EnvZ	0
IC80-M5	E7	15	6124605	EnvZ	0
IC80-M5	E7	3	393899	PtsP	0
IC80-M5	E7	5	393899	PtsP	0
IC80-M5	E7	7	393899	PtsP	0
IC80-M5	E7	9	393899	PtsP	0
IC80-M5	E7	11	393899	PtsP	0
IC80-M5	E7	13	393899	PtsP	0.01
IC80-M5	E7	15	393899	PtsP	0.15
IC80-M5	E7	3	394249	PtsP	0
IC80-M5	E7	5	394249	PtsP	0
IC80-M5	E7	7	394249	PtsP	0
IC80-M5	E7	9	394249	PtsP	0
IC80-M5	E7	11	394249	PtsP	0
IC80-M5	E7	13	394249	PtsP	0.01
IC80-M5	E7	15	394249	PtsP	0.7
IC80-M5	F7	3	5637204	PmrB	0.9
IC80-M5	F7	5	5637204	PmrB	0.8
IC80-M5	F7	9	5637204	PmrB	0.81
IC80-M5	F7	11	5637204	PmrB	0.72
IC80-M5	F7	13	5637204	PmrB	0.31
IC80-M5	F7	15	5637204	PmrB	0.06
IC80-M5	F7	3	732988	intergenic	0.6
IC80-M5	F7	5	732988	intergenic	0.38
IC80-M5	F7	9	732988	intergenic	0.3
IC80-M5	F7	11	732988	intergenic	0.32

IC80-M5	F7	13	732988	intergenic		0.17
IC80-M5	F7	15	732988	intergenic		0.02
IC80-M5	F7	3	393899	PtsP		0
IC80-M5	F7	5	393899	PtsP		0
IC80-M5	F7	9	393899	PtsP		0.07
IC80-M5	F7	11	393899	PtsP		0.33
IC80-M5	F7	13	393899	PtsP		0.3
IC80-M5	F7	15	393899	PtsP		0.58
IC80-M5	H7	3	5637204	PmrB		0.02
IC80-M5	H7	5	5637204	PmrB		0.21
IC80-M5	H7	7	5637204	PmrB		0.07
IC80-M5	H7	11	5637204	PmrB		0
IC80-M5	H7	13	5637204	PmrB		0
IC80-M5	H7	15	5637204	PmrB	NA	
IC80-M5	H7	3	393335	PtsP		0.01
IC80-M5	H7	5	393335	PtsP		0.21
IC80-M5	H7	7	393335	PtsP		0.26
IC80-M5	H7	11	393335	PtsP		0.42
IC80-M5	H7	13	393335	PtsP		0.34
IC80-M5	H7	15	393335	PtsP	NA	
IC80-M5	H7	3	394924	PtsP		0.01
IC80-M5	H7	5	394924	PtsP		0.3
IC80-M5	H7	7	394924	PtsP		0.51
IC80-M5	H7	11	394924	PtsP		0.57
IC80-M5	H7	13	394924	PtsP		0.47
IC80-M5	H7	15	394924	PtsP	NA	
IC80-M5	H7	3	3499294	RbsR		0.01
IC80-M5	H7	5	3499294	RbsR		0.14
IC80-M5	H7	7	3499294	RbsR		0.44
IC80-M5	H7	11	3499294	RbsR		0.41
IC80-M5	H7	13	3499294	RbsR		0.29
IC80-M5	H7	15	3499294	RbsR	NA	
IC80-M5	H7	3	1860256	hypothetical		0.01
IC80-M5	H7	5	1860256	hypothetical		0.09
IC80-M5	H7	7	1860256	hypothetical		0.14
IC80-M5	H7	11	1860256	hypothetical		0.16
IC80-M5	H7	13	1860256	hypothetical		0.05
IC80-M5	H7	15	1860256	hypothetical	NA	

Acknowledgements

First and foremost, I want to thank my supervisor Hinrich Schulenburg for all his support and mentoring over the past 4.5 years. Thank you for taking me on as a PhD student and exposing me to a lot of great people and topics. I may have tested your stoicism and patience more than once, but I could always rely on your advice and support. Thank you also for giving me the chance to experience the role of a university lecturer. In addition, I want to thank Gunther Jansen who facilitated this project and took me in as a PhD student. You did a terrific job as a mentor during my MSc thesis project and gave me the confidence to pursue a PhD. I will always be thankful for that.

For the longest stretch, this work was funded as part of the DFG priority program SPP 1819 “Rapid evolutionary adaptation: Potential and constraints”. I would like to thank the DFG for the funding and the program organizers for setting up the many meetings and courses that helped me develop my skills. I also want to thank all other funding sources: The Max Planck Society, the Leibniz-WissenschaftsCampus “EvoLUNG” and the Kiel University excellence cluster “Precision Medicine in Chronic Inflammation”.

I would like to thank all other members of my thesis advisory committee, Eva Stukenbrock, Jenna Gallie, Lutz Becks and Camilo Barbosa. Thank you for all your input and feedback over the years. The meetings I had with you were important milestones during my research and I took a lot of experience from them. These meetings and an important conference visit would not have been possible without the support of the IMPRS for Evolutionary Biology in Plön. Thank you to the committee for supporting my work!

I would also like to thank my collaborators Sven Künzel, Sören Franzenburg and Hildegard Uecker for taking the time to discuss important aspects of my thesis and providing the expertise and help that I needed to keep carrying this project forward.

I specifically would like to thank everybody who read previous versions of this dissertation and gave me a lot of valuable feedback that helped me improve it so much: Alejandra, Ashley, Camilo, Carmen, Florian and Nancy – I can’t express how thankful I am for your support! I also want to thank my awesome aunt Heike for helping me design the nice summary graph.

I would like to thank my colleagues in the AB group for all the long and interesting discussions we had that helped me form a better understanding of the bigger picture. Aditi, Ashley, Leif –

it was sometimes a pain but most often a pleasure to have all these intense discussion with you and your students. It also was a great experience to watch you grow as scientists along with me. Big thanks to my predecessors Camilo and Roderich for all that you have done for me and the group. I've always admired your passion and intellect and I will continue to look up to you.

To all my office mates over the last years, Andrei, Yang, Fan, Jack, Florian and Christina: It was my pleasure to share a room with all of you and a great experience to learn about you and your cultures. Special thanks to Christina for helping me taking care of the plants! Then, I really must thank the entire Schulenburg lab. The fantastic group atmosphere I experienced since I first set foot into the lab was a prime reason for me to stay on as a PhD student. I knew that it would be very difficult to find something comparable. I specifically would like to thank Alejandra, Nancy and Philipp for bringing so much joy and positive energy to the group every day, and Christina, Ashley and Julia for the occasional drama – because everyday life would be quite boring without any of it 😊. To any other member of the Schulenburg lab who I encountered during the last years and have not listed here before: Thank you for your contributions to building a great work environment!

I specifically want to acknowledge all undergrad students that I had the chance of supervising during my time as a PhD student. Max, Tessa, Alexandra, Carmen, Matze - thank you for all your hard work and for giving me the chance of experiencing the role of your supervisor. I am sorry if I not always could provide you the right amount of time that you deserved. But I hope you learned a lot from the time we had together. I am curious to find out where you will go in life, but I'm sure that you will go far!

Big thanks also to my cohort mates and „Leidensgenossen“ Leonie, Eike, Henry and Binia. Coming from a quite non-academic background, it was essential for me to have relatable friends that I can share and compare my experience and problems as an aspiring researcher. I am thankful for the time I shared with you and happy to see that we've all made it through the storm. Looking forward to whatever comes next!

Finally, I would like to thank my family and childhood friends for all the support they have given me not only during my time as a PhD student but for all my life. I encountered a fair amount of stress in the last couple of years and I often wished that I could have more time and energy for you. But I never lost any hope, because I know that I can always rely on your love. And this is more important to me than anything else in the world.

Curriculum vitae

Personal details

Date of birth	20.04.1988
Place of birth	Flensburg, Germany
Nationality	German
Place of residence	Kiel, Germany

Education

Since December 2015

PhD student at the Department of Evolutionary Ecology and Genetics, Christian-Albrechts-Universität zu Kiel, Germany, in association with the International Max-Planck Research School (IMPRS) for Evolutionary Biology

October 2012 - September 2015

Master of Science in Biology (Focus on Evolutionary Biology and Ecology), Christian-Albrechts-Universität zu Kiel, Germany

October 2009 - September 2012

Bachelor of Science in Biology, Christian-Albrechts-Universität zu Kiel, Germany

Attended courses, conferences and workshops during PhD

- Conferences: IMPRS Evolutionary Biology retreats 2016 (*poster*), 2017 (*poster*), 2018 (*talk*), 2019 (*talk*)
- Conference (*talk*): “EMPSEB 22”, Gotland, 12 – 16 Sep 2016
- Conference (*talk*): “Experimental Evolution & Community Dynamics”, MPI Evolutionary Biology Plön, 19 – 21 Sep 2016
- Conference (*talk*): “Rapid evolutionary adaptation: Potential and constraints”, University of Kiel, 17 – 19 Oct 2018
- Conference (*poster*): “EMBO | EMBL Symposium: New Approaches and Concepts in Microbiology”, EMBL Heidelberg, 10 – 13 Jul 2019
- Course: “Population genetic data analysis”, University of Hohenheim, Karl Schmid, 17 – 19 Oct 2016
- Course: “Experimental evolution: theory and current practises”, IBENS Paris, Henrique Teotonio, 7 – 11 Nov 2016
- Course: “Sequence analysis”, MPI Evolutionary Biology Plön, Bernhard Haubold, 19 – 23 Mar 2018
- Workshop (*talk*): “Pathogen evolution”, Kiel Evolution Center, 20 – 21 Jul 2017

- Workshop (*session chair*): "Evolutionary Biology meets the Antibiotic Crisis", MPI Evolutionary Biology Plön, 8 – 10 May 2019

Teaching during PhD (all at Christian-Albrechts-Universität zu Kiel, Germany)

- Teaching assistant "biol226 - Biostatistics" (MSc Biology), Winter semester 2015/16
- Teaching assistant "biol106 - Ökologie und Evolution" (BSc Biology), Winter semester 2017/18
- Teaching assistant "biol165 - Evolutionsökologie und -genetik" (BSc Biology), Winter semester 2018/19
- Lecturer "biol109 - Biostatistik" (BSc Biology), Winter semester 2019/20
- Lecturer "biol227 – Evolution, Evology and Genetics" (MSc Biology), Winter semester 2019/20

Supervised Bachelor theses during PhD

- Tessa Marciniak: "Influence of antibiotic concentrations on coexistence in multiclonal *Pseudomonas aeruginosa* populations", BSc Biology, Kiel 2018
- Alexandra Tietze "Evolutionary dynamics of gentamicin resistant mutants in *Pseudomonas aeruginosa* populations", BSc Biochemistry, Kiel 2019

Previous publications

Jansen G, Mahrt N, Tueffers L, Barbosa C, Harjes M, Adolph G, Friedrichs A, Krenz-Weinreich A, Rosenstiel P, Schulenburg H. (2016) "Association between clinical antibiotic resistance and susceptibility of *Pseudomonas* in the cystic fibrosis lung." *Evol Med Public Health* 2016(1):182-94:eow016. doi:10.1093/emph/eow016

Erklärung

Ich, Niels Jonas Mahrt, erkläre hiermit, dass

- ich die Abhandlung - abgesehen von der Beratung durch die Betreuerin oder den Betreuer - nach Inhalt und Form eigenständig und nur mit den angegebenen Hilfsmitteln verfasst habe,
- die Arbeit weder in Gänze noch zum Teil einer anderen Stelle im Rahmen eines Prüfungsverfahrens vorgelegt wurde, veröffentlicht worden ist oder zur Veröffentlichung eingereicht wurde;
- die Arbeit unter Einhaltung der Regeln guter wissenschaftlicher Praxis der Deutschen Forschungsgemeinschaft entstanden ist;
- kein akademischer Grad entzogen wurde.

Niels Jonas Mahrt

Kiel, 20.02.2020